Regulation of Diacylglycerol Acyltransferase-2 and Triacylglycerol Synthesis by Protein Ubiquitination

A Thesis Submitted to the College of Graduate Studies and Research
In Partial Fulfillment of the Requirements
For the Degree of Doctor of Philosophy
In the Department of Biochemistry
University of Saskatchewan
Saskatoon

By

CURTIS JAMES BRANDT

PERMISSION TO USE

In presenting this thesis/dissertation in partial fulfillment of the requirements for a Postgraduate degree from the University of Saskatchewan, I agree that the Libraries of this University may make it freely available for inspection. I further agree that permission for copying of this thesis/dissertation in any manner, in whole or in part, for scholarly purposes may be granted by the professor or professors who supervised my thesis/dissertation work or, in their absence, by the Head of the Department or the Dean of the College in which my thesis work was done. It is understood that any copying or publication or use of this thesis/dissertation or parts thereof for financial gain shall not be allowed without my written permission. It is also understood that due recognition shall be given to me and to the University of Saskatchewan in any scholarly use which may be made of any material in my thesis/dissertation.

DISCLAIMER

Reference in this thesis/dissertation to any specific commercial products, process, or service by trade name, trademark, manufacturer, or otherwise, does not constitute or imply its endorsement, recommendation, or favoring by the University of Saskatchewan. The views and opinions of the author expressed herein do not state or reflect those of the University of Saskatchewan, and shall not be used for advertising or product endorsement purposes.

Requests for permission to copy or to make other uses of materials in this thesis/dissertation in whole or part should be addressed to:

Head of the Department of Biochemistry
University of Saskatchewan
Saskatoon, Saskatchewan S7N 5E5 Canada

OR

Dean
College of Graduate Studies and Research
University of Saskatchewan
107 Administration Place
Saskatoon, Saskatchewan S7N 5A2 Canada

ABSTRACT

Triacylglycerol is the major source of stored energy in humans, yet, excessive accumulation of triacylglycerols in tissues leads to obesity, diabetes and heart disease. Triacylglycerol synthesis is catalyzed by diacylglycerol acyltransferase (DGAT) enzymes, DGAT1 and DGAT2. Although recent studies have shed light on the metabolic functions of these enzymes, little is known about their regulation.

We have found that DGAT2 is a short-lived protein and is degraded via the ubiquitin-proteasome pathway. Our objective was to identify the lysine residues that are ubiquitinated and determine the role of ubiquitination in regulating DGAT2 stability and triacylglycerol synthesis. Initial experiments found that a lysine-less DGAT2 mutant (Lys-less-DGAT2) was not degraded. Moreover, Lys-less-DGAT2 exhibited altered subcellular localization and disrupted lipid droplet biogenesis. Screening of a DGAT2 lysine-to-arginine mutant library demonstrated that several lysine residues are involved in regulating DGAT2 stability. Substitution of two lysine clusters was sufficient to mislocalize DGAT2 and perturb typical lipid droplet formation, suggesting that these lysines may have a role in targeting DGAT2 to lipid droplets. Interestingly, DGAT2 on lipid droplets was ubiquitinated and stimulating lipogenesis did not reduce DGAT2 degradation.

Monoacylglycerol acyltransferase (MGAT) enzymes, MGAT2 and MGAT3, are closely related to DGAT2 and produce the DGAT2 substrate, diacylglycerol. MGAT2 and MGAT3 interact with DGAT2 and appear to stabilize it. We determined that DGAT2, MGAT2 and MGAT3 are targeted for endoplasmic-reticulum-associated degradation (ERAD), as ERAD inhibition caused poly-ubiquitinated species of all three proteins to accumulate. Moreover, overexpression of DGAT2 and MGAT2 resulted in redistribution of the ERAD ATPase, valosin-containing protein (VCP/p97), where it becomes concentrated in the ER, co-localizing with both DGAT2 and MGAT2. Interaction of DGAT2 and MGAT2 with VCP/p97 was also demonstrated *in situ*.

We took a non-targeted mass spectrometry approach to identify proteins interacting with DGAT2. The carbohydrate binding protein, calnexin, was one of the candidates identified. This interaction was confirmed *in vitro* and *in situ*. The possible impacts of calnexin on triacylglycerol metabolism were examined in calnexin knockout mouse embryonic fibroblasts, which exhibited stunted lipid droplet size compared to wild-type cells.

Collectively, these investigations provide insight into the post-translational regulatory mechanisms of DGAT2 and DGAT2 family members.

ACKNOWLEDGEMENTS

I would like to first thank my supervisor, Dr. Scot Stone, whose mentorship has been an invaluable part of my graduate education. He has impressed upon me the qualities and practices necessary to become a successful researcher while providing the perfect balance of oversight and independence. Without your continued guidance this dissertation would not have been possible.

I am grateful to all past and present members of the Stone Lab for their assistance, direction and friendship. To Pamela McFie, getting to work with you and gaining the benefit of your expertise was one of the highlights of my time in this lab.

I would like to recognize Dr. George Katselis and the members of his lab for their assistance with components of this dissertation related to mass spectrometry; your time and efforts were greatly appreciated.

I want to thank my committee members: Dr. Terra Arnason, Dr. Ramji Khandelwal, Dr. Stanley Moore and Dr. Bill Roesler. The direction and constructive criticisms you supplied were instrumental in the completion of this work.

Thank you to my family. Your continued support and encouragement has meant so much to me. None of this would have been achievable without you.

Finally, thank you to the organizations that have financially contributed to my research. These include funding from: the College of Medicine, the Department of Biochemistry, The Heart and Stroke Foundation of Saskatchewan, the James Regan Cardiology PhD Scholarship and the John Spencer Middleton and Jack Spencer Gordon Middleton Bursary. Funding attained by Dr. Stone through the Canadian Institutes of Health Research and the Canadian Foundation for Innovation is also greatly appreciated.

DEDICATION

This dissertation is dedicated to Alyssa, my best friend and wife. It is hard to believe that this is finally done – I know that I could not have accomplished it without your love and support.

TABLE OF CONTENTS

LIST OF TABLES

LIST OF FIGURES

LIST OF ABBREVIATIONS

18:1	Oleic acid
ACAT	Acyl-CoA: cholesterol O-acyltransferase
AGPAT	Acyl-CoA: 1-Acyl-*sn*-glycerol-3-phosphate O-acyltransferase
AMFR	Autocrine motility factor receptor
BMI	Body mass index
BSA	Bovine serum albumin
C/EBP	CCAAT/enhancer-binding protein
CGI58	Comparative gene identification 58
CHX	Cycloheximide
CoA	Coenzyme A
CREB	cAMP responsive element binding protein
DGAT	Acyl-CoA: 1,2-diacyl-*sn*-glycerol O-acyltransferase
DMEM	Dulbecco's modified Eagle's medium
DMSO	Dimethyl sulfoxide
E1	Ubiquitin activating enzymes
E2	Ubiquitin conjugating enzymes
E3	Ubiquitin ligating enzymes
ER	Endoplasmic reticulum
ERAD	Endoplasmic reticulum-associated degradation
FABP	Fatty acid binding protein
FBS	Fetal bovine serum
GPAT	Acyl-CoA*: sn*-1-glycerol-3-phosphate O-acyltransferase
HA	Human influenza hemagglutinin
HECT	Homologous to E6AP carboxyl terminus
HMG	3-hydroxy-3-methyl-glutaryl
HRD1	HMG-CoA reductase degradation homolog 1
HRV	Human rhinovirus
Hsp70	Heat shock protein 70
INSIG	Insulin induced genes

LB	Luria-Bertani
LC-MS/MS	Liquid chromatography-tandem mass spectrometry
MAM	Mitochondria-associated membranes
MGAT	Acyl-CoA: 2-acylglycerol O-acyltransferase
NBD	N-[(7-nitro-2-1,3-benzoxadiazol-4-yl)-methyl]amino
p53	Tumor protein p53
PBS	Phosphate buffered saline
PGC	Peroxisome proliferator-activated receptor-gamma coactivator
PLA	Proximity ligation assay
PPAR	Peroxisome proliferator-activated receptor
RING	Really interesting new gene
Rpn	Regulatory particle non-ATPase
SCD	Stearoyl-coenzyme A desaturase
SNP	Single nucleotide polymorphism
TMD	Transmembrane domain
TRIM13	Tripartite motif containing protein 13
WAT	White adipose tissue

CHAPTER 1: Literature review

1.1 Obesity and complications

Obesity is a condition of energy imbalance. Excessive intake of food coupled with insufficient energy expenditure results in an over-abundance of adipose mass. Obesity is clinically estimated by body mass index (BMI) (Fig. 1.1) (Keys *et al.*, 1972). Guidelines endorsed by the World Health Organization (WHO) categorize a healthy weight as a BMI of 18.5-24.9 kg/m^2, overweight or pre-obesity as 25-29.9 kg/m^2 and obesity as BMI $\geq$ 30 kg/m^2. Obesity is further subdivided to represent the elevated health risk associated with increasing BMI: class I - moderately obese (30.0-34.9 kg/m^2), class II - severely obese (35.0-39.9 kg/m^2), class III - very severely obese ($\geq$ 40.0 kg/m^2) (World Health Organization, 2000; Lau *et al.*, 2007; Health Canada, 2003).

The 1970-1972 Nutrition Canada Survey identified that ~10% of Canadian adults were obese (Katzmarzyk, 2002). The 2009-2011 Canadian Health Measures Survey found that 34% of Canadian adults were overweight and an additional 26% considered obese. Moreover, 4% of the population was categorized as class III (Statistics Canada, 2012). Based on 2009-2011 data, 24% of Canadian obese adults were class II and 14% class III, representing an increase over 1978-1979 data which reported 17% were class II and 6% class III (Tjepkema, 2006; Statistics Canada, 2012). Childhood obesity has also increased in prevalence. In 1981, less than 2% of those under 18 years were obese, as of 2012 that had jumped to 9% (Tremblay, 2002; Statistics Canada, 2012). Obesity among most ethnic groups is similar, ranging from 14-16% for White, Black and Latin American Canadian adults. However, obesity in East/Southeast and South Asian Canadians is significantly lower at 3% and 8% respectively (Tremblay *et al.*, 2002). Conversely, obesity in Aboriginal populations is elevated. The 2000-2003 Canadian Community Health Survey identified obesity in 27% of off-reserve Aboriginals, while the 2008-2010 First Nations Regional Health Survey reported that obesity had reached 40% in reservation populations (Tremblay *et al.*, 2002; First Nations Information Governance Center, 2012). In the United States, based on 2011-2012 data, approximately 34% of adults were overweight and additional 35% were obese (Ogden *et al.*, 2014). As of 2014, roughly 39% of the global adult population was classified as overweight and 13% as obese (World Health Organization, 2000).

$$\text{BMI} = \frac{\text{Weight (kg)}}{(\text{Height (m)})^2}$$

Figure 1.1. Equation for the calculation of body mass index (BMI) - A Healthy weight is a BMI of 18.5-24.9 kg/m^2, overweight or pre-obesity ranges from 25-29.9 kg/m^2 and obesity is represented by a BMI $\geq$ 30 kg/m^2.

The clinical consequences of excess fat manifest in the predisposition towards a host of diseases. A causal link has been established between obesity and diseases such as metabolic syndrome, dyslipidemia, chronic obstructive pulmonary disease, hypertension, congestive heart failure, non-alcoholic fatty liver disease, deep vein thrombosis, gout, reproductive disorders and numerous cancers. It is clear that dangers associated with obesity extend far beyond classically associated type II diabetes. Researchers commonly express the increased likelihood of developing a disease secondary to elevated BMI, versus those with a normal BMI, as "relative risk". A weak effect is denoted by values of 1.01 – 1.49 and represents increased risk of 1% to 49%. Moderate risk is considered 1.5 (50%) – 2.99 (199%) and a strong risk is present above 3.0 (200%) (Oleckno, 2002). A 2009 report conducted meta-analysis on 89 studies to identify relative risk for overweight and obese individuals in relation to several diseases (Table 1.1) (Guh *et al.*, 2009; Janssen, 2013). Both obese men and women are at strong risk for type II diabetes and pulmonary embolism. Men are also at strong risk for osteoarthritis while women are at strong risk for endometrial cancer and coronary artery disease. A recent study found that all-cause mortality was 18% higher in obese adults and reached as high as 29% in class II and III adults (Flegal *et al.*, 2013).

Co-morbidity		Overweight		Obese	
		Male	Female	Male	Female
Endocrine and Metabolic	Type II Diabetes	2.40	3.92	6.74	12.41
	Gallbladder Disease	1.09	1.44	1.43	2.32
Cancer	Breast (postmenopausal)	-	1.08	-	1.13
	Colorectal	1.51	1.45	1.95	1.66
	Endometrial	-	1.53	-	3.22
	Esophageal	1.13	1.15	1.21	1.20
	Kidney	1.40	1.82	1.82	2.64
	Ovarian	-	1.18	-	1.28
	Pancreatic	1.28	1.24	2.29	1.60
	Prostate	1.14	-	1.05	-
Cardiovascular	Hypertension	1.28	1.65	1.84	2.42
	Coronary Artery Disease	1.29	1.80	1.72	3.10
	Congestive Heart Failure	1.31	1.27	1.79	1.78
	Stroke	1.23	1.15	1.51	1.49
Musculoskeletal	Osteoarthritis	2.76	1.80	4.20	1.96
	Chronic Back Pain	1.59	1.59	2.81	2.81
Respiratory	Asthma	1.20	1.25	1.43	1.78
	Pulmonary Embolism	1.91	1.91	3.51	3.51

Table 1.1. Summary relative risk of co-morbidities associated with elevated BMI - The summary relative risk of disease in overweight or obese individuals as determined by meta-analysis. Weak effect: 1.01 – 1.49 represents increased risk of 1% to 49%. Moderate risk: 1.5 – 2.99 represents increased risk of 50% - 199%. Strong risk: $\geq$ 3.0 represents increased risk of 200% (Guh *et al.*, 2009).

In addition to the medical complications attributable to excess weight, obesity has a profound economic impact. In terms of health care costs, Canadian studies have identified that average yearly medical expenses are increased by 25% for obese adults and 21% for obese children. Based on 2006 data, the direct and indirect costs associated with obesity were calculated (Janssen, 2013). Direct costs account for expenses of medical care while indirect costs cover aspects such as short-term and long-term disability, lost productivity and premature death. It is estimated that overweight adults in Canada added $2.1 billion in direct medical expenses while obesity accounted for an additional $3.9 billion. In-direct costs added $1.9 billion for overweight adults and a further $3.2 billion for obese adults. In total, the economic impact of excess weight in Canada can be estimated at $11 billion annually, as of 2006.

1.2 Storage lipids

Lipids are a biologically diverse group of compounds that play a variety of roles, including: energy storage molecules, membrane components, enzyme cofactors, chaperones, hormones, and intracellular signaling molecules. Fatty acids are the main reservoir of stored energy in eukaryotic cells. They are carboxylic acids with highly reduced hydrocarbon chains 4-36 carbons in length. Hydrocarbon chains can be saturated - containing no double-bonds, or unsaturated - containing at least one double-bond. The most prevalent fatty acids are composed of even numbers of carbon atoms between 12 and 24 units in unbranched chains (Fig. 1.2A). They are formed through sequential condensation reactions, resulting in the addition of two carbon units in the form of acetate. The polar carboxylic acid group is ionized at neutral pH and hydrophilic. However, the nonpolar hydrocarbon chains are very hydrophobic and therefore only short fatty acids exhibit any solubility in water. Fatty acids of increased length and fewer double-bonds exhibit increased hydrophobicity.

Three fatty acids esterified to a glycerol backbone form a triacylglycerol (Fig. 1.2B). Triacylglycerols are prevalent in eukaryotes such as fungi, plants and animals. They are non-polar and highly hydrophobic, which contributes to their efficiency in energy storage. Other energy storage molecules, such as glycogen and starch, while more readily accessible, must be hydrated, requiring the organism to carry extra water. In addition, the hydrocarbon chains of fatty acids are more reduced; oxidation of triacylglycerols produces over double the energy obtained from an equal mass of carbohydrate. A healthy (70 kg) person stores ~141,000 kcal as fat as compared with 24,000 kcal in the form of protein and 1000 kcal as carbohydrate (Wang *et al.*, 2013). In mammals, triacylglycerols also protect cells from the toxicity associated with free fatty acids (lipotoxicity), enabling fatty acid storage. Moreover, they provide ligands for nuclear hormone receptors and signal transduction pathways, in addition to substrates for the production of lipids important in maintaining the permeability barrier (Coleman and Lee, 2004; Listenberger *et al.*, 2003; Smith *et al.*, 2000; Farese *et al.*, 2000; Liu *et al.*, 2012)

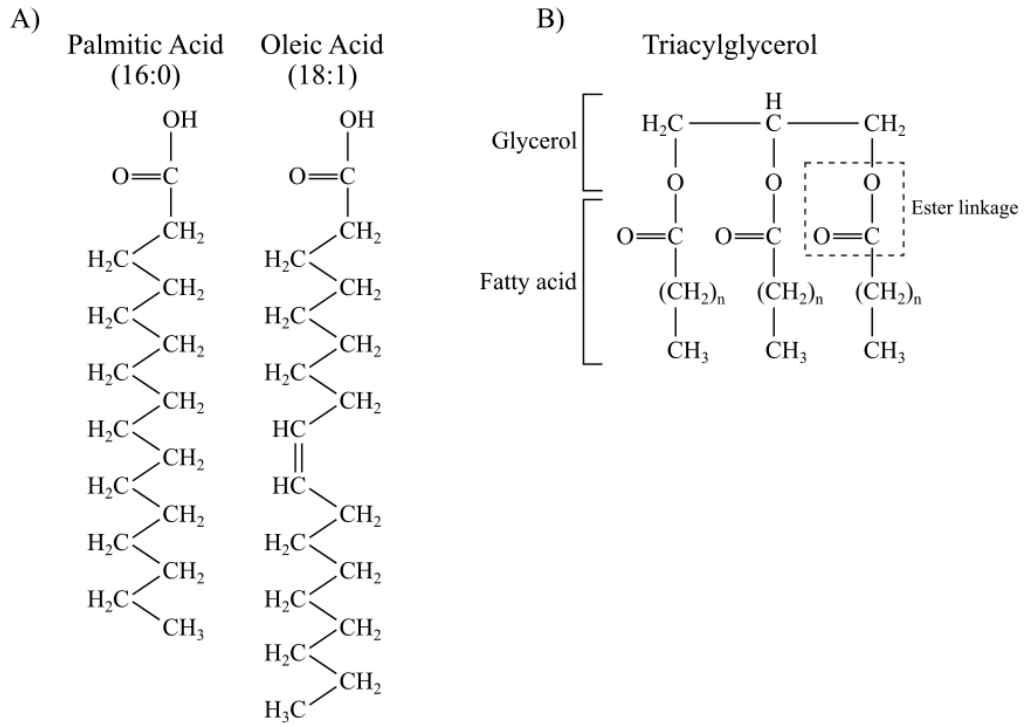

Figure 1.2. Lipid structure – *(A)* Fatty acid structure of palmitic acid (16:0) and oleic acid (18:1). *(B)* Representative structure of triacylglycerol noting the position of the ester linkage between the glycerol backbone and fatty acids.

1.3 Triacylglycerol biosynthesis

1.3.1 Mitochondria-associated membranes

Lipid biosynthetic enzyme activity is particularly enriched in a subdomain of the endoplasmic reticulum (ER) known as mitochondria-associated membranes (MAM). The ER has several morphologically and functionally distinct regions - the rough ER, smooth ER, transitional ER and MAM. MAM are characterized by their close proximity to mitochondria and delineated by the enrichment in lipid biosynthetic enzyme activities, such as: acyl-CoA: cholesterol O-acyltransferase (ACAT), acyl-CoA: 1,2-diacyl-*sn*-glycerol O-acyltransferase (DGAT)-2 and phosphatidylserine synthase (Franke and Kartenbeck, 1971; Morré *et al.*, 1971; Rusiñol *et al.*, 1994; Stone *et al.*, 2009, 2000). The only known marker protein to dependably distinguish MAM is phosphatidylethanolamine-N-methyltransferase-2, which is abundant in MAM but undetectable by Western blotting in other regions of the ER or mitochondria (Cui *et al.*, 1993). It is postulated that physical contact between MAM and the outer membrane of the mitochondria facilitates intracellular lipid transport between the ER and mitochondia (Shiao *et al.*, 1995, 1998; Stone and Vance, 2000; Vance and Shiao, 1996, Vance, 2014). MAM are also

closely apposed to intracellular sites of triacylglycerol storage, known as lipid droplets (Farese and Walther, 2009).

1.3.2 The Kennedy pathway

The Kennedy pathway, also known as the glycerol-3-phophate pathway, is the primary triacylglycerol synthesis mechanism in most mammalian cells (Fig 1.3) (Kennedy, 1957; Kindel *et al.*, 2010; Storch *et al.*, 2008). This four-step step pathway describes the sequential esterification of fatty-acyl groups to a glycerol backbone and occurs primarily on the ER membrane. Prior to incorporation in the Kennedy pathway, a fatty acid must be activated to form an acyl-coenzyme A (CoA) by acyl-CoA synthetase (Groot *et al.*, 1976; Cleland, 1963ab).

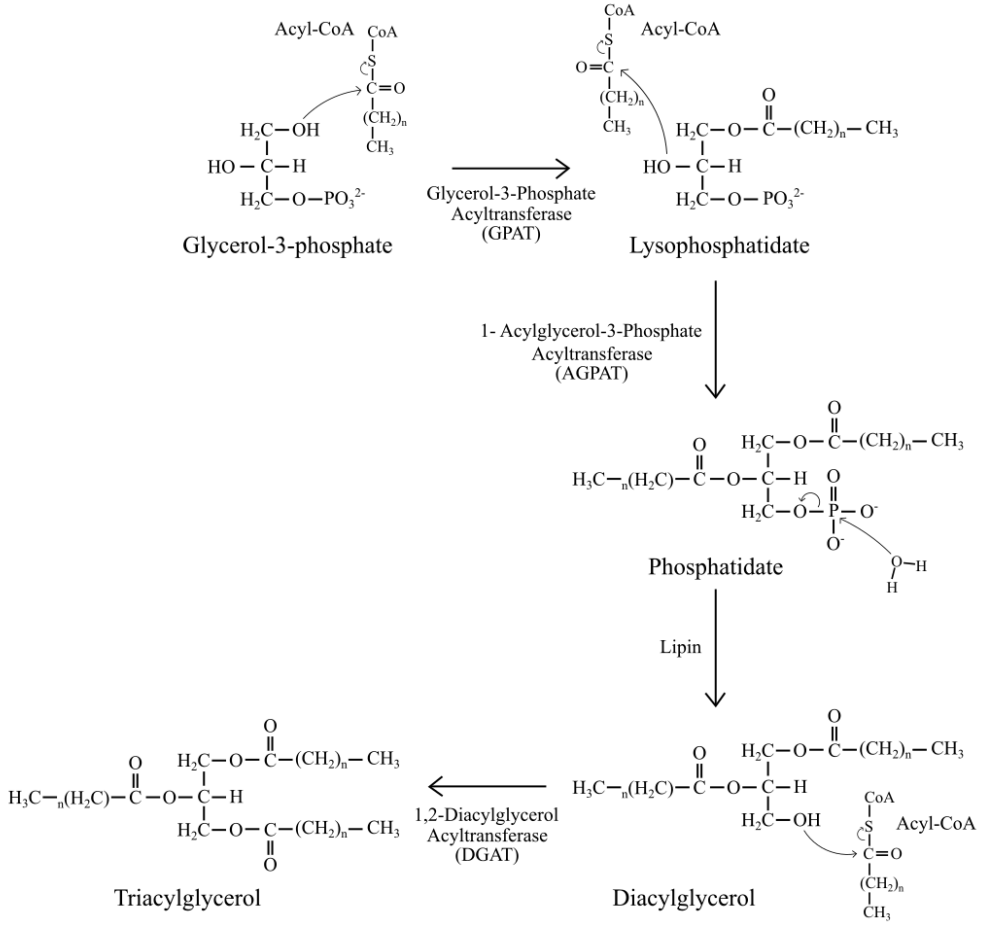

Figure 1.3. The Kennedy pathway - Alternatively known as the glycerol-3-phosphate pathway, it describes the sequential esterification of fatty acids to a glycerol backbone. The rate-limiting step in triacylglycerol synthesis is catalyzed by glycerol-3-phosphate acyltransferase isozymes, while the only committed step is performed by diacylglycerol acyltransferase isozymes. Triacylglycerol serves as a prominent energy storage molecule.

1.3.3 Glycerol-3-phosphate acyltransferase

Triacylglycerol synthesis begins through ester bond formation between glycerol-3-phosphate and an activated fatty acid (fatty acyl-CoA), forming lysophosphatidate. This reaction is catalyzed by acyl-CoA: *sn*-1-glycerol-3-phosphate O-acyltransferase (GPAT), the rate-limiting enzyme in triacylglycerol synthesis (Wendel *et al.*, 2009). Four GPAT isoforms (GPAT1-4), each an independent gene product, have been identified. GPAT isoforms differ mainly in localization, tissue expression, and substrate specificity (Lewin *et al.*, 2008). All isoforms are integral membrane proteins predicted to contain two transmembrane domains (TMD) and a cytosolic facing active site (Gonzalez-Baro *et al.*, 2001). Mammalian GPATs have yet to be crystallized. While the structure of a related GPAT isoform from squash has been determined, there are several key differences with mammalian GPATs (Turnbull *et al.*, 2001).

GPAT1 is localized to the outer membrane of the mitochondria and is enriched in MAM (Pellon-Maison *et al.*, 2007). Protein levels are greatest in the heart, however activity is low. Conversely, hepatocytes and adipocytes contain low GPAT protein levels but exhibit the highest GPAT activity (Lewin *et al.*, 2001). This discrepancy could be explained by regulation of GPAT activity by post-translational modification. Mitochondrial localization allows GPAT1 to compete with carnitine palmitoyl transferase-1 for acyl-CoA substrate. This shunts fatty acids into triacylglycerol synthesis and away from β-oxidation (Hammond *et al.*, 2005). Moreover, GPAT1 plays an important role in modulating triacylglycerol production in hepatocytes, as it accounts for 30-50% of totally liver GPAT activity (Wendel and Coleman unpublished; Hammond *et al.*, 2005). The *GPAT1* promoter is activated by sterol regulatory element-binding protein 1c, increasing GPAT1 expression and activity under lipogenic conditions (Ericsson *et al.*, 1997). GPAT1 activity is also stimulated by AMP-activated kinase, casein II kinase (through direct phosphorylation) and insulin (Collison and Jolly, 2006; Onorato *et al.*, 2005; Bronnikov, 2008). Little is known about GPAT2. Like GPAT1, it is localized to the mitochondria. It is expressed highly in the testes yet its significance is unknown (Lewin *et al.*, 2004; Wang *et al.*, 2007). GPAT3 is localized to the ER and protein levels are elevated in mouse tissues with increased triacylglycerol synthesis rates (adipose tissue, heart, small intestine). In humans, expression is highest in kidney, heart, thyroid, and skeletal muscle (Cao *et al.*, 2006). Triacylglycerol synthesis is increased in HEK-293 cells overexpressing GPAT3,

while knockdown in 3T3-L1 adipocytes reduced synthesis by 60% (Cao *et al.*, 2006; Shan *et al.*, 2010). Like GPAT3, GPAT4 is localized to the ER. GPAT4 has also been found to traffic to lipid droplet, facilitating droplet expansion (Wilfling *et al.*, 2013). Expression is highest in adipose tissue (brown and white), testes, liver and heart (Nagle *et al.*, 2008; Beigneux *et al.*, 2006; Vergnes *et al.*, 2006). Interestingly, *Gpat4*$^{-/-}$ mice presented with reduced subcutaneous fat deposits, yet knockdown of *Gpat4* in adipocytes had minimal effect on total GPAT activity or triacylglycerol production (Vergnes *et al.*, 2006). Activity of both GPAT3 and GPAT4 is induced by insulin-stimulated phosphorylation on serine and threonine residues in 3T3-L1 adipocytes (Shan *et al.*, 2010).

1.3.4 1-Acyl-glycerol-3-phosphate acyltransferase

Following GPAT acylation of glycerol-3-phosphate to lysophosphatidate, 1-Acyl-*sn*-glycerol-3-phosphate O-acyltransferase (AGPAT) carries out an analogous reaction, esterifying a second fatty acid (donated from a fatty acyl-CoA) to the second carbon position of lysophosphatidate to form phosphatidate. AGPATs, like GPATs, are integral transmembrane proteins and lysophosphatidate conversion to phosphatidate has been found to occur at the ER and mitochondrial membranes (Chakraborty *et al.*, 1999). While numerous AGPAT isoforms have been identified, only AGPAT1-3 isoforms have been confirmed to acylate lysophosphatidate to form phosphatidate (Leung, 2001; Lu *et al.*, 2005). Human *Agpat1* is expressed most highly in the liver, lungs, heart and pancreas - but is present in most tissues (Eberhardt *et al.*, 1997; West *et al.*, 1997). AGPAT1 overexpression in 3T3-L1 adipocytes or C2C12 myoblasts caused increased fatty acid uptake and lipogenesis (Ruan and Pownal, 2001). Regulation of AGPAT1 has gone largely uninvestigated, yet, neuron-derived orphan receptor 1 and peroxisome proliferator-activated receptor (PPAR) α binding sites in the gene promoter region suggest it may play a role in muscle development (Subauste *et al.*, 2010). AGPAT2 demonstrates high similarity with AGPAT1 in sequence and predicted topology. Transcript levels are most abundant in liver, heart and adipocytes (Agarwal *et al.*, 2002; West *et al.*, 1997). The *Agpat2* promoter region fosters consensus-binding regions for CCAAT/enhancer-binding protein (C/EBP) β and PPARγ, key transcriptional activators required for adipogenesis (Coleman and Mashek, 2011; Tanaka *et al.*, 1997; Gurnell *et al.*, 2000). This is supported by findings in 3T3-L1 differentiated adipocytes as *Agpat2* mRNA is increased 30-fold. Moreover,

Agpat2 specific siRNA suppressed C/EBPβ and significantly delayed PPARγ expression, thereby slowing adipogenesis. Intriguingly, cells produced 3-fold greater phosphatidate, yet triacylglycerol levels were low while phospholipids remained normal (Gale *et al.*, 2006). *Agpat3* transcripts are detectable in adipose tissue (brown and white), liver and testis - the protein localizes to membranes of the ER, Golgi and lipid droplets (Schmidt *et al.*, 2010; Wilfling *et al.*, 2013). Protease protection assays suggest AGPAT3 contains two TMDs and is oriented with the N-terminus in the cytosol and the C-terminus in the lumen of the ER or Golgi (Schmidt *et al.*, 2010). Studies have elucidated a role for AGPAT3 in the formation of Golgi membrane tubules and intracellular protein trafficking. Knockdown of *Agpat3* caused Golgi fragmentation in HeLa cells, possibly due to changes in membrane curvature triggered by aberrant ratios of lysophosphatidate and phosphatidate (Schmidt and Brown, 2009; Schmidt *et al.*, 2010; Bankaitis, 2009).

1.3.5 Lipin

The next step in the Kennedy pathway requires displacement of the phosphate group at the 3-carbon of phosphatidate. Lipins, alternatively known as phosphatidate phosphatases, traffic from the cytosol to the ER and hydrolyze phosphatidate to form 1,2-diacylglycerol. Depending on cellular needs, diacylglycerol can be utilized as a precursor for phospholipid or triacylglycerol synthesis (Carman and Han, 2006). Three mammalian isoforms of Lipin have been identified (Lipin1-3). It appears that structurally, these isoforms possess some common elements. These include a nuclear localization sequence, a DIDGT motif (containing the active site) and an LXXIL motif thought to confer activity as a transcriptional coactivator (Han *et al.*, 2006; Finck *et al.*, 2006).

Lipin1 mRNA is most abundant in adipose tissue, skeletal muscle and testes (Peterfy *et al.*, 2001). The human *LPIN1* gene has 3 splicing products designated α, β and γ (Han and Carman, 2010). Overexpression of Lipin1α or Lipin 1β in McA-RH7777 rat hepatoma cells increased glycerolipid abundance and triacylglycerol secretion while reducing degradation of apolipoprotein B-100, the primary apolipoprotein in liver derived lipoproteins. Moreover, knockdown of *Lipin1* in this cell line markedly reduced triacylglycerol secretion (Bou Khalil *et al.*, 2009; Khalil *et al.*, 2010). *Lipin1* transcription has been shown to be increased by glucocorticoids, sterol regulatory element binding protein 1 and nuclear factor Y (Manmontri *et*

al., 2008; Zhang *et al.*, 2008; Ishimoto *et al.*, 2009). Nuclear localization of Lipin1 is promoted by sumoylation and inhibited by interaction with cytosolic scaffold protein 14-3-3 (Peterfy *et al.*, 2010; Liu and Gerace, 2009). In the nucleus, Lipin1 interacts with, and enhances the activity of, transcription factors peroxisome proliferator-activated receptor-gamma coactivator (PGC)-1α and PPARα. These transcription factors also increase *LPIN1* expression. Lipin1 transcriptional coactivation of PPARγ, PPARδ and hepatocyte nuclear factor-4α has also been noted (Finck *et al.*, 2006). Accordantly, Lipin1 has been hypothesized to play a role in regulating the expression of numerous genes associated with glucose and fatty acid metabolism. Accordingly, mutation of the nuclear localization signal caused a reduction in triacylglycerol synthesis and secretion in McA-RH7777 cells (Bou Khalil *et al.*, 2009; Khalil *et al.*, 2010). Stimulation of the mammalian target of rapamycin pathway through insulin signaling has been shown to cause phosphorylation of serine and threonine residues on Lipin1, increasing interaction with 14-3-3 proteins and thereby promoting cytosolic localization (Peterfy *et al.*, 2010; Huffman *et al.*, 2002; Harris *et al.*, 2007). Similarly, stimulation of triacylglycerol synthesis by oleate loading in hepatocytes reduced Lipin1 phosphorylation and increased its phosphatidate phosphatase activity and membrane localization - enhancing triacylglycerol synthesis (Harris *et al.*, 2007; Cascales *et al.*, 1984; Hopewell *et al.*, 1985). Further, Lipin1 phosphorylation during mitosis reduces phosphatidate phosphatase activity (Grimsey *et al.*, 2008). Mice deficient in Lipin1 present with fatty liver dystrophy. As pups, they exhibit fatty liver and hypertriglyceridemia. After weaning, they experience lipoatrophy, a reduction in brown and white adipocytes. This appears to be caused by a lack of Lipin1-facillitated activation of adipogenic transcription factors PPARγ and C/EBPα rather than insufficient phosphatidate phosphatase activity (Phan *et al.*, 2004). Fatty liver dystrophy mice eventually experience neurodegeneration (Langner *et al.*, 1989; Langner *et al.*, 1991; Nadra *et al.*, 2008). In humans, mutations that compromise Lipin1 activity appear to cause myoglobinurea, a symptom of muscle destruction (Yen *et al.*, 2008).

Lipin2 and Lipin3 are not as well characterized as Lipin1. Expression of *Lipin2* appears to be highest in the liver, brain and kidney, and while it exhibits comparable transcriptional coactivation function, its phosphatidate phosphatase activity is reduced relative to Lipin1 (Csaki and Reue, 2010). A role distinct from that of Lipin1 is indicated, as *Lipin2* is not upregulated by glucocorticoids or PGC-1α and it is down-regulated during adipogenesis (Finck

et al., 2006; Grimsey *et al.*, 2008). Also of interest, Lipin2 is elevated in obesity while transcript levels remain unaltered (Gropler *et al.*, 2009). All that is currently known of Lipin3 is that transcripts are expressed most highly in the liver and intestine (Donkor *et al.*, 2007).

1.3.6 1, 2-Diacylglycerol acyltransferase

The terminal step in the Kennedy pathway is the conversion of 1,2-diacylglycerol to triacylglycerol. This occurs via the formation of an ester bond between a long chain fatty acid and the free hydroxyl group of diacylglycerol (Fig. 1.3). This reaction is catalyzed by the microsomal DGAT enzymes. Two DGAT genes have been identified, *DGAT1* and *DGAT2*, which produce distinct protein products of no sequence similarity. While both DGAT1 and DGAT2 catalyze the same reaction, *in vitro* evidence suggests structural dissimilarity (Cases *et al.*, 1998; Stone *et al.*, 2006). DGAT1 is a member of a large family of membrane-bound O-acyltransferases. This family includes ACATs, which catalyze acyl-group transfer to cholesterol, forming cholesterol esters (Klein and Rudel, 1983). DGAT2 belongs to the DGAT2/acyl CoA: monoacylglycerol acyltransferase family that includes several monoacylglycerol acyltransferases (MGAT) and a wax synthase (Cases *et al.,* 1998, 2001 Farese *et al.,* 2000; Hofmann, 2000; Buhman *et al.,* 2001; Yen *et al.,* 2002; Cao *et al.,* 2003a; Cheng *et al.,* 2003; Yen and Farese, 2003; Turkish and Sturley, 2007). Neither DGAT1 nor DGAT2 has an apparent preference in regard to acyl-CoA chain length or saturation; bias towards certain diacylglycerol species has yet to be determined (Cases *et al.*, 2001). *In vitro*, it has been noted that DGAT2 is more sensitive to alterations in Mg^{2+} concentration and may demonstrate increased activity at lower substrate concentration, however, the relevance *in vivo* is unknown (Cases et al., 2001). DGAT1 has retinol acyltransferase, MGAT and mono- and di-ester wax synthase activities. DGAT1 retinol acyltransferase activity, esterifying retinol esters to form retinyl esters, may be important in the absorption of dietary vitamin A (Yen *et al.*, 2005).

Upregulation of *Dgat1* and *Dgat2* mRNA has been identified during differentiation of 3T3-L1 adipocytes but neither gene is essential for differentiation (Harris *et al.*, 2011). C/EBPβ and C/EBPα have been implicated in the induction of the *DGAT2* gene during 3T3-L1 differentiation (Payne *et al.*, 2007). A PPAR binding site is present in the promoter of DGAT1; activators of PPARγ have been found to increase *Dgat1* mRNA in both adipocyte cell

lines and in mouse and human adipose tissue (Ludwig *et al.*, 2002; Ranganathan *et al.*, 2006). Both transcripts become more abundant following glucose treatment in mature adipocytes. Interestingly, *Dgat2*, but not *Dgat1*, transcripts accumulate in response to insulin (Meegala *et al.*, 2002). X-box binding protein 1, a transcription factor involved in the regulation of the unfolded protein response, augments expression of DGAT2 and other lipogenic genes in the liver (Lee *et al.*, 2008). DGAT2 expression was increased when X-box binding protein 1 was overexpressed in primary hepatocytes of wild-type and X-box binding protein 1-deficient mice (Lee *et al.*, 2008). mRNA levels of *Dgat2* appear to be elevated in genetic and chronic diet-induced obesity while *Dgat1* transcripts are reduced (Meegala *et al.*, 2002;Suzuki *et al.*, 2005). Further reciprocal regulation is observed as *Dgat2* transcripts are reduced in white adipose tissue (WAT) and liver during fasting but increase upon refeeding. *Dgat1* mRNA exhibits converse cycling (Meegala *et al.*, 2002; Yen *et al.*, 2008). There is evidence that leptin suppresses DGAT2. mRNA levels are induced 3-fold in WAT of leptin deficient *ob/ob* mice as well as in the WAT, skeletal muscle and small intestine of *db/db* (leptin receptor deficient) and *Agouti* KK-A^y (leptin resistant) mice (Chen *et al.*, 2002; Wakimito *et al.*, 2003).

DGAT1 and DGAT2 are highly expressed in WAT and to a lesser extent in liver, small intestine, mammary glands and skeletal muscle; tissues with a prominent role in triacylglycerol metabolism (Cases *et al.,* 1998; Cases *et al.,* 2001; Kennedy, 1957; Kuerschner *et al.,* 2008; Shockey *et al.,* 2006; Stone *et al.,* 2009; Weiss and Kennedy, 1956). Despite the fact that DGAT1 and DGAT2 catalyze the same reaction and show similar general localization to the ER, these enzymes have distinct roles in triacylglycerol metabolism. Results obtained from gene knockout studies in mice implicate DGAT2's involvement in bulk triacylglycerol synthesis while DGAT1 appears to play a modulatory role in whole body energy homeostasis (Smith *et al.,* 2000; Chen *et al.,* 2002; Chen *et al.,* 2003a; Stone *et al.,* 2004; Yen *et al.,* 2008). Mice lacking *Dgat1 (Dgat1*$^{-/-}$*)* exhibit a 50% reduction in adipose mass relative to wild-type. They are also resistant to diet-induced obesity through a mechanism involving increased activity and thermogenesis, and reduced rate of intestinal triacylglycerol absorption (Smith et al., 2000; Chen *et al.*, 2002, 2003b; Buhman *et al.*, 2002). Additionally, *Dgat1*$^{-/-}$ mice have decreased triacylglycerol levels in liver and skeletal muscle, as well as increased insulin sensitivity, resulting in improved glucose metabolism (Chen *et al.,* 2002; Chen *et al.,* 2003b; Wang *et al.,* 2007). *Dgat1*$^{+/-}$ mice exhibit an intermediate phenotype (Yen *et al.*, 2008). In

contrast, DGAT2 (*Dgat2*$^{-/-}$) deficient mice exhibit severe skin abnormalities, leading to rapid dehydration and death within hours of birth (Stone *et al.,* 2004). This phenotype is attributed to reduction in in the synthesis of acylceramide, a key lipid component of the skin barrier, as well as a ~90% decrease in triacylglycerol content - yielding insufficient quantities of substrate to sustain energy metabolism. *Dgat2*$^{+/-}$ mice are healthy and all physical and metabolic features are similar to wild-type mice (Yen *et al.*, 2008). Overexpression of DGAT2 in cells and mice resulted in significantly higher levels of intracellular triacylglycerol accumulation relative to DGAT1 overexpression, suggesting a larger role for DGAT2 in bulk triacylglycerol synthesis - consistent with mouse knockout studies (Monetti *et al.,* 2007; Stone *et al.,* 2004).

At present, information regarding the molecular structure and function of DGAT1 and DGAT2 is limited. DGAT1 contains three TMDs and is oriented with the N-terminus in the cytosol and the C-terminus in the ER lumen (Fig. 1.4A) (McFie *et al.,* 2010). A highly conserved histidine residue (H426 murine DGAT1) facing the ER lumen is essential for enzymatic activity and has been proposed to represent part of the active site (McFie *et al.,* 2010). Luminal residence of the active site implies DGAT1 involvement in the synthesis of triacylglycerol for incorporation into nascent lipoproteins and secretion into the circulation. The cytosolic N-terminus is not required for activity but may promote tetramer formation (Cheng *et al.*, 2001). This proposed topology of DGAT1 is supported by findings demonstrating latent DGAT activity in the ER lumen of liver microsomes (Waterman *et al.,* 2002).

Like DGAT1, DGAT2 is an integral membrane protein of the ER. DGAT2 is well conserved in fungi, plants, and animals – with most of the variation occuring in residues of the N-terminal region (Fig. 9.1). Studies have shown that murine DGAT2 has two TMDs and is oriented with both the N- and C-termini exposed to the cytosol (Fig. 1.4B) (Stone *et al.,* 2006; McFie *et al.*, 2014). Due to the presence of a short loop connecting the TMDs, it has been proposed that DGAT2 may not span the membrane. Rather, a hairpin like structure, consisting of the TMDs with a short loop between them, is inserted into the lipid bilayer. Yet, a recent study suggests that the short loop (≤ 8 amino acids) does extend into the ER lumen (McFie *et al.*, 2014). Interestingly, the topology of yeast DGAT2 ortholog, Dga1, differs significantly from that of murine DGAT2. Dga1 also has N- and C-termini facing the cytosol, but contains four transmembrane domains and two extended luminal regions (Liu *et al.*, 2011)

Catalytic activity of DGAT2 has been linked to a highly conserved (H/E)PH(G/S) (HPHG in most species) sequence present in all members of the DGAT2 family. Mutational analysis has demonstrated that this sequence, particularily the second histidine residue, is required for full enzymatic activity, suggesting that it may represent part of the active site (Cases *et al.,* 2001; Stone *et al.,* 2011). Additional regions of high conservation are present but their significance remains largely unknown (Fig. 9.1).

Interestingly, it appears that DGAT2 molecules form a large heterologous multimeric complex, likely facilitated by disulfide bond formation between adjacent members of the multimer (Man *et al.,* 2006; McFie *et al.,* 2011). A chemical-crosslinking study revealed that DGAT2 dimerizes and is also part of a large protein complex of ~650 kDa that is present in membranes and on lipid droplets (Jin *et al.*, 2014) The cytosolic orientation of the active site allows for deposition and storage of synthesized triacylglycerol into cytosolic lipid droplets, distinct cellular organelles key to lipid metabolism.

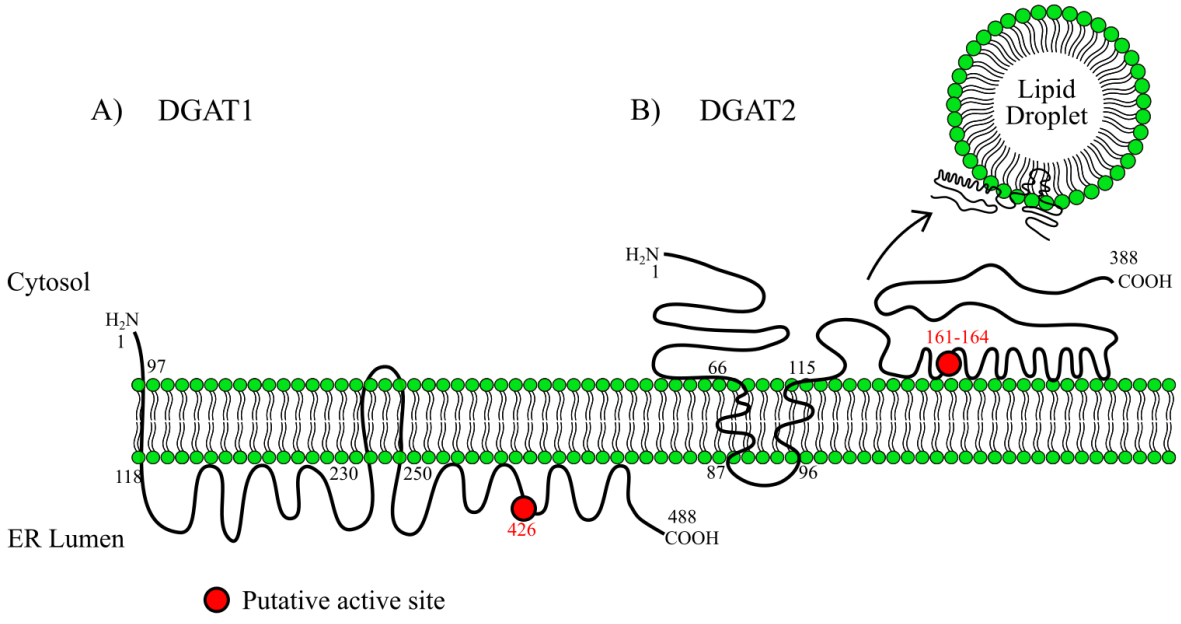

Figure 1.4. DGAT topology – Domain topology of *(A)* DGAT1 and *(B)* DGAT2. Included are locations of membrane spanning sections as well as positions of putative active sites.

DGAT2 is enriched in MAM of the ER (Cuie *et al.,* 1993; Rusinol *et al.,* 1994; Stone *et al.,* 2009; Stone and Vance, 2000). Studies focusing on the mechanism of DGAT2 localization have concluded that typical ER targeting signals are absent (Stone *et al.,* 2006; Stone *et al.,* 2009; Teasdale and Jackson, 1996). However, localization studies utilizing DGAT2 deletion mutants assert ER localization via the TMDs (amino acids 66-115) (McFie *et al.,* 2011). DGAT2 mutants lacking both TMDs continue to associate with membranes, however they do not localize to the ER. Rather, they localize to the mitochondria, most likely promoted by an N-terminal mitochondrial targeting sequence (McFie *et al.,* 2011; Stone *et al.,* 2009). Deletion of the TMDs in combination with a region predicted to contain two α-helices (amino acids 156-199), one amphipathic and the other hydrophobic and containing the putative acitve site, caused a significant portion of DGAT2 to localize to the cytosol (McFie *et al.*, 2014). Generation of chimeric proteins consisting of either TMD1 or TMD2 fused to a fluorescent reporter molecule (mCherry) revealed that TMD1, unlike TMD2, was sufficient to target the fluorescent construct to the ER (McFie *et al.,* 2011). While it is not entirely clear, it is possible that MAM situated DGAT2 interacts with mitochondria in order to promote channelling of substrates to DGAT2, increasing the production of triacylglycerols (Stone *et al.,* 2009; Coleman and Lee, 2004; Coleman *et al.*, 2000). MAM localization could increase access to activated fatty acyl-CoAs produced by acyl-CoA synthetases in the outer mitochondrial membrane (Ikeda *et al.*, 2001).

DGAT2, but not DGAT1, associates with lipid droplets. Oleate loading of COS-7 cells expressing DGAT2 was observed to stimulate DGAT2 accumulation on the surface of cytosolic lipid droplets (Kuerschner *et al.,* 2008; Stone *et al.,* 2009). Moreover, this localization pattern is found in adipocytes expressing endogenous DGAT2 (Kuerschner *et al.,* 2008). The current topology model, in conjunction with the unlikely ability for the phospholipid monolayer of lipid droplets to incorporate a bilayer spanning protein, suggests that DGAT2 remains imbedded in the ER membrane but is positioned in close proximity to droplets. This model is bolstered by electron micrographic data demonstrating lipid droplets in close proximity to the ER (Cinti, 2001; Kuerschner *et al.,* 2008; Stemberger *et al.,* 1984). However, if DGAT2 is imbedded in, but does not span the ER lipid bilayer, it is possible that the phospholipid monolayer of the lipid droplet could accommodate DGAT2 (Kuerschner *et al.,* 2008; Yen *et al.,* 2008). Findings by Xu *et al.* support the idea that DGAT2 does localize directly to droplets. A fusion protein expressed in DGAT2 mutant (lipid droplet defficient) round worms, consisting of an ER-

anchoring domain fused to the C-terminus of GFP-DGAT2, failed to initiate droplet growth. Disruption of ER tethering was sufficient to partially re-establish lipid droplet expansion and DGAT2 localization to lipid droplets. The group also generated convincing immunofluorescence data documenting co-localization with lipid droplet specific marker, perilipin-2, on the droplet surface (Xu *et al.,* 2012).

A study by Jacquier *et al.* provided insight into DGAT2 homolog, Dga1, ER to lipid droplet trafficking in S. *cerevisiae*. Using a fluorescence recovery after photobleaching approach, they found that the relocation of Dga1 occured independent of energy and temperature. Thus, Dga1 does not reach the lipid droplet surface through traditional vesicular transport. Noting that the observed rate of Dga1 fluorescence recovery was characteristic of two-dimensional diffusion, the group concluded that localization to lipid droplets may be attributed to lateral diffusion within a continuous membrane. This study advocates that lipid droplets are functionally connected to the ER membrane and that transport of membrane proteins between the lipid droplet and ER is mediated by this connection. Jacquier *et al.* also observed that droplet-localized Dga1 was able to shuttle back to the ER following stimulation of lipolysis (Jacquier *et al.,* 2011). Finally, a recent study suggested that the short transmembrane loop is important in allowing DGAT2 to function on lipid droplets; extension of the loop inhibited DGAT2 localization to droplets (McFie *et al.*, 2014)

DGAT2 interaction with other proteins involved in triacylglycerol synthesis has been noted. Stearoyl-coenzyme A desaturase (SCD) 1, responsible for catalyzing the desaturation of Δ9-cis fatty acids, was found to co-localize with DGAT2 in the ER of HeLa cells. Evidence of direct interaction was established by co-immunoprecipitation and fluorescence resonance energy transfer analysis. Co-expression of the two proteins resulted in accumulation of triacylglycerol levels above what was observed when either protein was expressed individually (Man *et al.*, 2006). Interaction with fatty acid transport protein 1, an acyl-CoA synthetase, was identified at the interface of the ER and lipid droplet and was found to facilitate lipid droplet expansion (Xu *et al.*, 2012). Recently, DGAT2 has been reported to interact with MGAT2, an enzyme responsible for producing diacylglycerol, particularly in the intestine. Interaction was found to be dependent on the DGAT2 TMDs. It was also discovered that incubation of McA-RH7777 cells with 2-monoacylglycerol caused DGAT2 to localize to, and produce, large lipid

droplets. This suggests that diacylglycerol produced by MGAT2 can be utilized by DGAT2 (Jin *et al.*, 2014)

DGAT activity has been divided into overt and latent fractions from studies in liver microsomes (Waterman *et al.*, 2002; Owen *et al.*, 1997; Abo-Hashema *et al.*, 1999). Overt activity is believed to represent catalysis on the cytosolic face of the ER, corresponding to storage of triacylglycerols in cytosolic lipid droplets. Latent activity is detected after membrane permeabilization and is thought to denote triacylglycerols synthesized in the ER lumen and destined for secretion. Elucidating the precise role of each DGAT in their contribution to triacylglycerol storage and secretion has yielded interesting and sometimes contradictory results. Based on the topologies, it would suggest that latent activity is that of DGAT1 while overt activity is provided by DGAT2. Evidence from transgenic mouse models suggests that over expression of DGAT1 or DGAT2 increases triacylglycerol production and storage in lipid droplets (Monetti *et al.*, 2007). Overexpression of DGAT1 in McA-RH7777 cells increased intracellular triacylglycerols and their secretion (Liang *et al.*, 2004). *In vivo*, short-term adenoviral overexpression of DGAT1 increased liver triacylglycerol abundance and secretion. DGAT2 overexpression increased liver triacylglycerols to a greater level than was observed for DGAT1 but had no effect on secretion (Yamazaki *et al.*, 2005). A similar study found that while both isoforms increased triacylglycerol levels in hepatocytes, overexpression of neither DGAT1 nor DGAT2 altered triacylglycerol secretion (Millar *et al.*, 2006). Studies utilizing antisense oligonucleotides directed against DGAT2 in the liver reduced hepatic triacylglycerol levels and triacylglycerol secretion (Yu *et al.*, 2005; Liu *et al.*, 2008). Recent work characterizing the effects of DGAT1 and DGAT2 inhibitors in mouse hepatocytes found that while DGAT1 and DGAT2 can compensate for one another in triacylglycerol synthesis, triacylglycerols produced by DGAT1 are primarily utilized for oxidation while those made by DGAT2 are directed towards secretion (Li *et al.*, 2015). It was also observed that inhibition of DGAT2, but not DGAT1, significantly reduced triacylglycerol secretion; tandem inhibition essentially abolished secretion. It is possible that interfering with the activity of one DGAT isoform could artificially impact the typical physiological processes of the other.

The beneficial effects observed in homozygous and heterozygous knockout mice made DGAT1 an attractive candidate for therapeutic intervention in the treatment of hyperlipidemias, obesity and type II diabetes. Several companies including Pfizer, Astrazeneca and Novartis

produced inhibitors that progressed to clinical trials (Maciejewski *et al.*, 2013; Denison *et al.*, 2013; Novartis, 2011; Serrano-Wu *et al.*, 2012). Unfortunately, not only was the efficacy of these compounds underwhelming but significant gastrointestinal side effects were noted. For this reason, as well as results obtained in the studies of DGAT2 directed antisense oligonucleotides in mice (detailed above), there has been renewed interest in targeting DGAT2. While several DGAT2 inhibitors have been developed, they have exhibited relatively weak potency - *in vitro* and *in vivo* effects are unknown (Qi *et al.*, 2012; Wurie *et al.*, 2012; Lee *et al.*, 2013; Kim *et al.*, 2013; Naik *et al.*, 2014; Kim *et al.*, 2014). A recent report detailed synthesis of several DGAT2 inhibitors; the most promising of which, compound 9 (PF-06424439), reduced plasma triacylglycerol levels by greater than 50% in rats (Futatsugi *et al.*, 2015). Moreover, in low-density lipoprotein receptor knockout mice fed a high fat and high cholesterol diet, 3 days of compound 9 treatment reduced plasma triacylglycerol by 61% and plasma cholesterol by 34% relative to control.

Recently, DGAT1 and DGAT2 associated diseases have been identified in humans. A case study detailed three children born from parents heterozygous for a DGAT1 splice variant in which exon 8 was skipped, resulting in an in-frame deletion of 75 base pairs; a 25 amino acid deletion in a highly conserved domain present in members of the membrane-bound O-acyltransferase family (Haas *et al.*, 2012). While the deletion did not affect the putative active site, the protein was rapidly degraded and inactive, culminating in an autosomal recessive congenital diarrheal disorder. Both parents exhibited elevated fasting triacylglycerol levels and total cholesterol. The first child (boy) was heterozygous for the mutant allele and was unaffected. The second child (girl), homozygous for the mutant allele, presented with hyperlipidemia, vomiting, colicky pain, diarrhea and associated protein-losing enteropathy - starting 3 days after birth. She was severely underweight despite tube-feeding and died at 17 months from malnutrition and sepsis. The third child (boy) presented similarly with hyperlipidemia, diarrhea and protein-losing enteropathy. The child was responsive to nutritional support and by 13 months the diarrhea had improved. At 46 months of age he was healthy and on an unrestricted diet. The authors determined that DGAT1, but not DGAT2, is expressed highly in the humnan intestine. This is contrary to tissue expression in mice where both DGAT1 and DGAT2 are present (Cases *et al.*, 1998, 2001). The authors hypothesized that diarrhea and protein-losing enteropathy may be caused by the accumulation of toxic DGAT1

substrates, diacylglycerol and fatty acids, or by bile acid malabsorption. Moreover, hyperlipidemia observed in both children and parents could be due to overcompensation by hepatic DGAT2 through secretion of triacylglycerols packaged as VLDL. The survival of the third child suggests the possibility of age or sex related differences in intestinal DGAT2 expression, compensating for defective DGAT1.

Aberrant DGAT2 was very recently reported to cause autosomal dominant early-onset axonal Charcot-Marie-Tooth Disease (Hong *et al.*, 2016). The report described a male, who as early as 8 years old, suffered from weakness in the lower limbs, ataxia and frequent falling. The disease progressed as the individual experienced hand tremors at 12 years and difficulty walking at 37 years of age. Analysis was undertaken at age 38. Serum triacylglycerol levels were mildly depressed while serum total cholesterol and low-density lipoprotein-cholesterol were average. The patient's son exhibited similar weakness of the lower limbs, ataxia, and frequent falling as early as 5 years of age. The cause was determined to stem from mutation of tyrosine 223 to histidine (Y223H). Overexpression of the mutant protein inhibited proliferation in NSC34 mouse motor neuron cells. Moreover, overexpression in zebrafish decreased axon branching as well as axon fasciculation in neurons of the neuromuscular junction. While the mechanism of pathology was unclear, reduced ER stress was noted, suggesting that DGAT2 Y223H does not trigger an unfolded protein response.

1.3.7 The monoacylglycerol pathway

In addition to the Kennedy pathway, the monoacylglycerol pathway is another prominent mechanism by which triacylglycerols are synthesized in mammals. The MGAT pathway describes the transfer of an acyl group from fatty acyl-CoA to 2-monoacylglycerol, forming 1,2-diacylglycerol (Fig. 1.5) (Kennedy, 1957; Bell and Coleman, 1980; Lehner and Kuksis, 1996; Ellis *et al.*, 2010; Coleman *et al.*, 2002). The MGAT and Kennedy pathways converge as 1,2-diacylglycerol is converted to triacylglycerol by DGATs (Cases *et al.*, 1998; Yen *et al.* 2008). The MGAT pathway is important for the absorption of dietary fat. Triacylglycerols are highly non-polar and cannot be absorbed intact; they must first be broken down to 2-monoacylglycerol by lipases. Monoacylglycerol is transported into enterocytes where triacylglycerols are re-synthesized by the MGAT pathway (Johnson and Rao, 1967).

The acylation of 2-monoacylglycerol is catalyzed by MGAT. There are three MGAT isoforms, MGAT1-3, encoded by genes *MOGAT1-3* respectively (Cases *et al.*, 2001). All three isoforms have been found to localize to the ER and demonstrate broad substrate specificity for monoacylglycerols and fatty-acyl CoA. Variation in MGAT tissue expression has been noted among isoforms. MGAT1 is expressed highly in the stomach and kidney of mice. It is also detectable in liver, uterus and adipose tissue but is absent in the intestine (Yen *et al.*, 2002). This expression pattern is conserved in humans but at reduced levels (Yen and Farese, 2003). Murine MGAT2 is expressed highly in the small intestine and at low levels in kidney and adipose tissue. Human MGAT2 is expressed highly in the intestine, stomach, liver and kidneys. It is detectable in mammary glands and adipose tissue as well (Yen and Farese, 2003; Cao *et al.* 2003b). MGAT3 is not present in mice but is expressed highly in the human intestine, particularly in the ileum (Yue *et al.*, 2011; Cheng *et al.*, 2003). Structural information on MGAT isoforms is very limited, however, MGAT2 appears to be an integral membrane ER protein with two TMDs - the second of which dictates ER targeting. Topology studies indicate that the short N-terminal region is partially embedded in the ER membrane bilayer. The extended C-terminal region faces the cytosol, while a short sequence containing the putative HPHG active site, is embedded in the cytosolic face of the membrane (McFie *et al.*, 2016).

Very little is known about the physiological role of MGAT1. A recent study found MGAT1 is highly expressed in fatty liver relative to normal liver; MGAT1 suppression is effective at blocking the fatty liver phenotype (Lee *et al.*, 2012). Moreover, *MOGAT1* gene activation is directly induced by PPARγ (Lee *et al.*, 2012). Evidence suggests that MGAT2 is the major intestinal MGAT in mice. Global MGAT2 knockout mice (*Mogat2*$^{-/-}$) appear to develop normally, however, they gain less weight than wild-type mice when fed a high fat diet, accordant with MGAT2's role in fat absorption. *Mogat2*$^{-/-}$ mice are also resistant to glucose intolerance, hypercholesterolemia, and hepatic steatosis induced by high-fat diet. Interestingly, MGAT2 knockout mice absorb sufficient dietary fat, even when fat accounts for 60% of caloric intake, such that levels of fecal fat and vitamin A and E are normal. This suggests that MGAT2 is not essential for absorbing typical fat quantities. Nevertheless, *Mogat2*$^{-/-}$ mice exhibit impaired triacylglycerol synthesis, slowed gastric emptying and perturbed fat absorption kinetics (Yen *et al.*, 2009). MGAT3 is only present in humans and higher mammals. While it functions as an MGAT, it shares higher sequence identity with DGAT2 (49%), than with

MGAT1 (44%) or MGAT2 (46%) (Cheng *et al.*, 2003). Also, like MGAT2, MGAT3 is upregulated in the liver of humans with nonalcoholic fatty liver disease; expression is greatly reduced following weight loss (Denison *et al.*, 2014). Analysis of MGAT3 found that it is present in the ER and may also function as a DGAT (Cheng *et al.*, 2003; Cao *et al.*, 2007; Brandt *et al.*, 2016a). Overexpression of MGAT3 in oleate treated COS-7 cells increased lipid droplet size and number; yet, MGAT3 did not traffick to lipid droplets (Brandt *et al.*, 2016a)

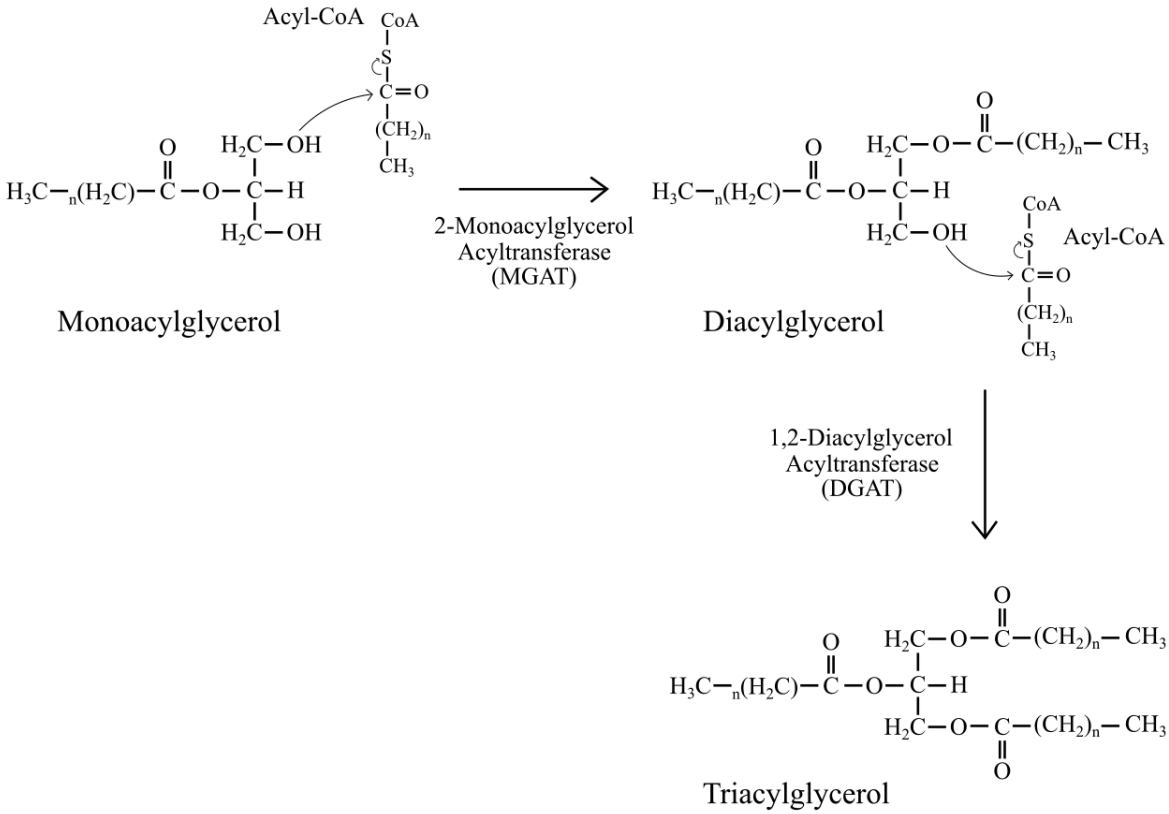

Figure 1.5. The monoacylglycerol pathway - In the monoacylglycerol pathway, 2-monoacylglycerol is acylated to produce 1,2-diacylglycerol. This reaction is catalyzed by the endoplasmic reticulum localized, MGAT, of which there are three isoforms (MGAT1-3). MGAT isoforms differ in tissue expression and substrate specificity. Diacylglycerol can be converted to triacylglycerol by the DGAT enzymes.

1.4 Digestion and transport of lipids

Triacylglycerol is the primary component of ingested animal fat and plant oils, and represents ~95% of dietary fat; the remaining 5% consists of phospholipids, sterols and fat-soluble vitamins (Yen *et al.*, 2015). Intestinal absorption of triacylglycerol is very efficient, allowing for almost complete assimilation of dietary fats even following a high fat meal (Kasper, 1970; Mansbach and Dowell, 2000). Also, processing of dietary fat and its transition to body fat requires less energy compared to carbohydrate or protein (Swaminathan *et al.*, 1985; Maffeis *et al.*, 2001).

Fat digestion is initiated in the stomach by lingual and gastric lipases, which preferentially hydrolyze medium chain triacylglycerols at the *sn*-3 position, producing 1,2-diacylglycerol (Carey and Hernell, 1992; Armand *et al.*, 1996). Emulsification, or the breakdown of large fat globules into smaller fat particles, begins in the stomach by mechanical contractions. The stomach regulates transition into the duodenum where food is mixed with bile acids and pancreatic secretions containing lipases. Bile acids function as detergents and are crucial in the solubilization of dietary fats, cholesterol and lipid-soluble vitamins (Zhou and Hylemon, 2014). The pancreas produces several lipases such as pancreatic lipase, carboxyl ester lipase, and phospholipase A_2, in addition to pancreatic lipase-related protein-1 and -2 (Wang *et al.*, 2013). In the duodenum, emulsion particles consist of a core of triacylglycerol and diacylglycerol covered by a monolayer of polar lipids, phospholipids and fatty acids. On the surface, small quantities of triacylglycerols and cholesterol are present - along with denatured dietary proteins, oligosaccharides and a bile salt coat (Carey and Hernell, 1992). Pancreatic lipase is a soluble enzyme and catalyzes hydrolysis at the interface between emulsion-oils and the aqueous phase (Verger, 1997; Roussel *et al.,* 1998). Pancreatic lipase hydrolyzes triacylglycerol primarily at *sn*-1 and *sn*-3 positions to produce monoacylglycerol and fatty acids. It can also hydrolyze monoacylglycerol, yielding glycerol and a fatty acid (Patton and Carey, 1979). Digestion of dietary phospholipids and cholesterol also occurs in the small intestine. Phospholipids are hydrolyzed by phospholipase A_2 at the *sn*-2 position, releasing fatty acids while lysophospholipids are integrated into micelles prior to uptake by mucosal cells (Wang *et al.*, 2013). Dietary cholesterol must be unesterified by cholesterol esterase, carboxylic ester lipase and sterol ester hydrolase before incorporation into micelles (Wang *et al.*, 2013).

Fatty acids released during digestion are taken up by enterocytes through passive diffusion and protein transport (Stahl *et al.*, 1999; Mashek and Coleman, 2006; Abumrad and Davidson, 2012). Passive diffusion via fatty acid "flip-flop" across the plasma membrane is believed to account for a large percentage of fatty acid uptake (Niot *et al.*, 2009). Several protein transporters have also been identified including, fatty acid transport protein 4, fatty acid binding proteins (FABP) and fatty acid translocase (Grevengoed *et al.*, 2014; Stremmel *et al.*, 1985; Abumrad and Davidson, 2012; Chen *et al.*, 2001). Monoacylglycerol is absorbed by the intestinal brush border membrane through passive diffusion (Schulthess *et al.*, 1994). As monoacylglycerol absorption can be saturated, the existence of a protein transporter has also been hypothesized (Ho and Storch, 2001). After uptake by enterocytes, fatty acids and monoacylglycerol are transported through the cytosol to the ER, likely by FABPs (Storch and Corsico, 2008). These include liver-type FABP, which is also expressed in the liver and kidney, and intestine-type FABP (Storch and McDermott, 2009). In addition to fatty acids, liver-type FABP binds monoacylglycerol and acyl-CoA (Lagakos *et al.*, 2013; Storch and Thumser, 2000). Data from liver-type FABP and intestine-type FABP knockout mice suggest that for triacylglycerol synthesis, fatty acids are channeled by intestine-type and monoacylglycerol by liver-type. Liver-type FABP may also play a role in fatty acid oxidation (Lagakos *et al.*, 2013).

Prior to triacylglycerol synthesis, fatty acids must be activated by an acyl-CoA synthetase, of which thirteen isoforms have been identified. Activation is achieved by thioesterification of the long-chain fatty carboxyl group (≥ 16 carbons) with CoA (Grevengoed *et al.*, 2014). The acyl-CoA synthetase 5 isoform is the most abundant in the intestinal mucosa and accounts for 60% of total intestinal acyl-CoA synthetase activity in mice (Meller *et al.*, 2013). In the intestine, the most prominent mechanism for triacylglycerol synthesis is via the MGAT pathway. It is estimated that >75% of intestinal triacylglycerol is produced via this route (Johnston and Rao, 1967). Interestingly, an alternate DGAT mechanism for triacylglycerol synthesis has been reported in rat intestine. In this reaction, an unidentified diacylglycerol transacylase catalyzes acyl-group transfer between two molecules of diacylglycerol to form triacylglycerol and monoacylglycerol (Lehner and Kuksis, 1993; Cases *et al.*, 2001).

It is believed that synthesized triacylglycerols are released into the phospholipid bilayer of the ER (Wilfling *et al.*, 2014a). These triacylglycerols either become incorporated into

cytosolic lipid droplets or enter the ER lumen for secretion (Thiam *et al.*, 2013; Demignot *et al.*, 2014; Lehner *et al.*, 2012; Martin and Parton, 2006; Murphy and Vance, 1999; Ohsaki *et al.*, 2009; Sturley and Hussain, 2012). In hepatocytes and enterocytes, cells responsible for the production of lipoproteins, accumulated triacylglycerols primarily partition into the ER lumen for secretion (Hussain, 2014). These accumulations are known as chylomicrons in the small intestine and very low-density lipoproteins in hepatocytes. For chylomicrons, the surface consists of a phospholipid monolayer and free cholesterol surrounded by apolipoprotein B48. Other proteins present on the surface of chylomicrons include apolipoprotein AI, apolipoprotein AIV and apolipoprotein C. The interior of chylomicrons primarily consists of triacylglycerol and cholesteryl esters. Chylomicrons are transported to the Golgi for modification prior to release into the circulation via the thoracic duct (Mansbach and Siddiq, 2010; Tso *et al.*, 2001). Chylomicrons function to transport triacylglycerol to peripheral tissues, especially skeletal muscle and adipose tissue. Triacylglycerol is subjected to hydrolysis by lipoprotein lipase in the blood vessel capillaries prior to entering tissues (Young and Zechner, 2013). Hydrolyzed chylomicrons are known as chylomicron remnants, which ultimately are taken up by the liver (Redgrave, 1970; Ji *et al.*, 1997). Following a lipid rich meal, when intake of fatty acids and monoacylglycerol surpasses the enterocytes ability to produce and secrete chylomicrons, triacylglycerol is stored in cytosolic lipid droplets (Nevin *et al.*, 1995). Triacylglycerol stored in lipid droplets can be liberated for secretion by adipose triglyceride lipase (Yang *et al.*, 1995; Obrowsky *et al.*, 2013; Xie *et al.*, 2014; Zhang *et al.*, 2014).

1.5 Lipid droplets

Originally viewed as inert deposits of intracellular lipids, lipid droplets are now recognized as functional organelles with a variety of roles (Fujimoto and Parton, 2011). Droplets in non-adipocytes range from 0.1-5 μm in diameter while those found in white adipocytes can be greater than 100 μm (Tauchi-Sato *et al.*, 2002). The exterior phospholipid monolayer consists of phosphatidylcholine, phosphatidylethanolamine, phosphatidylinositol, lysophosphatidylcholine and lysophosphatidylethanolamine (Tauchi-Sato *et al.* 2002; Leber *et al.* 1994; Bartz *et al.* 2007a). Phosphatidylcholine is the primary phospholipid in the monolayer, possibly because its cylindrical shape reduces surface tension (Thiam *et al.*, 2013). Free cholesterol is also present on the lipid droplet surface (Prattes *et al.*, 2000). The interior is

composed of stored triacylglycerols and cholesterol esters in varying ratios, depending on cell-type. Cryoelectron microscopy has revealed segregation between triacylglycerols and cholesterol esters in the droplet core (Czabany *et al.* 2008; Chang *et al.* 2009). Proteins are known to associate with the lipid droplet surface through insertion into, or interaction with, the phospholipid monolayer and have also been detected in the droplet core (Dvorak *et al.*, 1992; Bozza *et al.*, 1997; Robenek *et al.*, 2004, 2005). How proteins are inserted into the phospholipid monolayer remains an important question. Caveolin, a scaffold protein with several functions, is known to interact with the plasma membrane and lipid droplets. Topological evidence indicates cytosolic localization of the N- and C-termini with the presence of a long central hydrophobic membrane helix that is embedded in the membrane (Glenney and Soppet, 1992; Ostermeyer *et al.*, 2004). This is very similar to DGAT2 (Stone *et al.*, 2006; McFie *et al.*, 2014). Possibly, these long internal hydrophobic sequences are central in facilitating embedment in both membrane bilayers and the lipid droplet monolayer.

Triacylglycerol synthesized by DGATs and deposited in the ER membrane bilayer has limited solubility, leading to the formation of lipid droplets (Wang *et al.*, 2010). There are three prominent hypotheses for how lipid droplets are formed. The first of which suggests that lipid esters accumulate in the ER bilayer, leading to bulging of the cytosolic monolayer. The cytosolic leaflet eventually buds off to form an enclosed lipid droplet. Whether this is driven solely by the accumulation of neutral lipids in the ER or by cytosolic proteins that bind to the ER and induce budding, is unknown (Fig. 1.6A) (Murphy and Vance, 1999; Walther and Farese, 2009). The bicelle formation model is very similar. Lipid esters accumulate between the ER membranes prior to both leaflets of the membrane being excised (Fig. 1.6B) (Ploegh, 2007). One issue with this model is that excision of the droplet would create a hole in the ER membrane, allowing release of segregated calcium and altering the redox environment of the ER (Walther and Farese, 2009). Finally, the vesicular budding model describes accumulation of triacylglycerols in bilayer vesicles produced by vesicle machinery of the secretory pathway (Fig. 1.6C) (Walther and Farese, 2009; Walther *et al.*, 2009). The vesicle, which remains tethered or in close proximity to the ER, has neutral lipids deposited into the intermembrane space, causing the vesicle lumen to either fuse with the outer membrane or form an inclusion within the droplet interior.

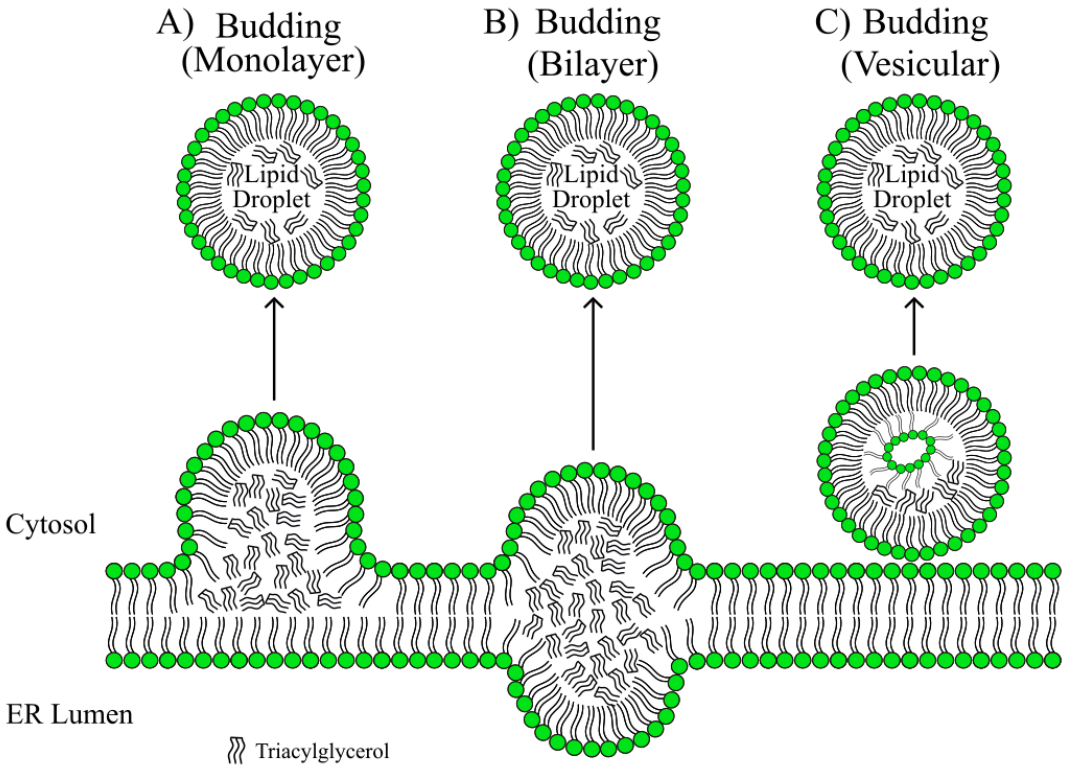

Figure 1.6. Theories of lipid droplet formation – *(A)* The monolayer budding theory suggests that triacylglycerol s accumulate in the ER membrane, causing bulging of the cytosolic leaflet, which eventually pinches off into the cytosol. *(B)* The bilayer budding model differs in that both the ER and cytosolic faces of the bilayer form the lipid droplet. *(C)* The vesicular budding model posits that triacylglycerols accumulate in the membrane bilayer of vesicles that are in close proximity to the ER membrane.

Following droplet formation, lipid droplets grow through coalescence, ripening and *in situ* expansion (Thiam *et al.*, 2013). Coalescence is driven by increasing surface tension brought on by the incorporation of lipids with negative curvature such as cholesterol, diacylglycerol, phosphatidylethanolamine and fatty acids. Insufficient levels of phosphatidylcholine also drives coalescence of lipid droplets, reducing surface tension by decreasing surface-to-volume ratio (Fujimoto and Parton, 2011). This has been shown in *Drosophila* and mammalian cells (Guo *et al.*, 2008; Jacobs *et al.*, 2008). Droplet ripening refers to transfer of neutral lipids from one lipid droplet to another. Triacylglycerols flow from the smaller droplet to the larger droplet, down the Laplace pressure gradient. Laplace pressure describes pressure differences between the inside and outside of a curved surface. Fat-specific protein 27 is known to induce ripening in adipose tissue during adipogenesis (Gong *et al.*, 2011;

Sun *et al.*, 2013). Finally, *in situ* expansion describes triacylglycerol synthesis on the formed droplet and is facilitated by localization of triacylglycerol synthesis enzymes to the lipid droplet surface. Isoforms of acyl-CoA synthetase, GPAT4, AGPAT3 and DGAT2 have all been found to traffic to lipid droplets (Wilfling *et al.*, 2014b).

The PAT protein family consists of perilipin, adipophilin/adipose differentiation-related protein and tail-interacting protein of 47 kDa - recently renamed perilipin-1, perilipin-2 and perilipin-3 respectively - along with S3-12 (perilipin-4) and OXPAT/MLDP/LSDP5 (perilipin-5) (Londos *et al.*, 2005; Kimmel *et al.,* 2010). These proteins localize to lipid droplets and play crucial structural and regulatory roles. They differ slightly in tissue expression and cellular localization. Perilipin-1 is expressed in adipocytes and steroidogenic cells (Greenberg *et al.*, 1991). Following feeding, when insulin levels are high, perilipin-1 is dephosphorylated. Perilipin-1 sequesters comparative gene identification 58 (CGI58), an activator of adipose triglyceride lipase, and also inhibits hormone-sensitive lipase interaction with lipid droplets - promoting triacylglycerol storage (Brasaemle, 2007; Lass *et al.*, 2011). Deletion of perilipin-1 in mice decreased WAT and increased ectopic fat deposition (Martinez-Botas *et al.*, 2000; Tansey *et al.*, 2001). Moreover, loss of function in humans causes partial lipodystrophy, dyslipidemia and type II diabetes (Gandotra *et al.*, 2011). Perilipin-1 is typically found on large lipid droplets (Grahn *et al.*, 2013). Perilipin-2 is expressed most highly in the liver, heart, and skeletal muscle, but it ubiquitous in tissues (Jiang and Serrero, 1992; Heid *et al.*, 1998). Similar to perilipin-1, it reduces adipose triglyceride lipase induced lipolysis but cannot compensate for loss of perilipin-1 activity in adipose tissue (Listenberger *et al.*, 2007). Perilipin-3 is elevated in small intestine, liver and macrophages but is detectable in all tissues (Grasselli *et al.*, 2010). Data suggests that perilipin-3 functions in the organization of the lipid droplet phospholipid monolayer and knockdown in hepatic tissue inhibits triacylglycerol storage (Sztalryd *et al.*, 2006). Perilipin-4 is expressed in WAT, heart and skeletal muscle; expression is controlled by PPARγ (Wolins *et al.*, 2006; Dalen *et al.*, 2004; Nagai *et al.*, 2004; Shimizu *et al.*, 2006). Its role in adipose tissue is unknown but loss of perilipin-4 in cardiac tissue correlated with attenuated triacylglycerol storage (Chen *et al.*, 2013). Perilipin-5 is largely found in organs with prominent fatty acid oxidation, like liver, muscle and brown adipose tissue (Fujimoto and Parton, 2011). Overexpression of perilipin-5 has been found to promote cardiac steatosis by blocking lipolysis (Pollak *et al.*, 2013). Accordantly, reduced

perilipin-5 expression correlated with reduced storage of triacylglycerols.

It is believed that PAT proteins may bind lipid droplets using a similar mechanism to that of apolipoprotein E, which utilizes a four-helix bundle of amphipathic helixes capable of binding the monolayer surface (Wilson *et al.*, 1991). A very similar four-helix bundle has been identified in perilipin-3 (Lu *et al.*, 2000). Additionally, a sequence of N-terminal 11-mer repeats forming an amphipathic helical structure is common to all PAT proteins and is likely involved in lipid droplet interaction (Hickenbottom *et al.*, 2004). Interestingly, PAT proteins demonstrate preferential binding based on lipid droplet size. In adipocytes, perilipin-3 and perilipin-4 localize to small droplets while perilipin-2 and perilipin-1 are found on medium and large droplets respectively (Wolins *et al.*, 2005). The mechanism for this is unknown, however, PATs may preferentially bind lipid droplets of a certain curvature, or interact with certain proteins or phospholipid head groups more abundant on or in droplets of a given size (Walther and Farese, 2009).

1.6 Triacylglycerol catabolism

Stored triacylglycerols can be liberated from cytosolic lipid droplets to meet cellular energy requirements through fatty acid catabolism, for thermogenesis, or for the assembly of lipoproteins and intracellular signaling molecules (Walther and Farese, 2009). Lipolysis can occur in the cytosol, ER and in late endosomes (Hornick *et al.*, 1992; Lass *et al.,* 2011). This process is largely modulated by lipases; the location and substrate specificity dictates which pathway fatty acids are directed to. All lipases belong to the α/β hydrolase superfamily of serine esterases (Duncan *et al.*, 2007). While there are some examples of integral membrane lipases, most are soluble proteins and act at the interface of the lipid droplet and the cytosol.

In WAT, insulin present in the fed-state inhibits lipolysis, however, during fasting, increased catecholamines and stress hormones stimulate lipolysis - utilizing triacylglycerol to meet energy requirements (Fain and Garcija-Sainz, 1983; Arner, 2005). Stimulation of β-adrenergic signaling by catecholamines increases cAMP, thereby activating protein kinase A (Fain and Garcija-Sainz, 1983; Carmen and Victor, 2006). Protein kinase A phosphorylates perilipin-1 and hormone sensitive lipase. Perilipin-1 phosphorylation inhibits its ability to interact with and sequester CGI58, an activator of adipose triglyceride lipase (Tansey *et al.*, 2001; Sztalryd *et al.*, 2003; Yamaguchi *et al.*, 2006). It also allows hormone sensitive lipase to

interact with lipid droplets, promoting hydrolysis (Tansey *et al.*, 2003). Adipose triglyceride lipase is abundant in adipose tissue but is also expressed in heart, intestine, muscle, liver and pancreas (Ahmadian *et al.*, 2011; Chandak *et al.*, 2010; Haemmerle *et al.*, 2006, 2011; Ong *et al.*, 2011; Wu *et al.*, 2012). It catalyzes hydrolysis of triacylglycerol at *sn*-1 and *sn*-2, producing *sn*-1,3-diacylglycerol or *sn*-2,3-diacylglycerol respectively (Zimmerman *et al.*, 2004, 2009). Hormone sensitive lipase is present mainly in white and brown adipocytes as well as steroid producing tissues (Holm *et al.*, 1988; Kraemer *et al.*, 1993; Holm, 2003). It functions primarily as a diacylglycerol lipase, exhibiting a preference for fatty acids at the *sn*-3 position, while it also demonstrates cholesteryl ester- and retinyl ester-lipase activity (Rodriguez *et al.*, 2010; Cook *et al.*, 1982; Wei *et al.*, 1997). Triacylglycerol lipase activity has been noted *in vitro*, yet hormone sensitive lipase is not sufficient to rescue adipose triglyceride lipase loss *in vivo* (Morak *et al.*, 2012). Protein kinase A phosphorylates and activates hormone sensitive lipase (Anthonsen *et al.*, 1998; Su *et al.*, 2003). In addition, phosphorylated perilipin-1 binds and recruits hormone sensitive lipase to the lipid droplet surface (Wang *et al.*, 2009a; Krintel *et al.*, 2009). Monoacylglycerol lipase localizes to the cytosol and lipid droplets, catalyzing the hydrolysis of monoacylglycerol (Karlsson *et al.*, 1997). Little is known regarding the mechanisms governing monoacylglycerol lipase but mice with aberrant monoacylglycerol lipase-activity display reduced fatty acid and glycerol release in WAT (Taschler *et al.*, 2011). Throughout this sequence, it is believed that diacylglycerol and monoacylglycerol are constantly being re-acylated by DGATs and MGATs (Salter *et al.*, 1998). In rats, 57% of free fatty acids released by lipolysis are re-esterified into triacylglycerols (Kalderon *et al.*, 2000). This futile cycle is believed to allow for rapid change and fine tuning of fatty acid oxidation in response to fluctuating energy demands (Wolfe *et al.*, 1990; Newsholme and Crabtree, 1976). Finally, FABP4 binds free fatty acids and transports them to the plasma membrane prior to albumin-facilitated distribution to other tissues via circulation (Coe *et al.*, 1999).

Oxidation of fatty acids to produce energy, also known as β-oxidation, requires sequential cleavage of two-carbon units from a fatty acid as a molecule of acetyl-CoA (Fig. 1.7). Acetyl-CoA is then oxidized to CO_2 in the citric acid cycle. NADH and $FADH_2$ produced through these processes drive the electron transport chain to generate ATP. β-oxidation takes place in the mitochondrial matrix. Fatty acids of ≤ 12 carbons are able to pass through the mitochondrial membrane unassisted. However, the more prevalent fatty acids of ≥

14 carbons must use the carnitine shuttle (Nelson and Cox, 2008). This involves ATP dependent activation of fatty acids by acyl-CoA synthetases in the outer mitochondrial membrane to form fatty acyl-CoAs (Nelson and Cox, 2008). Fatty acyl-CoAs can be utilized by mitochondrial GPATs to produce lysophosphatidate in the glycerol-3-phosphate pathway, or can be processed by carnitine acyltransferase I, replacing the CoA group with a molecule of carnitine (Nelson and Cox, 2008). Fatty-acyl carnitine passes through the inner mitochondrial membrane via the acyl-carnitine/carnitine transporter, where carnitine is immediately replaced with a CoA group by carnitine acyltransferase II (Nelson and Cox, 2008). Carnitine-dependent trafficking of acyl groups into the matrix forms the rate-limiting step of β-oxidation (Nelson and Cox, 2008). Through the coordinated processing by enzymes, acyl-CoA dehydrogenase, enoyl-CoA hydratase, β-hydroxyacyl-CoA dehydrogenase and ketoacyl-CoA thiolase - a two-carbon unit is removed to form one acetyl-CoA, one $FADH_2$, one NADH and a proton (Nelson and Cox, 2008). The fatty acid goes through successive rounds of this sequence. For example, palmitic acid (16-carbons) passes through this cycle 7 times, generating: 8 acetyl-CoA, 7 $FADH_2$, 7 NADH and 7 protons. Acetyl-CoA formed through fatty acid oxidation is further oxidized to CO_2 in the citric acid cycle (Nelson and Cox, 2008). Electrons generated by β-oxidation and carried by $FADH_2$/NADH are used to drive the electron transport chain, producing ATP. Complete oxidation of palmitate results in the production of 129 ATP (Nelson and Cox, 2008).

The glycerol backbone remaining after hydrolysis of the fatty-acyl groups can be released into the circulation and taken up by the liver where it is phosphorylated by glycerol kinase to produce glycerol-3-phosphate. This can be oxidized to dihydroxyacetone phosphate by glycerol-3-phosphate dehydrogenase. Triose phosphate isomerase can then convert dihydroxyacetone phosphate to the glycolytic intermediate, glyceraldehyde-3-phosphate (Nelson and Cox, 2008).

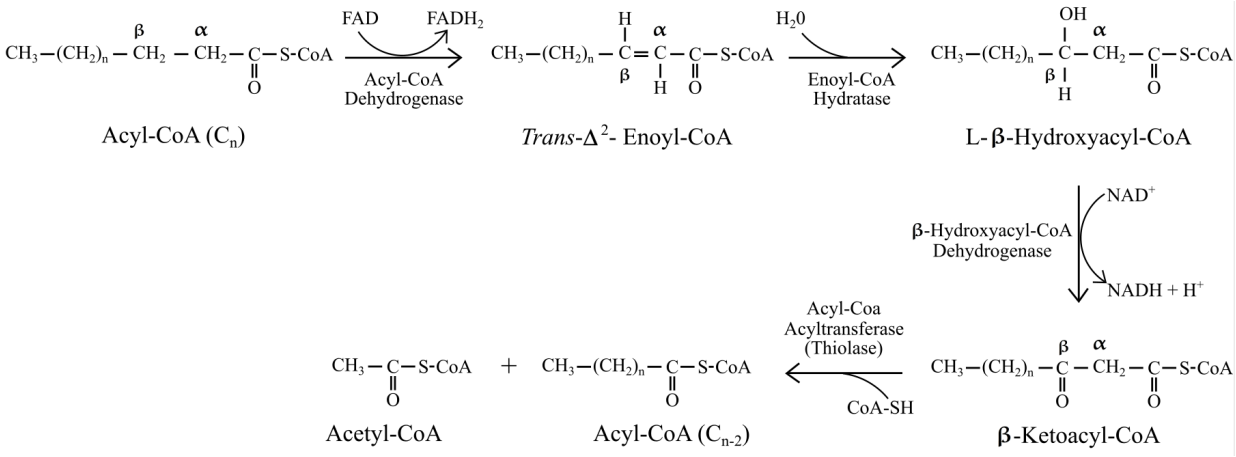

Figure 1.7. The β-oxidation pathway – Energy is released from fatty acids through β-oxidation as two-carbon units in the form of acetyl-CoA; electrons are transferred to carriers FAD and NAD^+. Acetyl-CoA can enter the citric acid cycle while electrons are delivered to the electron transport chain.

Regulation of β-oxidation enables efficient transition between triacylglycerol anabolism and catabolism in order to respond to cellular energy requirements. There are several key regulatory steps in this process. Malonyl-CoA, the first intermediate in long-chain fatty acid biosynthesis, inhibits carnitine acyltransferase I - blocking transport of fatty acids into the mitochondria (Nelson and Cox, 2008). An additional layer is present in this mechanism as high AMP (low ATP) levels activate AMP-activated protein kinase, which inhibits several lipogenic enzymes via phosphorylation. These targets include acetyl-CoA carboxylase 1 and 2, which converts acetyl-CoA to malonyl-CoA (Nelson and Cox, 2008). Reduction in malonyl-CoA alleviates inhibition of carnitine acyltransferase I, allowing β-oxidation to restore ATP levels (Nelson and Cox, 2008). β-oxidation is also inhibited by elevated energy levels in the form of NADH/NAD^+ ratio. Elevated NADH levels indicate abundant energy and inhibit β-hydroxyacyl-CoA dehydrogenase, which catalyzes the conversion of hydroxyacyl-CoA to α-ketoacyl-CoA in the third reaction of β-oxidation (Nelson and Cox, 2008). Finally, regulation at the transcriptional level is mediated by PPARα and cAMP responsive element binding protein (CREB). During fasting, PPARα upregulates the expression of acetyl-CoA synthetase I, carnitine acyltransferase I and II, and acyl-CoA dehydrogenase - increasing ATP production

in oxidative tissues such as liver, brown adipose tissue and muscle. CREB is activated through cAMP signaling (Nelson and Cox, 2008). This is triggered by glucagon released due to low blood glucose. CREB also activates genes that promote β-oxidation, such as sirtuin 1 (Li, 2013)

1.7 Ubiquitin and the ubiquitin proteasome system

Ubiqutin is an 8.5 kDa regulatory protein expressed in all eukaryotes. Covalent linkage of ubiquitin to a target protein is achieved through the concerted action of three types of enzymes: ubiquitin activating enzymes (E1), ubiquitin conjugating enzymes (E2) and ubiquitin ligating enzymes (E3). E1 catalyzes the ATP dependent activation of ubiquitin C-terminal Gly76, conjugating ubiquitin to the E1 by a high energy thioester bond (Haas *et al.*, 1982). Ubiquitin is then transferred to a cysteine residue located in the active site of an E2 enzyme. Transfer of ubiquitin to the target protein is achieved through different mechanisms depending on the class of E3 enzyme involved. E3 enzymes are the most important element of the ubiquitination machinery in determining substrate specificity. There are three classes of E3s, characterized by the presence of one of two general domains – really interesting new gene (RING)/RING-like and homologous to E6AP carboxyl terminus (HECT). RING and RING-like E3s bind to both the E2 and the ubiquitination target and catalyze the direct transfer from E2 to target protein. In contrast, HECT E3s catalyze the transfer of the thioester bonded ubiquitin from E2 to a conserved cysteine residue in the HECT domain before being conjugated to the target protein (Ravid and Hochstrasser, 2008). The third class of E3s are known as RING-between-RING E3 ligases (Aguilera et al., 2000). They consist of a standard RING domain (RING1) that is responsible for recruiting the ubiquitin bound E2, while a second RING domain (RING2), containing a catalytic cysteine, transfers ubiquitin to the substrate - similar to HECT E3s (Wenzel et al., 2011; Duda et al., 2013).

Post-translational linkage of ubiquitin to a target molecule is most often achieved through the formation of an amide bond between Gly76 of ubiquitin and the ε-NH_2 of an internal lysine residue. While less common, ubiquitin can also be linked to the substrate N-terminal residue α-NH_2 group (Ciechanover and Ben, 2004). In addition, recent studies have documented ubiquitin linkages to cysteine via a thioester bond as well as to serine and threonine residues by an oxyester bond (Fig. 1.8) (Wang *et al.,* 2012b). The linkage of a single ubiquitin molecule to

an amino acid residue is termed monoubiquitination. However, additional ubiquitins can be covalently attached to the first, creating a polyubiquitin chain. Each subsequent ubiquitin can be linked to any of seven lysine residues (Lys6, Lys11, Lys27, Lys29, Lys33, Lys48, Lys63) or the amino-terminal methionine (Met1) of the preceding ubiquitin in the chain. Therefore eight different homotypic polyubiquitin chains and variety of atypical chains consisting of heterologous, forked and/or mixed linkages are possible (Ye and Rape, 2009; Ikeda and Dicik, 2008; Iwai and Tokunaga, 2009). In some cases E4 enzymes, which support chain elongation, are necessary for polyubiquitin chain formation (Koegl *et al.,* 1999).

Ubiquitin signaling has been implicated in several cellular processes including protein degradation, DNA repair, endoplasmic reticulum-associated degradation (ERAD), receptor endocytosis, apoptosis and autophagy (Ravid and Hochstrasser, 2008; Finley, 2009; Ulrich and Walden, 2010; Hirsch *et al.,* 2009; Raiborg and Stenmark, 2009; Wertz and Dixit, 2010; Kirkin *et al.,* 2009). Specialized proteins containing ubiquitin-binding domains recognize specific ubiquitin chain linkages in order to differentially activate signaling pathways (Dikic *et al.,* 2009).

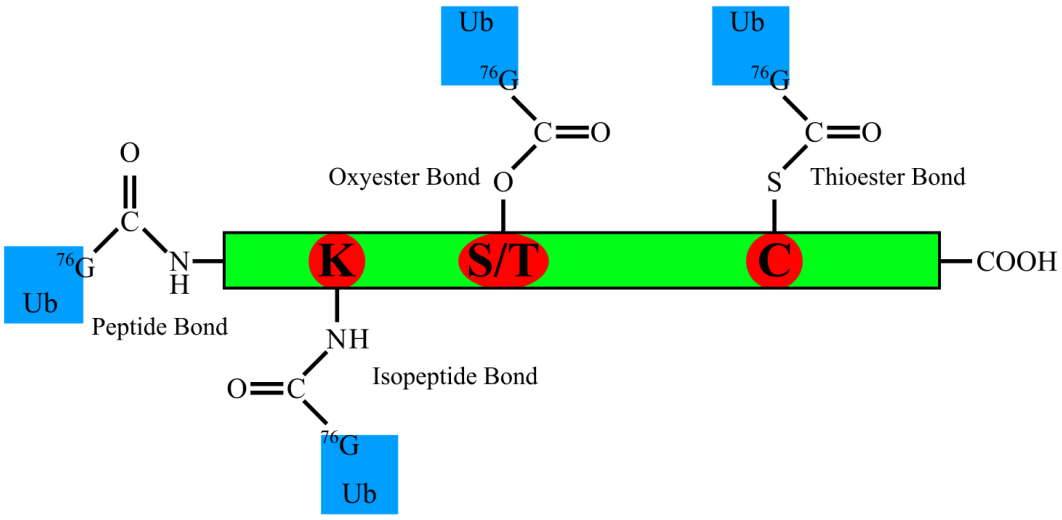

Figure 1.8. Protein ubiquitination - Ubiquitination is most often achieved through the formation of an amide bond between Gly76 of ubiquitin and the ε-NH_2 of an internal lysine residue. Ubiquitin can also be linked by peptide bond to the N-terminal α-NH_2, to cysteine via a thioester bond or to serine and threonine residues by an oxyester bond.

The most extensively studied branch of ubiquitin signaling is the ubiquitin-proteasome system (Fig. 1.9). A ubiquitin chain consisting of at least four Lys48 linked ubiquitin monomers represents a tag, targeting the protein to which it is linked for degradation by the 26S proteasome (Ikeda and Dikic, 2008; Thrower *et al.*, 2000). The signal presented by a protein, rendering it recognizable as a proteasomal substrate, is known as a degron. Degrons include the presence of hydrophobic or basic amino acids at the N-terminus of the protein (N-end rule) and phosphorylation at serine and/or threonine residues (phosphodegron) (Rao *et al.*, 2001; Orlicky, 2003).

The 26S proteasome consists of an inner 20S core particle flanked on either side by a 19S regulatory subunit. Ubiquitin mediated protein targeting to the proteasome can be achieved through either a direct or indirect recognition pathway. Direct targeting refers to recognition of the ubiquitin chain by one of two subunits in the 19S regulatory particle. The regulatory particle non-ATPase (Rpn) 10 (S5A in mammals) subunit contains one-to-three ubiquitin interaction motifs (dependent on species) while the Rpn13 (ADRM1 in mammals) contains a ubiquitin-binding domain known as pleckstrin homology receptor for ubiquitin (Finley, 2009; Husnjak *et al.,* 2008; Schreiner *et al.,* 2008). Indirect targeting refers to ubiquitin chain recognition by proteasomal shuttle factor proteins such as radiation gene 23, dominant suppressor of Kar2 and DNA-damage inducible homolog 1 (Glickman and Raveh, 2005; Grabbe and Dikic, 2009). These factors utilize their ubiquitin-associated domains to bind ubiquitinated substrates followed by their N-terminal ubiquitin-like domain in order to dock to subunits Rpn10, Rpn13 or Rpn1 (PSMD2 in mammals) of the 19S base (Dikic *et al.,* 2009; Finley, 2009). The function of proteasomal shuttle factors is critical as they provide a means of recognition and transport for ubiquitin marked proteins distant from the proteasome.

Prior to translocation of the ubiquitinated protein into the 20S proteolytic cavity, proteins in the base of the 19S cap are responsible for ATP-dependent unfolding and deubiquitination of the target. Entrance to the 20S cavity is regulated by the cap protein, regulatory particle ATPase 2 (Kohler *et al.,* 2001). Protein degradation within the 20S cavity is achieved through threonine-dependent nucleophilic attack, reducing the protein to short 7-9 amino acid peptides (Voges *et al.,* 1999).

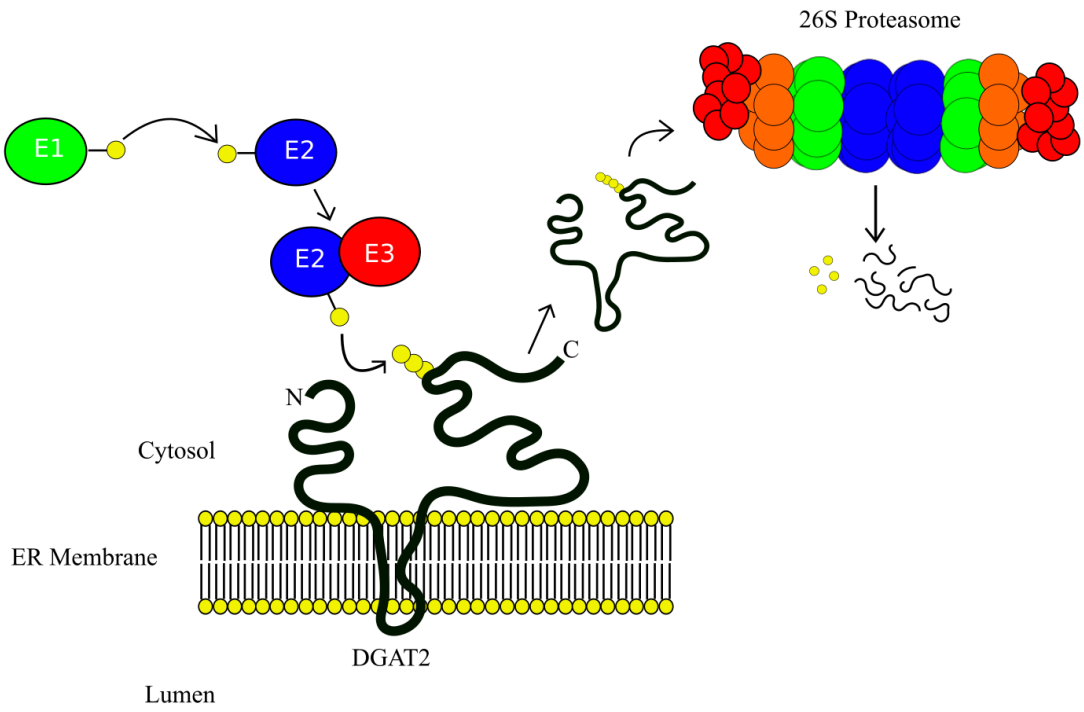

Figure 1.9. The ubiquitin proteasome system – The covalent attachment of an ubiquitin tag to a target protein is accomplished by the concerted effort of E1- ubiquitin activating enzymes, E2- ubiquitin conjugating enzymes and E3- ubiquitin ligases. A chain of at least four Lys48 linked ubiquitin molecules is sufficient for recognition by subunits of the 19S regulatory particle or shuttle factors. ATP-dependent unfolding and deubiquitination occurs at the 19S cap prior to threonine-dependent nucleophilic attack in the 20S proteolytic cavity.

1.8 Endoplasmic reticulum-associated degradation

ERAD is an indispensable process in maintaining ER homeostasis in eukaryotic organisms. Polypeptides entering the ER through the translocon achieve their native state by chaperone assistance and commonly, the acquisition of post-translation modifications (Rapoport, 2007; Braakman and Hebert, 2013). However, due to factors such as mutation and insufficient chaperone levels, a portion of these proteins fail to achieve the proper folded conformation (Hartl and Hayer-Hartl, 2009). The accumulation of misfolded proteins in the lumen and membrane of the ER results in ER stress and proteotoxicity. A variety of diseases have been linked to retarded ERAD function including Wilson disease, Hirschprung disease and severe congenital neutropenia (Walter and Ron, 2011; Guerriero and Brodsky, 2012).

ERAD substrates appear to be detected by the exposure of hydrophobic regions normally inaccessible in the native structure. Recognition factors complexed to multi-pass

integral membrane RING E3 ligases are responsible for substrate recognition. These recognition factor/ligase complexes appear to demonstrate specificity dependent on the location of the misfolded domain, whether cytosolic, intramembrane, or luminal (Plemper *et al.,* 1999, 1999; Bhamidipati *et al.,* 2005; Kim *et al.,* 2005; Szathmary *et al.,* 2005; Carvalho *et al.,* 2006; Denic *et al.,* 2006; Gauss *et al.,* 2006). There are nine confirmed ER-membrane localized E3 ligases functioning in the ERAD pathway: 3-hydroxy-3-methyl-glutaryl (HMG)-CoA reductase degradation homolog 1 (HRD1), autocrine motility factor receptor (AMFR), tripartite motif containing protein 13 (TRIM13), membrane-associated RING finger protein 6, and RING finger proteins- 5, 103, 139, 170, and 204 (Nakatsukasa and Brodsky, 2008; Ravid and Hochstrasser, 2008; Hirsch *et al.*, 2009). Furthermore, there are an additional 15 ER-membrane localized E3 ligase candidates that may play a role in ERAD and while less common, a host of cytoplasmic E3 ligases such as Parkin and carboxy terminus of heat-shock 70-interacting protein (CHIP), involved in ERAD of some substrates (Neutzner *et al.,* 2011; Imai *et al.,* 2002; Meacham *et al.,* 2001).

Following substrate recognition, the misfolded protein is retrotranslocated across the ER membrane to the cytosol. How the targeted protein crosses the membrane is not fully understood. Current lines of evidence implicate the Sec61 complex, degradation in endoplasmic reticulum protein-1 and/or intrinsic retrotranslocation function of the ERAD E3 ligases (Wiertz *et al.,* 1996; Ye *et al.,* 2001; Lilley and Ploegh, 2004; Kalies *et al.,* 2005; Kreft *et al.,* 2006; Scott and Schekman, 2008; Wang *et al.*, 2008a; Horn *et al.,* 2009; Carvalho *et al.,* 2010; Mehnert *et al.,* 2014). Upon partial exposure of the protein to the cytosol, it can be ubiquitinated by an E3 ligase, permitting detection by a homohexameric complex of the valosin containing protein (mammals, VCP/p97; yeast, Cdc48) ATPase complex and cofactors ubiquitin fusion degradation 1 like protein and nuclear protein localization 4 homolog (Bays *et al.,* 2001; Ye *et al.,* 2001, 2003; Jarosch *et al.,* 2002; Rabinovich *et al.,* 2002). Targeting of this complex to the ER membrane is modulated by the ubiquitin-binding domain of fas-associated factor family member 2 in mammals (Neuber *et al.,* 2005; Schuberth and Buchberger, 2005; Mueller *et al.,* 2008). The VCP/p97 complex also facilitates interaction of de-ubiquitinating enzymes with the ubiquitinated substrate (Rumpf and Jentsch, 2006; Jentsch and Rumpf, 2007; Ernst *et al.*, 2009). Disruption of deubiquitinating enzymes YOD1 or ataxin-3 inhibits retrotranslocation. This suggests that cycles of ubiquitination and de-ubiquitination are

necessary for ERAD (Wang *et al.,* 2006; Ernst *et al.,* 2009; Zhang *et al.,* 2013). It appears that dislocation of the ubiquitinated substrate from the membrane is coupled to ATP hydrolysis by VCP/p97; the precise mechanism is currently unknown (Ye *et al.*, 2003). Following membrane dislocation, cytosolic chaperones such as B-cell CLL/lymphoma-2-associated athanogene 6 or proteasomal shuttle factors Rad23 and Dsk2 maintain substrate solubility and mediate transfer to the proteasome for degradation (Medicherla *et al.,* 2004; Claessen and Ploegh, 2011; Wang *et al.,* 2011; Xu *et al.,* 2012).

Mammalian ERAD, for the majority of substrates, appears to involve RING E3 ligases HRD1 and/or AMFR (Nadav *et al.,* 2003; Kikkert *et al.,* 2004; Fang *et al.,* 2001). The activities of other known E3 ligases are implicated in the destruction of a smaller group of substrates. Based on current data, it appears that there is a high level of cooperativity among E3 ligases of ERAD and that processing by several ligases is required for complete ERAD. Several versions of cooperativity have been proposed: 1) several E3s working in parallel, demonstrating equal specificity to a given substrate; 2) E3s simultaneously targeting a substrate with specificity to different sites on said substrate; 3) monoubiquitination by one E3 coupled to chain extension E4 activity of another E3; 4) sequential rounds of ubiquitin conjugation and removal (Olzmann *et al.,* 2013a). Joint activity of AMFR and ring finger protein 139, specific to different sites on the protein, has been documented in the degradation of HMG-CoA reductase while ring finger protein 5 has been found to accompany cytoplasmic E3, CHIP, in directing the degradation of cystic fibrosis transmembrane conductase regulator ΔF508 (Jo *et al.,* 2011; Younger *et al*., 2006). Ring finger protein 5 may also monoubiquitinate certain substrates, serving to prime chain elongation by AMFR (Morito *et al.,* 2008). While Hrd1p has reportedly been found to form dimers in yeast, E3s have yet to be observed forming heteromeric complexes of multiple E3s (Horn *et al.,* 2009; Carvalho *et al.,* 2009). Several groups postulate that ERAD E3s can ubiquitinate each other (Morito *et al.* 2008; Shmueli *et al.* 2009; Ballar *et al.,* 2010; Jo *et al.,* 2011). It is possible that inter-ubiquitination among ERAD E3s could function as a mechanism to regulate ERAD function - monoubiquitination of a single or set of E3s altering activity, while polyubiquitination controls E3 degradation (Olzmann *et al.*, 2013a).

1.8.1 ERAD of native proteins and its role in lipid metabolism

While ERAD is predominantly thought of as a “garbage removal” process in the cell, it

has also been implicated in the regulation of many native proteins. Moreover, several of these proteins are involved in lipid synthesis pathways. ERAD of functional proteins is a highly specific process appearing to require a diverse set of signals that prompt identification by the recognition factor/E3 ligase complex. Perhaps the best characterized of native ERAD substrates is HMG-CoA reductase, which catalyzes the rate-limiting step in the conversion of HMG-CoA to mevalonate in the synthesis of cholesterol and non-sterol isoprenoids (Goldstein and Brown, 1990). A complex feedback mechanism is utilized in order to target HMG-CoA reductase for ERAD. As cholesterol synthesis proceeds, an intermediate, 24,25-dihydrolanosterol, accumulates, triggering binding of ER-membrane proteins known as insulin induced genes (INSIG) to the membrane domain of HMGR (Song *et al.,* 2005). Interactions between a subset of INSIG proteins with E3 ligase AMFR results in ubiquitination at lysine residues 89 and 248, subsequently triggering proteasomal degradation (Song *et al.,* 2005; Lee *et al.,* 2007; Sever *et al.,* 2003).

Additional examples of functional proteins regulated through ERAD include: cytochrome P450 3A4, cyclooxygenase-2, apolipoprotein B-100 and SCD1. Interestingly, there appears to be diversity in signaling to E3 ligases that a particular protein is an ERAD substrate. For example, cytochrome P450 3A4 requires phosphorylation at residues Ser478, Thr264 and Ser420 by protein kinase A and protein kinase C in order to be degraded through ERAD by the concerted effort of the E2 conjugase, ubiquitin conjugating enzyme E2G 2, and E3 ligase, AMFR (Wang *et al.,* 2001; Wang *et al.,* 2009b). Further research using mass spectrometry revealed additional protein phosphorylation sites as well as eight ubiquitinated lysine residues tagged by ubiquitin conjugating enzyme E2G 2/AMFR and/or non-ERAD associated E2/E3 ubiquitin conjugating enzyme E2D1/CHIP (Wang *et al.,* 2012a). Conversely, cyclooxygenase-2, an integral membrane protein of the ER responsible for catalyzing the committed step in prostanoid biosynthesis, is targeted for ERAD by a 19 amino acid cassette near its C-terminus, which contains an N-glycosylation site at Asn594. While substitution of Asn594 stabilizes cyclooxygenase-2 mutants glycosylated at Asn594, a mutant containing glycosylated Asn594 yet lacking the rest of the 19-amino acid cassette is also stable (Mbonye *et al.,* 2006).

Like HMG-CoA reductase, SCD1 and apolipoprotein B-100 are involved in lipid synthesis pathways and degraded by ERAD. Mammalian SCD1 is an integral membrane protein in the ER and is involved in the catalysis of mono-unsaturated fatty acids (Shimakata *et*

al., 1972; Strittmatter *et al.,* 1974). In this case, detection by recognition factors/E3 ligase appears to be dependent on an N-terminal 66-residue PEST sequence. Rich in Pro, Glu, Ser and Thr residues, the PEST sequence is typical of short-lived proteins in which degradation appears to be facilitated by the ubiquitin-proteasome system or non-lysosomal cysteine protease, calpain (Reverte *et al.,* 2001; Spencer *et al.,* 2004; Shumway *et al.,* 1999). Proteasomal inhibition by MG132 results in the accumulation of polyubiquitinated SCD1 in the ER that is found to interact with VCP/p97, suggesting ERAD. Deletion of the N-terminal PEST sequence increases SCD1 stability. Likewise, fusion of the PEST sequence to a normally stable ER membrane protein results in its degradation by the proteasome (Kato *et al.,* 2006).

In contrast, apolipoprotein B-100 ERAD is regulated by lipidation. Apolipoprotein B-100 is the primary constituent of very low-density lipoprotein produced by hepatocytes, playing an integral role in lipoprotein transport. It contains prominent hydrophobic regions that must be lipidated during synthesis in order to avoid ERAD (Lapierre et al., 2004). Co-translational lipidation is facilitated by microsomal triglyceride transfer protein (Hussain *et al.,* 2003). Insufficient lipidation of the nascent peptide causes delay of co-translational entry through the Sec61 translocon, resulting in regions of apolipoprotein B-100 being exposed to the cytosol (Mitchell *et al.,* 1998). The E3 ligase AMFR is responsible for apolipoprotein B-100 ubiquitination (Fisher *et al.*, 1997, 2008).

While the main trends and players in the ERAD pathway appear to be consistent, the diversity in signaling mechanisms responsible for targeting a native protein for ERAD appears extensive; this is highlighted by comparing the examples outlined above. Sterol sensitive INSIG proteins are responsible for the turnover of HMG-CoA reductase, while phosphorylation by protein kinases A and C is necessary for destruction of cytochrome P450 3A4. Finally, apolipoprotein B-100 degradation is triggered by its insufficient co-translational lipidation. While the mechanisms are very dissimilar, all of these proteins are ubiquitinated by the same E3 ligase, AMFR. A complex network of recognition factors allows for this heterogeneity in signaling mechanisms.

It has been proposed that there may be a functional link between ERAD and lipid droplets. This is based on the inference that a traditional protein-based channel is unlikely to accommodate the size of folded ERAD substrates, many of which may have large post-translational modifications such as glycosylations (Ploegh, 2007). In addition, ERAD

components fas-associated factor family member 2, VCP/p97, ancient ubiquitous protein 1 and ubiquitin-conjugating enzyme E2G 2 - as well as ERAD substrates HMG-CoA reductase and apolipoprotein B-100 - are isolated in a lipid droplet-enriched fraction following proteasomal inhibition (Hartman *et al.*, 2010; Ohsaki *et al.*, 2006). Also, HMG-CoA reductase is stabilized when droplet formation is inhibited via acyl-CoA synthetase inhibitor, triacsin c (Hartman, 2010). Further findings illustrate that sterol treatment caused relocation of HMG-CoA reductase to buoyant lipid droplet-associated ER membranes, preceding dislocation to the cytosol. Moreover, chemical inhibition of lipid droplet formation reduced cytosolic dislocation of native ERAD targets (Hartman *et al.*, 2010; Klemm *et al.*, 2011). This suggests that lipid droplets may play a role in substrate dislocation or possibly serve as a waypoint for substrates traveling to the proteasome (Ploegh, 2007). Contrasting evidence in S. *cerevisiae* revealed that lipid droplets are not necessary for ERAD, illustrating differences between mammalian and yeast ERAD pathways (Olzmann and Kopito, 2011).

CHAPTER 2: Hypothesis and objectives

Hypothesis

A principle mechanism of DGAT2 and DGAT2 family regulation is through post-translational ubiquitination and degradation by the proteasome. Moreover, DGAT2 exists in a multi-protein triacylglycerol synthesis complex and interaction with members of this assembly further influence DGAT2 regulation.

Objectives

1. Identify ubiquitinated residues of DGAT2.
2. Determine the role of protein ubiquitination in regulating DGAT2 stability, triacylglycerol synthesis and storage.
3. Identify proteins interacting with DGAT2.
4. Examine the role(s) of proteins interacting with DGAT2.

CHAPTER 3: Materials and methods

3.1 Reagents

Names of reagents and their corresponding supplier are listed in Table 3.1. Supplier addresses are shown in Table 3.2. Table 3.3 outlines cDNA and expression vectors. The sequences of mutagenic primers used in this work are detailed in Table 3.4.

Table 3.1. Reagents and suppliers

General reagents and consumables	**Supplier**
Anti-FLAG M2 affinity gel	Sigma-Aldrich
Ezview HA agarose	Sigma-Aldrich
BODIPY 493/503	Invitrogen
Bovine serum albumin - fatty acid free	Sigma-Aldrich
Coumaric acid	Sigma-Aldrich
Cycloheximide	Sigma-Aldrich
Dimethyl sulfoxide	Sigma-Aldrich
1,2 Dioleoyl-sn-glycerol	Sigma-Aldrich
Eeyarestatin I	Santa Cruz
3X-FLAG peptide	Sigma-Aldrich
HRV 3C protease	Novagen
Hyblot Cl film	Denville Scientific
Insulin	Sigma-Aldrich
2x Laemmli sample buffer	Bio-Rad
Luminol	Sigma-Aldrich
MG132	Sigma-Aldrich
NBD-palmitoyl CoA	Avanti
Oleic acid	Sigma-Aldrich
PfuUltra DNA polymerase	Stratagene
10x PfuUltra DNA polymerase buffer	Stratagene
Polyethylenimine	Polysciences
Polyvinylidene difluoride membrane	Bio-Rad
Trypsin	Sigma-Aldrich
Tunicamycin	Sigma-Aldrich
Bacterial cell culture reagents	**Supplier**
Ampicillin	Fisher
Bacto agar	Difco
DH5α Competent *E. coli*	Invitrogen
NZ-Amine A from bovine milk	Sigma-Aldrich
Tryptone	EMD
XL10-Gold Ultracompetent E .coli	Agilent

Yeast extract	EMD
Mammalian cell culture reagent	**Supplier**
Antibiotic-Antimycotic 100x	Gibco
Dulbecco's modified eagle's medium	Lonza
Fetal bovine serum	Gibco
Commercial kits	**Supplier**
Duolink® *In Situ* Proximity Ligation Assay	Sigma-Aldrich
Primary antibodies	**Supplier**
Mouse anti-ADRP/perilipin-2 (10R-A117ax)	Fitzgerald
Rabbit anti-calnexin (ADI-SPA-865)	Enzo
Rabbit anti-DGAT2 C-term (N/A)	Invitrogen
Mouse anti-FLAG (F3165)	Sigma-Aldrich
Rabbit anti-FLAG (F7425)	Sigma-Aldrich
Mouse anti-HA (H9658)	Sigma-Aldrich
Mouse anti-Hsp70 (MA3-028)	Thermo Pierce
Rabbit anti-lamin (A+C) (ab108922)	Abcam
Mouse anti-Myc (N/A)	N/A
Rabbit anti-Myc (C3956)	Sigma-Aldrich
Mouse anti-ubiquitin (sc-8017)	Santa Cruz
Mouse anti-VCP/p97 (MA3-004)	Thermo Pierce
Secondary antibodies	**Supplier**
Goat anti-mouse 594 (A11005)	Invitrogen
Donkey anti-rabbit 594(A21207)	Invitrogen
Goat anti-mouse 488 (A11001)	Invitrogen
Donkey anti-rabbit 488 (A21206)	Invitrogen
Donkey anti-rabbit 405(ab175651)	Abcam
Goat anti-mouse horseradish peroxidase (170-6516)	Bio-Rad
Goat anti-rabbit horseradish peroxidase (170-65-15)	Bio-Rad

Table 3.2. Reagent supplier addresses

Supplier	Location
Abcam	Cambridge, UK
Agilent	Santa Clara, California, USA
Bio-Rad	Mississauga, Ontario, Canada
Denville Scientific	Holliston, Massachusetts, USA
Difco	Franklin Lakes, New Jersey, USA
EMD	Chicago, Illinois, USA
Enzo	Farmingdale, New York, USA
Fisher	Waltham, Massachusetts, USA
Fitzgerald	Acton, Massachusetts, USA

Gibco	Waltham, Massachusetts, USA
Invitrogen	Waltham, Massachusetts, USA
Lonza	Basel, Switzerland
Polysciences	Washington, Pennsylvania, USA
Sigma Aldrich	St. Louis, Missouri, USA
Stratagene	San Diego, California, USA
Thermo Pierce	Waltham, Massachusetts, USA

Table 3.3. cDNA and expression vectors

cDNA	Vector	Promoter
FL-DGAT2	pcDNA3	CMV
FL-DGAT2 3C Mutants 1-4	pcDNA3	CMV
FL-DGAT2 K-to-R Mutants	pcDNA3	CMV
FL-Lys-less-DGAT2	pcDNA3	CMV
FL-Lys-less-DGAT2 R-to-K Mutants	pcDNA3	CMV
FL-Lys-less-DGAT2-HA	pcDNA3	CMV
Lys-less-DGAT2-HA	pcDNA3	CMV
Lys-Less-DGAT2 (untagged)	pcDNA3	CMV
FL-DGAT2/Δ2-30	pcDNA3	CMV
FL-DGAT2/Δ30-67	pcDNA3	CMV
FL-DGAT2/Δ66-115	pcDNA3	CMV
FL-DGAT2/Δ2-119	pcDNA3	CMV
FL-DGAT2/Δ327-388	pcDNA3	CMV
FL-DGAT2/Δ2-35	pcDNA3	CMV
FL-DGAT2/HA-insert	pcDNA3	CMV
Myc-DGAT2	pcDNA3	CMV
DGAT2-HA	pcDNA3	CMV
LacZ	pcDNA3	CMV
FL-Lipin1	pcDNA3	CMV
FL-MGAT2	pCMV6	CMV
MGAT2-Myc-FL	pCMV6	CMV
MGAT2-Myc	pCMV6	CMV
FL-MGAT3	pcDNA3.1+	CMV
MGAT3-Myc-FL C265Y	pCMV6	CMV
HA-Ubiquitin	pRK5	CMV

Table 3.4. Mutagenic primers

Primer name	Primer sequence
FL-DGAT2 3C protease mutants	
Mutant 1 F	5'-CTGGAAGTTCTGTTTCAGGGGCCCAAGACCCTCATCGCCGCC-3'
Mutant1 R	5'-GGGCCCCTGAAACAGAACTTCCAGATCATCATCATCTTTGTAAT CTCCCATGC-3'
Mutant 2 F	5'-CTGGAAGTTCTGTTTCAGGGGCCCCTGGTGAAGACACACAACC TG-3'
Mutant 2 R	5'-GGGCCCCTGAAACAGAACTTCCAGCTGGATGGGAAAGTAGTCT CG-3'
Mutant 3 F	5'-CTGGAAGTTCTGTTTCAGGGGCCCGCTGATCTGGTTCCCACTTA TTCCTTTGG-3'
Mutant 3 R	5'-GGGCCCCTGAAACAGAACTTCCAGTCCATGGCGCAGGGCCAGC TT C-3'
Mutant 4 F	5'-CTGGAAGTTCTGTTTCAGGGGCCCCCCCAAGCTGGAGCACCCGA CC-3'
Mutant 4 R	5'-GGGCCCCTGAAACAGAACTTCCAGGACAGTGATGGGCTCCCCC AC-3'
FL-DGAT2 Lys-to-Arg mutants	
K2R F	5'-GGAGATTACAAAGATGATGATGATAGGACCCTCATCGCCGCC-3'
K2R R	5'-GGCGGCGATGAGGGTCCTATCATCATCATCTTTGTAATCTCC-3'
K26, 28R F	5'-GCCCGCAGCGAAAACAGGAATAGAGGATCTGCCCTG-3'
K26, 28R R	5'-CAGGGCAGATCCTCTATTCCTGTTTTCGCTGCGGGC-3'
K63, 66R F	5'-GGCTCAACAGATCTAGGGTGGAAAGACAGCTGCAGGTC-3'
K63, 66R R	5'-GACCTGCAGCTGTCTTTCCACCCTAGATCTGTTGAGCC-3'
K118, 119R F	5'-GACTGGAACACGCCCAGGAGAGGTGGCAGGAGATCGC-3'
K118, 119R R	5'-GCGATCTCCTGCCACCTCTCCTGGGCGTGTTCCAGTC-3'
K146R F	5'-CCAGCTGGTGAGGACACACAACCTGCTG-3'
K146R R	5'-CAGCAGGTTGTGTGTCCTCACCAGCTGG-3'
K183, 184R F	5'-GCTACTGAAGTCAGCAGGAGGTTTCCTGGCATAAGGCCC-3'
K183, 184R R	5'-GGGCCTTATGCCAGGAAACCTCCTGCTGACTTCAGTAGC-3'
K227R F	5'-GACTACTTGCTCTCCAGGAATGGGAGTGGC-3'
K227R R	5'-GCCACTCCCATTCCTGGAGAGCAAGTAGTC-3'
K286, 301, 302, 305R F	5'-GTATACAGGCAGGTGATCTTTGAGGAGGGTTCCTGGGGCCGAT GGGTCCAGAGGAGGTTCCAGAGGTATATTGG-3'
K286, 301, 302, 305R R	5'-CCAATATACCTCTGGAACCTCCTCTGGACCCATCGGCCCCAGG AACCCTCCTCAAAGATCACCTGCCTGTATAC-3'
K251R F	5'-CCCTGAGCTCCATGCCTGGCAGGAACGCAGTCACCC-3'
K251R R	5'-GGGTGACTGCGTTCCTGCCAGGCATGGAGCTCAGGG-3'
K257R F	5'-CGCAGTCACCCTGAGGAACCGC-3'

K257R R	5'-GCGGTTCCTCAGGGTGACTGCG-3'
K260R F	5'-CCGCAGAGGCTTTGTG-3'
K260R R	5'-CACAAAGCCTCTGCGG-3'
K264R F	5'-GGCTTTGTGAGGCTGGCCCTGCGCC-3'
K264R R	5'-GGCGCAGGGCCAGCCTCACAAAGCC-3'
K332, 346, 353R F	5'-GCCCTACTCCAGGCCCATCACCACCGTCGTGGGGGAGCCCATC ACTGTCCCCAGGCTGGAGCACCCGACCCAGAGAGACATCGACC-3'
K332, 346, 353R R	5'-GGTCGATGTCTCTCTGGGTCGGGTGCTCCAGCCTGGGGACAGT GATGGGCTCCCCCACGACGGTGGTGATGGGCCTGGAGTAGGGC-3'
K368, 374, 376R F	5'-GGAGGCCCTGGTGAGGCTCTTTGACAATCACAGGACCAGATTT GGCCTTCC-3'
K368, 374, 376R F	5'-GGAAGGCCAAATCTGGTCCTGTGATTGTCAAAGAGCCTCACCA GGGCCTCC-3'
FL-Lys-less-DGAT Arg-to-Lys mutants	
R2K F	5'-GGAGATTACAAAGATGATGATGATAAGACCCTCATCGCCGCC-3'
R2K R	5'-GGCGGCGATGAGGGTCTTATCATCATCATCTTTGTAATCTCC-3'
R26, 28K F	5'-GCCCGCAGCGAAAACAAGAATAAAGGATCTGCCCTG-3'
R26, 28K R	5'-CAGGGCAGATCCTTTATTCTTGTTTTCGCTGCGGGC-3'
R63, 66K F	5'-GGCTCAACAGATCTAAGGTGGAAAAACAGCTGCAGGTC-3'
R63, 66K R	5'-GACCTGCAGCTGTTTTTCCACCTTAGATCTGTTGAGCC-3'
R118, 119K F	5'-GACTGGAACACGCCCAAGAAAGGTGGCAGGAGATCGC-3'
R118, 119K R	5'-GCGATCTCCTGCCACCTTTCTTGGGCGTGTTCCAGTC-3'
R146K F	5'-CCAGCTGGTGAAGACACACAACCTGCTG-3'
R146K R	5'-CAGCAGGTTGTGTGTCTTCACCAGCTGG-3'
R183, 184K F	5'-GCTACTGAAGTCAGCAAGAAGTTTCCTGGCATAAGGCCC-3'
R183, 184K R	5'-GGGCCTTATGCCAGGAAACTTCTTGCTGACTTCAGTAGC-3'
R227K F	5'-GACTACTTGCTCTCCAAGAATGGGAGTGGC-3'
R227K R	5'-GCCACTCCCATTCTTGGAGAGCAAGTAGTC-3'
R251, 257, 260,264K F	5'-CCTGGCAAGAACGCAGTCACCCTGAAGAACCGCAAAGGCTTT GTGAAGCTGGCC-3'
R251, 257, 260,264K R	5'-GGCCAGCTTCACAAAGCCTTTGCGGTTCTTCAGGGTGACTGCGTTCTTGCCAGG-3'
R286K F	5'-GAGGTATACAAGCAGGTGATCTTTGAGGAGGG-3'
R286K R	5'-CCCTCCTCAAAGATCACCTGCTTGTATACCTC-3'

R301K F	5'-CCGATGGGTCCAGAAGAGGTTCCAGAGG-3'
R301K R	5'-CCTCTGGAACCTCTTCTGGACCCATCGG-3'
R302K F	5'-CCGATGGGTCCAGAGGAAGTTCCAGAGG-3'
R302K R	5'-CCTCTGGAACTTCCTCTGGACCCATCGG-3'
R305K F	5'-GGAGGTTCCAGAAGTATATTGGTTTCGCCCCC-3'
R305K R	5'-GGGGGCGAAACCAATATACTTCTGGAACCTCC-3'
R332K F	5'-GCCCTACTCCAAGCCCATCACCACC-3'
R332K R	5'-GGTGGTGATGGGCTTGGAGTAGGGC-3'
R346K F	5'-CCCATCACTGTCCCCAAGCTGGAGCACCCG-3'
R346K R	5'-CGGGTGCTCCAGCTTGGGGACAGTGATGGG-3'
R353K F	5'-CCGACCCAGAAAGACATCGACCTG-3'
R353K R	5'-CAGGTCGATGTCTTTCTGGGTCGG-3'
R368K F	5'-GAGGCCCTGGTGAAGCTCTTTGAC-3'
R368K R	5'-GTCAAAGAGCTTCACCAGGGCCTC-3'
R374K F	5'-GACAATCACAAGACCAGATTTGGCC-3'
R374K R	5'-GGCCAAATCTGGTCTTGTGATTGTC-3'
R376K F	5'-GACAATCACAGGACCAAATTTGGCC-3'
R376K R	5'-GGCCAAATTTGGTCCTGTGATTGTC-3'
FL-Lys-less-DGAT tag change	
Remove N-Term FL F	5'-CATCTAGATGACCCAATATG_AGGACCCTCATCG-3'
Remove N-Term FL R	5'-CGATGAGGGTCCT_CATATTGGGTCATCTAGATG-3'
Add C-Term HA F	5'-GGATACCCATACGATGTTCCAGATTACGCTTGAGACCCAATAT CGGATCCCGGGC-3'
Add C-Term HA R	5'-AGCGTAATCTGGAACATCGTATGGGTATCCGTTCACCTCCAGC ACCTCAGTCTC-3'

3.2 Site directed mutagenesis

Mutations and epitope tags were introduced into cDNA by PCR with PfuUltra DNA polymerase. Mutagenic primers are detailed in Table 3.4. PCR reactions were conducted in a final volume of 50 µL containing the following reagents: 29 µL cross-linked ultrapure water, 5 uL 10x Pfu buffer, 0.2 mM dNTPs, 10% dimethyl sulfoxide (DMSO), 125 ng of each mutagenic primer (forward and reverse), 50 ng of template DNA and 1 µL of PfuUltra DNA

polymerase. The general thermal cycler protocol used was: 1) 1 min. at 95°C. 2) 18 cycles: 50 sec. at 95°C, 50 sec. at 60°C and 1 min./kilobase at 68°C. 3) 7 min. at 68°C. Methylated DNA was digested with 20 units of DpnI for 2 h at 37°C.

FL-Lys-less-DGAT2, in which all of 25 DGAT2 lysines were mutated to arginine, was manufactured by GenScript.

The cDNA of all constructs was verified by sequencing prior to use.

3.3 Bacterial strains and media preparations

XL10-Gold Ultracompetent *E. coli* were used for the amplification of PCR products following mutagenesis. Transformation was conducted according to manufacturers instructions. Transformation required the use of NZY^+ broth consisting of 10 g NZ-amine, 5 g yeast extract and 5 g NaCl in 1 L of double-distilled water. The broth was adjusted to pH 7.5 and autoclaved for 20 min at 15 psi. Prior to use, filter sterilized components were added at final concentrations of: 12.5 mM $MgCl_2$, 12.5 mM $MgSO_4$ and 0.4% glucose. The bacterial transformation mixture was plated onto Luria-Bertani (LB) broth agar plates. LB broth, consisting of 10 g tryptone, 5 g yeast extract and 10 g of NaCl in 1 L of double-distilled water, was supplemented with 15 g of agar and autoclaved as previously described. Once cooled, ampicillin was added at 100 μg/mL and the LB agar solution was transferred into petri dishes.

DH5α Competent *E. coli* were used for bulk amplification of plasmid DNA. Transformation was conducted according to manufacturer specifications. Transformation required the use of LB broth. The bacterial transformation mix was again transferred to LB agar plates containing ampicillin at a final concentration of 100 μg/mL. Colonies were cultured in Terrific broth, composed of 2.4 g tryptone, 4.8 g yeast extract and 0.8 mL glycerol - brought to a final volume of 200 mL with double-distilled water. The solution was autoclaved for 20 min at 15 psi, before the addition of a 20 mL solution containing 0.17 M KH_2PO_4 and 0.72 M K_2HPO_4. Ampicillin was added at a final concentration of 100 μg/mL.

3.4 Mammalian cell culture

HEK-293T and COS-7 (American Type Culture Collection) cells were grown in Dulbecco's modified eagle's medium (DMEM) supplemented with 10% fetal bovine serum (FBS) in a 37°C incubator (5% CO_2). Cells were grown in the presence of 1x antibiotic-

antimycotic. Triacylglycerol synthesis and lipid droplet formation was stimulated by treatment with 0.5 mM oleic acid complexed to 0.67% fatty acid-free bovine serum albumin (BSA).

3.5 Cell transfection

For HEK-293T transfection, 20 μg of plasmid DNA was added to 430 μL of 0.15 M NaCl and 120 uL of 0.1% polyethylenimine (pH 7.0). For transfection of COS-7 cells, polyethylenimine volume was reduced to 60 μL. The transfection solution was incubated 10 min. at room temperature prior to drop-wise addition to a 100 mm culture dish (containing 10 mL of media) with cells at ~50% confluency. After 4 h, cells were washed with phosphate buffered saline (PBS) and re-fed fresh media. Experiments were conducted 20-48 h post-transfection.

3.6 Immunoprecipitation

FLAG or human influenza hemagglutinin (HA) epitope containing proteins were expressed in HEK-293T cells. Approximately 20 h post-transfection, cells were washed with PBS, pelleted at 600 x *g* for 2 min. and resuspended in a 0.5% CHAPS, 1x PBS (pH 7.4) solution. Cells were disrupted by 20 passages through a 27 gauge needle. Insoluble material was pelleted at 20,800 x g for 10 min. and solubilized material transferred to a new tube. Samples were incubated with 10 μL of anti-FLAG or anti-HA agarose in 0.5% CHAPS, 1x PBS (pH 7.4) in a final volume of ~1mL and rotated for 2-3 h at room temperature. Alternatively, samples were rotated overnight at 4^{o}C. Agarose was pelleted for 30 sec. at 5000 x g and washed three times with 0.5% CHAPS in 1x PBS (pH 7.4). FLAG-tagged proteins were eluted from beads by incubation with 3x FLAG peptide or by boiling in an equal volume of 2x SDS-PAGE sample buffer containing 5% β-mercaptoethanol. HA-tagged proteins were displaced by boiling in an equal volume of 2x SDS-PAGE sample buffer (+5% β-mercaptoethanol).

Some experiments were conducted using total cell extracts in a solution of 8 M Urea, 1x PBS (pH 7.4). Immunoprecipitation of epitope tagged proteins was carried out at a final urea concentration of 1 M urea, 1x PBS (pH 7.4). Urea was removed from immunoprecipitates through washing in 1x PBS. Tagged proteins were eluted by boiling in 2x SDS-PAGE sample buffer containing 5% β-mercaptoethanol.

3.7 3C protease assay

Approximately 20 h post-transfection, cells were washed twice with PBS prior to harvest by scraping. Cells were pelleted at 600 x *g* for 2 min. and resuspended in a 0.5% CHAPS, 1x PBS (pH 7.4) solution. Cells were disrupted by 20 passages through a 27 gauge needle. Insoluble material was pelleted at 20,800 x g for 10 min. and solubilized material was transferred to a new tube. An aliquot was taken to determine protein concentration. Immunoprecipitation was conducted in a solution of 0.5% CHAPS in 1x PBS, using anti-FLAG agarose as described in section 3.6. Total cell extracts or anti-FLAG immunoprecipitates were incubated with 5 units of human rhinovirus (HRV) 3C protease for 16 h at 4^{o}C. Anti-FLAG agarose and bound N-terminal fragments were pelleted by centrifugation at 600 x g for 2 min., the supernatant fraction containing C-terminal fragments was transferred to a fresh tube. An equal volume of 2x SDS-PAGE sample buffer (+5% β-mercaptoethanol) was added to total cell extracts as well as to pelleted and supernatant fractions of the immunoprecipitation. Samples were boiled for 5 min. The pelleted immunoprecipitation fraction was centrifuged 20,800 x g for 1 min. to pellet anti-FLAG agarose, and the supernatant, containing displaced N-terminal fragments, was transferred to a fresh tube. Samples were analyzed by SDS-PAGE and immunoblotting.

3.8 Standard protein degradation assay

Approximately 20 h post-transfection, cells were washed with PBS and re-fed 100 μg/mL cycloheximide (CHX) diluted in DMEM (+10% FBS). Time zero samples were harvested immediately at the onset of CHX incubation and received no treatment. Samples were harvested at various time intervals of CHX treatment. Cells were washed twice with PBS prior to harvest by scraping. Cells were pelleted at 600 x *g* for 2 min. and suspended in 8M urea, 1x PBS (pH 7.4). Cells were disrupted by 20 passages through a 25 gauge needle followed by 15 passages through a 27 gauge needle. Insoluble material was pelleted at 20,800 x g for 10 min. and solubilized material was transferred to a new tube. Samples were incubated in 2x SDS-PAGE sample buffer (+5% β-mercaptoethanol) for 30 min. at 37^{o}C. Samples were not boiled due to the presence of urea. Protein degradation was observed by SDS-PAGE and immunoblotting.

3.9 Protein degradation assay under lipogenic conditions

HEK-293T cells were transfected with FL-DGAT2. Four hours after transfection, cells were re-fed DMEM (+10% FBS) in the presence or absence of 0.5 mM oleic acid. Approximately 18 h later, cells were washed with PBS and re-fed in the presence or absence of 0.5 mM oleic acid with 100 μg/mL CHX in DMEM (+10% FBS). Time zero samples were harvested immediately after the 18 h incubation and received no CHX. Cells were washed twice with PBS and harvested by scraping after 0-6 h of CHX treatment. Cells were pelleted at 600 x g for 2 min. and resuspended in 0.5% Triton X-100, 1x PBS (pH 7.4). Cells were disrupted by 20 passages through a 27 gauge needle. Insoluble material was pelleted at 20,800 x g for 10 min. and solubilized material transferred to a new tube. An aliquot was removed for lipid extraction (3.10). Samples were boiled in 2x SDS-PAGE sample buffer with 5% β-mercaptoethanol for 5 min. Protein degradation was observed by SDS-PAGE and immunoblotting.

Alternatively, lipogenesis was stimulated with insulin treatment. Four hours post-transfection, cells were re-fed DMEM (+10% FBS) in the presence or absence of 5 μg/mL insulin. One hour later, cells were washed with PBS and re-fed in the presence or absence of 5 μg/mL insulin with 100 μg/mL CHX in DMEM (+10% FBS). Time zero samples were harvested immediately after the 18 h incubation and received no CHX. Cells were washed twice with PBS and harvested by scraping after 0-6 h of CHX treatment. Cells were pelleted at 600 x g for 2 min. and resuspended in 8 M urea, 1x PBS (pH 7.4). Cells were disrupted by 20 passages through a 25 gauge needle, followed by 15 passages through a 27 gauge needle. Insoluble material was pelleted at 20,800 x g for 10 min. and solubilized material was transferred to a new tube. Samples were incubated in 2x SDS-PAGE sample buffer with 5% β-mercaptoethanol for 30 min. at 37^{o}C. Samples were not boiled due to the presence of urea. Protein degradation was observed by SDS-PAGE and immunoblotting.

3.10 Lipid extraction

Sample total cell extracts prepared in a buffer of 0.5% Triton X-100, 1x PBS (pH 7.4) were brought to a final volume of 1 mL with double-distilled water in 16 x 100 mm glass tubes. Four mL of $CHCl_3$:MeOH (2:1, v/v) was added and samples were vortexed for 30 sec. prior to centrifugation at 775 x g for 5 min. The aqueous supernatant was discarded and the lower

organic phase was evaporated. Air-dried samples were resuspended in 65 μL of $CHCl_3$:MeOH (2:1, v/v), vortexed and applied to a channeled silica gel G60 thin layer chromatography plate. The plate was developed in a hexane:ethyl ether:acetic acid (80:20:1, v/v/v) solvent system. Plates were air-dried and then briefly submerged in a solution of 10% cupric sulfate (w/v) and 8% phosphoric acid. Lipids were observed by charring at approximately 180^{o}C until bands appeared. Pictures were taken using a VersaDoc 4000 molecular imaging system (Bio-Rad Laboratories, Inc.) and Quantity One software (Bio-Rad Laboratories, Inc.).

3.11 Co-immunoprecipitation

Approximately 20 h post-transfection, HEK-293T cells were washed with PBS. Cells were pelleted at 600 x *g* for 2 min. and resuspended in a 0.5% CHAPS, 1x PBS (pH 7.4) solution. To reduce non-specific interactions, a detergent to protein ratio of approximately 10:1 was used, representing the critical micelle concentration for CHAPS. Cells were disrupted by 20 passages through a 27 gauge needle. Insoluble material was pelleted at 20,800 x g for 10 min. and solubilized material was transferred to a new tube. An aliquot was taken to determine protein abundance. The detergent to protein ratio was then adjusted to 10:1. Samples were incubated with 10 μL of anti-FLAG or anti-HA agarose in 0.5% CHAPS, 1x PBS (pH 7.4) at a final volume of ~1mL and rotated for 2-3 h at room temperature. Alternatively, samples were rotated overnight at 4^{o}C. Anti-FLAG agarose was pelleted for 30 sec. at 5000 x g and washed three times with 0.5% CHAPS, 1x PBS (pH 7.4). Proteins were eluted from beads by boiling in an equal volume of 2x SDS-PAGE sample buffer containing 5% β-mercaptoethanol.

3.12 Isolation of crude mitochondria and lipid droplet fractions

Approximately 20 h post-transfection, HEK-293T were washed with PBS. Cells were pelleted at 600 x *g* for 2 min. and resuspended in 1x PBS (pH 7.4). Cells were disrupted by 20 passages through a 27 gauge needle followed by centrifugation 2 min. at 1000 x g to pellet cellular debris and nuclei. The supernatant was centrifuged for 10 min. at 10,000 x g (4^{o}C) to pellet crude mitochondria (containing mitochondria and mitochondria-associated membranes). Crude mitochondria were resuspended in a solution of 50 mM Tris-HCl (pH 7.4), 250 mM sucrose.

The supernatant obtained following the 10,000 x g centrifugation was adjusted to 20% sucrose and dispensed onto a 1 mL sucrose cushion of 60 % sucrose, 20 mM Tris-HCl (pH 7.4), 1 mM EDTA. Six mL of 5% sucrose, 20 mM Tris-HCl (pH 7.4), 1 mM EDTA was then layered on top of the sample; 20 mM Tris-HCl (pH 7.4) 1 mM EDTA was added until the tube was nearly brimmed. The sample was then centrifuged at 200,000 x g for 30 min (4^{o}C). The floating fat layer, containing lipid droplets, was isolated and diluted with 20 mM Tris-HCl (pH 7.4), 1 mM EDTA.

3.13 SDS-PAGE and Western blotting

Samples were incubated in an equal volume of 2x SDS sample buffer (+5% β-mercaptoethanol) and boiled for 5 min. (unless indicated otherwise), to denature and solubilize proteins. SDS-PAGE was carried out on a polyacrylamide gel (8 – 12%) in a running buffer of 25 mM Tris-HCl, 192 mM glycine, and 0.1 % (w/v) SDS at approximately 160 volts for 1 h. Proteins were transferred to a polyvinylidene difluoride membrane in a buffer of 62 mM boric acid (pH 8.0) at 360 mA for a period of 1.5 h. Alternatively, transfer was conducted overnight at 25 volts and 4^{o}C. Membranes were blocked for 30 min. in 10 % skim milk powder (w/v), 1x PBST to reduce non-specific binding. Primary antibody was diluted in 1x PBST (1:50 – 4000). Membranes were incubated with primary antibody for approximately 2 h at room temperature or overnight at 4^{o}C. Membranes were incubated with species-specific secondary antibody conjugated to horseradish peroxidase (1:10,000) for 40 min. at room temperature. Proteins were detected by incubation in a solution of 100 mM Tris-HCl (pH 8.6), 1.25 mM luminol, 0.225 mM p-coumaric acid and 9.0 x10^{-3} % (w/w) hydrogen peroxide for 1 min. and exposed to Hyblot Cl film.

3.14 DGAT activity assay

The activity assay reaction mixture consisted of: 100 mM Tris-HCl (pH 7.6), 20 mM $MgCl_2$, 0.625 mg/mL of BSA (fatty acid free), 200 μM 1,2 dioleoyl-sn-glycerol, 25 μM N-[(7-nitro-2-1,3-benzoxadiazol-4-yl)-methyl]amino (NBD)-palmitoyl CoA, 100 mM sucrose, brought to a final volume of 150 μL with double-distilled water. Aliquots of reaction mixture were pre-heated at 37^{o}C for 2 min. The reaction was initiated upon the addition 50 μg of total cell extract (diluted to 1 μg/μL in 50 mM Tris-HCl pH 7.6, 250 mM sucrose) and incubated at

37°C for 10 min. The reaction was terminated by the addition of 4 mL $CHCl_3$/methanol (2:1, v/v) and mixed by brief vortex. Water, at a volume of 800 µL was added, followed by a 10 sec. vortex at top speed. Samples were centrifuged at room temperature for 5 min. at 775 x g. The upper aqueous layer was aspirated followed by air-drying of the organic phase. Sixty-five µL of $CHCl_3$ was added to each sample tube prior to brief vortex and application to a channeled 20 x 20 cm thin layer chromatography plate. The plate was developed in a solvent system of ethyl ether/hexane/methanol/acetic acid (55:45:5:1, v/v/v/v). The plate was then allowed to air dry for 1 h prior to NBD-triacylglycerol quantification using a VersaDoc 4000 molecular imaging system (Bio-Rad Laboratories, Inc.) and Quantity One software (Bio-Rad Laboratories, Inc.).

3.15 Immunofluorescence microscopy

COS-7 cells were cultured in 6-well plates containing glass coverslips. Cells were fixed for 10 min. in 4% paraformaldehyde, 1x PBS (pH 7.4) and permeabilized for 5 min. in 0.2% Triton X-100, 1x PBS (pH 7.4). Blocking, in 3% BSA, 1x PBS (pH7.4) for 5 min. was conducted to reduce non-specific binding. Primary antibodies specific to protein or epitope tags were diluted (1:50 – 300) and applied to cells for 1 h. Fluorescent secondary antibodies (1:200) and neutral lipid stain BODIPY 493/503 (1:50-100) were incubated with samples for 30 min. All incubation steps were carried out at 37°C in a humidity chamber. Images were obtained using Leica SP5 and Zeiss LSM700 laser scanning confocal microscopes. Image processing was conducted using ImageJ

3.16 Lipid droplet counting and size analysis

The size and number of lipid droplets were assessed in COS-7 cells expressing DGAT2 or DGAT2 mutant constructs. Cells were prepared for immunofluorescence microscopy (3.15) and images were taken with a Leica SP5 laser scanning confocal microscope. Lipid droplet analysis was conducted using ImageJ analysis software. All analysis was conducted on fourteen cells per construct; lipid droplets with an area of ≥ 0.2 micron^2 were counted.

Variation among groups was analyzed using a one-way analysis of variance test and Tukey test.

3.17 Proximity ligation assay (PLA)

Approximately 20 h post transfection, COS-7 cells were fixed and permeabilized as outlined under section 3.15. Blocking was conducted for 30 min at 37^{o}C in a pre-heated humidity chamber in a solution of 3% BSA, 1x PBS (pH 7.4). Primary antibodies were diluted to 1:50 – 1:300 in 3% BSA, 1x PBS (pH 7.4). Cells were incubated with primary antibody for 30 min at 37^{o}C in a pre-heated humidity chamber. Duolink® *in situ* proximity ligation assay was conducted according to manufacturer's instructions. Cell nuclei were visualized with DAPI containing mounting medium. Images were obtained using Leica SP5 and Zeiss LSM700 laser scanning confocal microscopes. Image processing was conducted with ImageJ

In some experiments, cells were "co-stained" with protein or epitope specific primary antibody. Chemical staining of lipid droplets by BODIPY 493/503 was also carried out. This was done after the completion of the proximity ligation assay protocol and was conducted as described in section 3.15.

3.18 Protein identification by mass spectrometry

HEK-293T cells were transfected with FL-DGAT2 or control Myc-DGAT2 and incubated for approximately 18 hours in 0.5 mM oleic acid to stimulate lipogenesis. Cells were harvested in 0.5% CHAPS, 1x PBS (pH 7.4) and the detergent to protein ratio adjusted to 10:1. Co-immunoprecipitations were conducted using anti-FLAG agarose beads in a 0.5% CHAPS, 1x PBS (pH 7.4) solution. Proteins were dissociated from anti-FLAG agarose by boiling in 2x SDS-PAGE sample buffer (+5% β-mercaptoethanol). Sample preparation and analysis by mass spectrometry was conducted in collaboration with Dr. George Katselis' Lab at the University of Saskatchewan. Samples were buffered in 100 mM ammonium bicarbonate prior to addition of an equal volume of tetrafluoroethylene. Samples were then reduced in 10 mM dithiothreitol and alkylated in 55 mM indole-3-acetic acid. Tetrafluoroethylene was removed by SpeedVac and proteins were precipitated using acetone. The precipitant was re-suspended in ammonium bicarbonate buffer and trypsinized before drying and re-suspension in 0.1% formic acid in water/acetonitrile (97:3) for liquid chromatography-tandem mass spectrometry (LC-MS/MS). Samples were analyzed by 6550 iFunnel Q-TOF (Agilent Technologies) equipped with a chip cube interface and with 1260 infinity nano and cap pumps. The liquid chromatography separation of peptides was carried out on a chip consisting of a 160 nL trapping column and 75

μL × 150 mm analytical column. Columns were packed with Zorbax 300SB-C-18 5 μm using a gradient solvent system comprised of 0.1% formic acid in water and 0.1% formic acid in acetonitrile. Data extractor, SpectrumMill Proteomics Workbench Version B.04.00.127 (Agilent Technologies) was used for identification of MS/MS spectra. Data were searched against the SWISS-PROT *Homo sapiens* database with fixed cysteine carbamidomethylation and variable methionine oxidation parameters.

CHAPTER 4: Identification of ubiquitinated residues on DGAT2

4.1. Introduction

DGAT2 regulation has not been extensively studied, especially at the post-translational level. Recent research has demonstrated that DGAT2 is rapidly degraded by the ubiquitin proteasome system via the ERAD pathway (Choi *et al.*, 2014).

DGAT2 is present on the long arm of chromosome 11 (11q13), a region linked to body mass index and obesity-associated phenotypes in humans (Saar *et al.*, 2003; Norman *et al.*, 1997; Pratley *et al.*, 1998; Watanabe *et al.*, 2000; Hirschhorn *et al.*, 2001). As the enzyme responsible for bulk triacylglycerol synthesis, it is reasonable to hypothesize that genomic variance in DGAT2 could correlate with predisposition or resistance to elevated adiposity and related conditions. Currently, studies have not found a link between DGAT2 genetic variants and total body fat in humans (Friedel *et al.*, 2007). However, a single nucleotide polymorphism (SNP), rs1944438, has been linked to liver fat levels (Kantartzis *et al.*, 2009). Additionally, DGAT2 SNPs have been found to affect fat deposition in pigs (Yin *et al.*, 2012; Renaville *et al.*, 2015).

We were interested in identifying ubiquitinated residues of DGAT2 responsible for modulating DGAT2 destruction. If SNPs are present at or surrounding ubiquitin acceptor sites, the turnover rate of DGAT2 could be altered, potentially affecting triacylglycerol synthesis. There are examples of proteins such as elongator complex protein 3 in *S. cerevisiae*, which is ubiquitinated at only 1 of its 42 lysine residues (Peng *et al.*, 2003). Other proteins contain multiple ubiquitinated lysines. In the case of yeast cell cycle regulating protein, SIC1, the six N-terminal-most of its twenty lysines are involved in ubiquitin dependent degradation. Interestingly, *in vitro*, the kinetics of degradation differ up to five-fold depending on the lysine chosen as acceptor (Petroski and Deshaies, 2003). Conversely, proteins such as cyclins A and B1 are also ubiquitinated on several lysine residues, yet degradation rate does not vary with the acceptor lysine (Fung *et al.*, 2005; Kirkpatrick *et al.*, 2006). As DGAT2 has 25 lysines, identifying residues important in dictating protein turnover was challenging and several different approaches were taken (see Fig 9.1 for the position of lysine residues in DGAT2 orthologs).

Attempts to examine endogenous DGAT2 turnover were unsuccessful. Numerous "in house" and commercial antibodies specific to N-terminal, C-terminal and internal regions were

evaluated. Cell lines tested include adipocytes (3T3-L1 and OP9), liver (HepG2) and kidney (HEK-293T). Other researchers recently reported degradation of endogenous DGAT2 by the ubiquitin-proteasome system in HEK-293T cells using a commercial antibody (Choi *et al.*, 2014). We have since acquired this antibody and do not believe that the band detected is endogenous DGAT2, as the size does not align with our positive control; a positive control was not included in the aforementioned study. For these reasons, an overexpression system was used for the characterization of DGAT2 post-translational regulation.

4.2. Results

4.2.1. The 3C protease assay was ineffective at identifying ubiquitinated DGAT2 residues

In order to map ubiquitinated lysine residues of DGAT2, we employed a method previously utilized in ubiquitin mapping of tumor protein p53 (p53) (Chan *et al.*, 2006). This approach requires the production of several mutants, each containing a single protease cleavage site. DGAT2 mutant constructs were produced through PCR based insertion of a 3C protease recognition site (amino acid sequence: LEVLFQGP). This method of ubiquitin mapping relies on the use of HRV 3C protease to cleave (between Gln and Gly residues) the inserted 3C sites in mutant constructs bound to anti-FLAG agarose. The agarose bound fraction is then pelleted while the fragment is released into the supernatant (Fig. 4.1). Through SDS-PAGE and immunoblotting, comparison of the ubiquitin signal generated from the N- and C-terminal fragments of each mutant can reveal ubiquitinated regions of the protein.

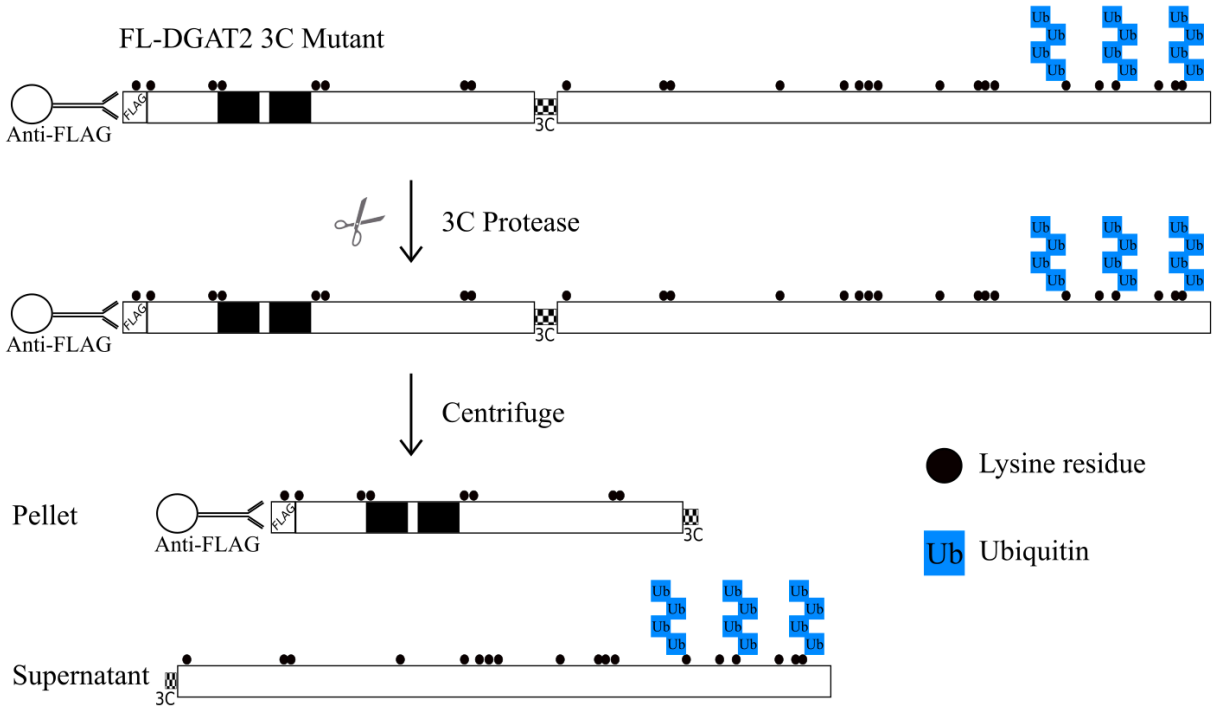

Figure 4.1. The 3C protease method – HEK-293T cells were transfected with FL-DGAT2 or a FL-DGAT2 3C mutant construct. Cells were harvested and subjected to immunoprecipitation with anti-FLAG agarose. Isolates bound to anti-FLAG agarose were incubated with HRV 3C protease prior to centrifugation. FL-DGAT2 and N-terminal fragments of 3C mutants bound to anti-FLAG agarose would be pelleted while fragments C-terminal of the cleave site would be present in the supernatant. Samples were analyzed by SDS-PAGE and immunoblotting with anti-FLAG and anti-DGAT2 (C-terminus) to demonstrate efficient cleavage. Subsequent immunoblotting with anti-ubiquitin antibody was conducted to identify ubiquitinated regions of DGAT2.

Four mutants were designed, each containing a single 3C encoding site inserted strategically into the DNA sequence - avoiding regions of predicted secondary structure (Fig. 4.2). HEK293T cells were transfected with 3C mutants (Section 3.5) and expression of all mutants was confirmed (Fig. 4.3A). Protease efficiency was confirmed on total cell extracts of FL-DGAT2 and FL-DGAT2 3C Mutant 1 transfected HEK-293T cells (Fig. 4.3B). Protease incubation with FL-DGAT2 3C Mutant 1 lysates resulted in cleavage of the 3C site and removal of the FLAG-tag as was detected by immunoblotting with anti-FLAG antibody. Conversely, incubation of the 3C protease with FL-DGAT2 lysates had no effect.

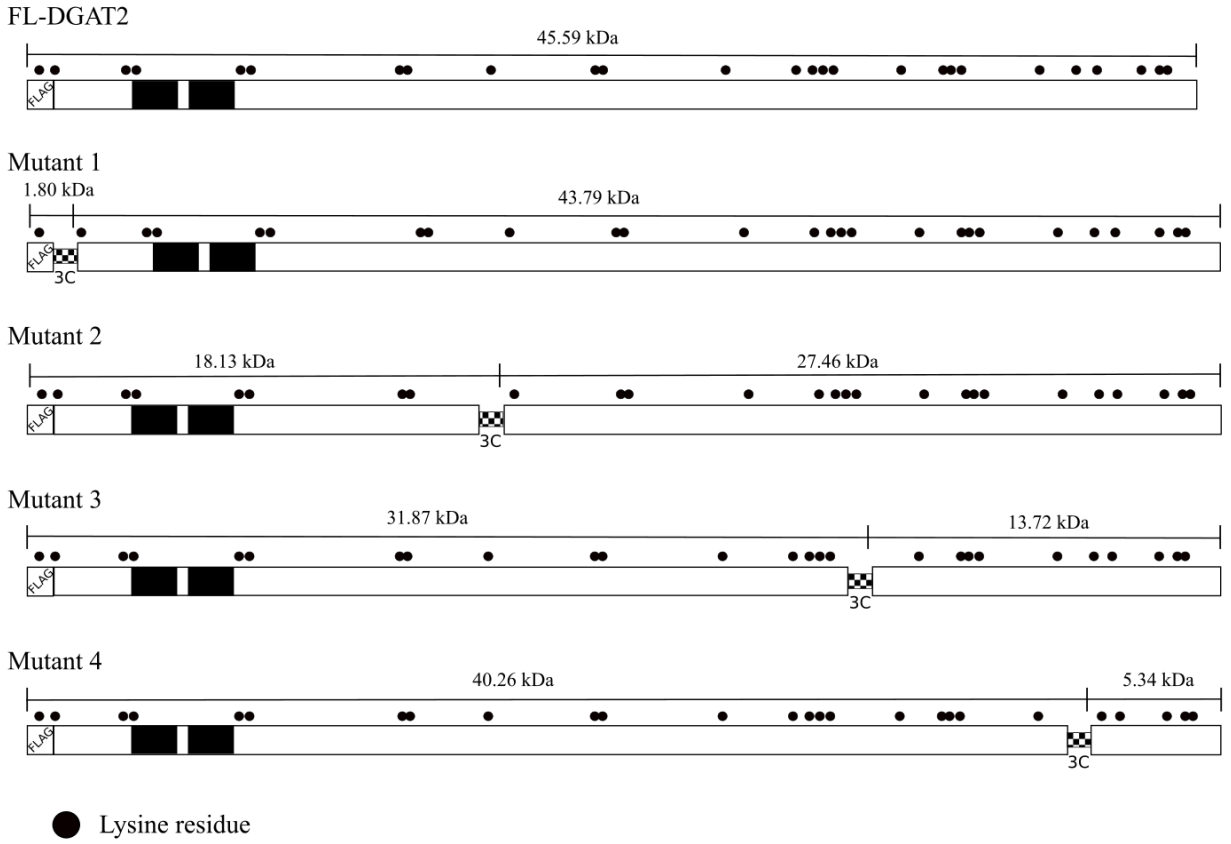

Figure 4.2. DGAT2 3C mutant constructs - Mutants were produced through PCR insertion of a 3C protease recognition sequence (LEVLFQGP), denoted "3C". Included are the positions of lysine residues within FL-DGAT2 and FL-DGAT2 mutants, as well as the size in kDa of N- and C-terminal fragments following cleavage by HRV 3C protease. Black bars represent the relative position of TMDs (amino acids 66–87 and 93–116).

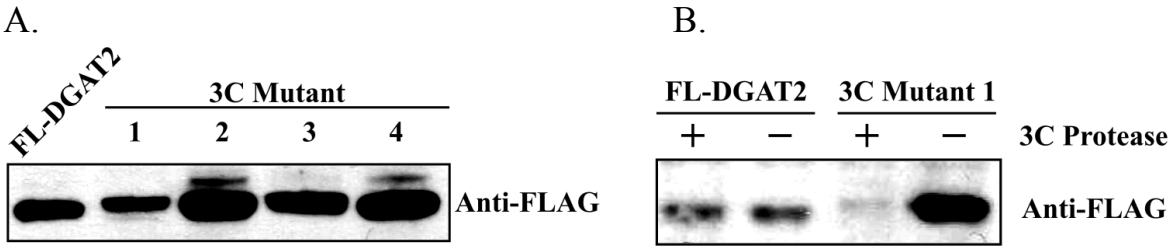

Figure 4.3. The 3C mutant 1 protease site is effectively cleaved in total cell extracts – HEK-293T cells were transfected with FL-DGAT2 or 3C mutants as indicated. *(A)* Mutant expression in total cell extracts was confirmed by SDS-PAGE and anti-FLAG immunoblotting. *(B)* Total cell extracts were incubated for 16 h in the presence or absence of HRV 3C protease to demonstrate protease efficiency and specificity. Samples were separated by SDS-PAGE and immunoblotted with anti-FLAG antibody.

In order to identify ubiquitinated regions of DGAT2, subsequent cleavage reactions were carried out on FL-DGAT2 and 3C mutants conjugated to anti-FLAG beads (Section 3.6). Following protease incubation, the pellet fraction (anti-FLAG beads and associated N-terminal bound protein fragment) was separated from the supernatant fraction (containing protein fragments C-terminal of the 3C cleavage site). Cleavage efficiency was evaluated by immunoblotting with an anti-DGAT2 C-terminus specific antibody. The ubiquitination status of N- and C-terminal fragments was to be evaluated with an anti-ubiquitin antibody. Experiments using 3C Mutants 1-3 in the presence of the protease yielded results of limited success (Fig. 4.4). It was noted that following protease incubation, C-terminal fragments of approximately the correct size were detected for all mutants. However, a significant amount of the construct was not cleaved as the full-size ~46 kDa band was readily detectable in the pellet fractions. In addition, the majority of the C-terminal fragment for each mutant was detected in the pellet rather than in the supernatant. Attempts to examine the ubiquitination of C-terminal fragments successfully released into the supernatant fractions were ineffective (data not shown), likely due to insufficient quantities of these ubiquitinated fragments to be detected by anti-ubiquitin immunoblotting. Numerous buffers, detergents, 3C protease brands and incubation conditions were evaluated in order to optimize this process, however, no conditions were effective at solubilizing 3C mutants while still remaining conducive to immunoprecipitation and protease digestion. For these reasons, this approach was abandoned.

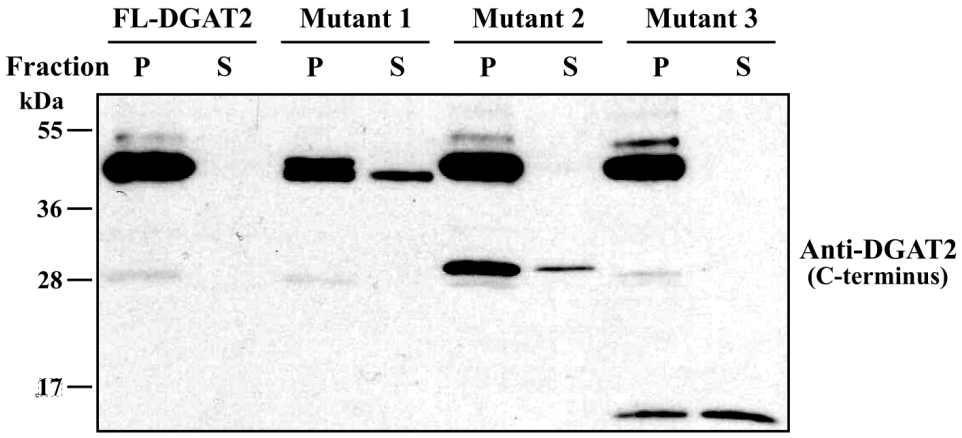

Figure 4.4. Cleavage of 3C mutant immunoprecipitates was incomplete – Immunoprecipitates derived from HEK293T cells transfected with FL-DGAT2 and FL-DGAT2 3C mutants 1-3 were incubated with HRV 3C protease for 16 h. Samples were centrifuged, separating the supernatant (S) from the pelleted (P) beads. Cleavage efficiency was evaluated by SDS-PAGE and immunoblotting with an anti-DGAT2 C-terminus specific antibody. Expected fragment sizes can be found in Fig. 4.2.

4.2.2. Conservative substitution of all DGAT2 lysine residues to arginine abolished DGAT2 degradation

We sought to confirm that degradation of DGAT2 is a lysine dependent process. While ubiquitin mediated degradation is most commonly associated with internal lysine residues, several proteins have been shown to be ubiquitinated at the N-terminal residue or at serine, threonine and/or cysteines (Johnson *et al.*, 1995; Tait *et al.*, 2007; Shimizu *et al.*, 2010). To address this possibility, we designed a FL-DGAT2 construct in which all lysine residues, with the exception of one lysine present in the middle of the FLAG-tag, were mutated to arginine (FL-Lys-less-DGAT2). The FL-DGAT2 and FL-Lys-less-DGAT2 constructs were transfected into HEK-293T cells and protein stability was assessed via CHX protein degradation assay (Section 3.8). CHX binds to the E-site of the 60S ribosomal subunit, inhibiting translation elongation and thereby protein synthesis (Schneider-Poetsch *et al.*, 2010; Klinge *et al.*, 2011; Pestova and Hellen, 2003). Protein degradation was examined by treating cells with CHX and harvesting at several time intervals. Samples were separated by SDS-PAGE and analyzed by immunoblotting (Fig. 4.5). We found that mutation of all twenty-five lysines was sufficient to abrogate DGAT2 degradation, suggesting that DGAT2 turnover is lysine dependent. Blotting for calnexin was conducted to demonstrate that assay conditions did not induce general protein degradation and that sample protein concentrations were consistent.

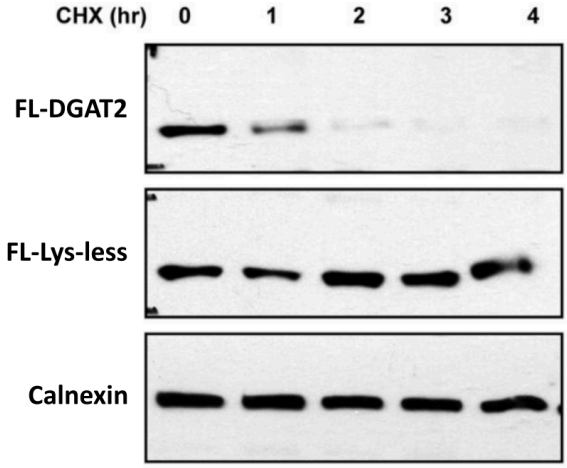

Figure 4.5. Lys-less-DGAT2 is not degraded - HEK-293T cells expressing either FL-DGAT2 or FL-Lys-less-DGAT2 were treated with CHX for 0–4 h. Samples were separated by SDS-PAGE and immunoblotted with anti-FLAG and anti-calnexin antibodies.

4.2.3. Lys-less-DGAT2 remained polyubiquitinated, likely through N-terminal ubiquitination

Having shown that Lys-less-DGAT2 is stable, we expected that it was no longer ubiquitinated. FL-DGAT2 and FL-Lys-less-DGAT2 were expressed in HEK-293T cells and isolated by anti-FLAG immunoprecipitation prior to SDS-PAGE and immunoblotting (Fig. 4.6A). Unexpectedly, Lys-less-DGAT2 was still ubiquitinated at a similar level to DGAT2. As the running buffer contained 5% β-mercaptoethanol, which would remove ubiquitin chains conjugated through a thioester linkage, cysteine ubiquitination would not be detected. To test for serine/threonine ubiquitination, immunoprecipitates were treated with sodium hydroxide (Fig. 4.6A). Ubiquitin linkage to these residues, via an oxyester bond, is sensitive to mild alkaline hydrolysis. Sodium hydroxide treatment had no effect on the intensity of the ubiquitin signal, ruling out conjugation at serine or threonine residues. As one lysine residue is remaining in the middle of the FLAG-tag, we generated FL-Lys-less-HA and Lys-less-HA (containing no lysines) constructs to examine whether this lysine is a potential ubiquitin acceptor site. The aforementioned constructs, along with untagged Lys-less-DGAT2, were transfected in HEK-293T cells and proteins were isolated with anti-FLAG agarose. Blotting for ubiquitin revealed signals of approximately equal intensity for FL-Lys-less-HA and Lys-less-HA while controls showed no ubiquitin signal (Fig. 4.6B). By process of elimination, ubiquitination through peptide bond formation at the α-NH_2 is the most likely scenario. As this modification does not appear to effect stability, its function is unknown. It is unclear whether N-terminal ubiquitination occurs on native DGAT2 or is merely an artifact related to the mutation of 25 lysine residues.

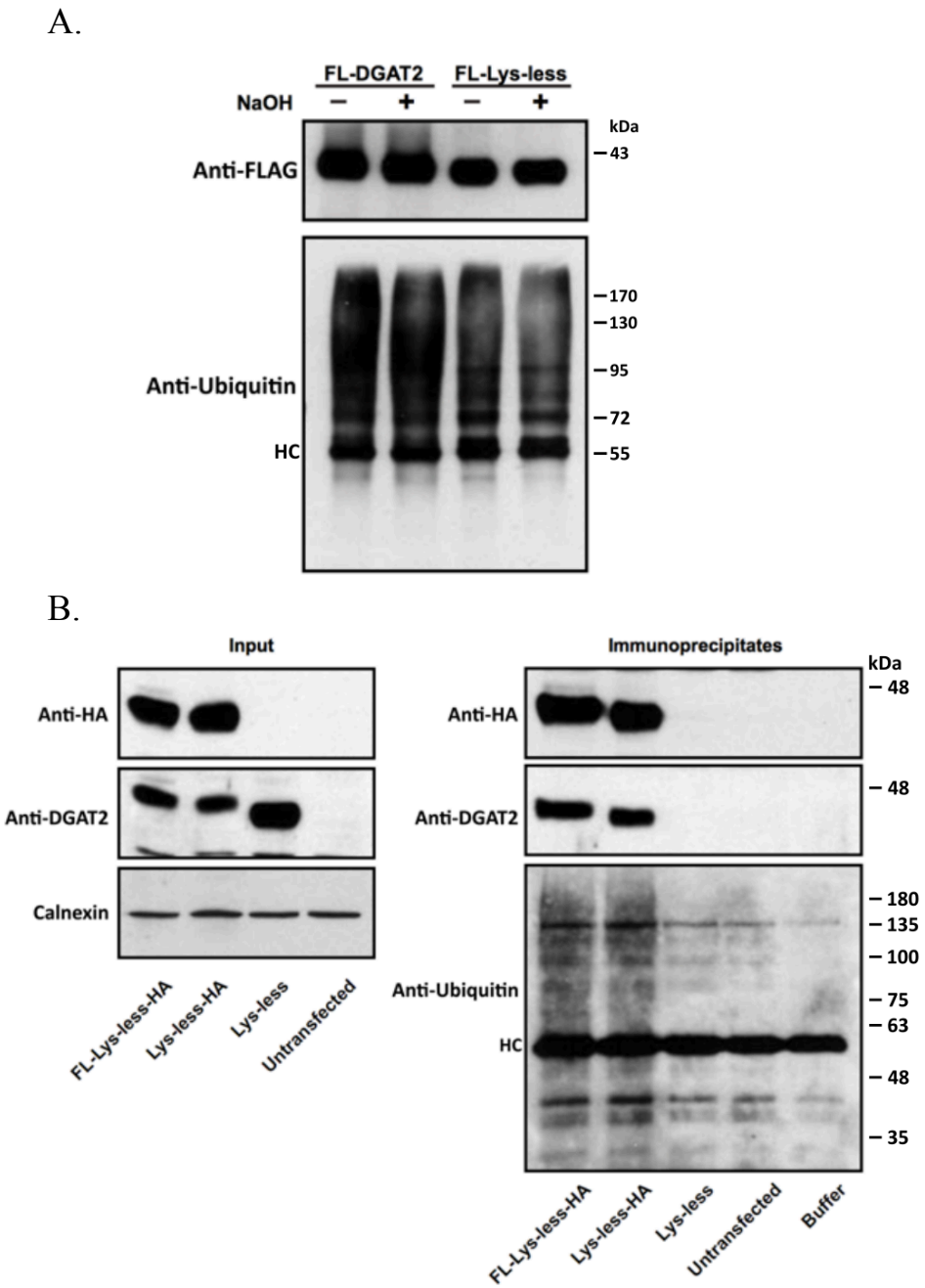

Figure 4.6. Lys-less-DGAT2 is ubiquitinated, likely at the N-terminus - (*A*) FL-DGAT2 and FL-Lys-less expressed in HEK-293T cells were immunoprecipitated with anti-FLAG agarose. Proteins were eluted by boiling in an equal volume of 2x Laemmli buffer containing 5% β-mercaptoethanol. Eluted proteins were incubated with or without 100 mM NaOH at 37°C for 2 h. NaOH treated samples were neutralized with HCl while those that did not receive NaOH were treated with an equal volume of 1x PBS. Immunoprecipitates were analyzed by immunoblotting with anti-FLAG and anti-ubiquitin antibodies. *(B)* FL-Lys-less-HA and Lys-less-HA expressed in HEK-293T cells were immunoprecipitated with anti-HA. Untagged Lys-less was included as a negative control. Immunoprecipitates were then separated by SDS-PAGE and probed with anti-HA, anti-DGAT2 and anti-ubiquitin antibodies. HC denotes heavy chains.

4.2.4. Deletion of amino acids 327-388 increased DGAT2 stability

As the 3C protease method was ineffective at identifying regions of DGAT2 that were ubiquitinated, we chose to evaluate the turnover and ubiquitination status of several DGAT2 deletion mutants (Fig. 4.7). HEK-293T cells were transfected with each construct and their stability was assessed. We identified that the N-terminus had little-to-no role in dictating DGAT2 stability as none of these deletion mutants - including a deletion of residues 2-119, removing the first 5 lysine residues - had an appreciable effect in reducing turnover (Fig. 4.8A). Notably, a deletion of amino acids 327-388, lacking the 6 C-terminal most lysines, was greatly stabilized. Further highlighting the importance of the DGAT2 C-terminus, a mutant in which all 20 lysines C-terminal of the TMDs (FL-DGAT2 K118-376R) were conservatively substituted to arginine, demonstrated little degradation over the course of the experiment (Fig. 4.8B).

In addition to analyzing degradation of DGAT2 deletion mutants, we examined their ubiquitination. Each construct was expressed in HEK-293T cells and isolated by anti-FLAG-immunoprecipitation. Samples were then subjected to SDS-PAGE and immunoblotting with anti-FLAG and anti-ubiquitin antibodies (Fig. 4.8C). While ubiquitination in deletion mutants Δ2-119 and Δ66-115 was reduced relative to other constructs, the abundance of the unmodified protein was also less than that of other mutants. Additionally, Δ2-30, Δ30-67 and Δ327-388 - while expressed at levels at or below that of FL-DGAT2 - they demonstrated increased ubiquitination. Ultimately, no deletion was sufficient to abolish DGAT2 ubiquitination, consistent with the CHX degradation results (Fig. 4.8A).

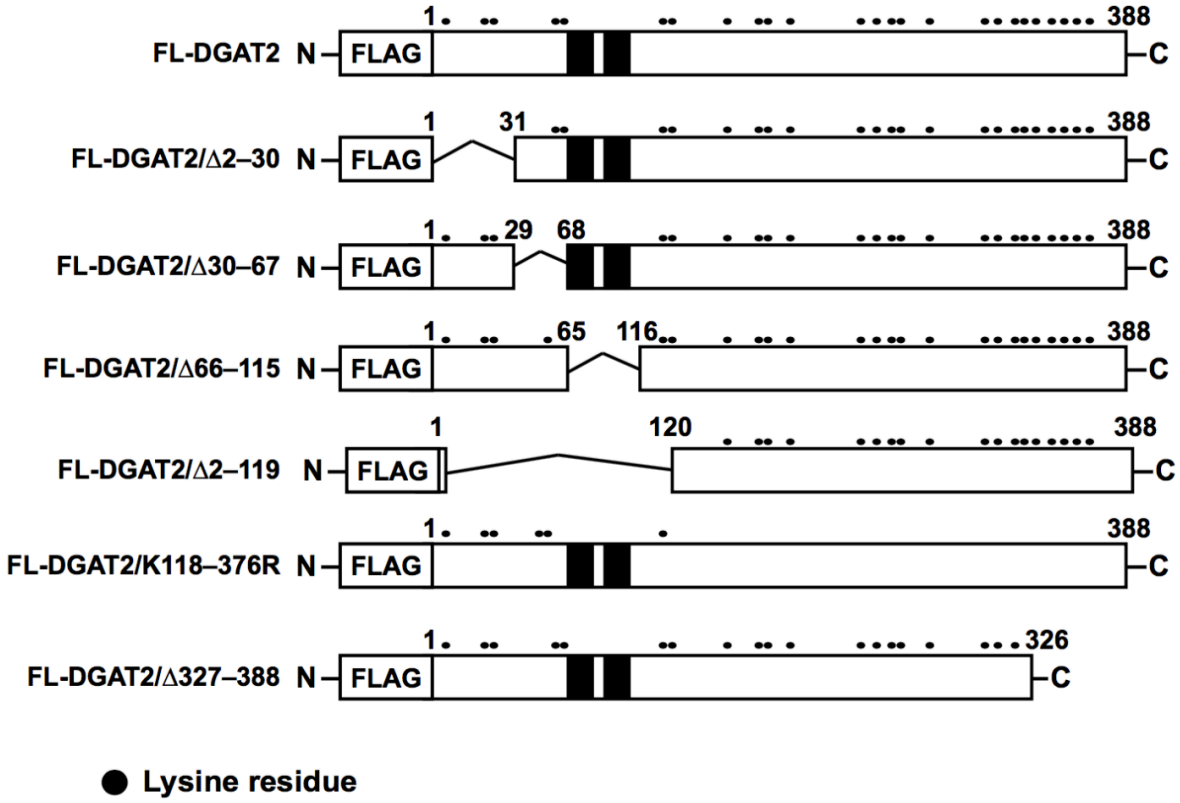

Figure 4.7. DGAT2 deletion mutants - DGAT2 mutants used to identify regions of DGAT2 that have a role in mediating its degradation. *Black circles* represent individual lysine residues present in DGAT2. Black boxes represent the transmembrane domains of DGAT2 (amino acids 66–87 and 93–116).

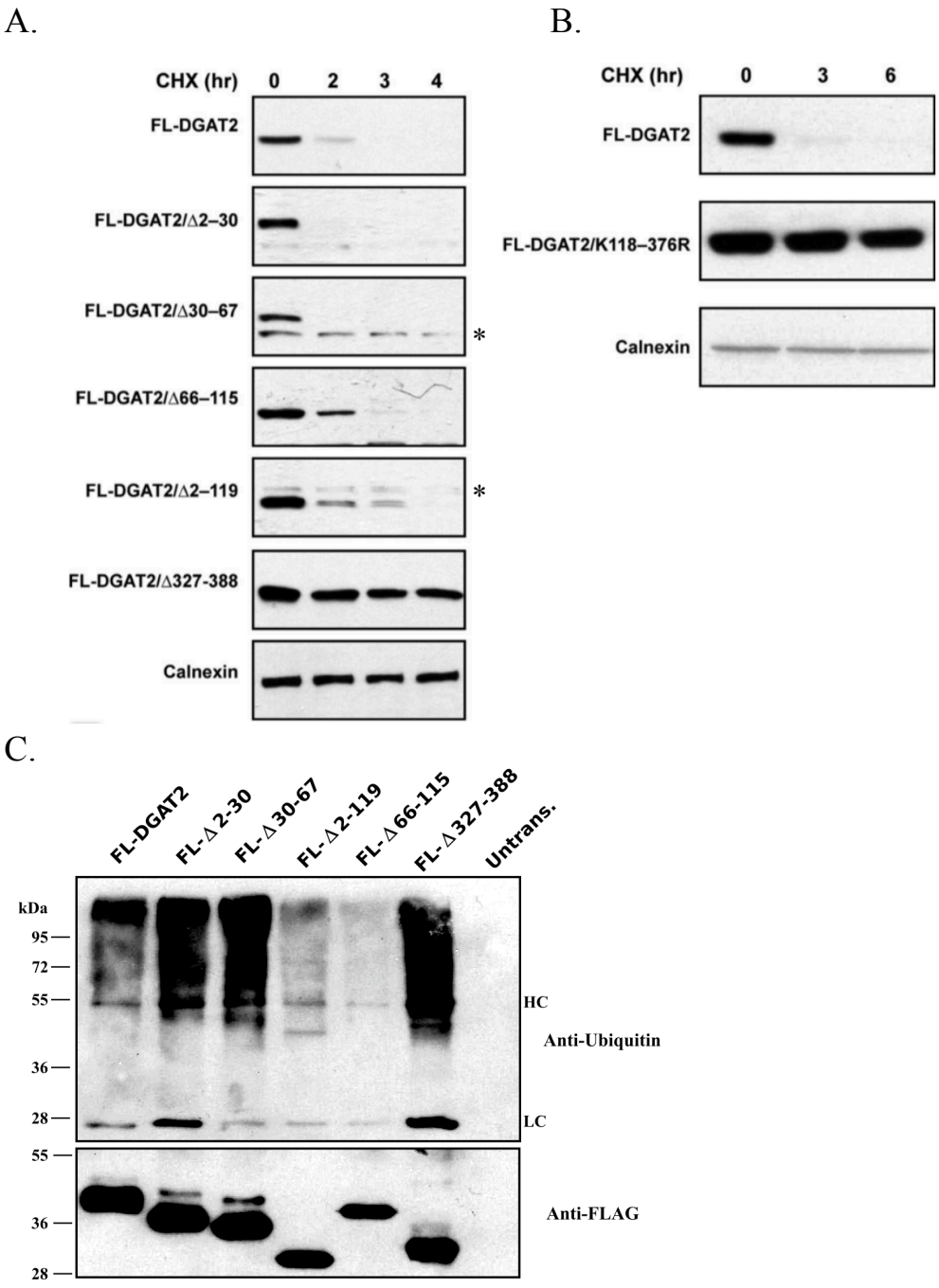

Figure 4.8. Lysine residues in the C-terminal half of DGAT2 are important for its degradation - *(A and B)* HEK-293T cells expressing FL-DGAT2 and the DGAT2 mutants shown in Fig. 4.7 were exposed to 100 μg/mL CHX for the time indicated. Samples were separated by SDS-PAGE and analyzed by immunoblotting with anti-FLAG and anti-calnexin antibodies. An asterisk denotes the position of a non-specific band. *(C)* HEK-293T cells were transfected with DGAT2 deletion mutants. Samples were subjected to anti-FLAG immunoprecipitation. Immunoprecipitates were displaced by 3X FLAG peptide prior to SDS-PAGE and subsequent immunoblotting with anti-ubiquitin primary antibody. Re-blotting with anti-FLAG antibody was conducted to confirm mutant isolation.

4.2.5. Identification of lysines involved in regulating DGAT2 stability by systematic restoration in Lys-less-DGAT2

In order to identify specific lysine residues important for DGAT2 degradation signaling, we took a site directed mutagenesis approach. Early experiments found that mutations of single lysine residues to arginines had little effect in reducing DGAT2 degradation (data not shown). This suggested that many lysines might be involved. In addition, it was challenging to interpret which lysines were important as it relied on detecting slight differences in mutant stability for rapidly degraded proteins. For these reasons, we chose to use the Lys-less construct and systematically restore lysine residues. Detecting changes in degradation was much simpler with the stable Lys-less-DGAT2 as a baseline. Constructs were transfected into HEK-293T cells and analyzed by CHX degradation assay. Samples were harvested and subjected to SDS-PAGE and immunoblotting with anti-FLAG and anti-calnexin antibodies (Fig. 4.9). Notably, as identified with the Δ327-388 deletion mutant, the 6 C-terminal lysines were important in regulating DGAT2 degradation as individual restoration resulted in ~60-90% degradation following 6 h of CHX treatment. Tandem restoration of K63 and K66, as well as K183 and K184, also strongly increased degradation - as did lysines K302 or K305. All remaining lysines, apart from K2, K26 and K28, which had no effect on degradation, triggered an intermediate rate of turnover.

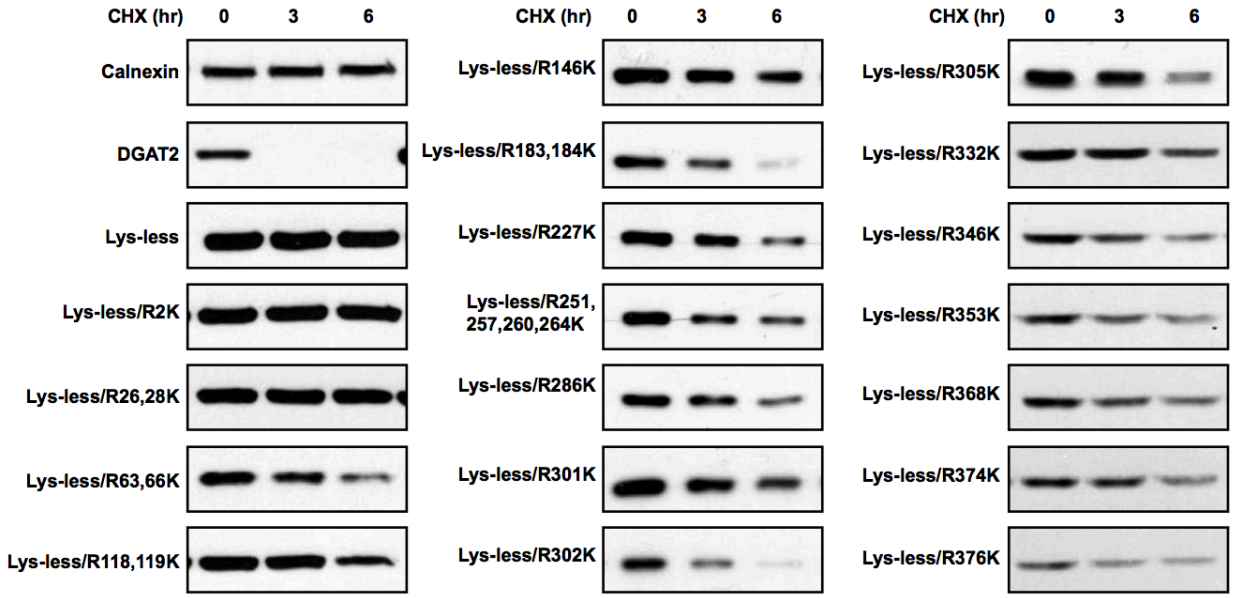

Figure 4.9. Addition of specific lysine residues back to a lysine-less mutant of DGAT2 promoted its degradation - Individual or clusters of lysine residues were added back to FL-Lys-less-DGAT2. HEK-293T cells expressing FL-DGAT2, FL-Lys-less-DGAT2, or FL-Lys-less-DGAT2 lysine restoration mutants were exposed to 100 µg/mL CHX for the time indicated. Samples were separated by SDS-PAGE and analyzed by immunoblotting with anti-FLAG and anti-calnexin antibodies.

4.3. Discussion

The 3C protease method of ubiquitin mapping originally described by Chen *et al.* (2006) is advantageous as it streamlines ubiquitinated lysine detection by grouping lysines into clusters of those N-terminal or C-terminal to an engineered protease site. By comparing the ubiquitination of the N- and C-terminal fragments of 3C mutants, it is possible to pinpoint candidate acceptor lysines. Ideally, this should eliminate exhaustive mutagenesis in which every lysine must be individually examined. In the original study, the authors used this method to determine that of the 20 lysines present in p53, five situated in the DNA binding domain were potentially ubiquitinated; mutation of all five lysines abolished ubiquitination (Chen *et al.*, 2006). While ultimately effective, the authors identified several caveats to this method. First, the fragment C-terminal to the protease site was consistently isolated along with the N-terminal fragment during immunoprecipitation. This becomes problematic upon anti-ubiquitin immunoblotting as a ubiquitin signal detected in the pellet could be provided by contamination from the C-terminal fragment rather than ubiquitination of the N-terminal immunoprecipitated fragment. Therefore, only the supernatant fraction, containing the successfully released C-

terminal fragment, is reliable. Secondly, this method is only ideal for mapping ubiquitinated lysines in those proteins with either few ubiquitinated lysines or those in which they are closely grouped. A protein with several ubiquitinated residues spread throughout the length of the protein would be a poor candidate for analysis by this method. Unfortunately both of these issues made this method a poor tool to examine DGAT2. We found that not only was a significant portion of the C-terminal fragment isolated along with the immunoprecipitated N-terminal fragment, but the overall cleavage efficiency at the 3C protease site was weak. We postulate this occurred because DGAT2 molecules interact with each other to form a multimeric complex stabilized by disulfide bonds (Man *et al.*, 2006; McFie *et al.*, 2011). We believe that incomplete cleavage was most likely caused by interaction of 3C mutant proteins physically obstructing the 3C site, and was likely compounded by the presence of the anti-FLAG agarose. In addition, it is likely that C-terminal fragments were interacting with uncleaved constructs still bound to anti-FLAG beads and thus remained in the pellet fraction following centrifugation. Several alterations to the protocol were evaluated in order to resolve these issues, however, detergents and other reagents necessary to solubilize DGAT2 and reduce interactions were not conducive to maintaining protease activity. Ultimately, through mutagenesis, we found that DGAT2 also fell victim to caveat two as it contained multiple ungrouped ubiquitinated residues and therefore was not a suitable candidate for analysis by the 3C protease method.

To show that DGAT2 degradation was lysine dependent, we utilized a construct in which all 25 lysine residues were mutated to arginine. As expected, this mutant was not degraded, yet surprisingly, it was still polyubiquitinated. We identified that peptide bond formation at the α-NH_2 was the most likely site of ubiquitin conjugation. The significance of N-terminal ubiquitination is not well understood. It has been found to function as a degradation signal, forming a distinct pathway dubbed the ubiquitin fusion degradation pathway (Johnson *et al.*, 1995). While degradation of Lys-less-DGAT2 was not apparent, it might occur over a longer time period as the longest CHX assay conducted was six hours. Additionally, N-terminal ubiquitination found on the Lys-less construct could be an artifact of mutating all lysine residues in the protein.

Analysis of pre-existing DGAT2 deletion mutants demonstrated the importance of the C-terminus in dictating DGAT2 stability. Deletion of the C-terminal-most residues (Δ327-388)

greatly stabilized DGAT, suggesting the six lysine residues in this region may be of importance. A previous report implicated the first TMD as a degradation signal (Choi *et al.*, 2014). Our findings demonstrated that deletion of the TMDs (amino acids 66-116 in mutants FL-Δ66-115 and FL-Δ2-119) had no significant effect on DGAT2 stability. One possible explanation for this disparity is that the previous study utilized a fusion protein containing the N-terminal 398 amino acids of firefly luciferase linked to the N-terminus of DGAT2. Thus, the sizable tag could elicit significant structural changes in DGAT2. While this fusion protein, when intact, is rapidly degraded, it is possible that deletions in the TMD region cause structural rearrangements that mask normal DGAT2 degradation signals.

In agreement with the finding that no deletion mutant was invulnerable to degradation, all DGAT2 deletion mutants were polyubiquitinated. Polyubiquitination of FL-Δ327-388 was greater than that of FL-DGAT2 despite reduced abundance of the unmodified protein. This suggested that a larger fraction of this mutant was in the polyubiquitinated form. However, the FL-Δ327-388 mutant exhibited increased stability. It is possible that deletion of this region caused improper folding that targets the mutant to degradation through a quality control mechanism, which facilitates turnover at a lesser rate. While the ubiquitin signal was reduced in FL-Δ2-119 and FL-Δ66-115, the monomeric form of the mutant was also less abundant.

Early attempts at mutating individual lysines to arginines in DGAT2 and assessing stability were largely unsuccessful. The rapid rate of DGAT2 degradation made fine distinctions in turnover time difficult to discern. Only when larger groups of lysines were mutated simultaneously could a noticeable reduction in turnover be elicited (ex. mutant FL-K118-376R). As identifying the contribution of individual lysine residues in dictating DGAT2 stability was not possible, we used the Lys-less-DGAT2 mutant – which was stable over a 6 h CHX degradation assay. Therefore, restoration of lysines in Lys-less-DGAT2 allowed us to distinguish those that facilitated degradation. In agreement with data from the deletion mutants, the N-terminal most lysines (K: 2, 26 and 28) did not trigger turnover in the Lys-less construct. However, restoration of lysines directly flanking the TMDs (K: 63, 66, 118 and 119) (TMD1: 66-87; TMD2: 93-116) was sufficient to induce turnover. Moreover, re-introduction of lysines K346, K353, K368, K374 or K376 - all removed in the degradation resistant Δ327-388 mutant - served as potent turnover signals. All remaining lysines - excluding K2, K26 and K28 - also facilitated degradation to varying degrees. Mass spectrometry was attempted in order to

confirm these findings, but was unsuccessful due to poor sequence coverage. As there are so many potential ubiquitin acceptor sites, it is unsurprising that the substitution of individual lysines in DGAT2 had little effect. Moreover, the rapid turnover of DGAT2 could simply be a function of the abundance of ubiquitin chain acceptor sites, therby increasing the likelihood that DGAT2 is recognized and targeted for destruction.

All lysine residues of DGAT2 are present on the cytosolic face of the ER membrane, potentially exposing them to ubiquitination by E3 ligases localized to the ER membrane or cytosol (Stone *et al.,* 2006; McFie *et al.*, 2014). It is possible that substitution of 25 lysine residues in the Lys-less-DGAT2 construct causes significant structural changes. Moreover, when the lysines are reintroduced into the Lys-less construct they may be present in regions with significantly different structure than is observed in the native protein. This could lead to ubiquitination of lysines that are not normally accessible for post-translational modification; knowledge of DGAT2 structural domains could identify these residues. It is also possible that Lys-less-DGAT2 is ubiquitinated by a different group E3 ligases. This would likely be dependent on whether the degron(s) of DGAT2 that are traditionally identified are substantially altered in the mutant protein.

Notably, a mass spectrometry based study of ubiquitination patterns in mouse tissues revealed greater than 20,000 unique ubiquitination sites (Wagner *et al.*, 2012). DGAT2, ubiquitinated at Lys264 in heart tissue, was detected. Incidentally, we found that restoration of the K251, K257, K260 and K264 cluster of lysines induced degradation in the Lys-less construct.

CHAPTER 5: Examining the role of lysines in triacylglycerol synthesis and the effects of lipogenesis on DGAT2 stability and ubiquitination

5.1. Introduction

For some time there has been debate as to whether DGAT2 is capable of trafficking from the ER to lipid droplets. An alternative hypothesis is that it may remain in the ER with its cytoplasmic domains interacting with lipid droplets via the close proximity of the two membranes. Recent evidence suggests that DGAT2 does in fact exist on the lipid droplet (Jacquier *et al.* 2011; Xu *et al.*, 2012; Wilfling *et al.*, 2013; McFie *et al.*, 2014). One of the preeminent unresolved aspects of DGAT2 is elucidating the events that allow this transition to the droplet. It may move to the lipid droplet in a manner similar to that of GPAT4, which diffuses on membrane bridges that connect the ER and lipid droplets (Wilfling *et al.*, 2013). Post-translational modification of DGAT2 during lipogenesis could be a crucial factor in DGAT2 relocalization.

Lysine is the most commonly post-translationally modified amino acid (Zhang *et al.*, 2011). Potential modifications include: methylation, acetylation, biotinylation, propionylation, butylation, succinylation, ubiquitination and ubiquitin-like modification. Post-translational modifications can have a variety of implications in cell signaling, including dictating changes in protein localization. Notably, the role of ubiquitination in affecting protein localization has been detailed in many cases. For example, p53 requires multi-monoubiquitination for nuclear export (Li *et al.*, 2003)

Lipid concentrations have been shown to affect the turnover rate of multiple proteins involved in triacylglycerol metabolism, such as perilipin-2, apolipoprotein B, lipoprotein (a), and apolipoprotein E (Xu *et al.*, 2005, 2006; Taghibiglou *et al.*, 2000; White *et al.*, 1999; Wenner *et al.*, 2001). Supplementation with fatty acids stabilizes these proteins, increasing the efficiency of triacylglycerol storage in lipid droplets. Conversely, as fatty acid levels fall, these proteins are ubiquitinated and degraded by the proteasome. As DGAT2 is rapidly degraded under basal conditions, it is possible that lipogenesis and lipolysis prompt alterations in stability (Choi *et al.*, 2014).

5.2. Results

5.2.1. Lys-less-DGAT2 retained *in vitro* DGAT activity

We were interested to see if Lys-less-DGAT2, containing 25 lysine substituted arginines, was active and able to efficiently catalyze the acylation of diacylglycerol to triacylglycerol. FL-DGAT2 and FL-Lys-less-DGAT2 were expressed in HEK-293T cells and total cell extracts were isolated. Triacylglycerol synthesis activity of cell lysates was assessed by measuring the incorporation of fluorescent NBD-palmitoyl-CoA, producing NBD-triacylglycerol (Fig. 5.1) (Section 3.14) (McFie and Stone, 2011). We identified that Lys-less-DGAT2 retained *in vitro* activity equal to that of DGAT2. This suggests that lysines are not necessary for DGAT2 activity.

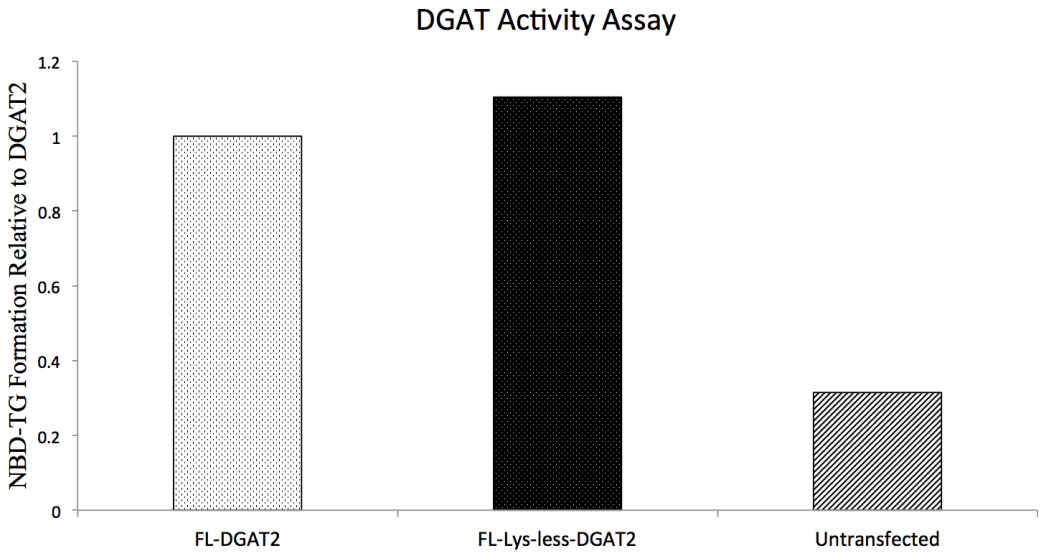

Figure 5.1. Lys-less-DGAT2 is active *in vitro* – *In vitro* DGAT activity of total cell extracts isolated from HEK-293T cells transiently expressing FL-DGAT2, FL-Lys-less-DGAT2 or untransfected control were analyzed as described in Section 3.14. Fifty micrograms of total cell extract was used for each reaction. DGAT2 and FL-Lys-less-DGAT2 were expressed at similar levels (data not shown). Results shown represent the average values obtained from duplicate samples in one experiment; the experiment was repeated, yielding similar results.

5.2.2. Lys-less-DGAT2 exhibited altered localization and reduced the average size of lipid droplets in COS-7 cells

Having identified that Lys-less-DGAT2 was stable and retained *in vitro* activity comparable to DGAT2, we were particularly interested to examine the effect of the Lys-less mutant on triacylglycerol synthesis *in situ*. We expected the degradation resistance of the Lys-less construct to translate to increased triacylglycerol synthesis and elevated lipid droplet size and/or number. COS-7 cells were transfected with FL-DGAT2 or FL-Lys-less-DGAT2 and treated with oleic acid to stimulate lipid droplet formation. Analysis was conducted by immunofluorescence microscopy (Section 3.15). We found that Lys-less-DGAT2 exhibited altered localization (Fig. 5.2). While some cells showed Lys-less-DGAT2 localization to the ER, typical of DGAT2, a population of cells also displayed strong staining in or around the nucleus with distinct punctate structures. Additionally, Lys-less-DGAT2 did not localize to the surface of lipid droplets when triacylglycerol synthesis was stimulated by the addition of oleic acid. As DGAT2 localization to the lipid droplet aids in droplet expansion, a lack of large lipid droplets was apparent in Lys-less-DGAT2 transfected cells (Monetti *et al.*, 2007; Stone *et al.* 2004).

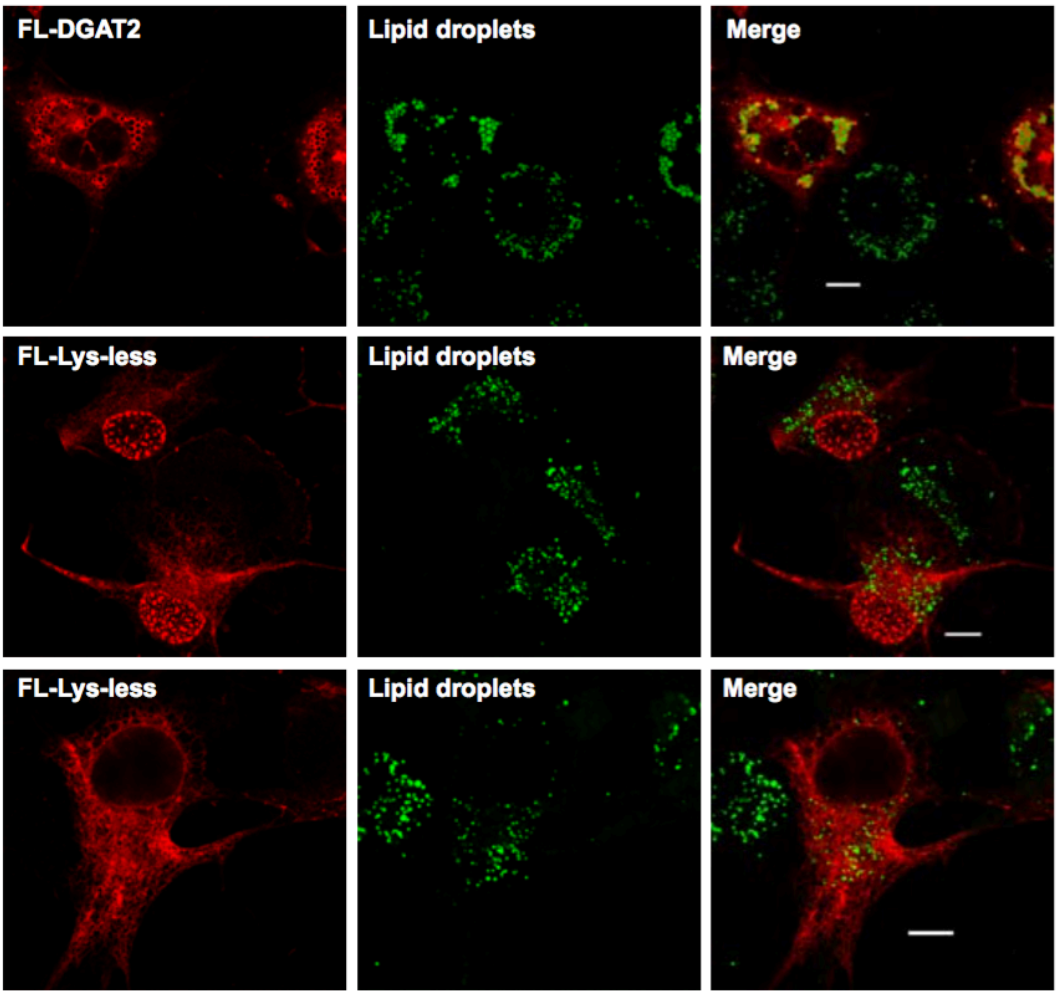

Figure 5.2. Lys-less-DGAT2 exhibited altered localization and reduced the size of lipid droplets - COS-7 cells transiently expressing FL-DGAT2 or FL-Lys-less-DGAT2 were treated with 0.5 mM oleate for 12 h and then stained with anti-FLAG. BODIPY 493/503 was used to visualize lipid droplets. Two different staining patterns for FL-Lys-less-DGAT2 are shown. Scale bars, 10 μm.

5.2.3. Mutation of two DGAT2 lysine clusters caused mislocalization of DGAT2 and perturbed lipid droplet formation

Having noted that Lys-less-DGAT2 exhibited altered localization and produced smaller lipid droplets, we chose to screen our DGAT2 Lys-to-Arg mutant library to identify regions which may be responsible. A cluster of Lys residues - K251, K257, K260, K264 - that when mutated to Arg (FL-DGAT2 K251, 257, 260, 264R) was sufficient to cause nuclear/perinuclear localization, similar to Lys-less-DGAT2 (Fig. 5.3). Conversely, reintroduction of these four lysines into the Lys-less construct (FL-Lys-less-DGAT2 R251, 257, 260, 264K) was not able to correct mislocalization, suggesting that additional regions may be able to produce this phenotype.

Lipid droplet analysis was conducted on confocal images of FL-DGAT2, FL-DGAT2 K251, 257, 260, 264R, FL-Lys-less-DGAT2 and FL-Lys-less-DGAT2 R251, 257, 260, 264K transfected COS-7 cells (Section 3.16). Lipid droplet number in cells expressing DGAT2 K251, 257, 260, 264R was significantly higher post-oleate treatment than in those expressing other constructs (Fig. 5.4A). Examination of mean droplet area revealed that DGAT2 transfected cells produced larger droplets than those observed with the DGAT2 mutants (Fig. 5.4B). In addition, DGAT2 and DGAT2 K251, 257, 260, 264R transfected cells exhibited a greater total lipid droplet area per cell than the Lys-less mutants (Fig. 5.4C). While DGAT2 K251, 257, 260, 264R appeared to result in an overall increase in total droplet area relative to DGAT2, this finding was not statistically significant. To summarize, substitution of lysine residues 251, 257, 260 and 264 for arginine caused cells to produce an elevated number of lipid droplets with a lower mean area relative to DGAT2. Ultimately, the total lipid droplet area was relatively similar when comparing cells expressing each construct. While restoration of the 251-264 cluster of lysines in the Lys-less construct appeared to increase the mean droplet area above that of Lys-less, the mean sum of total lipid droplet area remains similar. Likely, there are additional regulatory lysine residues important in the production of lipid droplets.

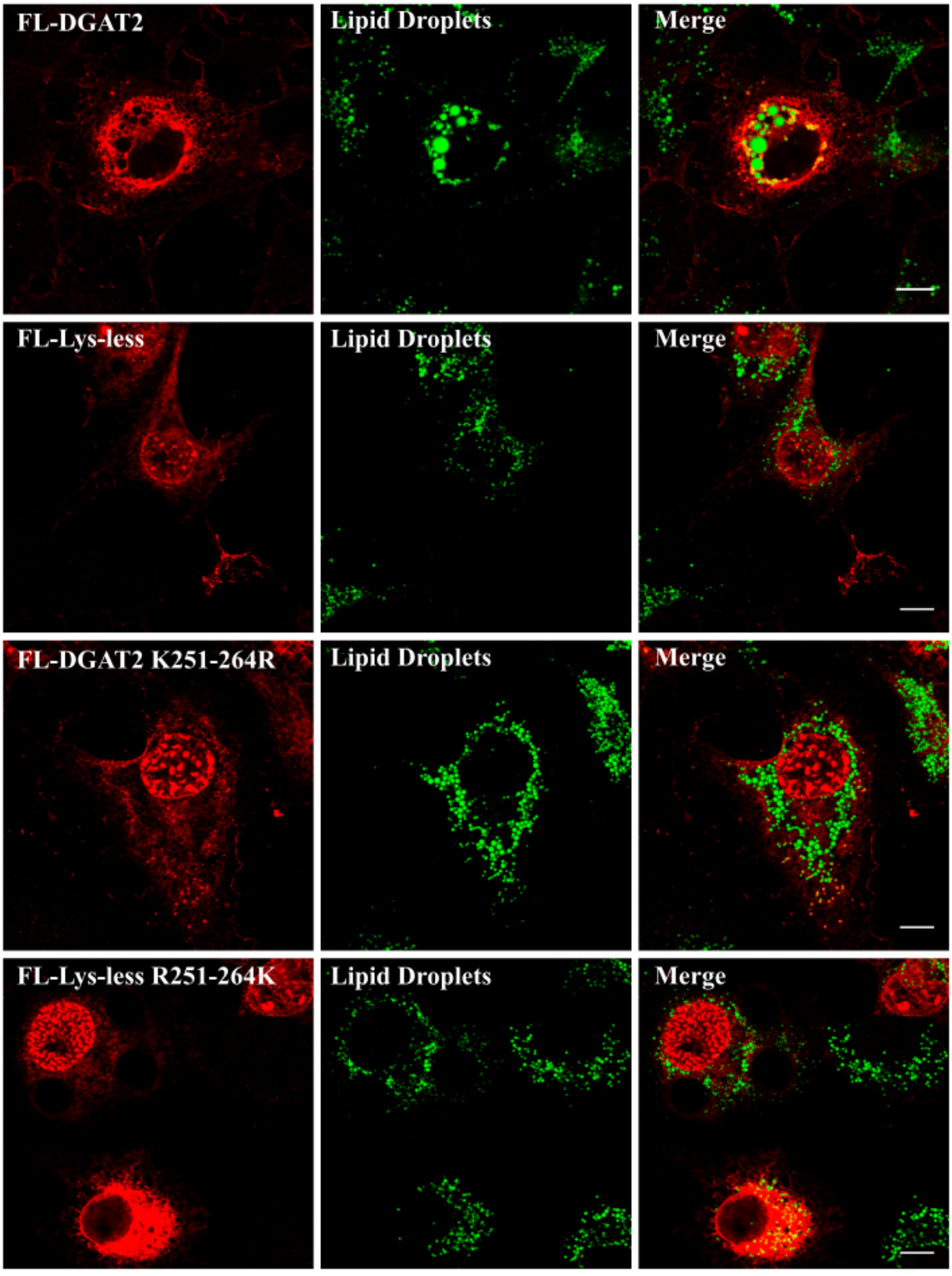

Figure 5.3. Lipid droplet analysis of cells expressing DGAT2 lysine mutants - COS-7 cells transiently expressing FL-DGAT2, FL-Lys-less-DGAT2, FL-DGAT2 K251, 257, 260, 264R or FL-Lys-less-DGAT2 R251, 257, 260, 264K were treated with 0.5 mM oleate for 18 h and then stained with anti-FLAG and BODIPY 493/503 to visualize lipid droplets. Scale bar, 10 μm

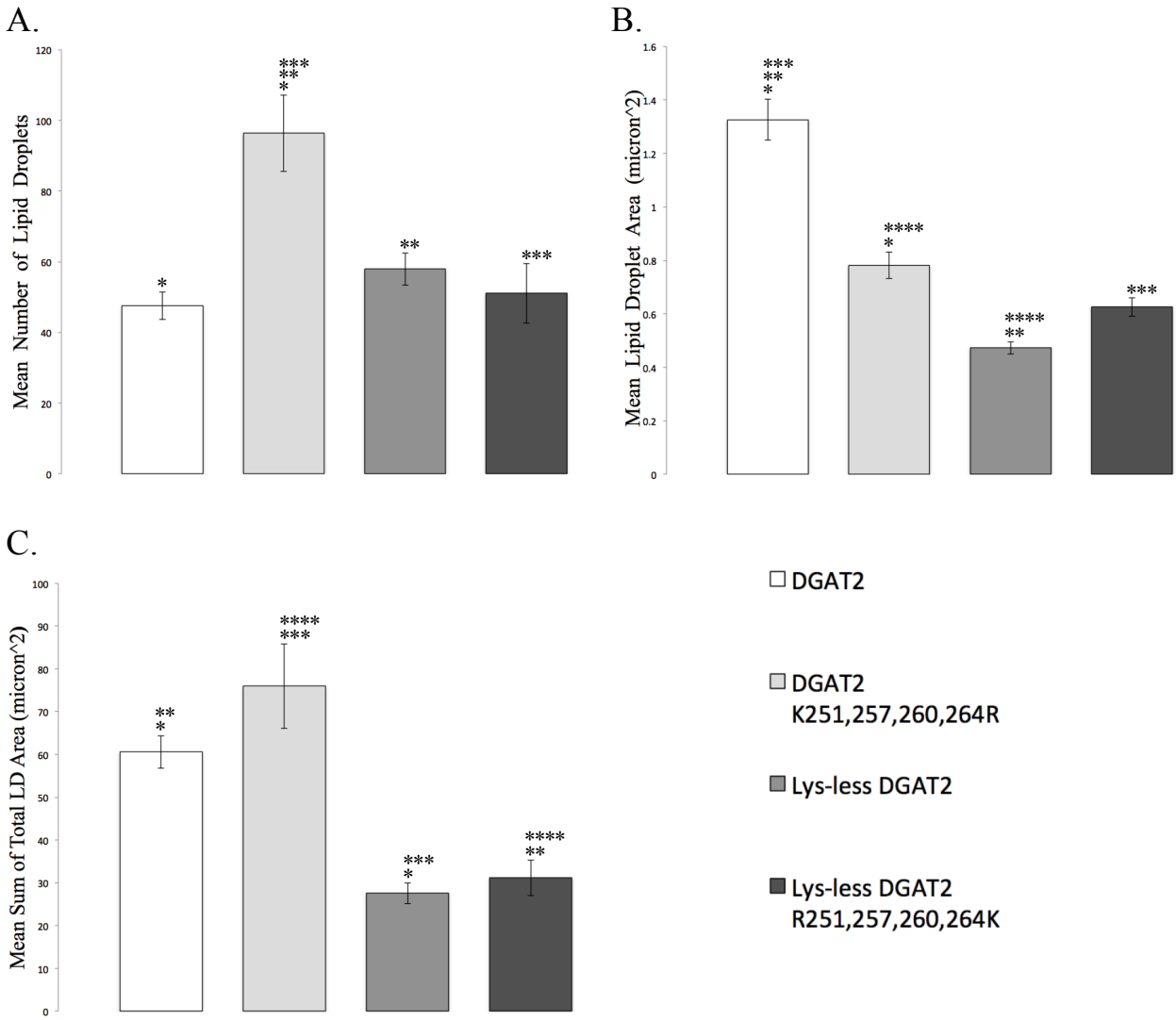

Figure 5.4. DGAT2 lysines 251-257 are important in normal lipid droplet formation - COS-7 cells were transfected with FL-DGAT2, FL-DGAT2 K251, 257, 260, 264R, FL-Lys-less-DGAT2 or FL-Lys-less-DGAT2 R251, 257, 260, 264K prior to 18 h treatment with 0.5 mM oleic acid (18:1). Samples were stained with anti-FLAG and BODIPY 493/503 to visualize lipid droplets. Images were taken with a confocal system and analyzed using ImageJ analysis software. All analysis was conducted on fourteen cells per construct. Lipid droplets with an area of ≥ 0.2 micron^2 were counted. *(A)* Mean lipid droplet number was calculated. *, **, ***, $p < 0.05$ *versus* DGAT2, Lys-less-DGAT2 and Lys-less-DGAT2 R251, 257, 260, 264 transfected cells respectively. *(B)* Mean lipid droplet area was calculated. *, **, ***, $p < 0.05$ *versus* DGAT2 K251, 257, 260, 264R, Lys-less-DGAT2 and Lys-less-DGAT2 R251, 257, 260 ,264K transfected cells respectively. ****, $p < 0.05$ *versus* Lys-less-DGAT2 transfected cells. *(C)* Mean sum of lipid droplet area was calculated *, **, $p < 0.05$ *versus* Lys-less-DGAT2 and Lys-less-DGAT2 R251, 257, 260, 264K transfected cells respectively. ***, ****, $p < 0.05$ *versus* Lys-less-DGAT2 and Lys-less-DGAT2 R251, 257, 260, 264K transfected cells respectively.

Through further screening of our mutant library, we identified that mutation of the six C-terminal lysines - 332, 346, 353, 368, 374 and 376 - to Arg caused a similar nuclear pattern to that observed in the Lys-less and K251, 257, 260, 264R mutants (Fig. 5.5). We previously identified these six residues as strong promoters of DGAT2 degradation (Chapter 4.2.5). Unfortunately, re-establishment of these ten residues in the Lys-less construct was insufficient to restore typical DGAT2 localization (data not shown).

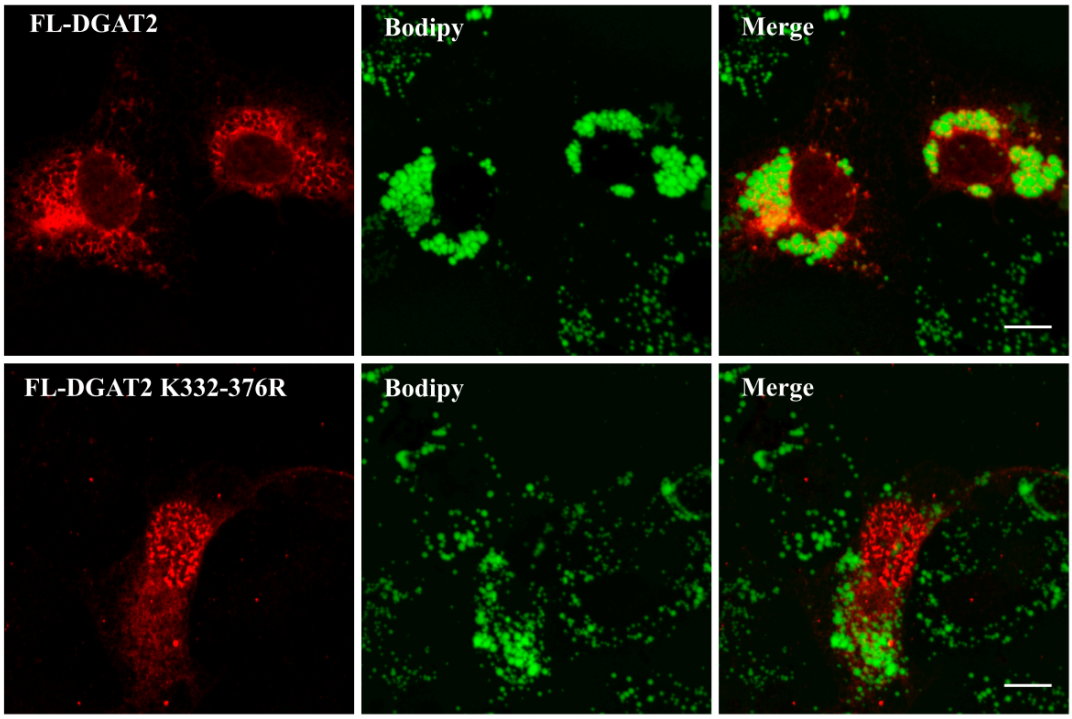

Figure 5.5. Mutation of the six C-terminal DGAT2 lysines caused nuclear localization - COS-7 cells transiently expressing FL-DGAT2 or FL-DGAT2 K332, 346, 353, 368, 374, 376R (FL-DGAT2 K332-376R) were treated with 0.5 mM oleate for 12 h and then stained with anti-FLAG and BODIPY 493/503 to visualize lipid droplets. Scale bar, 10 μm.

5.2.4. Stimulation of lipogenesis did not reduce DGAT2 turnover

We were interested in determining if DGAT2 stability is altered by the stimulation of lipogenesis. It is possible that when the cell is producing triacylglycerols, DGAT2 turnover could be reduced in order to increase the rate of triacylglycerol synthesis. Two separate methods of lipogenic induction were evaluated (Section 3.9). Treatment with oleic acid, a DGAT2 substrate, drives the acylation of 1,2-diacylglycerol to form triacylglycerol. HEK-293T cells were transfected with FL-DGAT2 and cultured in the presence or absence of oleic acid followed by re-feeding a solution of CHX with or without oleic acid (Fig. 5.6A). DGAT2 was rapidly degraded independent of oleic acid. Examination of triacylglycerol levels revealed a large increase in triacylglycerol synthesis in oleate treated cells, which remained relatively constant throughout the CHX time course (Fig. 5.6B). While DGAT2 is reduced over this period, a fall in triacylglycerol levels is not necessarily expected, as the bulk of triacylglycerol would be formed over the 18 h oleic acid incubation. Thus, variations in triacylglycerol abundance over the 6 h CHX treatment would be heavily influenced by the rate of triacylglycerol breakdown, which may happen at a lesser rate.

DGAT2 turnover was also analyzed under insulin-induced lipogenesis. Treatment with insulin stimulates lipogenesis through the activation of pyruvate dehydrogenase and acetyl-CoA carboxylase. Pyruvate dehydrogenase is responsible for the conversion of pyruvate into acetyl-CoA, a substrate for acetyl-CoA carboxylase. Acetyl-CoA carboxylase then converts acetyl-CoA to malonyl-CoA, providing the two-carbon units in the production of long chain fatty acids. FL-DGAT2 transfected cells were treated in the presence or absence of insulin, preceding co-treatment with CHX (Fig. 5.6C). Samples were harvested, isolating total cell extracts, and DGAT2 protein levels were analyzed by anti-FLAG-immunoblotting. The data showed that stimulation of lipogenesis, triggered by insulin, did not affect the rate of DGAT2 turnover.

A.

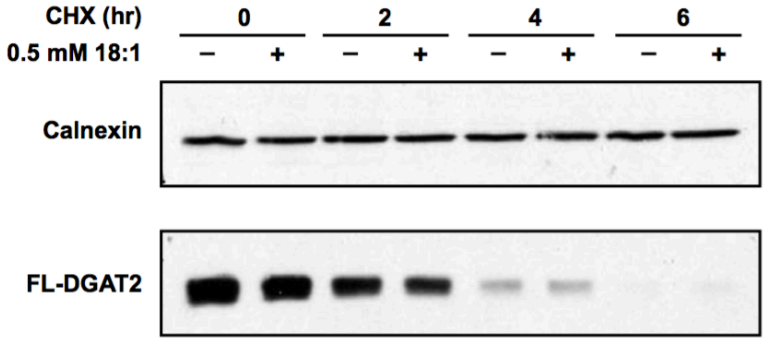

B.

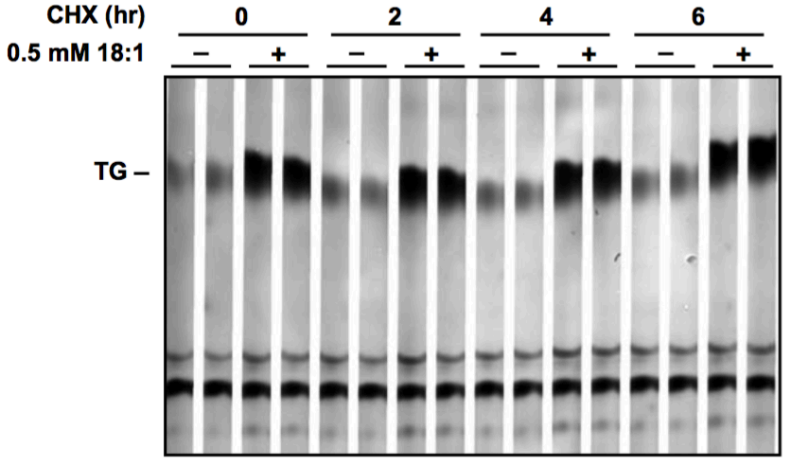

C.

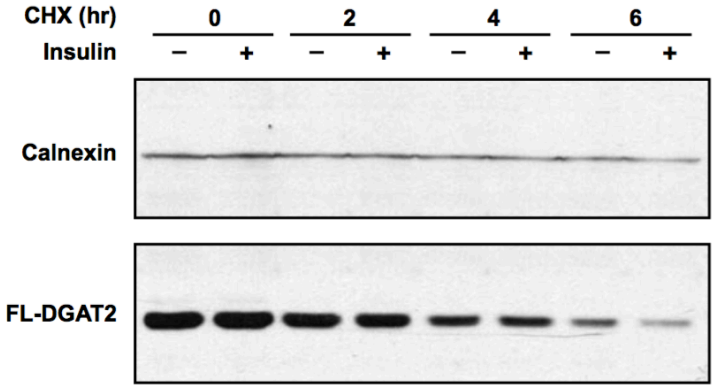

Figure 5.6. Neither oleic acid nor insulin stabilized DGAT2 - *(A)* HEK-293T cells expressing FL-DGAT2 were incubated with or without 0.5 mM oleate for 18 h. Cells were then treated with 100 µg/mL CHX in the presence or absence of 0.5 mM oleate for 0–6 h. Time zero refers to cells harvested after the 18 h incubation, in the presence or absence of oleate, without any CHX. *(B)* Lipids were extracted from equal amounts of cellular protein from the samples in Fig. 2*A* and separated by thin layer chromatography. *(C)* Cells were treated with or without 5 µg/mL insulin for 1 h. The growth media was replaced with media containing 100 µg/mL CHX with or without 5 µg/mL insulin and cells were harvested at the indicated time points. Time zero refers to cells harvested after the 1 h insulin treatment with no CHX. Samples were separated by SDS-PAGE and immunoblotted with anti-FLAG and anti-calnexin. TG represents triacylglycerol.

5.2.5. Polyubiquitinated DGAT2 was detected in mitochondrial and fat fractions

Stimulation of lipogenesis did not appear to alter DGAT2 degradation, however, we chose to use subcellular fractionation to examine whether lipid droplet localized DGAT2 was ubiquitinated. HEK-293T cells were transfected with FL-DGAT2 and HA-ubiquitin or a Myc-DGAT2 and HA-ubiquitin negative control. Through differential- and sucrose gradient-centrifugation, crude mitochondria and the lipid droplet/fat fractions were isolated (Section 3.12). MAM, in which DGAT2 is enriched, is present in the crude mitochondria fraction. DGAT2 was immunoprecipitated with anti-FLAG agarose and analyzed by SDS-PAGE and immunoblotting (Fig. 5.7). Relative fraction purity was assessed by the presence of marker proteins. Heat shock protein 70 (Hsp70) was detectable only in the crude mitochondria input fraction while lipid droplet protein, perilipin-2, was observed only in the fat input fraction. FL-DGAT2 was detected in crude mitochondria and fat fractions. The Myc-DGAT2 control, not bound by anti-FLAG agarose, was only detected in fraction inputs and not isolated in the anti-FLAG immunoprecipitates. Detection of HA-ubiquitin conjugates with an anti-HA primary antibody revealed DGAT2 polyubiquitination in both crude mitochondria and fat fraction immunoprecipitations. No ubiquitin signal was detected in anti-FLAG immunoprecipitates of fractions derived from Myc-DGAT2 transfected cells. This demonstrates that DGAT2 isolated from MAM and lipid droplets is polyubiquitinated.

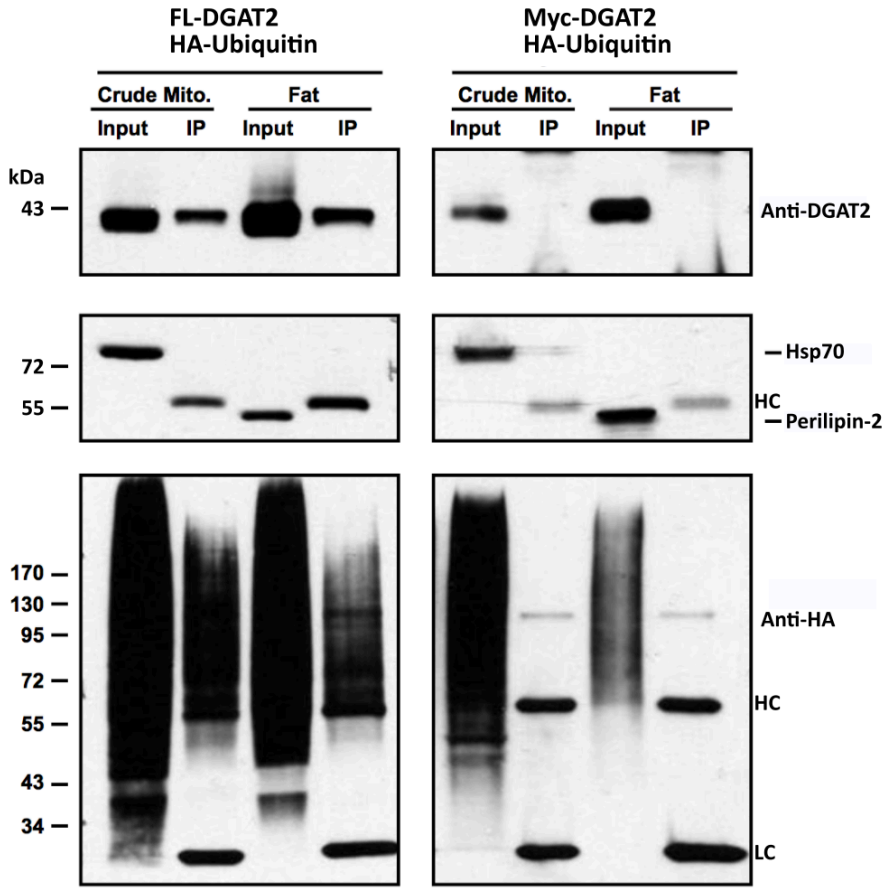

Figure 5.7. DGAT2 localized to both MAM and lipid droplets is ubiquitinated - HEK-293T cells expressing either FL-DGAT2 or Myc-DGAT2 along with HA-ubiquitin were incubated with 0.5 mM oleate for 43 h to stimulate triacylglycerol synthesis. Crude mitochondria and floating fat fractions were then isolated by ultracentrifugation. Purity of the crude mitochondrial membrane and floating fat fractions were assessed by sequential immunoblotting with anti-Hsp70 (mitochondria) and perilipin-2 (lipid droplet) antibodies. FL-DGAT2, but not Myc-DGAT2, was immunoprecipitated with anti-FLAG agarose from detergent solubilized material. Immunoprecipitates (IP) were separated by SDS-PAGE and were then probed with anti-FLAG and anti-HA antibodies. HC and LC represent antibody heavy and light chains respectively.

5.2.6. Inhibiting lipid droplet localization did not affect DGAT2 degradation

Having identified that DGAT2 on the ER and lipid droplets is ubiquitinated, we chose to determine whether DGAT2 localization to the lipid droplet has an impact on its turnover. This was examined using a mutant that is retained in the ER, FL-DGAT2-HA-insert, which has an artificially extended lumenal loop between its TMDs. The extended region is comprised of 22 amino acids, containing an HA-tag flanked by additional primary sequence normally present in the loop. This mutant has been shown to retain full catalytic activity *in vitro*, but does not migrate from the ER following oleate loading (McFie *et al.* 2014). HEK-293T cells transiently

expressing FL-DGAT2 or the ER anchored mutant were pre-treated in the presence or absence of oleic acid prior to CHX assay. Samples were analyzed by SDS-PAGE and anti-FLAG immunoblotting (Fig. 5.8). In the absence and presence of oleic acid, the HA-insert mutant was rapidly degraded at a rate very similar to DGAT2. This suggests that DGAT2 degradation is not dependent on localization to lipid droplets.

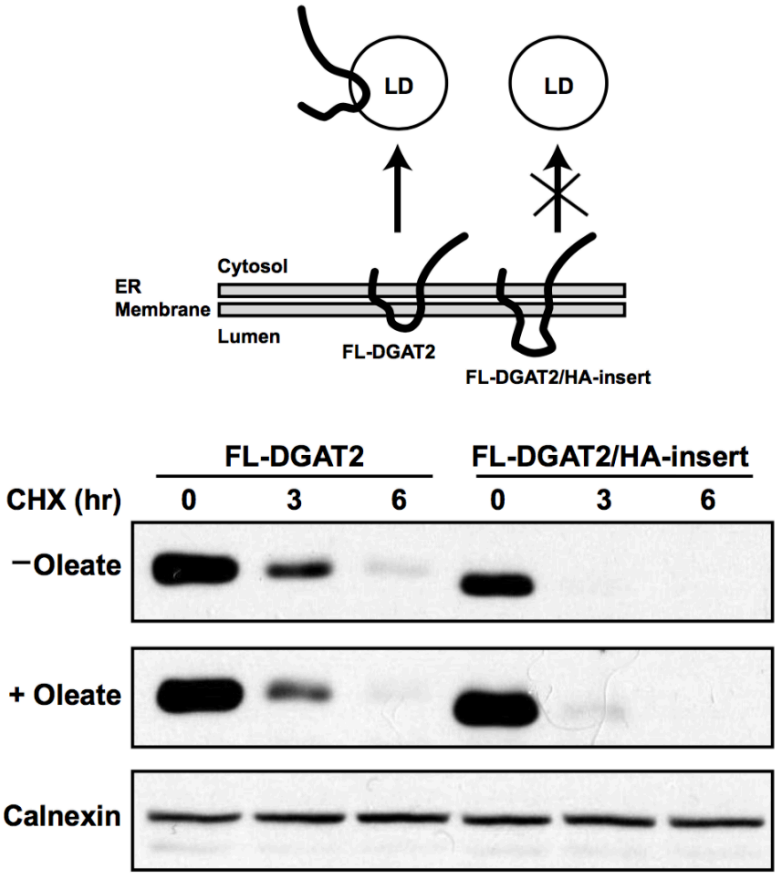

Figure 5.8. Inhibiting lipid droplet localization did not affect DGAT2 degradation - HEK-293T cells expressing FL-DGAT2 or FL-HA-insert were treated with or without 0.5 mM oleate for 18 h. Cells were then treated with 100 µg/mL CHX in the presence or absence of 0.5 mM oleate for 0–6 h. Samples were analyzed by immunoblotting with anti-FLAG and anti-calnexin antibodies. LD denotes a lipid droplet.

5.2.7. DGAT2 is ubiquitinated *in situ* under basal and lipogenic conditions

Stimulation of lipogenesis did not have an effect on DGAT2 turnover. Similarly, a DGAT2 mutant confined to the ER was rapidly degraded at a rate closely resembling that of DGAT2. However, the ubiquitination status of DGAT2 may be altered during lipogenesis, possibly playing a role in migration to the lipid droplets during triacylglycerol synthesis. We were interested in identifying which cellular pools of DGAT2 were ubiquitinated, as well as any differences in the ubiquitination of DGAT2 populations under basal and lipogenic conditions. COS-7 cells were co-transfected with FL-DGAT2/HA-ubiquitin or control Myc-DGAT2/HA-ubiquitin and incubated with or without oleic acid prior to Duolink® *In Situ* Proximity Ligation Assay (PLA) analysis (Fig. 5.9) (Section 3.17). Anti-FLAG and anti-HA primary antibodies were detected by species specific PLUS and MINUS PLA probes. Addition of the ligation mixture results in hybridization of the oligonucleotide tails if the PLUS and MINUS PLA probes are within 40 nm of each other. The hybridized circular DNA is then amplified and detected with a fluorescent probe.

Following completion of the PLA, cells were co-stained with BODIPY 493/503 to visualize ubiquitinated DGAT2 relative to lipid droplet position. Alternatively, cells were co-stained using anti-DGAT2 specific antibody in order to compare ubiquitinated DGAT2 to the total DGAT2 population. A strong interaction signal was detected in cells expressing FL-DGAT2 and HA-ubiquitin in both oleate treated and untreated samples - signifying ubiquitinated DGAT2. The population of ubiquitinated DGAT2 appeared to align very closely with total DGAT2 population, independent of oleate treatment (Fig. 5.10A). Ubiquitinated DGAT2 was also observed closely associated with BODIPY stained lipid droplets (Fig. 5.10B), confirming our subcellular fractionation findings (Fig. 5.7). Whether the ubiquitination of lipid droplet localized DGAT2 functions as a lipid droplet targeting signal, in DGAT2 degradation, or in both, is unknown.

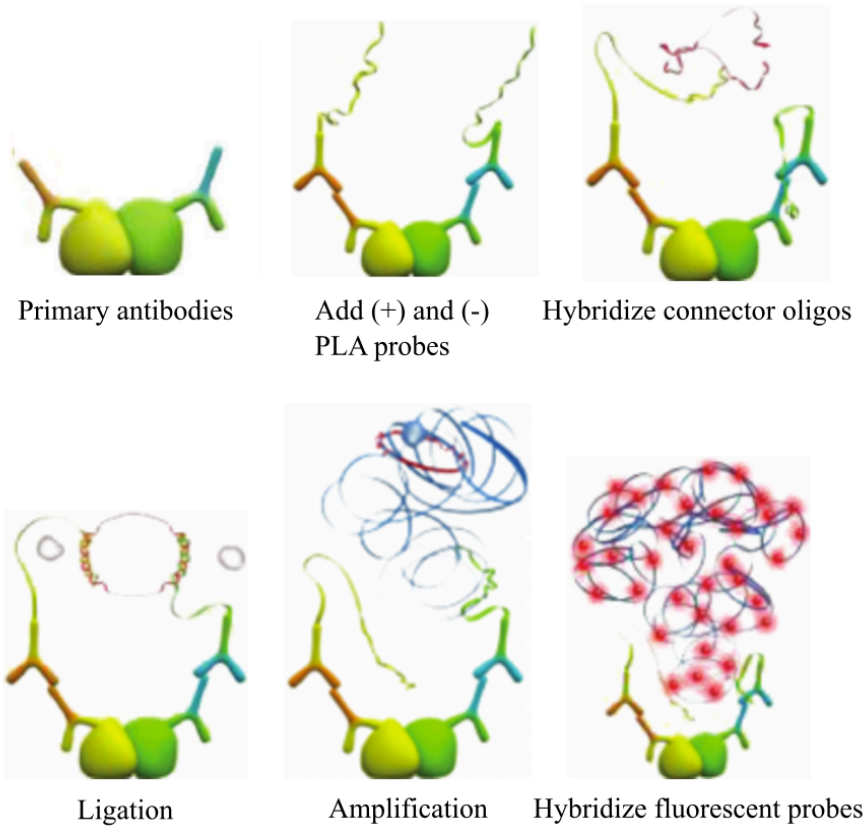

Figure 5.9. Duolink® *in situ* proximity ligation assay – *In situ* identification of protein-protein interactions or post-translational modifications using PLA requires primary antibodies specific to each target. Species-specific secondary antibody PLA probes bind to the primary antibodies. Oligonucleotide tails on the PLA probes hybridize with connector oligonucleotides if the two target proteins are within 40 nm, forming a complete circularized oligonucleotide that is ligated together. Addition of polymerase replicates the circular oligonucleotide to amplify the interaction signal. Fluorescent probes hybridize to the amplified sequence allowing for detection. A d protocol is described in Section 3.17. This figure has been adapted from product literature produced by Sigma Aldrich.

A.

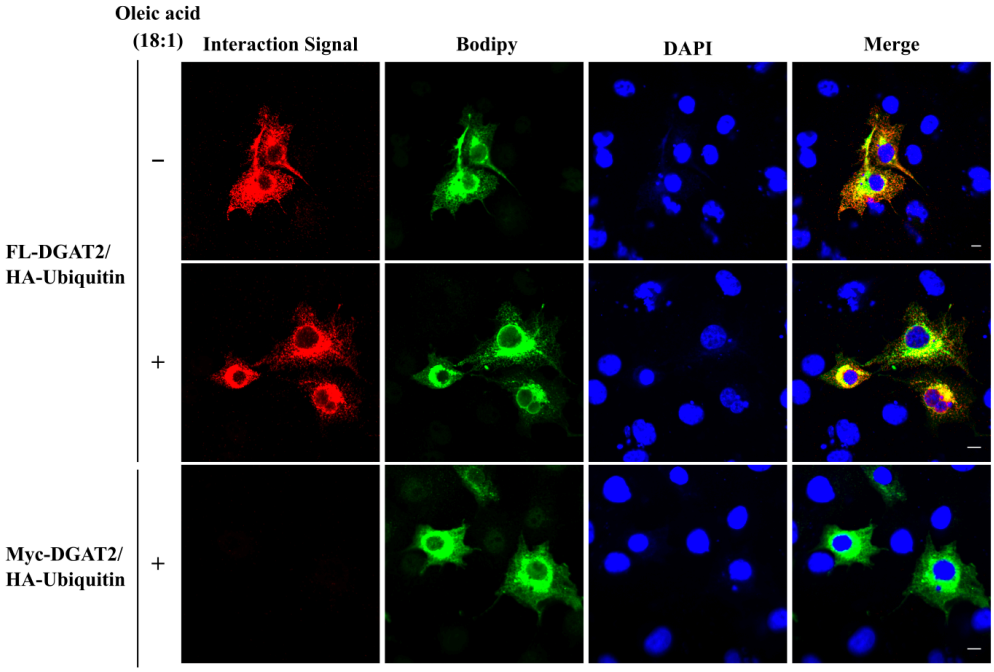

B.

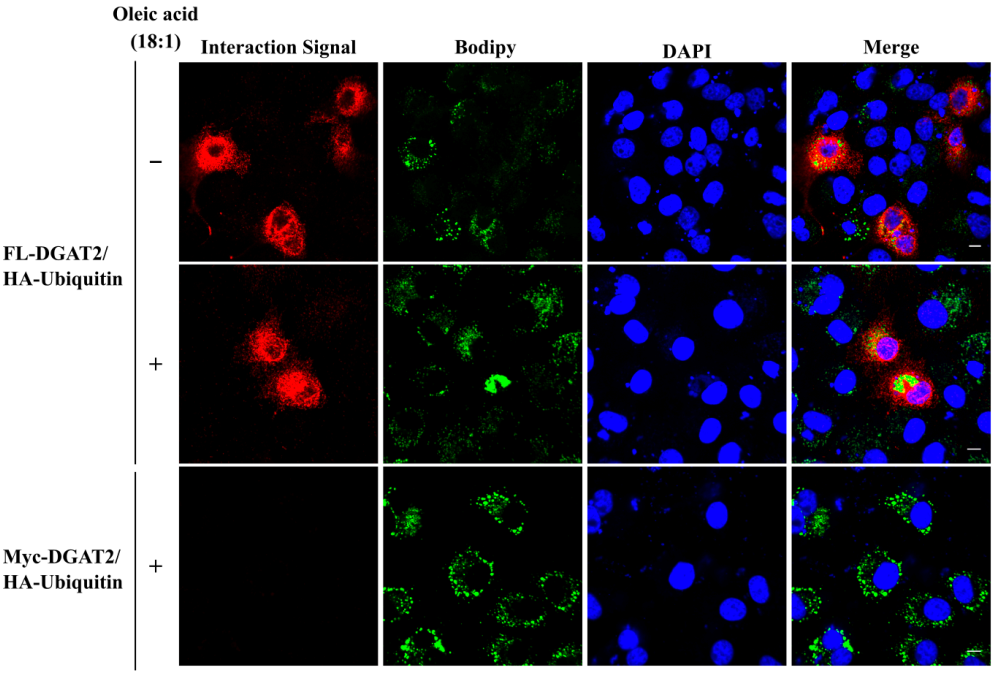

Figure 5.10. DGAT2 ubiquitination patterns are not affected by oleic acid - COS-7 cells were co-transfected with FL-DGAT2/HA-ubiquitin or control Myc-DGAT2/HA-ubiquitin and incubated approximately 18 h in the presence or absence of 0.5 mM oleic acid prior to PLA analysis. In order to visualize ubiquitinated DGAT2 relative to the total population of DGAT2 and lipid droplet position, cells were co-stained with *(A)* anti-DGAT2 or *(B)* BODIPY 493/503 respectively. Cover slips were mounted with DAPI containing medium and visualized using a confocal system. Scale bar, 10 μm.

5.3. Discussion

We used Lys-less-DGAT2 to determine if lysine residues play a catalytic role in DGAT activity. From our *in vitro* assay, it is clear that lysines are dispensable for triacylglycerol synthesis. More interesting were the effects *in situ*, in which the Lys-less mutant exhibited aberrant localization and disrupted typical lipid droplet formation. The nuclear foci observed in Lys-less-DGAT2 transfected cells are most likely accumulations of degradation resistant DGAT2. This conclusion is bolstered by similar findings from mutants DGAT2 K251, 257, 260, 264R and DGAT2 K332, 346, 353, 368, 374, 376R which contain mutation of lysines shown to induce degradation when restored in the Lys-less construct (Chapter 4.2.5.) Why DGAT2 accumulates in or around the nucleus is unclear. However, like the ER, the nucleus is enriched in components of the ubiquitin-proteasome system (Palmer *et al.*, 1996). Moreover, DGAT2 was recently discovered in intranuclear membranes and on nuclear lipid droplets, thus, it is possible there is a nuclear pathway for DGAT2 degradation (Ohsaki *et al.*, 2016). Our findings did not clearly distinguish whether the Lys-less mutant was present as insoluble aggregates in the nucleoplasm, in nuclear membranes, or in closely apposed ER membranes. This could be resolved through examining co-localization with known nuclear proteins or by isolation and analysis of nuclear fractions.

How the Lys-less-DGAT2 mutant has such a dramatic effect on triacylglycerol synthesis and lipid droplet formation *in situ*, yet retains normal *in vitro* activity is difficult to reconcile. Analysis clearly revealed that lipid droplet size and number were altered in Lys-less-DGAT2 expressing cells. Interestingly, mutation of lysines 251, 257, 260 and 264 in DGAT2 caused a significant reduction in the average size of lipid droplets, with a corresponding increase in average number of droplets. This did not affect total lipid droplet area within the cell, suggesting that some or all of these lysines may be involved in targeting DGAT2 to expanding droplets. Restoration of these residues in the Lys-less construct did not elevate total cellular lipid droplet area, again implying that additional lysines play a role in regulating DGAT activity *in situ*.

As mentioned previously, lipid concentrations have been shown to affect the turnover rate of multiple proteins involved in triacylglycerol metabolism. We identified that stimulating triacylglycerol synthesis through substrate loading or insulin treatment did not alter DGAT2 turnover. These results suggest that DGAT2 degradation is held relatively constant and

DGAT2 levels are likely controlled primarily at the level of transcription. However, it is possible that at the time of the degradation assay, after sustained treatment with oleic acid, the cells were no longer lipogenic. This was recently re-evaluated, using tandem treatment with CHX and oleic acid while omitting the oleic acid pre-treatment; DGAT2 degradation was still not inhibited (data not shown). SCD1 is another protein involved in triacylglycerol synthesis that is rapidly degraded by the ubiquitin-proteasome system independent of lipid concentrations. Incidentally, SCD1 and DGAT2 have been shown to interact when co-expressed, elevating triacylglycerol synthesis above levels when either protein was transfected individually (Man *et al.*, 2006). This cooperation could indicate similarities in post-translational regulation.

As stimulation of triacylglycerol synthesis, which triggers DGAT2 movement to lipid droplets does not stabilize DGAT2, DGAT2 situated on droplets must still be vulnerable to degradation. Consistent with this notion, DGAT2 isolated from both crude mitochondria and lipid droplet fractions was polyubiquitinated. Several questions still remain. For one, does ubiquitin have a role in targeting DGAT2 to lipid droplets? Use of linkage-specific antibodies to detect chains not typically associated with degredation may be useful in determining this. The inability of the Lys-less-DGAT2 construct to migrate to droplets provides some evidence that the process is at least lysine dependent. Secondly, can DGAT2 on lipid droplets be sent directly to the proteasome or must it first move back to the ER? Oleosins and PAT-domain containing proteins are reportedly degraded on lipid droplets (Deruyffelaere *et al.*, 2015; Kaushik and Cuervo, 2015). Multiple proteins involved in protein degradation, such as ancient ubiquitous protein 1, are present on droplets and could facilitate this process (Jo *et al.*, 2013; Klemm *et al.*, 2011; Spandl *et al.*, 2011; Olzmann *et al.*, 2013b). Yeast DGAT2 ortholog, Dga1, shuttles back to the ER under lipolytic conditions (Jacquier *et al.*, 2011). A similar mechanism could be present for DGAT2 degradation. Unfortunately, analysis of DGAT2 degradation using an ER anchored mutant provided little insight. Moreover, PLA analysis revealed that ubiquitinated DGAT2 is abundant under basal and lipogenic conditions. Also, it appeared that all DGAT2 can be potentially ubiquitinated rather than a specifically localized sub-population. Linkage specific poly-ubiquitin antibodies could again be useful in identifying traditionally non-degradative linkages.

These findings point to a protein that is constitutively ubiquitinated and rapidly degraded independent of its location or metabolic signals. As DGAT2 transcript levels have been shown to fall during fasting and increase upon refeeding, it is possible that regulation is imposed primarily at the transcriptional level (Meegalla *et al.*, 2002). This study is limited by reliance on an overexpression system; the ability to monitor endogenous DGAT2 would be beneficial. Recent findings in our lab, indirectly measuring DGAT2 turnover, support the conclusions of our overexpression system in that it is a rapidly degraded protein. 3T3-L1 adipocytes were pre-treated with DMSO or MG132 for 30 min., CHX was added to the culture media and cells were incubated for two hours. *In vitro* DGAT assays were conducted in the presence of a DGAT1 inhibitor to observe triacylglycerols produced only by DGAT2. We found that lysates obtained from cells treated with MG132, blocking DGAT2 degradation, produced significantly more triacylglycerols. This indicates that over the two hour CHX incubation, DGAT2 proteins levels fell considerably (Brandt *et al.*, 2016b). Repeating this experiment in cells treated with oleic acid or insulin would be valuable in validating our findings that DGAT2 is degraded independent of lipogenic stimuli. Additionally, it must be acknowledged that DGAT2 regulation could vary widely between tissues and what applies in human kidney cells may not be replicated in hepatocytes or adipocytes – tissues exhibiting prominent DGAT2 expression and activity.

CHAPTER 6: Identification of proteins interacting with DGAT2

6.1. Introduction

Very little is known about the identity of proteins interacting with DGAT2. Until recently, the only experimentally validated interacting partners included SCD1, MGAT2, fatty acid transport protein 1 and GPAT8 (Man *et al.*, 2006; Jin *et al.*, 2014; Xu *et al.*, 2012; Gidda *et al.*, 2011). These interactions suggest that DGAT2 is part of a large triacylglycerol synthesis complex. Identification of other binding partners could be valuable in understanding the regulatory network of DGAT2.

MGAT2 is responsible for producing diacylglycerol in the MGAT pathway, which is particularly prominent in the intestine (Johnston and Rao, 1967). Interaction of DGAT2 with MGAT2 was recently discovered (Jin *et al.*, 2014). This interaction was found to be dependent on DGAT2 TMDs. Moreover, diacylglycerol produced by MGAT2 may be utilized by DGAT2. Like MGAT2, MGAT3 exhibits a high degree of sequence similarity with DGAT2 (Cheng *et al.*, 2003). In addition to MGAT activity, MGAT3 also appears to possess significant DGAT activity (Cheng *et al.*, 2003; Cao *et al.*, 2007; Brandt *et al*., 2016a). Association of DGAT2 with MGAT3, and the possible metabolic implications have yet to be studied.

Calnexin is an integral membrane protein of the ER (Schrag *et al.*, 2001). It functions as a lectin, binding monoglucosylated glycans covalently attached to proteins undergoing folding in the ER (Hammond and Helenius, 1993, Hammond *et al.*, 1994; Helenius, 1994). The glycan acts as a tag, the composition of which signals the folding status of the protein to which it is attached. Calnexin interaction with a protein undergoing folding occurs until the glucose molecule is removed, at which point it is either properly folded or structural aberrations trigger re-glucosylation, signaling further chaperone assistance by calnexin (Hammond and Helenius, 1993, Hammond *et al.*, 1994; Helenius, 1994). Persistent interaction with lectin chaperones leads to ERAD of the improperly folded protein (Tannous *et al.*, 2015; Hebert and Molinari, 2007). Inhibition of the proteasome causes calnexin to accumulate in regions of the ER enriched in several ERAD factors and substrates (Frenkel *et al.*, 2003; Benyair *et al.*, 2015). Interestingly, calnexin has also been found to bind non-glycosylated proteins (Danilczyk and Williams, 2001). *In vitro*, calnexin binding to non-glycosylated proteins appears to inhibit aggregation (Saito *et al.*, 1999).

6.2. Results

6.2.1. Identification of DGAT2 interacting proteins by LC-MS/MS

To identify proteins interacting with DGAT2, we chose to take an unbiased mass spectrometry proteomics-based approach. HEK-293T cells were transfected with FL-DGAT2 or control Myc-DGAT2 and incubated with oleic acid to stimulate lipogenesis. Co-immunoprecipitation was conducted on total cell extracts using anti-FLAG agarose. Sample preparation and analysis by mass spectrometry was conducted in collaboration with Dr. George Katselis' Lab at the University of Saskatchewan. Samples were trypsinized prior to analysis by LC-MS/MS. Data were searched against the SWISS-PROT *Homo sapiens* database (Table 9.1). Data extractor, SpectrumMill Proteomics Workbench Version B.04.00.127 (Agilent Technologies) was used for identification of MS/MS spectra. Peptide identifications were accepted if they could be established at greater than 90.0% probability. Additionally, protein identifications were accepted if they could be established at greater than 99.0% probability and contained at least one identified peptide. Proteins identified in Myc-DGAT2 transfected samples were judged to interact non-specifically with the anti-FLAG agarose and excluded from further analysis. DGAT2 was successfully identified in the FL-DGAT2 transfected sample with 3 unique peptides and 3 unique spectra detected (Fig. 6.1 A, B). DGAT2 sequence coverage was 5.15% (Table 9.1). DGAT2 was not identified in the Myc-DGAT2 transfected control.

A.

Sequence	Observed	Actual Mass	Charge	Intensity
(K)THNLLTTR(N)	319.18	954.51	3	1.64E+06
(R)DTIDYLLSK(N)	534.27	1066.53	2	4.17E+07
(K)YIGFAPCIFHGR(G)	719.35	1436.68	2	6.84E+06

B.

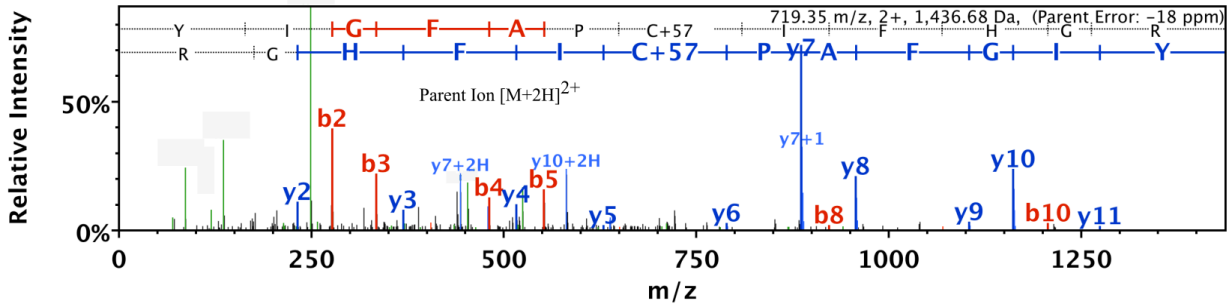

Figure 6.1. DGAT2 was successfully detected by LC-MS/MS - HEK-293T cells were transfected with FL-DGAT2 or control Myc-DGAT2 and incubated for approximately 18 h in 0.5 mM oleic acid to stimulate lipogenesis. Cells were harvested and total cell extracts prepared for co-immunoprecipitation with anti-FLAG agarose. Proteins were dissociated from anti-FLAG agarose by boiling in 2x SDS-PAGE sample buffer (+5% β-mercaptoethanol). Samples were trypsinized prior to analysis by LC-MS/MS. Data extractor, SpectrumMill Proteomics Workbench Version B.04.00.127 (Agilent Technologies) was used for identification of MS/MS spectra. Data were searched against the SWISS-PROT *Homo sapiens* database. (*A*) Three unique peptides from DGAT2 were isolated from trypsinized co-immunoprecipitation samples. Included are values for observed and actual mass, as well as peptide charge and intensity. (*B*) Representative spectrum identifying DGAT2 in co-immunoprecipitation samples.

One hundred thirty-three proteins were isolated along with DGAT2. This list was compared against The Contaminant Repository for Affinity Purification Mass Spectrometry Database. This database contains the frequency of identification for ~4500 different proteins isolated across 334 separate mass spectrometry experiments, aiding in the discrimination of common contaminants from genuine interactions (Mellacheruvu *et al.*, 2013). Frequency of identification was included for proteins present in the database (Table 9.1). Twenty of the 134 proteins identified by LC-MS/MS had a frequency of greater than 25% when scanned against the Contaminant Repository database; other proteins were also present in the database but at lower frequency (Table 9.1).

DGAT2 immunoprecipitated with several components of the proteasome, including: 26S proteasome non-ATPase regulatory subunits 11 and 14 as well as 26S protease regulatory

subunit 7. Interestingly, the E3 ubiquitin ligase, TRIM13, was isolated. Co-immunoprecipitation of these proteins with DGAT2 provides further evidence of DGAT2 regulation by the ubiquitin-proteasome system.

We were interested in the identification of calnexin in the DGAT2 immunoprecipitates (Fig. 6.2 A, B). Two unique peptides of calnexin were detected, representing 2.53% sequence coverage. In this chapter, experiments focus on confirming DGAT2 interaction with calnexin and gaining insight into the functional significance of this relationship.

A.

Sequence	Observed	Actual Mass	Charge	Intensity
(K)AEEDEILNR(S)	544.75	1087.50	2	1.98E+06
(R)KIPNPDFFEDLEPFR(M)	621.97	1862.88	3	1.31E+05

B.

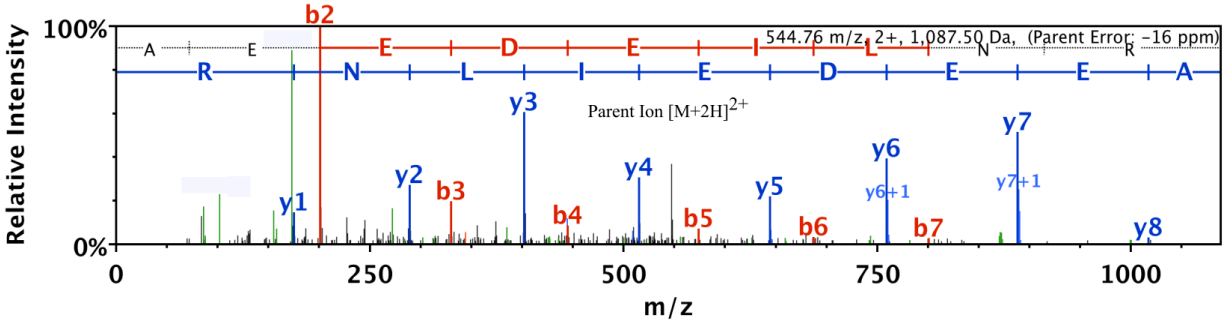

Figure 6.2. Calnexin was detected by LC-MS/MS in DGAT2 co-immunoprecipitates - HEK-293T cells were transfected with FL-DGAT2 or control Myc-DGAT2 and incubated for approximately 18 h in 0.5 mM oleic acid to stimulate lipogenesis. Cells were harvested and total cell extracts prepared for co-immunoprecipitation with anti-FLAG agarose. Proteins were dissociated from anti-FLAG agarose by boiling in 2x SDS-PAGE sample buffer (+5% β-mercaptoethanol). Samples were trypsinized prior to analysis by LC-MS/MS. Data extractor, SpectrumMill Proteomics Workbench Version B.04.00.127 (Agilent Technologies) was used for identification of MS/MS spectra. Data were searched against the SWISS-PROT *Homo sapiens* database. (*A*) Two unique peptides from calnexin were isolated from trypsinized co-immunoprecipitation samples. Included are values for observed and actual mass, as well as peptide charge and intensity. (*B*) Representative spectrum identifying calnexin in co-immunoprecipitation samples.

6.2.2. DGAT2 co-immunoprecipitated with MGAT2 and MGAT3

MGAT2 and MGAT3 are members of the DGAT2 family. They also exhibit substantial sequence similarity with DGAT2 (Fig. 6.3). Knowing that DGAT2 and MGAT2 interact, we also expected MGAT3 to interact with DGAT2. HEK-293T cells were transfected with DGAT2-HA, MGAT2-Myc-FL, MGAT3-Myc-FL, Lipin1 or LacZ. Reciprocal anti-HA and anti-FLAG immunoprecipitations were conducted on total cell extracts. Samples were separated by SDS-PAGE and analyzed by immunoblotting (Fig. 6.4). Anti-HA immunoprecipitation, followed by immunoblotting for HA, revealed DGAT2-HA isolation was successful. An identical blot was probed with anti-FLAG antibody, detecting MGAT2 and MGAT3. Lipin1 was not detected. Re-probing with an anti-calnexin antibody found calnexin only in samples transfected with DGAT2-HA. Therefore, immunoprecipitation of DGAT2 also isolated MGAT2, MGAT3 and calnexin. Conversely, anti-FLAG immunoprecipitation followed by anti-FLAG immunoblotting showed that MGAT2, MGAT3 and Lipin1 were successfully isolated. Calnexin was detectable only in MGAT2 transfected samples. Anti-FLAG immunoprecipitates probed with an anti-HA antibody revealed DGAT2-HA was present in MGAT2, MGAT3 and Lipin1 isolates. Our lab has previously identified interaction of DGAT2 with Lipin1 (Jin *et al.*, 2014). Why DGAT2 was present in Lipin1 immunoprecipitates but Lipin1 was not detected in DGAT2 immunoprecipitates is unclear. Immunoblotting with an anti-Hsp70 antibody returned no signal, demonstrating co-immunoprecipitation specificity. To summarize, reciprocal interaction between DGAT2 and MGAT2/MGAT3 were demonstrated. Immunoprecipitation of DGAT2 did not isolate Lipin1 while DGAT2 did co-immunoprecipitate with Lipin1. Calnexin was detected in all DGAT2-HA derived co-immunoprecipitations.

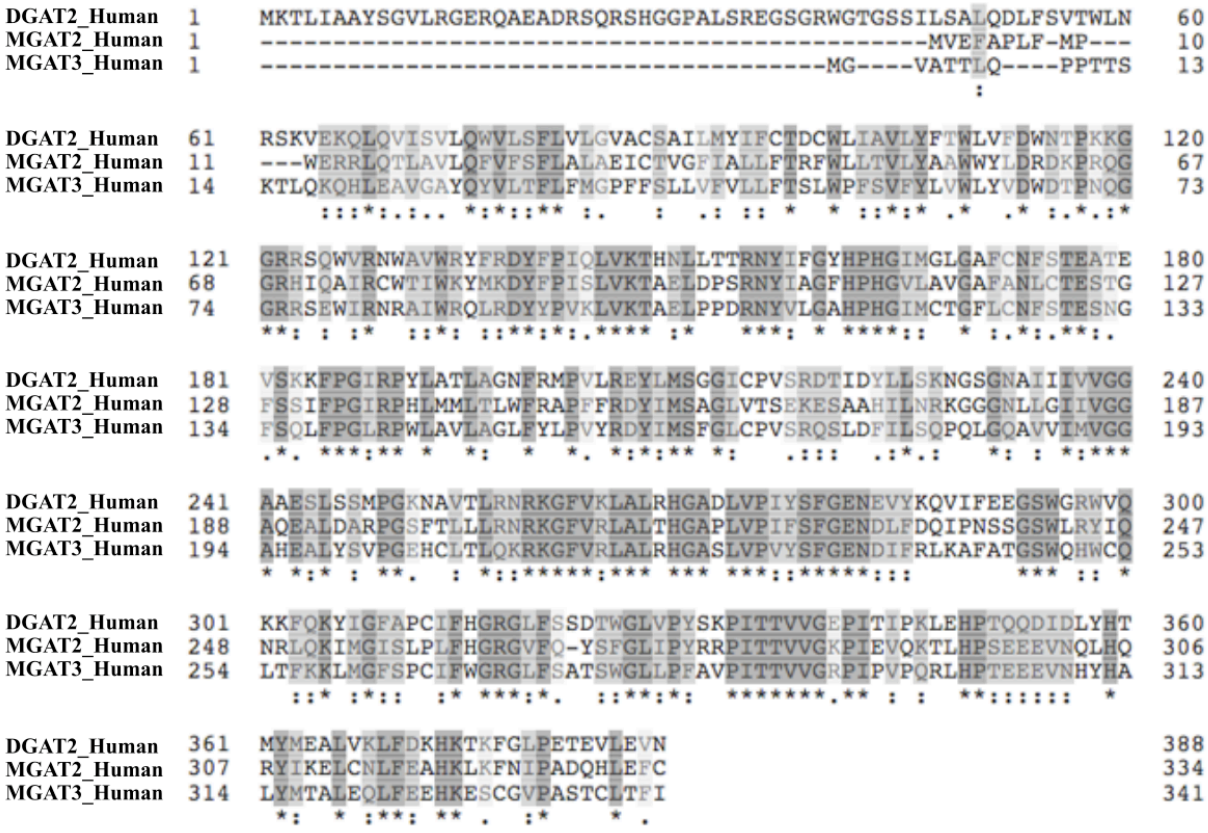

Figure 6.3. DGAT2, MGAT2 and MGAT3 exhibit high sequence similarity – Multiple sequence alignment comparing human DGAT2, MGAT2 and MGAT3. '*' denotes identical residues. ':' refers to conservation between groups of strongly similar properties. '.' refers to conservation between groups of weakly similar properties.

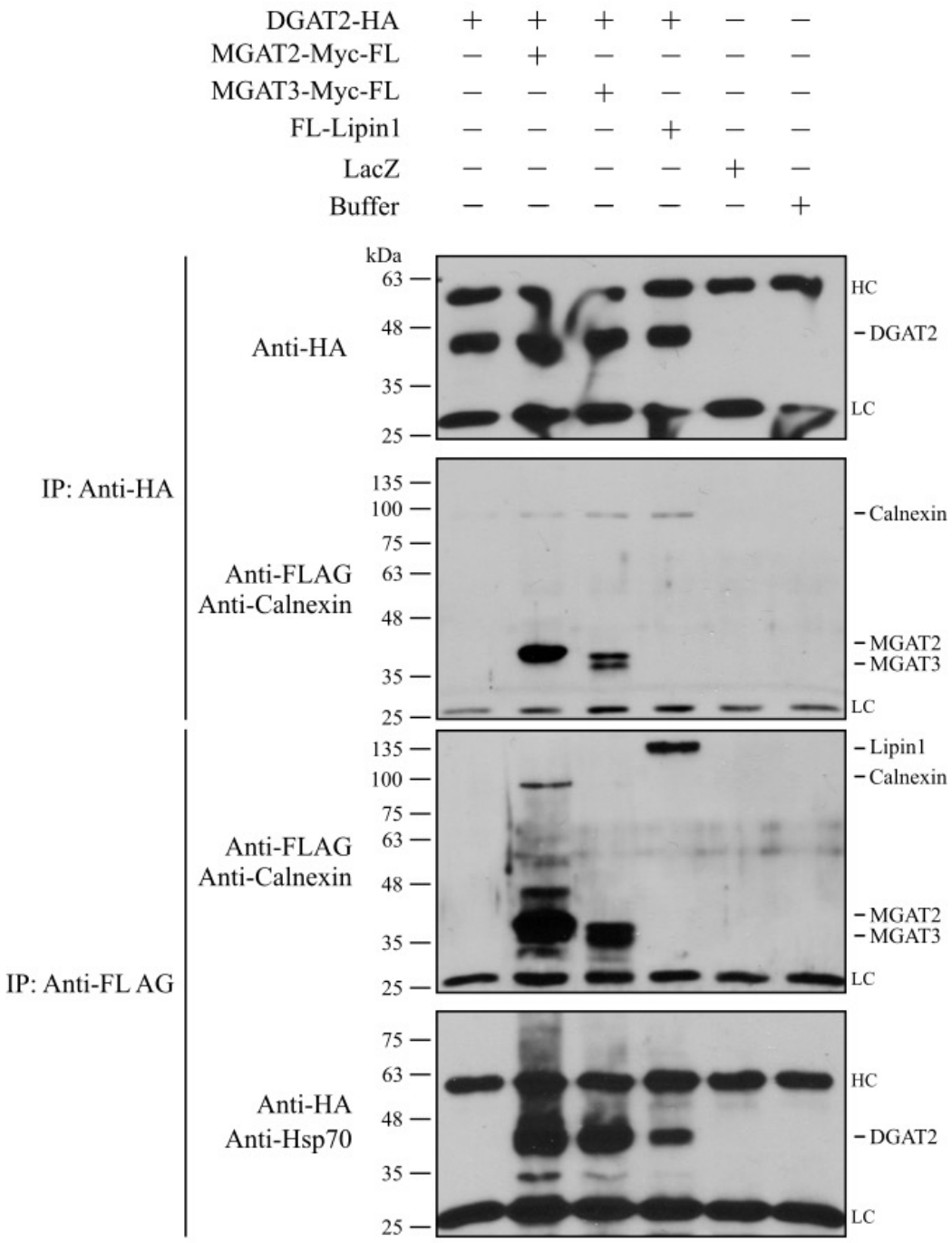

Figure 6.4. DGAT2 co-immunoprecipitated with MGAT2 and MGAT3 – HEK-293T cells were transfected with DGAT2-HA, MGAT2-Myc-FL, MGAT3-Myc-FL, Lipin1 or LacZ. Reciprocal anti-HA and anti-FLAG co-immunoprecipitation were conducted on total cell extracts. Samples were analyzed by SDS-PAGE and immunoblotting with anti-HA, anti-FLAG, anti-calnexin and anti-Hsp70 specific antibodies. IP represents immunoprecipitation. HC and LC represent antibody heavy and light chains respectively.

6.2.3. DGAT2 interacts with MGAT2 and MGAT3 *in situ*

To confirm *in vitro* evidence of DGAT2 interaction with MGAT2 and MGAT3, we used a proximity ligation assay to examine the interactions *in situ*. FL-DGAT2 and Myc-DGAT2 were transfected into COS-7 cells individually or in tandem. PLA analysis was conducted as previously described. Samples were probed with anti-FLAG and anti-Myc specific antibodies. No interaction signal was detected when either protein was transfected individually. When co-transfected, a strong interaction signal was observed, indicating DGAT2 interaction with MGAT2 (Fig. 6.5). An analogous experiment was conducted to confirm DGAT2 *in situ* interaction with MGAT3. COS-7 cells were co-transfected with Myc-DGAT2 and FL-MGAT3 or with DGAT2-HA and FL-MGAT3. Samples were probed with anti-Myc and anti-FLAG specific antibodies (Fig. 6.6). No signal was detected in the DGAT2-HA/FL-MGAT3 samples, as the Myc-tag is absent. An interaction signal was visible in the Myc-DGAT2/FL-MGAT3 co-transfection, thus DGAT2 does interact with MGAT3 *in situ*.

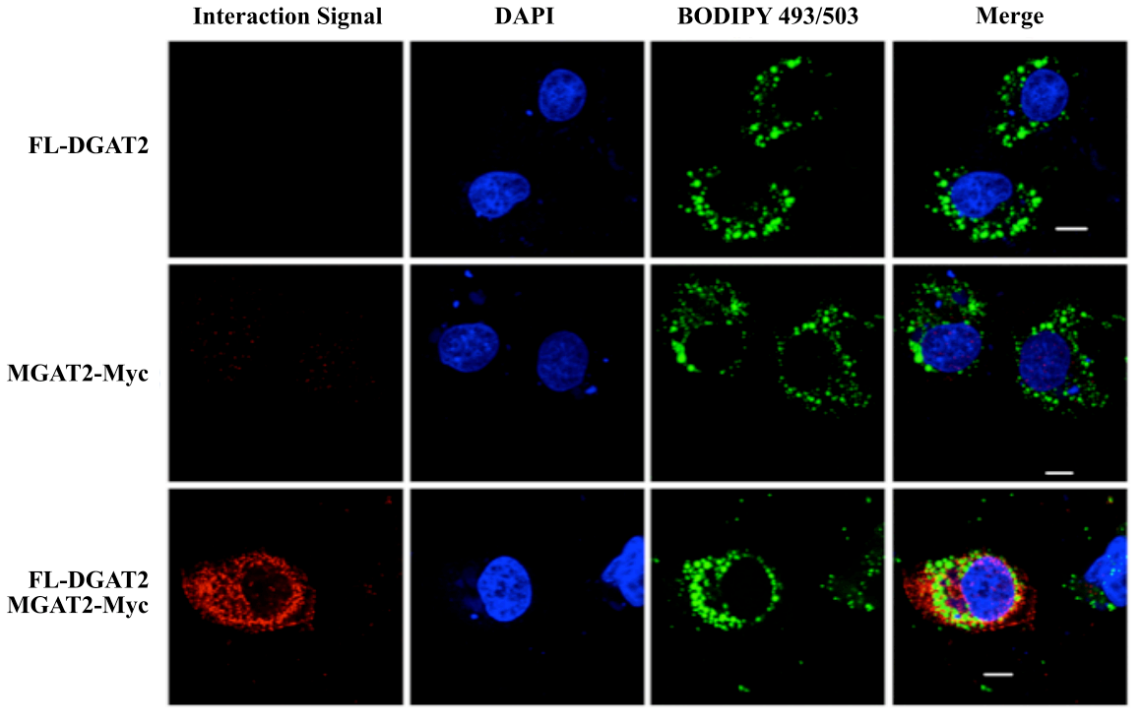

Figure 6.5. Interaction of DGAT2 and MGAT2 was detected *in situ* by proximity ligation assay - COS-7 cells expressing either FL-DGAT2, MGAT2-Myc, or both together were stained with anti-FLAG and anti-Myc antibodies. Interaction signals were detected using a Duolink® detection kit. Nuclei were stained with DAPI and lipid droplets were stained with BODIPY 493/503. Scale bar, 10 µm.

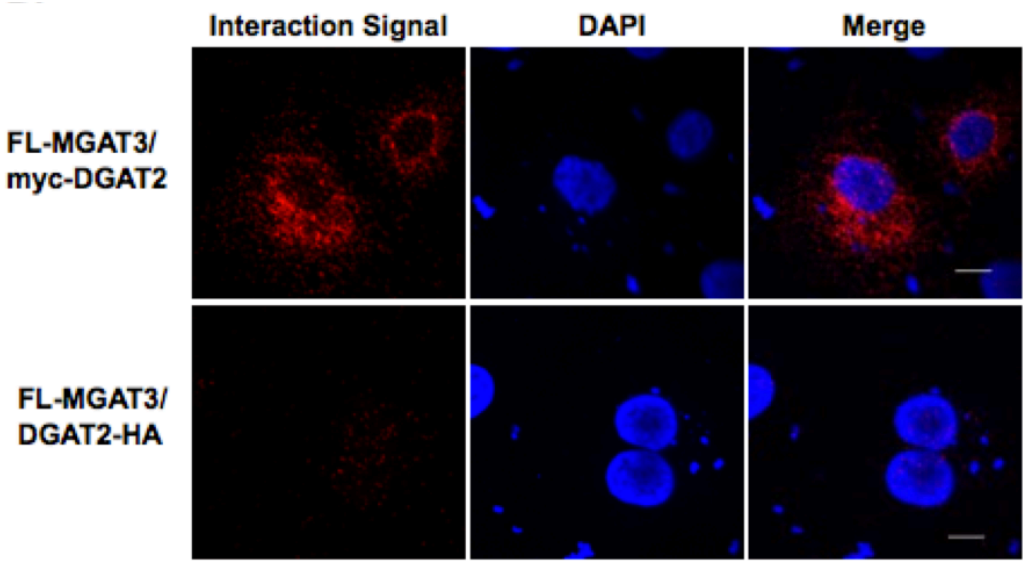

Figure 6.6. Interaction of DGAT2 and MGAT3 was detected *in situ* by proximity ligation assay - COS-7 cells expressing either myc-DGAT2 and FL-MGAT3 or DGAT2-HA and FL-MGAT3 were incubated with anti-FLAG and anti-Myc antibodies. Interaction signals were detected using a Duolink® detection kit. Nuclei were stained with DAPI. Scale bar, 10 μm.

6.2.4. Calnexin co-immunoprecipitated with DGAT2 and MGAT2

Like DGAT2, calnexin is an integral membrane protein of the ER. It has also been identified as a member of the lipid droplet proteome through mass spectrometry studies (Hodges and Wu , 2010; Bouchoux *et al.*, 2011). Calnexin was one of the proteins identified to interact with DGAT2 by mass spectrometry and was also isolated with DGAT2 when analyzing DGAT2 interaction with MGAT2/3 (Fig. 6.2, 6.4). We chose to examine whether MGAT2 and MGAT3 also interact with calnexin and if these interactions were glycosylation dependent. HEK-293T cells were transfected with FL-DGAT2, FL-MGAT2, FL-MGAT3 or Myc-DGAT2. Cells were treated in the presence or absence of tunicamycin, an inhibitor of N-glycosylation. Tunicamycin inhibits the transfer of N-acetylglycosamine 1-phosphate to dolichol monophosphate (Heifetz *et al.*, 1979). Samples were subjected to anti-FLAG immunoprecipitation prior to SDS-PAGE and immunoblotting. Anti-FLAG immunoblotting revealed that FL-DGAT2, FL-MGAT2 and FL-MGAT3 were successfully expressed and immunoprecipitated (Fig. 6.7A, B). Anti-Myc immunoblotting showed Myc-DGAT2 was only

detected in total cell extracts. Blotting with an anti-calnexin antibody revealed that it was present in anti-FLAG isolates from DGAT2 and MGAT2, but not MGAT3, transfected cells (Fig. 6.7B). The calnexin band is slightly obscured by a non-specific band located marginally above it in the anti-FLAG immunoprecipitates, but is still visible. Re-blotting with an antibody specific to lamin isoforms A and C yielded a signal in total cell extracts but not immunoprecipitates, demonstrating interaction specificity. Tunicamycin did not have any apparent effect on calnexin interaction with DGAT2 and MGAT2, suggesting that the interaction is not glycosylation dependent.

A.

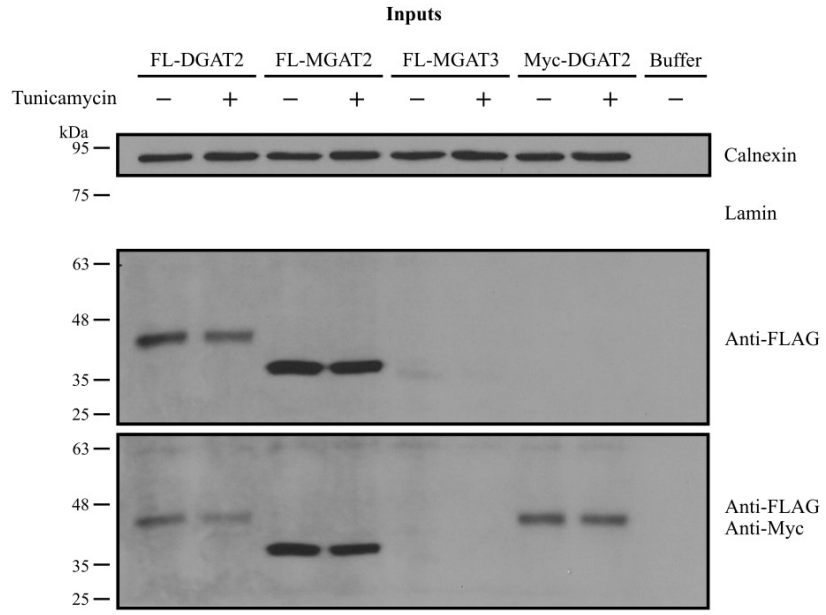

B.

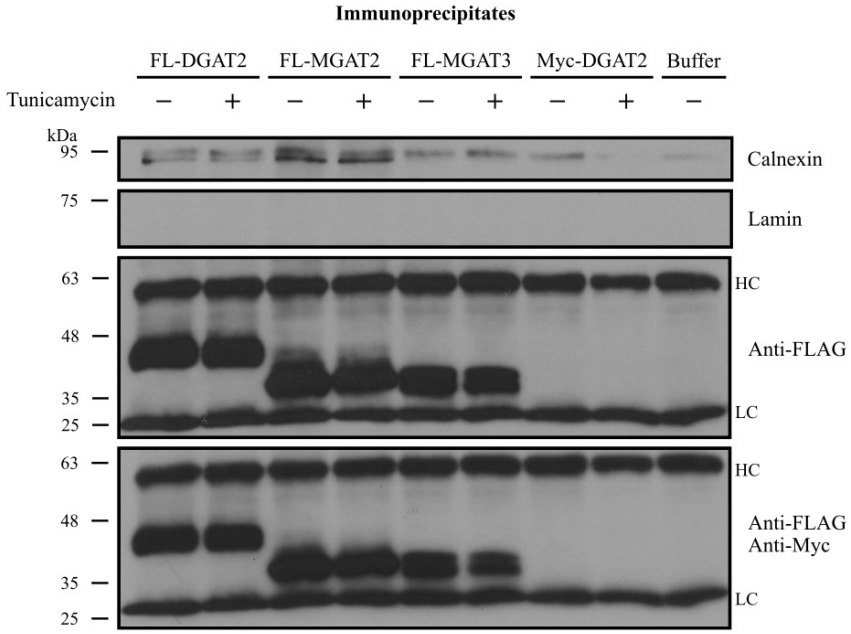

Figure 6.7. Calnexin co-immunoprecipitated with DGAT2 and MGAT2 via a glycosylation independent mechanism – *(A)* HEK293T cells were transfected with FL-DGAT2, FL-MGAT2, FL-MGAT3 or Myc-DGAT2 and treated with 5 μg/mL of glycosylation inhibitor, tunicamycin, or an equal volume of DMSO, for 21 h. Total cell extracts were isolated and analyzed by SDS-PAGE and immunoblotting with anti-FLAG, anti-Myc, anti-calnexin and anti-lamin specific antibodies. (*B)* Total cell extracts were subjected to anti-FLAG immunoprecipitation. Immunoprecipitates were analyzed by SDS-PAGE and immunoblotting with anti-FLAG, anti-Myc, anti-calnexin and anti-lamin specific antibodies. Control immunoprecipitations were performed on Myc-DGAT2 transfected cells and with buffer alone. HC and LC represent antibody heavy and light chains respectively.

6.2.5. Calnexin interacts with DGAT2 *in situ*

Having identified that calnexin interacts with DGAT2 *in vitro*, we chose to examine this relationship *in situ.* COS-7 cells were transfected with FL-DGAT2 or Myc-DGAT2. Interaction with endogenous calnexin was tested by PLA using anti-FLAG and anti-calnexin antibodies. A clear interaction signal was observed in FL-DGAT2 transfected samples but not in those transfected with Myc-DGAT2 (Fig. 6.8). This demonstrates that DGAT2 interacts with calnexin *in situ*.

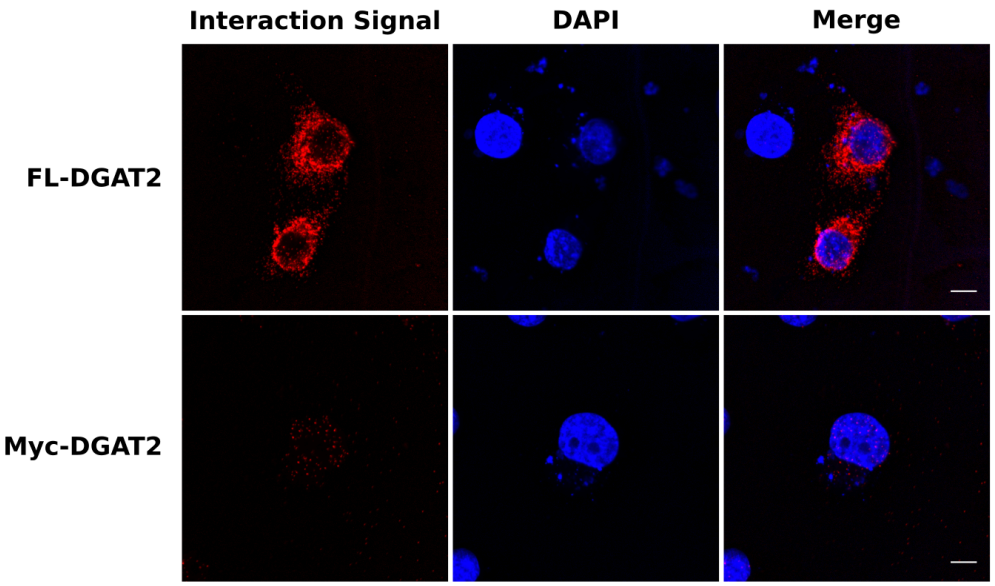

Figure 6.8. Calnexin interaction with DGAT2 was detected *in situ* by proximity ligation assay - COS-7 cells expressing either FL-DGAT2 or Myc-DGAT2 were incubated with anti-FLAG and anti-calnexin antibodies. Interaction signals were detected using a Duolink® detection kit. Nuclei were stained with DAPI. Scale bar, 10 μm.

6.2.6. Calnexin is present in the lipid droplet fraction in MGAT2 and DGAT2 transfected cells

We have identified that calnexin interacts with DGAT2 and MGAT2 *in vitro* and confirmed DGAT2 interaction *in situ*. We next decided to determine if calnexin is present on lipid droplets in MGAT2 and DGAT2 transfected cells. HEK-293T cells were transfected with FL-DGAT2, MGAT2-Myc or both in tandem. Crude mitochondria and lipid droplet fractions were isolated through differential- and sucrose gradient–centrifugation. Samples were subsequently analyzed by SDS-PAGE and immunoblotting (Fig. 6.9). Fraction identity was

evaluated with marker protein specific antibodies for Hsp70 (mitochondria) and perilipin-2 (lipid droplet). FL-DGAT2 and FL-DGAT2/MGAT2-Myc co-transfection increased lipid droplet production, as signified by the accumulation of perilipin-2. Anti-calnexin immunoblotting showed that calnexin was in crude mitochondria and fat fractions for each transfection group. Like DGAT2, calnexin is enriched in MAM present in the crude mitochondria fraction (Cuie *et al.* 1993; Rusinol *et al.* 1994; Stone *et al.* 2009; Stone and Vance 2000; Lynes *et al.*, 2013).

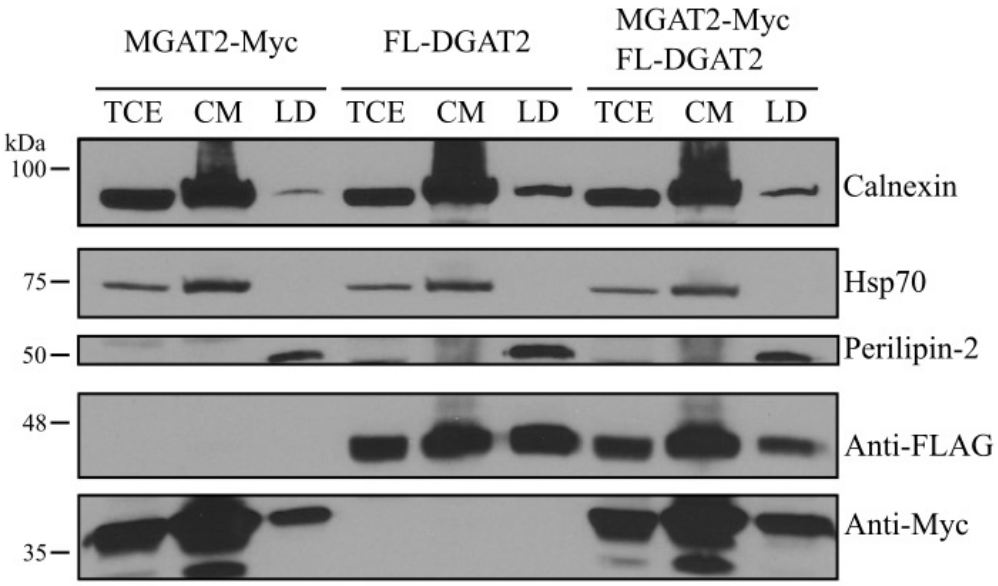

Figure 6.9. Calnexin is localized to lipid droplets in MGAT2 and DGAT2 transfected cells - HEK-293T cells were transfected with MGAT2-Myc or FL-DGAT2, individually or in tandem. Crude mitochondria (CM) and lipid droplet (LD) fractions were isolated from total cell extracts (TCE) through differential- and sucrose gradient–centrifugation. Samples were subsequently analyzed by SDS-PAGE and immunoblotting. Fraction identity was evaluated with marker protein specific antibodies for Hsp70 (mitochondria) and perilipin-2 (lipid droplet). DGAT2 and MGAT2 were detected with anti-FLAG and anti-Myc antibodies respectively.

6.2.7. Calnexin knockout mouse embryonic fibroblasts exhibited reduced lipid droplet size

To gain insight into the role of calnexin in lipid droplet metabolism, we chose to examine lipid droplet production in calnexin knockout versus wild-type mouse embryonic fibroblasts. Wild-type and calnexin knockout cell lines were a gift from Dr. Marek Michalak at the University of Alberta. To first confirm that calnexin is efficiently knocked-out, cells were harvested and total cell extracts analyzed by SDS-PAGE and immunoblotting (Fig. 6.10A). Calnexin was abundant in wild-type mouse embryonic fibroblasts and in the HEK-293T

control, but absent in the knockout cell line. Immunoblotting with an anti-Hsp70 specific antibody demonstrated equal protein levels in all samples. To compare lipid droplet production in each cell line, cells were treated with oleic acid for 18 h to stimulate lipogenesis prior to preparation for immunofluorescence microscopy. Lipid droplets were visualized by BODIPY 493/503 staining; representative images of total cell populations were obtained by immunofluorescence microscopy (Fig. 6.10B). Lipid droplet production was clearly hindered in calnexin knockout mouse embryonic fibroblasts. The wild-type cells typically produced lipid droplets of larger average size when compared to the calnexin knockout cell line.

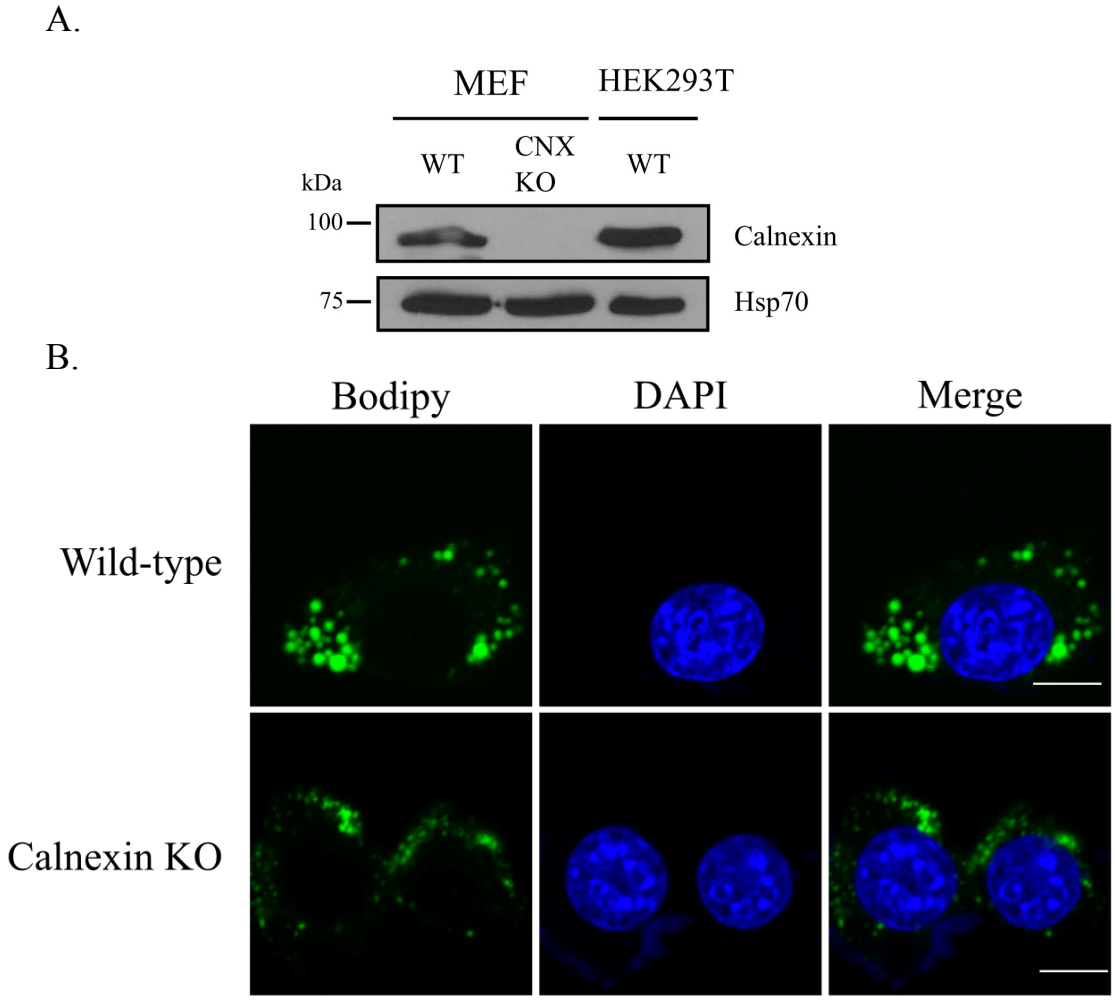

Figure 6.10. Calnexin knockout mouse embryonic fibroblasts produced smaller lipid droplets than wild-type - (*A*) Wild-type and calnexin knockout mouse embryonic fibroblasts total cell extracts were analyzed by SDS-PAGE and immunoblotting with calnexin and Hsp70 specific antibodies. (*B*) Mouse embryonic fibroblasts were treated for 18 h with oleic acid prior to immunofluorescence microscopy. Lipid droplets were visualized with BODIPY 493/503 and cell nuclei with DAPI containing mounting medium. These images are representative of the total cell populations. Scale bar, 10 μm.

6.3. Discussion

Relatively little is known about proteins that interact with DGAT2. We chose to take a mass spectrometry approach in order to identify proteins that bind and potentially influence post-translational regulation of DGAT2. As detection of endogenous DGAT2 is not possible with current tools, we overexpressed an epitope tagged construct in human kidney cells. While DGAT2 was successfully detected by mass spectrometry, the sequence coverage was lower than we would have hoped. The exact reason for this is unclear but the large number of potential trypsin cleavage sites within DGAT2 could yield relatively short peptides, reducing the probability of identification. Nevertheless, many interesting proteins were found to precipitate with DGAT2. In addition to subunits of the proteasome, several other proteins involved in the ubiquitin-proteasome and associated ERAD pathways were revealed. For example, B-cell receptor–associated protein 31 is a chaperone that plays a role in targeting proteins to the ERAD pathway, while COP9 signalosome complex (CSN) subunit 1 is essential in CSN mediated regulation of SCF E3 ligases (Wang et a., 2008; Wang *et al.*, 2015). Also, the E3 ubiquitin ligase, TRIM13, was recognized. To this point, the only E3 ligase implicated in DGAT2 regulation was AMFR (Choi *et al.*, 2014). The TRIM family of proteins, of which there are greater than 70, are RING-type E3 ligases (Ozato *et al.*, 2008). TRIM13 is ER anchored and has been implicated in degradation of ERAD substrates through the proteasome and autophagy pathways (Lerner *et al.*, 2007; Tomar *et al.*, 2012).

Several proteins involved in lipid metabolism were also found to interact with DGAT2. Sterol-4-alpha-carboxylate 3-dehydrogenase is involved in cholesterol biosynthesis, while tafazzin and stomatin-like protein 2 both play roles in cardiolipin metabolism (Caldas and Herman, 2003;Vaz *et al.*, 2003; Christie *et al.*, 2011). Finally, very-long-chain enoyl-CoA reductase catalyzes the final four reactions of the long-chain fatty acid elongation cycle (Moon and Horton, 2003). Unfortunately, MGAT proteins were not detected. In human kidney, MGAT2 is higly expressed, however, protein levels may be low, as MGAT activity appears to be modest (Yen and Farese, 2003).

Intriguingly, several proteins involved in nuclear trafficking were detected, including: importin subunit beta-1, importin-4, exportin-7 and nuclear pore complex protein Nup98-Nup96 (Jaekel and Goerlich, 1998, Jaekel *et al.*, 2002; Mingot *et al.* 2004; Krull *et al.*, 2004). The existence of lipid droplets in the nucleus has been reported, however, until recently it has

been unclear whether these lipid droplets are in the nucleoplasm or are situated on the cytoplasmic face of invaginations in the nuclear envelope (Hillman and Hillman, 1975; Layerenza *et al.*, 2013; Uzbekov and Roingeard, 2013). Recent evidence suggests that lipid droplets do exist in the nucleoplasm in cell lines such as Huh7, HepG2 and Mc-RH7777 (Ohsaki *et al.*, 2016). It appears that triacylglycerols can be synthesized in the nucleus, as newly produced lipid esters were directly incorporated into nuclear lipid droplets; DGAT2 was able to localize to these same lipid droplets. The physiological role of nuclear lipid droplets and the mechanism of DGAT2 relocalization are currently unknown.

Calnexin was one of the proteins discovered to interact with DGAT2 by mass spectrometry. We chose to confirm this finding and examine whether other DGAT2 family members shared this interaction. We found that calnexin co-immunoprecipitated with DGAT2 and MGAT2 but not MGAT3. DGAT2 interaction with calnexin was also demonstrated *in situ*. DGAT2, MGAT2, and likely MGAT3, containing only a short luminal loop with no aspartate residues, are unlikely targets for N-glycosylation (Stone *et al.*, 2006; McFie *et al.*, 2014; McFie *et al.*, unpublished; Anderson *et al.*, 1996). Yet, there is evidence that calnexin can bind non-glycosylated proteins via a region in close proximity to the glycan-binding site within the globular domain (Danciczyk *et al.*, 2001; Wijeyesakere *et al.*, 2013). Additionally, it has been reported that calnexin is able to monitor the assembly of transmembrane domains within the ER membrane, binding to misfolded regions in a glycan-independent manner (Swanton *et al.*, 2003). To address whether DGAT2 and MGAT2 interaction with calnexin was glycosylation dependent, cells were treated with the glycosylation inhibitor, tunicamycin, prior to co-immunoprecipitation. We found that calnexin was still isolated with DGAT2 and MGAT2 in the presence of tunicamycin. These results need to be confirmed in the presence of a positive control whose interaction with calnexin is disrupted upon inhibition of glycosylation.

Like DGAT2, calnexin is enriched in MAM of the ER (Cuie *et al.* 1993; Rusinol *et al.* 1994; Stone *et al.* 2009; Stone and Vance, 2000; Lynes *et al.*, 2013). Under normal conditions, calnexin is preferentially relegated to MAM; ER stress causes calnexin to become palmitoylated and transition to the rough ER where it aids in protein quality control (Lynes *et al.*, 2013). Calnexin has previously been detected in the lipid droplet proteome but its function remains unknown (Brasaemle *et al.*, 2004; Turró *et al.*, 2006; Bartz *et al.*, 2007b; Cho *et al.*, 2007; Bouchoux *et al.*, 2011). As MGAT2 does not traffic to lipid droplets unless co-expressed

with DGAT2, it suggests that the interaction detected through co-immunoprecipitation was between ER localized MGAT2 and calnexin (Jin *et al.*, 2014). Because DGAT2 is highly similar to MGAT2, interaction with calnexin at the ER can likely be extrapolated. Whether DGAT2 or MGAT2 can interact with calnexin on the surface of lipid droplets has yet to have been explored.

We demonstrated that calnexin knockout mouse embryonic fibroblasts were unable to produce large lipid droplets when treated with oleate. This provides evidence that calnexin may play a role in lipid droplet biogenesis. Nevertheless, it is still possible that perturbed lipid droplet formation could be a result of loss of calnexin chaperone function, leading to insufficient quantities of proteins involved in pathways of triacylglycerol synthesis and lipid droplet formation. Quantification of lipid droplets in calnexin knockout and wild-type cells would be beneficial. Treating wild-type cells with tunicamycin to inhibit glycosylation could help to illuminate whether this effect if dependent on calnexin lectin function. Alternatively, if expression of mutant calnexin, deficient in carbohydrate binding, restored droplet formation in knockout cells, it would demonstrate that calnexin plays a more direct role in lipid droplet production.

The functional significance of DGAT2 family member interactions has not been extensively studied. We identified that DGAT2 co-immunoprecipitated with MGAT2 and MGAT3; this interaction was confirmed *in situ*. Interestingly, further characterization of the MGAT3 construct used in the DGAT2 co-immunoprecipitation study (Fig. 6.4) revealed that it contained an inactivating C265Y mutation that was initially undetected. Co-immunoprecipitation of DGAT2 and MGAT3 was repeated using a wild-type MGAT3 construct. It was verified that C265Y did not alter MGAT3 interaction with DGAT2 (data not shown). Unfortunately, the manufacturer of the mutant MGAT3 cDNA would not disclose the origin of the cDNA. All additional experiments utilizing MGAT3 were performed with the wild-type construct.

As DGAT2 has been shown to form homodimers, it is possible that the high degree of sequence conservation allows for heterodimer formation between DGAT2, MGAT2 and MGAT3 (Jin *et al.*, 2014). Co-expression of DGAT2 and MGAT2 has been shown to increase triacylglycerol synthesis (Jin *et al.*, 2014). Increased efficiency in substrate channeling,

through DGAT2/MGAT2 interaction, is one mechanism by which this could occur. The metabolic effects of DGAT2 and MGAT3 interaction have not been studied.

CHAPTER 7: DGAT2 family protein interactions and regulation by ERAD

7.1. Introduction

ERAD is responsible for clearing polypeptides that fail to achieve the proper folded confirmation, an indispensible process in maintaining ER homeostasis in eukaryotes (Hartl and Hayer-Hartl, 2009). Dysfunction can lead to the accumulation of misfolded proteins in the lumen and membrane of the ER, causing proteotoxicity that has been linked to several diseases (Walter *et al.*, 2011; Guerriero and Brodsky, 2012). In addition to its role in the degradation of improperly folded proteins, ERAD is involved in the targeted degradation of several native proteins of the ER membrane and lumen. The ERAD pathway is required for the destruction of these proteins as they must transition across the ER membrane to the cytosol prior to being delivered to the proteasome (Wiertz *et al.* 1996; Ye *et al.* 2001; Lilley and Ploegh, 2004; Kalies *et al.*, 2005; Kreft *et al.*, 2006; Scott and Shekman, 2008; Horn *et al.*, 2009; Carvalho *et al.*, 2010; Mehnert *et al.*, 2014). Many of the native proteins regulated by ERAD are involved in lipid metabolism (Shimakata *et al.*, 1972; Mitchell *et al.*, 1998; Lee *et al.*, 2006; Choi *et al.*, 2014). A functional relationship between ERAD and lipid droplets has been proposed on the evidence that several ERAD substrates and factors have been identified in the lipid droplet proteome following proteasome inhibition (Hartman *et al.* 2010; Ohsaki *et al.* 2006).

DGAT2 has been found to be part of a triacylglycerol synthesis complex with several proteins, one of which is MGAT2 (Man *et al.*, 2006; Jin *et al.*, 2014; Xu *et al.*, 2012; Gidda *et al.*, 2011). DGAT2 and MGAT2 possess a high degree of sequence identity and have been observed to cooperate in the synthesis of triacylglycerols (Jin *et al.*, 2014). MGAT3 exhibits greater sequence identity with DGAT2 than with other MGATs. Also, it possesses both MGAT and DGAT activity, suggesting it may have arisen from a gene duplication event (Hall *et al.*, 2012; Cheng *et al.*, 2003; Cao *et al.*, 2007). DGAT2, MGAT2 and MGAT3 are all believed to be transmembrane proteins of the ER, with similar membrane topographies (Stone *et al.* 2006; McFie *et al.*, 2014; McFie *et al.*, 2016). We believe than MGAT2 and MGAT3, like DGAT2, are regulated by the ubiquitin proteasome system and that the ERAD pathway plays a role in their destruction (Choi *et al.*, 2014)

7.2. Results

7.2.1. MGAT2 is ubiquitinated

We chose to examine MGAT2 ubiquitination, believing that the considerable sequence similarity with DGAT2, coupled with its ability to interact with DGAT2, made MGAT2 a likely candidate for ubiquitin conjugation. HEK-293T cells were transfected with MGAT2-Myc-FL or MGAT2-Myc and treated in the presence or absence MG132. MGAT2-Myc-FL was isolated by anti-FLAG immunoprecipitation prior to analysis by immunoblotting (Fig. 7.1). MGAT2-Myc-FL was detected in total cell extracts and immunoprecipitates. Probing for ubiquitin revealed the typical polyubiquitin smear both in the presence and absence of MG132, signifying MGAT2 is polyubiquitinated. No ubiquitin signal was observed in anti-FLAG immunoprecipitates from MG132 treated MGAT2-Myc expressing cells. Notably, a strong increase in ubiquitin signal was not seen in MG132 treated MGAT2 samples, however the increase in ubiquitination of the corresponding total cell extracts was also modest.

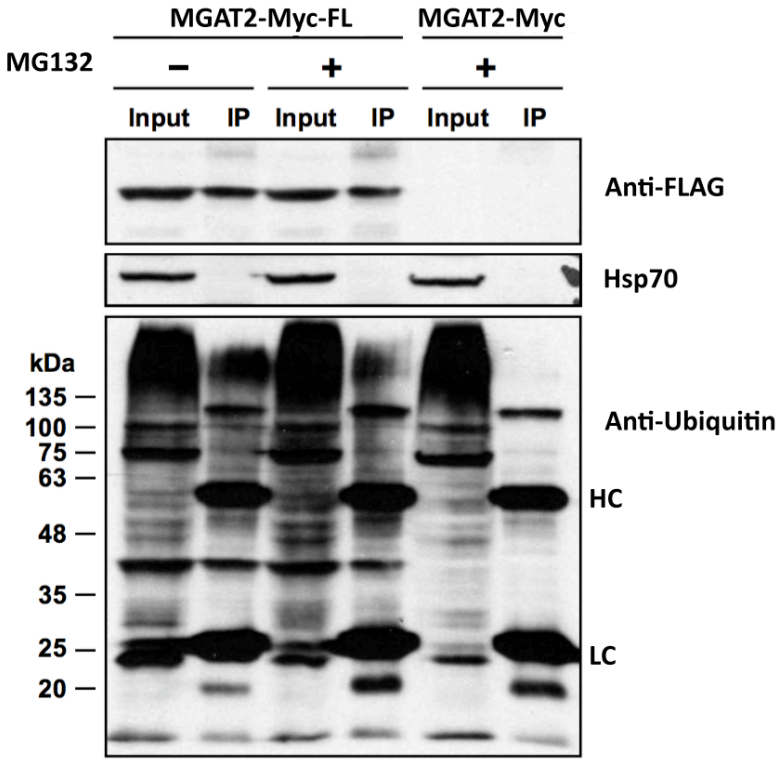

Figure 7.1. MGAT2 is ubiquitinated - HEK-293T cells were transfected with MGAT2-Myc-FL or MGAT2-Myc constructs. Cells were incubated with 10 μM MG132 or an equal volume of DMSO for a period of 2 h prior to isolation of total cell extracts. FLAG-tagged proteins were precipitated with anti-FLAG agarose. Samples were separated by SDS-PAGE and immunoblotted with anti-FLAG, anti-ubiquitin and anti-Hsp70.

Proximity ligation assay was utilized to confirm MGAT2 ubiquitination. COS-7 cells were co-transfected with MGAT2-Myc-FL and HA-ubiquitin in the presence or absence of oleic acid. Transfection with Myc-DGAT2 and HA-ubiquitin was included as a negative control. Anti-FLAG and anti-HA antibodies were used to detect interaction. Ubiquitinated MGAT2 was detected in the presence and absence of oleic acid; no signal was observed in the negative control (Fig. 7.2). Co-staining to detect MGAT2, lipid droplets and DGAT2 was also included. These results confirm that MGAT2 is ubiquitinated *in situ*.

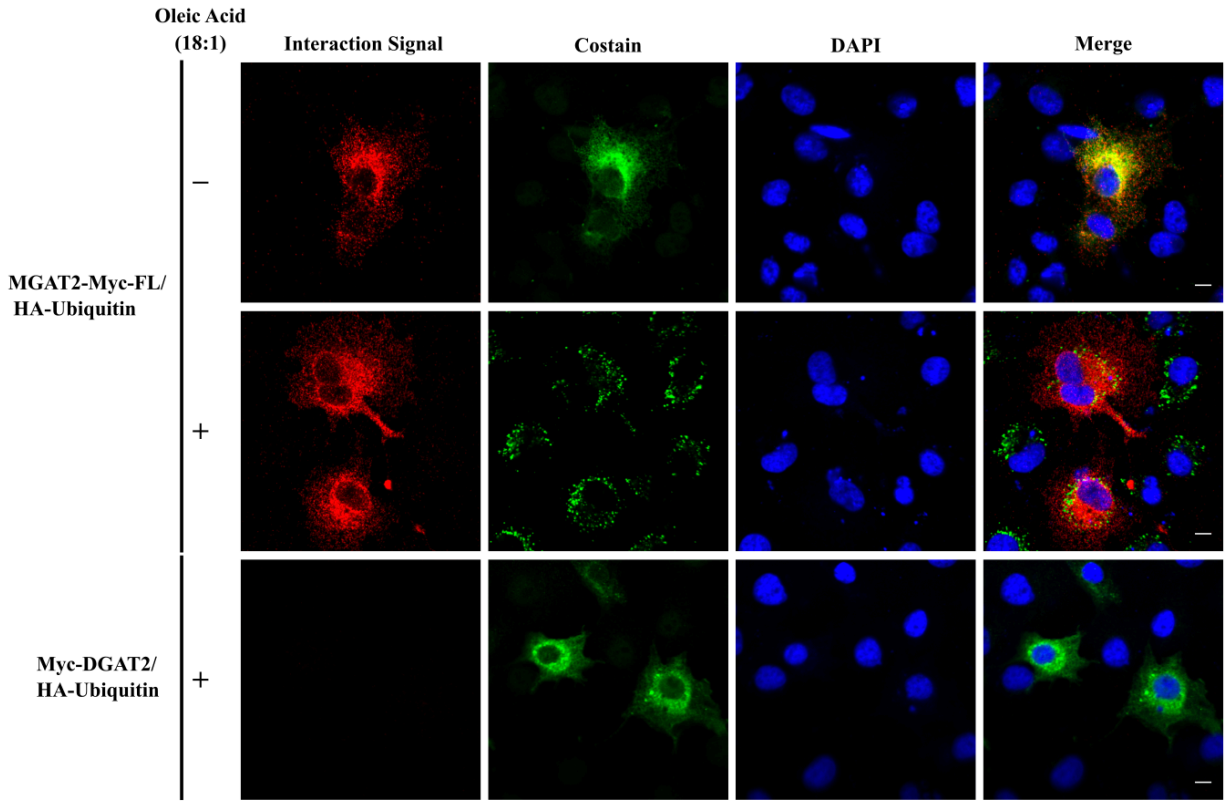

Figure 7.2. MGAT2 is ubiquitinated *in situ* - COS-7 cells were co-transfected with MGAT2-Myc-FL and HA-ubiquitin or with control Myc-DGAT2 and HA-ubiquitin prior to incubation in the presence or absence of 0.5 mM oleic acid for ~18 hr. Samples were probed with anti-FLAG and anti-ubiquitin antibodies and analyzed by proximity ligation assay. Cells were co-stained with anti-Myc and anti-DGAT2 to show MGAT2 and DGAT2 respectively. Lipid droplets were stained with BODIPY 493/503 and cell nuclei with DAPI. Scale bar, 10 μm.

7.2.2. DGAT2 and MGAT2 are regulated by ERAD

As DGAT2 and MGAT2 are both ubiquitinated membrane proteins of the ER, they are likely regulated by the ERAD pathway. To examine this, HEK-293T cells were co-transfected with FL-DGAT2 and HA-ubiquitin or control Myc-DGAT2 and HA-ubiquitin prior to treatment with eeyarestatin I (EerI). EerI directly inhibits VCP/p97 and the associated deubiquitinase, ataxin-3 (Wang *et al.*, 2008, 2010). Ultimately, this inhibits ERAD by blocking retrotranslocation out of the ER and into the cytosol (Cross *et al.*, 2009; Aletrari *et al.*, 2011). Samples were analyzed by SDS-PAGE and immunoblotting. Probing with anti-FLAG and anti-Myc antibodies demonstrated that FL-DGAT2 was successfully isolated, while Myc-DGAT2, as expected, was not present following ant-FLAG IP (Fig. 7.3). Interestingly, a band the approximate size of a DGAT2 dimer (~85 kDa) was detectable in total cell extracts in EerI treated cells. It was not present in the IP sample but may have been visible with a longer exposure. Detection of ubiquitin conjugates with anti-HA clearly revealed a shift toward higher molecular weight ubiquitin chains following EerI treatment. Inhibiting substrate deubiquitination by ataxin-3 should lead to the accumulation of longer and/or more polyubiquitin chains. Ubiquitin was not detected in the negative control. Taken together, these data provide strong evidence that DGAT2 is regulated by ERAD.

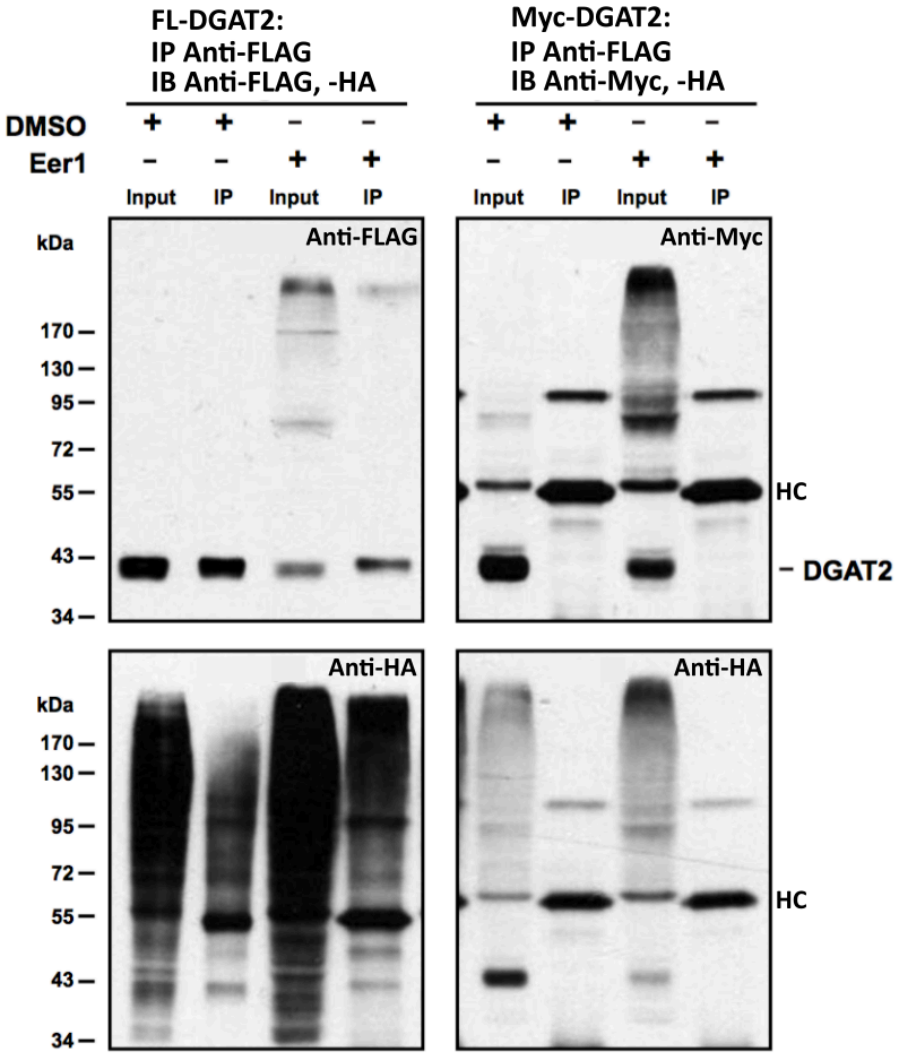

Figure 7.3. DGAT2 is regulated by ERAD - HEK-293T cells were co-transfected with either FL-DGAT2 or Myc-DGAT2 and HA-ubiquitin. Cells were treated with 8 μM of ERAD inhibitor, EerI, or an equal volume of DMSO for 3 h. FL-DGAT2 was immunoprecipitated (IP) with anti-FLAG agarose from detergent solubilized material. Immunoprecipitates were separated by SDS-PAGE and were then immunoblotted (IB) with anti-FLAG, anti-Myc and anti-HA antibodies. HC represents antibody heavy chains.

An analogous experiment was conducted to analyze MGAT2 regulation by ERAD. HEK-293T cells were transfected with MGAT2-Myc-FL or positive control, FL-DGAT2. Cells were subjected to treatment with DMSO, MG132 or EerI prior to anti-FLAG-immunoprecipitation and immunoblotting (Fig. 7.4). We found that DGAT and MGAT2 were successfully isolated in all treatment groups. As we previously identified, MG132 does not appear to increase MGAT2 ubiquitination, however it is highly ubiquitinated under both DMSO

and MG132 treatments. Similar to DGAT2, treatment with EerI caused a distinct shift towards higher molecular weight polyubiquitin conjugates in MGAT2 transfected samples. Also of note, EerI treatment appeared to reduce the signal of a band at ~45 kDa, roughly 8-10 kDa above the primary MGAT2 band, possibly representing mono-ubiquitinated MGAT2. This reduction is accompanied by an increased signal at ~75-80 kDa - the approximate size of an MGAT2 dimer. The identity of these bands has not been confirmed.

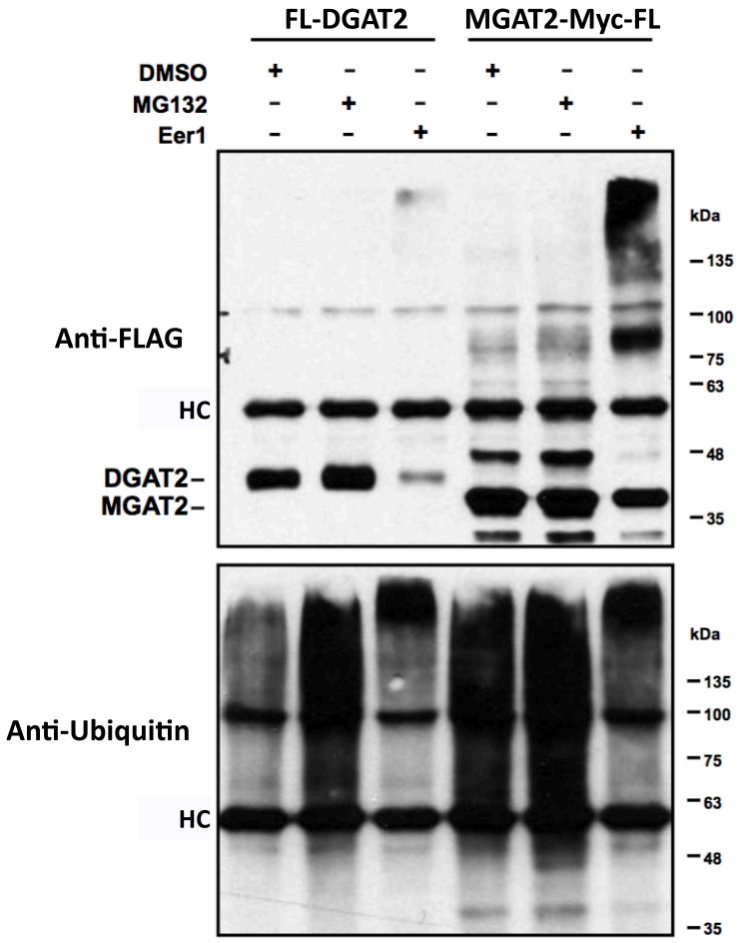

Figure 7.4. MGAT2 is regulated by ERAD - HEK-293T cells expressing either FL-DGAT2 or MGAT2-myc-FL were treated with 8 µM EerI, 10 µM MG132 or an equal volume of DMSO for 3 h. Samples were then anti-FLAG immunoprecipitated prior to SDS-PAGE and immunoblotting with anti-FLAG and anti-ubiquitin antibodies. HC represents antibody heavy chain.

7.2.3. MGAT3 is ubiquitinated and regulated by ERAD

Having identified that MGAT2 is ubiquitinated and regulated by ERAD, we were interested to look at MGAT3 as it contains even greater sequence identity with DGAT2 than MGAT2. HEK-293T cells were transfected with FL-MGAT3 or LacZ control prior to treatment with MG132, EerI or an equal volume of DMSO. MGAT3 was isolated by anti-FLAG immunoprecipitation before SDS-PAGE and immunoblotting with anti-FLAG and anti-ubiquitin specific antibodies. MGAT3 was detected in total cell extracts and in immunoprecipitates (Fig. 7.5A, B). MG132 treatment yielded a sharp increase in polyubiquitination relative to DMSO treated sample, revealing that MGAT3 is likely degraded by the ubiquitin-proteasome system. Treatment with EerI caused a shift towards high molecular weight polyubiquitination that was detected by both anti-FLAG and anti-ubiquitin antibodies. EerI caused a distinct accumulation at ~70 kDa when probing with anti-FLAG, possibly representing a dimer. This trend was also observed when MGAT2 was isolated following treatment with EerI (Fig. 7.4).

A.

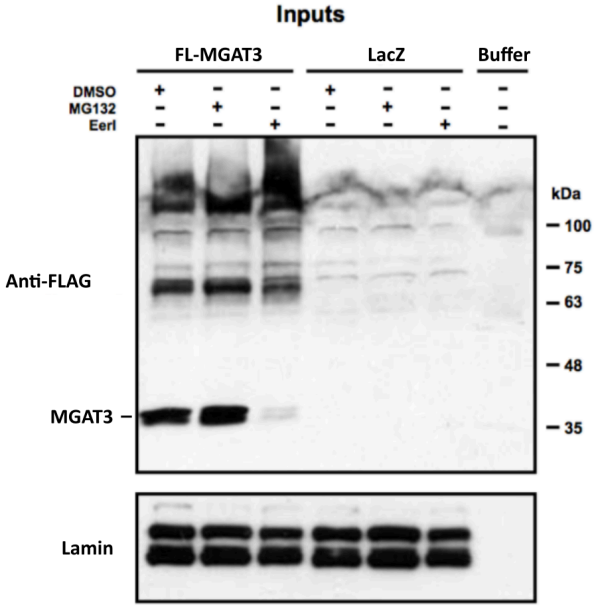

B.

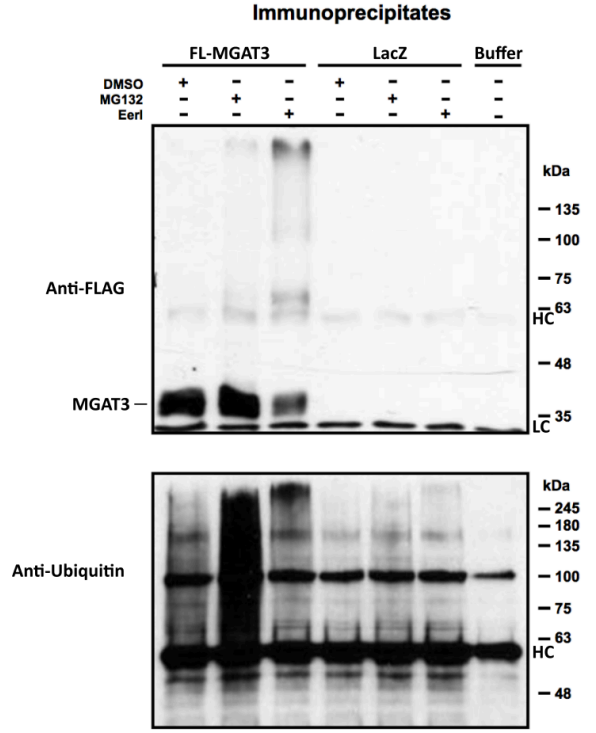

Figure 7.5. MGAT3 is ubiquitinated and is a substrate for ERAD - *(A)* HEK-293T cells expressing either FL-MGAT3 or LacZ were incubated with 10 μM MG132, 8 μM EerI or an equal volume of DMSO for 3 h. Cell lysates were then prepared and analyzed by immunoblotting with anti-FLAG and anti-lamin antibodies. *(B)* FL-MGAT3 was immunoprecipitated with anti-FLAG agarose. Immunoprecipitates were separated by SDS-PAGE and probed with anti-FLAG and anti-ubiquitin antibodies. Control immunoprecipitations were performed on LacZ transfected cells and with buffer alone. HC represents antibody heavy chains.

7.2.4. VCP/p97 co-localizes with DGAT2 and MGAT2

To gain additional evidence of DGAT2 and MGAT2 regulation by ERAD we looked at co-localization with the ERAD ATPase, VCP/p97. COS-7 cells were transfected with FL-DGAT2, MGAT2-Myc-FL or FL-DGAT1 prior to oleate treatment for ~18 h. DGAT1, DGAT2 and MGAT2 were detected with anti-FLAG antibody. Endogenous VCP/p97 localization was detected with an anti-VCP/p97 antibody (Fig. 7.6). For both FL-DGAT2 and MGAT2-Myc-FLAG transfected samples there was a clear correlation between DGAT2/MGAT2 signal intensity and VCP/p97 localization, particularly in the rough-ER directly surrounding the nucleus. In contrast, VCP/p97 staining in FL-DGAT1 transfected samples was more diffuse and co-localization much less pronounced. This was to be expected as even if DGAT1 was regulated by ERAD, it is stable with a half-life of ~18 h when overexpressed in adipocytes. Thus, we would anticipate minimal DGAT1 interaction with VCP/p97 (Yu *et al.*, 2002). Additionally, we noted VCP/p97 localization on lipid droplets in FL-DGAT2 transfected samples (Fig. 7.7). Concentrated co-localization of MGAT2 with VCP/p97 in the ER and with DGAT2 in the ER and on lipid droplets, provides further evidence that both are ERAD substrates.

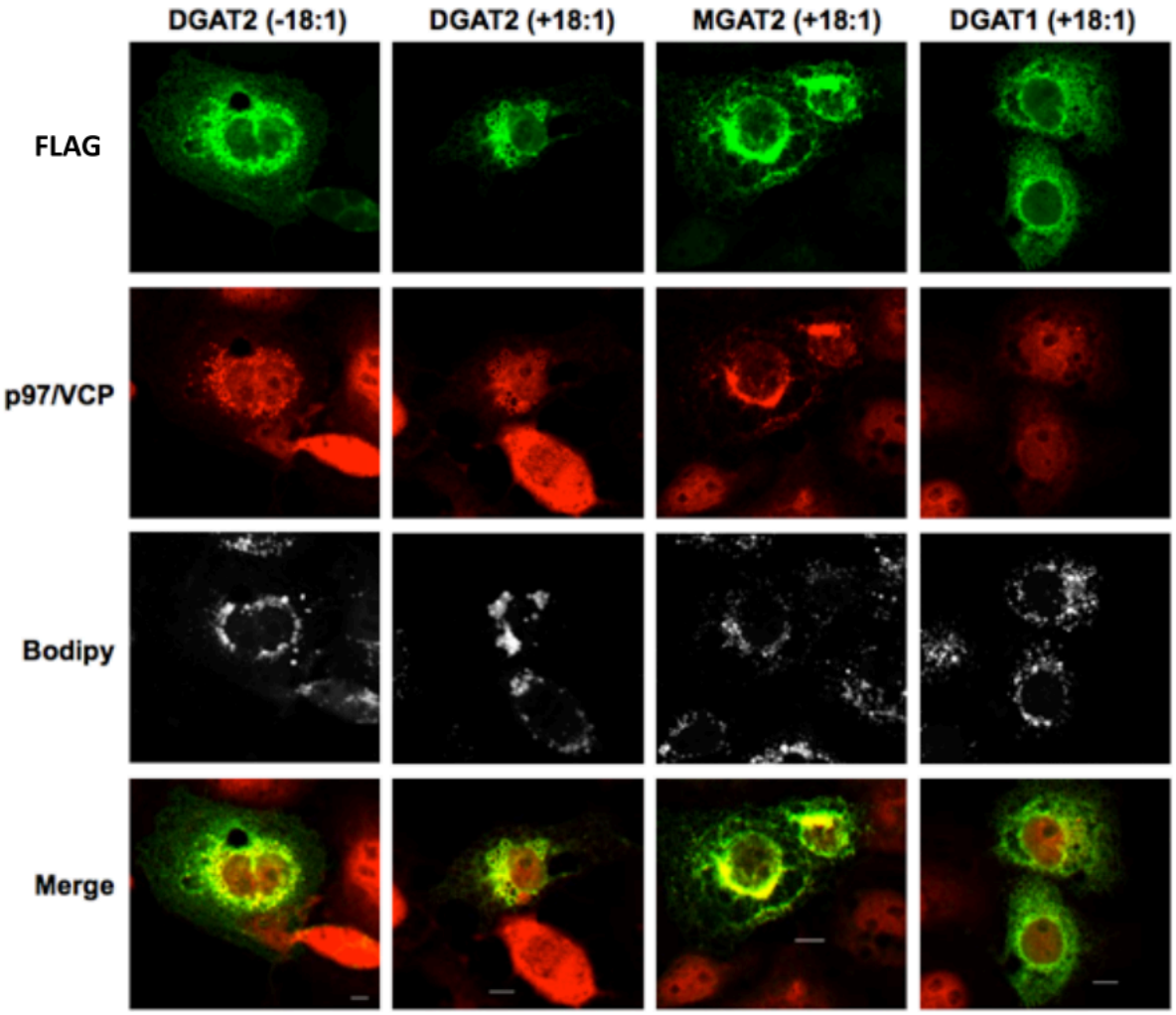

Figure 7.6. DGAT2 and MGAT2, but not DGAT1, co-localize with VCP/p97 - COS-7 cells were transfected with FL-DGAT2, MGAT2-myc-FL or FL-DGAT1 and then treated with 0.5 mM oleate for 18 h. Cells were then stained with anti-FLAG (*green*), anti-p97/VCP (*red*) and BODIPY 493/503 (*white*). The bottom panels only show merged images of each acyltransferase and p97/VCP. Yellow color shows regions of co-localization. Scale bars, 10 μm.

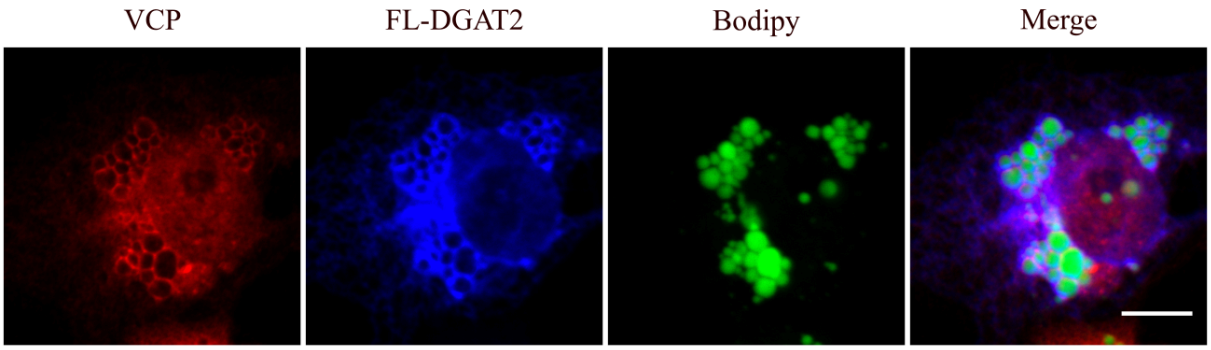

Figure 7.7. VCP/p97 is present on lipid droplets in DGAT2 transfected cells - COS-7 cells were transfected with FL-DGAT2 and treated with 0.5 mM oleate for 18 h. Cells were then stained with anti-FLAG, anti-p97/VCP and BODIPY 493/503. Scale bars, 10 μm.

7.2.5. DGAT2 and MGAT2 interact with VCP/p97 *in situ*

To demonstrate that DGAT2 and MGAT2 co-localization with VCP/p97 is indicative of direct protein-protein interaction, we conducted a proximity ligation assay. COS-7 cells were transfected with FL-DGAT2 or Myc-DGAT2 (Figure 7.8A). Alternatively cells were transfected with MGAT2-Myc-FL or MGAT2-Myc (Figure 7.8B). Interaction was detected with anti-FLAG and anti-VCP/p97 specific antibodies. Following completion of the PLA protocol, cells were co-stained with anti-DGAT2 or anti-Myc in order to confirm DGAT2 and MGAT2 expression respectively. An interaction signal was detected for both FL-DGAT2 and MGAT2-Myc-FL with VCP/p97, demonstrating physical interaction of both proteins with endogenous VCP/p97. There was no interaction signal in cells expressing negative controls Myc-DGAT2 or MGAT2-Myc.

A.

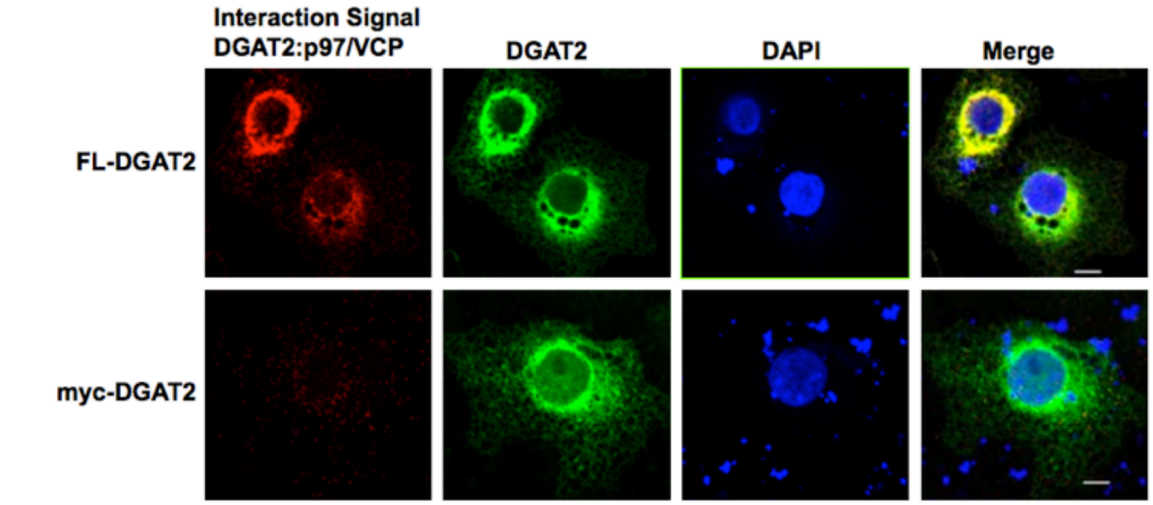

B.

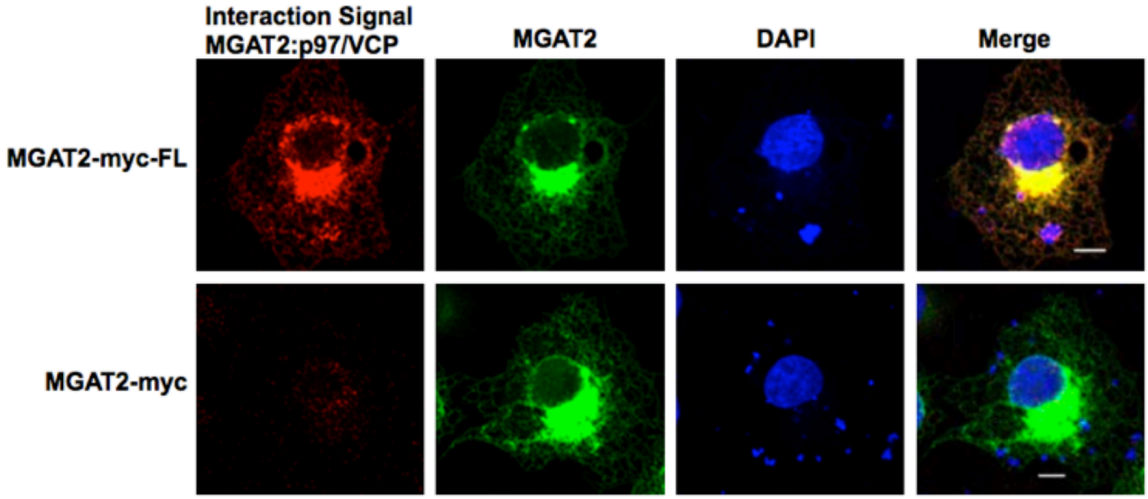

Figure 7.8. VCP/p97 interacts with DGAT2 and MGAT2 *in situ* - Protein interactions were detected using a proximity ligation assay. COS-7 cells were transfected with *(A)* FL-DGAT2 or Myc-DGAT2. In an analogous experiment, COS-7 cells were transfected with *(B)* MGAT2-myc-FL or MGAT2-Myc. Myc-DGAT2 and MGAT2-Myc expressing cells represent negative controls. Samples were stained with rabbit anti-FLAG and mouse anti-p97/VCP antibodies. Interaction signals were detected using a Duolink® detection kit. Nuclei were stained with DAPI. After the interaction assay was performed, DGAT2 and MGAT2 were visualized by staining cells with rabbit anti-DGAT2 and rabbit anti-Myc antibodies. Scale bar, 10 μm.

7.2.6. MGAT2 is more stable than DGAT2, and when co-expressed, inhibited DGAT2 turnover

As MGAT2 shares a great deal of primary sequence similarity with DGAT2 and is ubiquitinated, we expected it to be rapidly degraded. HEK-293T cells were transfected with FL-DGAT2 or MGAT2-Myc-FL individually or in tandem prior to CHX degradation assay. Samples were separated by SDS-PAGE and analyzed by anti-FLAG immunoblotting (Fig. 7.9). While DGAT2 was unstable, with very little protein detectable after 6 h, MGAT2 showed no apparent decline. What was more interesting was that co-expression with MGAT2 dramatically reduced DGAT2 turnover; ~70% of DGAT2 remained at 6 h. MGAT2 degradation appeared to be unaffected by co-transfection.

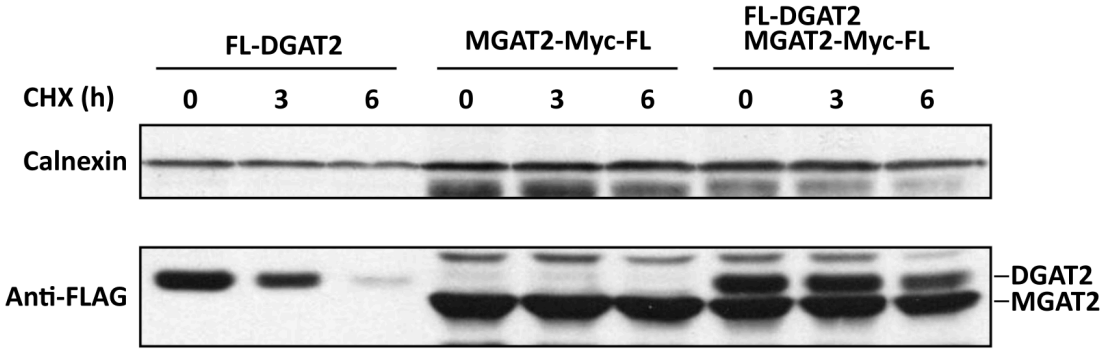

Figure 7.9. MGAT2 is more stable than DGAT2, and when co-expressed, inhibited DGAT2 turnover – HEK-293T cells were transfected with FL-DGAT2 or MGAT2-Myc-FL individually or in tandem. *pcDNA3.1/LacZ* was used in individual transfections to keep total transfection DNA constant. Cells were treated with 100 μg/mL CHX and harvested at the time indicated. Samples were analyzed by SDS-PAGE and immunoblotting. Proteins were detected simultaneously with anti-FLAG primary antibody. Re-probing for calnexin was used to establish equal loading. The total amount of plasmid DNA was kept constant for each transfection, using pcDNA3.1/LacZ when transfecting with only DGAT2 or MGAT2.

7.2.7. MGAT2 does not stabilize DGAT2 by reducing its ubiquitination

A possible mechanism by which MGAT2 could stabilize DGAT2 is through reducing DGAT2 ubiquitination. To examine this, HEK-293T cells were transfected with FL-DGAT2, MGAT2-Myc-FL, FL-DGAT2 and MGAT2-Myc in tandem, or Myc-DGAT2 alone. Cells were treated with DMSO or MG132 to observe effects under proteasomal inhibition. In order to examine the ubiquitination of DGAT2 in isolation, samples were harvested so as to minimize co-immunoprecipitation of MGAT2 and other proteins with DGAT2. Analysis of total cell extracts by SDS-PAGE and immunoblotting, with anti-FLAG followed by anti-Myc specific antibodies, revealed that all constructs were expressed (Fig 7.10A). Anti-FLAG immunoprecipitation was conducted on total cell extracts prior to analysis by SDS-PAGE and immunoblotting (Fig. 7.10B). Probing for FLAG showed that FL-DGAT2 and MGAT2-Myc-FL were successfully isolated in the appropriate samples. Re-probing of the blot with a Myc-specific antibody revealed that interaction of MGAT2-Myc with FL-DGAT2 was largely eliminated and only a very faint MGAT2-Myc band was visible for both DMSO and MG132 treated samples. Myc-DGAT2 control was not detected following anti-FLAG pull-down. A separate blot was probed to detect endogenous ubiquitin. As expected, no signal was detected in the Myc-DGAT2 transfected control. Comparison of the FL-DGAT2 and FL-DGAT2/MGAT2-Myc transfections revealed that in the presence or absence of MG132, MGAT2 did not appear to have any observable effect on the polyubiquitination of DGAT2.

A.

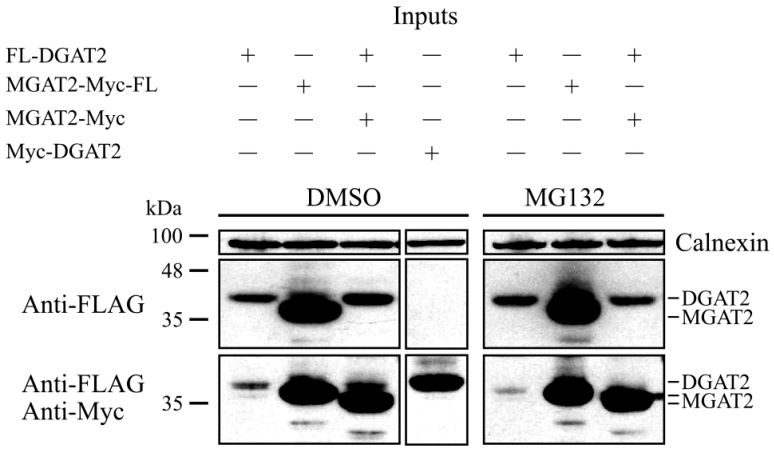

B.

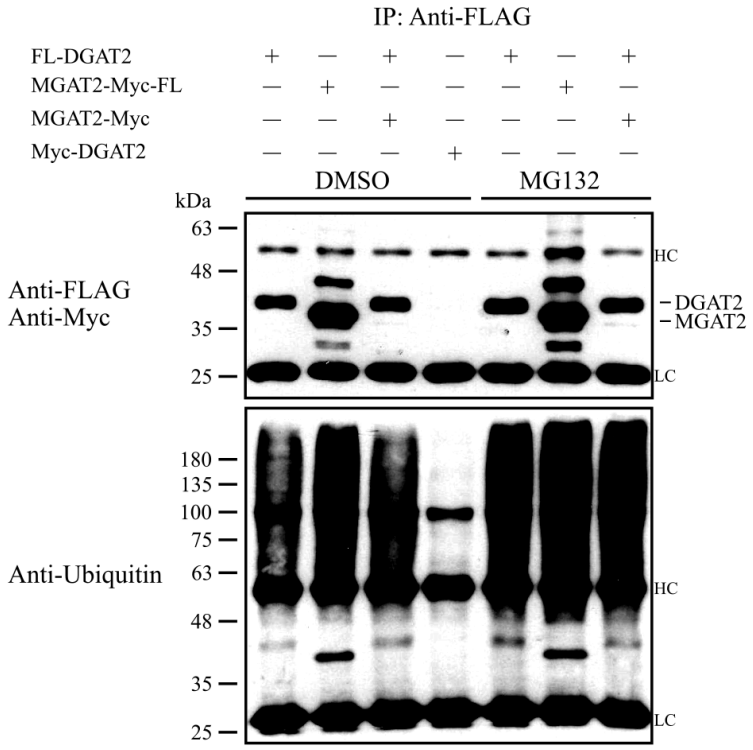

Figure 7.10. MGAT2 does not reduce DGAT2 ubiquitination when co-expressed - HEK-293T cells were transfected with FL-DGAT2, MGAT2-Myc-FL, FL-DGAT2/MGAT2-Myc or Myc-DGAT2 control and treated with 10 μM MG132 or an equal volume of DMSO. Samples were harvested in order to minimize DGAT2 and MGAT2 interaction. *(A)* Total cell extracts were separated by SDS-PAGE and analyzed by immunoblotting with anti-FLAG followed by anti-Myc specific antibodies. Blotting for calnexin was included to establish equal loading. *(B)* Anti-FLAG immunoprecipitation was conducted on total cell extracts prior to analysis by SDS-PAGE and immunoblotting. A blot was probed sequentially with anti-FLAG and anti-Myc specific antibodies. A separate blot was probed with anti-ubiquitin specific antibody. IP represents immunoprecipitation. HC and LC represent antibody heavy and light chains respectively.

7.2.8. MGAT3 is more stable than DGAT2, and when co-expressed, inhibited DGAT2 turnover

We were interested to examine the stability of MGAT3. As MGAT3 sequence homology is greater with DGAT2 than MGAT2, we expected the turnover rate to be rapid. HEK-293T cells were transfected with FL-DGAT2, FL-MGAT2, or FL-MGAT3 and turnover rates evaluated by treatment with CHX. Samples were analyzed by SDS-PAGE and anti-FLAG immunoblotting (Fig. 7.11A). We identified that MGAT3 existed as a doublet; to our knowledge this had not been previously reported. Past studies expressed MGAT3 in COS-7 or sf9 insect cells, providing a possible explanation for this difference (Hall *et al.*, 2012; Cheng *et al.*, 2003). At 3 h ~70% of MGAT3 remained, this was reduced to ~50% at 6 h of CHX treatment. Comparatively, very little DGAT2 remained at 3 h and was undetectable at 6 h. MGAT2 did not show any appreciable degradation after 6 h CHX treatment. Thus, MGAT3 is more stable than DGAT2 but less stable than MGAT2. Having found that MGAT2 is able to reduce DGAT2 turnover, we were curious to see whether MGAT3 could as well. HEK-293T cells expressing FL-DGAT2 individually, or in conjunction with FL-MGAT3, were analyzed by CHX degradation assay. Total cell extracts were analyzed by SDS-PAGE and anti-FLAG immunoblotting (Figure 7.11B). Despite modest expression relative to DGAT2, MGAT3 had a strong stabilizing effect. When expressed on its own, DGAT2 was not detectable after 6 h. Comparatively, 30% of DGAT2 remained at 6 h when co-expressed with MGAT3. Thus, MGAT3 also reduced DGAT2 degradation.

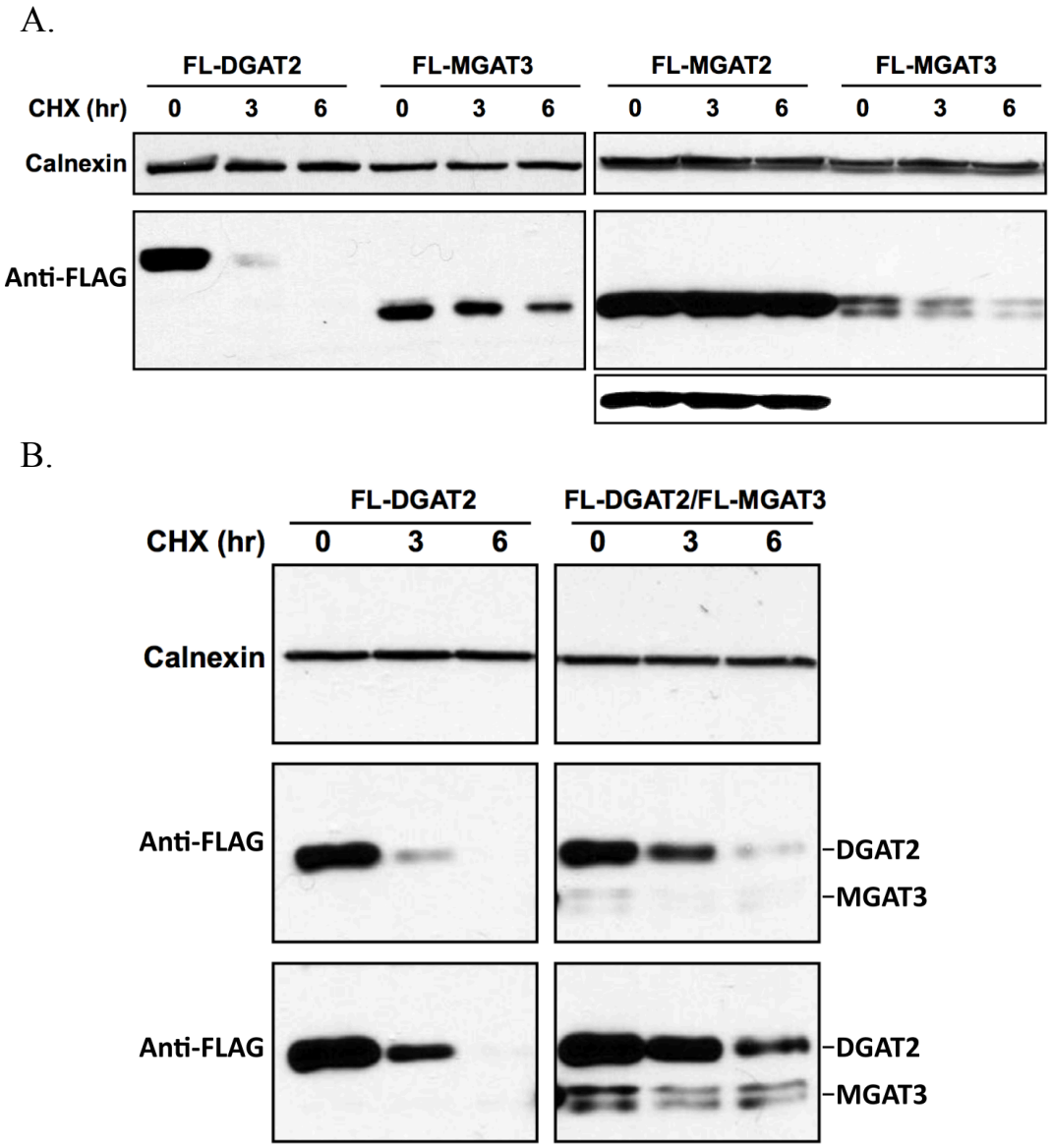

Figure 7.11. MGAT3 is more stable than DGAT2, and when co-expressed, inhibited DGAT2 turnover - *(A)* HEK-293T cells were transfected with FL-DGAT2, FL-MGAT2 or FL-MGAT3 and treated with 100 μg/mL CHX prior to harvest at the indicated time points. Cells lysates were separated by SDS-PAGE and analyzed by anti-FLAG immunoblotting. Calnexin was used as a degradation control. Two exposures of FL-MGAT2/FL-MGAT3 are shown. *(B)* HEK-293T cells were transfected with FL-DGAT2 or FL-MGAT3 individually or in tandem and incubated with 100 μg/mL CHX prior to harvest at the indicated time point. Cell lysates were separated by SDS-PAGE and analyzed by anti-FLAG immunoblotting. FL-DGAT2 and FL-MGAT3 were detected simultaneously. Two separate exposures are shown. The total amount of plasmid DNA was kept constant for each transfection, using pcDNA3.1/*LacZ* when transfecting with only DGAT2 or MGAT3. Samples were separated on the same SDS-PAGE gel but images were cropped for clarification.

7.3. Discussion

Due to the high sequence identity between DGAT2 and MGAT2, we were unsurprised to find that MGAT2 was also polyubiquitinated. However, the substantial difference in degradation rate was unexpected. Human MGAT2 used in this experiment contains 13 lysine residues compared to 25 present in murine DGAT2. Of these lysines, only 6 are conserved between the two proteins, all of which we identified to induce degradation when restored in the Lys-less-DGAT2 construct. It is possible that the stability of MGAT2 is a result of having fewer ubiquitin-acceptor lysines. Yet, MGAT2 is polyubiquitinated at similar levels in the presence and absence of MG132. The lack of polyubiquitin accumulation upon proteasome inhibition is consistent with a reduced turnover rate, however, it seems that MGAT2 is highly ubiquitinated even under basal conditions. How polyubiquitinated MGAT2 evades destruction is unknown. One possible answer is that ubiquitination of MGAT2 may have additional functions. Poly-ubiquitin antibodies specific to traditionally non-degradative chain linkages (ex. K6, K63) could be useful in confirming this. Ubiquitination and turnover of MGAT3 was more similar to DGAT2 than MGAT2. A sharp spike in ubiquitination was observed upon MG132 treatment and there was an appreciable reduction in protein following 6 h of CHX. Comparison of the human MGAT3 and mouse DGAT2 utilized in the study shows that MGAT3 contains 10 lysine residues, only four of which directly align with those in DGAT2. Finally, comparison of the mouse MGAT2 and human MGAT3 constructs that were used revealed that again, four lysine residues align. The four lysines conserved between MGAT3 and DGAT2, and MGAT3 and MGAT2 are the same, corresponding to lysines 146, 260, 305 and 374 of mouse DGAT2.

The effect of EerI treatment on DGAT2, MGAT2 and MGAT3 provide additional evidence that all three proteins are regulated by the ubiquitin-proteasome system. EerI inhibits ERAD deubiquitination that is necessary for substrate retrotranslocation from the ER into the cytosol prior to degradation by the proteasome (Wang *et al.* 2006; Ernst *et al.* 2009; Zhang *et al.* 2013). The observed shift towards high MW polyubiquitin conjugates suggests that DGAT2, MGAT2 and MGAT3 experience deubiquitination by ERAD associated deubiquitinases. EerI also caused an increase in what may be dimer formation of MGAT2 and MGAT3. This was also observed in DGAT2 total cell extracts but could not be detected in immunoprecipitates - possibly because the amount of DGAT2 isolated in EerI treated samples

was relatively low. MGAT2 also exhibited a reduction in a band ~8 kDa above the unmodified protein. The identity of these bands is currently unknown. DGAT2 has been shown to form dimers, the significance of which is unclear (Jin *et al.*, 2014). The considerable sequence identity with MGAT2 and MGAT3 makes it likely they may form dimers as well. We are unsure as to why inhibition of ERAD associated deubiquitination would cause a transition to dimer formation. However, there is evidence that disulfide bonds must be reduced prior to dislocation from the membrane (Riemer *et al.*, 2011; Christianson *et al.*, 2012)

For VCP/p97 to perform its role in ERAD, it must be recruited from the cytosol to the ER. This is facilitated by cofactors such as fas-associated factor family member 2 and the E3 ligase AMFR (Ye *et al.*, 2001, 2003, 2005; Ballar *et al.*, 2006, 2011; Madsen *et al.*, 2011). We identified that overexpression of DGAT2 or MGAT2 caused a clear reorganization of VCP/p97. VCP/p97 became localized to the ER and was particularly concentrated in areas that DGAT2 or MGAT2 were abundant. Conversely, VCP/p97 staining remained very diffuse and cytosolic in those cells, which were unsuccessfully transfected. This was also observed in cells transfected with the very stable DGAT1. Lack of VCP/p97 relocalization in DGAT1 transfected cells suggests VCP/p97 relocalization following DGAT2 and MGAT2 transfection is specific and not an artifact of overexpression. Detection of VCP/p97 on the surface of lipid droplets was not surprising. VCP/p97 trafficking to lipid droplets has been previously noted, its migration controlled by fas-associated factor family member 2 (Olzmann *et al.* 2013b).

Co-expression studies in HEK-293T and COS-7 cells have identified that DGAT2 and MGAT2 interact to promote triacylglycerol accumulation above levels observed when either protein is expressed individually (Jin *et al.*, 2014). We identified that MGAT2 is much more stable than DGAT2. Furthermore, when co-expressed, MGAT2 reduced DGAT2 degradation. This, in conjunction with substrate channeling of diacylglycerol, potentially provides the mechanistic basis for elevated triacylglycerol accumulation upon co-expression. MGAT2 induced stabilization of DGAT2 did not appear to be mediated by curbing DGAT2 ubiquitination. As MGAT2 itself is highly ubiquitinated, it is possible that the less potent, or potentially non–degradative, ubiquitination of MGAT2 obfuscates recognition of ubiquitinated DGAT2. DGAT2 mRNA levels in adipose tissue and liver are decreased during fasting and increased upon re-feeding (Meegalla *et al.*, 2002). Liberation of fatty acids from triacylglycerol stored in cytosolic lipid droplets during fasting could explain the necessity for DGAT2 to be

rapidly degraded. In contrast, mRNA levels in the intestine, where MGAT2 is expressed most highly, are held relatively constant, as are protein and activity levels (Chon *et al.*, 2007). MGAT2 stability could be physiologically important, as the need to absorb dietary fats in the intestine could be required any moment a meal is consumed.

MGAT3 function and regulation has not been extensively characterized. In humans, MGAT3 expression appears to be confined to the gastrointestinal tract (Cheng *et al.*, 2003). As so little is known about the enzyme, it is difficult to predict the significance of its degradation rate and stabilizing effect on DGAT2.

CHAPTER 8: General discussion

8.1 Conclusions

Obesity has reached epidemic proportions in the developed world. The consequences associated with excess weight have dramatic impacts at personal, societal and economic levels. Therapeutic intervention in pathways involved in the synthesis and storage of triacylglycerols has shown clinical benefits. Additional research is necessary to increase the efficiency of these treatments, enhancing manipulation of existing targets, while also identifying novel targets and means of treatment. Understanding the regulatory network of key proteins involved in synthesis and degradation of dietary lipids provides crucial insight to attain these goals. DGAT2, catalyzing the final and only committed step in this process, represents a logical point at which to direct therapeutic influence. Previous DGAT2 inhibitors have suffered from weak activity, however, recent reports show some promise.

We identified that DGAT2 is ubiquitinated and degraded by the ubiquitin proteasome system. DGAT2 has a very short half-life. Degradation is lysine dependent and controlled by numerous lysines C-terminal of the second transmembrane domain. Confirmation of ubiquitinated lysine residues through mass spec analysis would be beneficial; our attempt was unsuccessful. *In vitro,* a lysine-less mutant retained full cataytic activity. However, *in situ*, this mutant exhibited a nuclear/perinuclear-staining pattern and disrupted typical lipid droplet formation. Two lysine clusters were identified; when mutated, they could recapitulate the abnormal nuclear localization. As both of these clusters contained lysines found to promote degradation, this phenotype could be caused by the accumulation of degradation resistant protein.

As lipid concentrations have been found to influence the degradation rate of several proteins involved in triacylglycerol metabolism, we chose to examine whether DGAT2 was similarly regulated. Stimulation of lipogenesis did not reduce DGAT2 degradation, suggesting that DGAT2 turnover may be controlled primarily at the transcriptional level. Moreover, following the discovery that DGAT2 on both lipid droplets and the ER is ubiquitinated, we found that inhibiting re-localization to the lipid droplet during lipogenesis had no effect on DGAT2 turnover rate. Finally, analysis of DGAT2 ubiquitination *in situ* demonstrated no apparent changes in the quantity or localization of ubiquitinated DGAT2 under basal or lipogenic conditions.

In order to gain insight into DGAT2 regulation, we took a non-targeted mass spectrometry approach to identify interacting proteins. Notably, the ERAD E3 ligase, TRIM13, was detected. Further experiments to confirm and characterize this interaction would be beneficial. Calnexin was also detected by LC-MS/MS in DGAT2 isolates; this interaction was confirmed *in vitro* and *in situ*. MGAT2 was also found to co-immunoprecipitate with calnexin. DGAT2 and MGAT2 interaction with calnexin did not appear to be dependent on glycosylation, implying that these interactions are not simply due to calnexin chaperone function. The possible impacts of calnexin on triacylglycerol metabolism were examined in calnexin knockout mouse embryonic fibroblasts, which exhibited stunted lipid droplet size compared to wild-type cells. Additional experiments are necessary to determine whether this is simply a result of loss of chaperone function or if calnexin has a secondary role in lipid droplet formation. The presence of calnexin on lipid droplets provides some evidence for the latter.

DGAT2, MGAT2 and MGAT3 have many commonalities in sequence, localization and function. We were interested to examine interactions between these family members and check for similarities in regulation. We reported that DGAT2 was able to interact with MGAT2 and MGAT3 *in vitro* and *in situ*. As expected, both MGAT2 and MGAT3 were also found to be ubiquitinated, pointing to regulation by the ubiquitin-proteasome system. Differences in stability were observed, with MGAT2 being much more stable than DGAT2, and MGAT3 exhibiting an intermediate rate of degradation. The functional significance of these interactions were examined in co-expression studies. We recognized that MGAT2 and MGAT3 stabilized DGAT2, dramatically reducing its rate of degradation. These interactions could serve to increase triacylglycerol synthesis capacity during lipogenesis. In investigating MGAT2 induced stabilization of DGAT2, we found that MGAT2 co-expression did not reduce DGAT2 ubiquitination. The mechanism of stabilization requires further analysis.

Accumulation of high molecular weight polyubiquitinated DGAT2, MGAT2 and MGAT3 were observed upon ERAD inhibition. This provides evidence that these proteins are degraded through the ERAD pathway. Additionally, DGAT2 and MGAT2 were found to co-localize and interact with the ERAD ATPase, VCP/p97.

This project has provided insight into the post-translational regulatory mechanisms of DGAT2 and DGAT2 family members. Furthermore, results from mass spectrometry based identification of DGAT2 interacting proteins offer numerous avenues of potential research.

Finally, MGAT2 and MGAT3 mediated stabilization of DGAT2 has potential physiological implications. It has been noted that MGAT2 and DGAT2 can cooperate to increase triacylglycerol production (Jin *et al.*, 2014). The prospect of increased triacylglycerol synthesis through the stabilization of DGAT2 bound to a triacylglycerol synthesis complex requires additional inquiry.

8.2 Future directions

Further mapping of DGAT2 post-translational modifications by mass spectrometry would be very beneficial. While our attempt was unsuccessful, we would like to confirm findings from our mutagenic studies that numerous lysines C-terminal of the TMDs are ubiquitinated and responsible for destabilizing DGAT2. Identification of other modifications would also help to elucidate the regulatory mechanisms of DGAT2.

The recent finding that DGAT2 is present in the nucleus suggests that a mechanism must be present to transport it there (Ohsaki *et al.*, 2016). This provides some explanation as to why the degradation resistant Lys-less-DGAT2 mutant is found in the nuclear region. Why it accumulates in or around the nucleus rather than the ER or cytosol is unclear. Finding the sequence(s) in DGAT2 that modulates this localization would be valuable.

We identified that mutation of lysine residues 251, 257, 260 and 264 significantly reduced the size of lipid droplets and appeared to block DGAT2 localization to the lipid droplet surface. It would be interesting to further examine this mechanism and determine whether this region is post-translationally modified or involved in protein-protein interactions that serve to target DGAT2 to lipid droplets. An alternate explanation is that these residues directly interact with the lipid droplet monolayer.

Convincing evidence linking genomic variance in DGAT2 to increased adiposity has yet to be found. Differences among individuals in the activity of proteins responsible for regulating DGAT2 abundance could also play a role. Currently, AMFR is the only E3 ligase experimentally verified to regulate DGAT2 turnover (Choi *et al*., 2014). We identified TRIM13 E3 ligase in DGAT2 co-immunoprecipitates. This interaction should be further examined. An *in vitro* ubiquitination assay would be useful to show DGAT2 is a substrate for TRIM13. Additionally, siRNA mediated knockdown of TRIM13 would be expected to stabilize DGAT2.

We were very interested to find that DGAT2 and MGAT2 interact with calnexin in a glycosylation independent manner. In characterizing this interaction, we would first like to pinpoint the interacting regions of each protein. We also found that lipid droplet production appeared to be inhibited in a calnexin knockout cell line. Introduction of a calnexin mutant in these cells, made deficient in chaperone function through inactivation of its carbohydrate-binding domain, could illuminate the role of calnexin in lipid droplet formation. If this construct restored lipid droplet production, it would imply that calnexin plays a role in triacylglycerol metabolism that is not attributable to its function as a folding chaperone.

Finally, the observation that MGAT2 and MGAT3 stabilize DGAT2 has possible physiological implications. As tools to examine endogenous DGAT2 protein levels are not available, this needs to be examined indirectly. We intend to transfect human liver cells with MGAT2/MGAT3 and subject them to CHX degradation assay. Total cell extracts would then be isolated and analyzed by *in vitro* DGAT activity assay in the presence of a DGAT1 inhibitor. If MGAT2 and MGAT3 reduce DGAT2 turnover, we would expect to see a more gradual reduction in DGAT activity over the time course of CHX incubation. Additionally, it would be interesting to examine the effects of combined inhibition of MGAT2/MGAT3 and DGAT2 in obese mice.

CHAPTER 9: Supplementary material

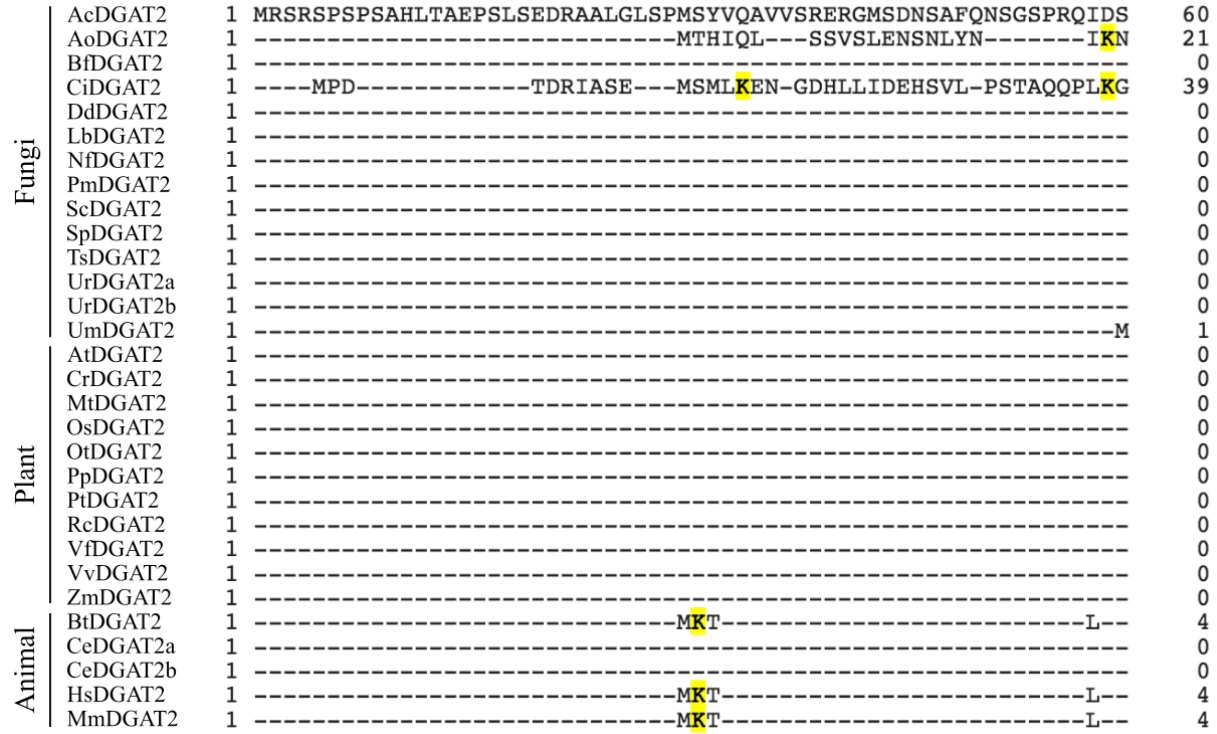

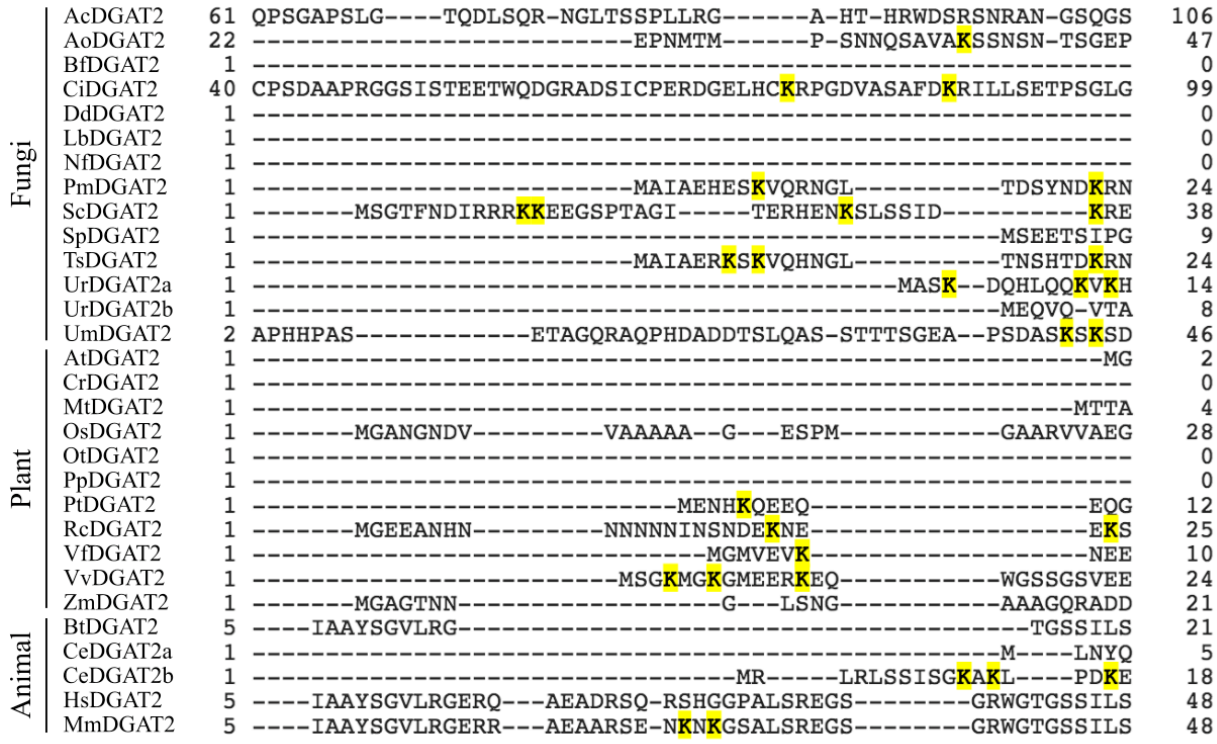

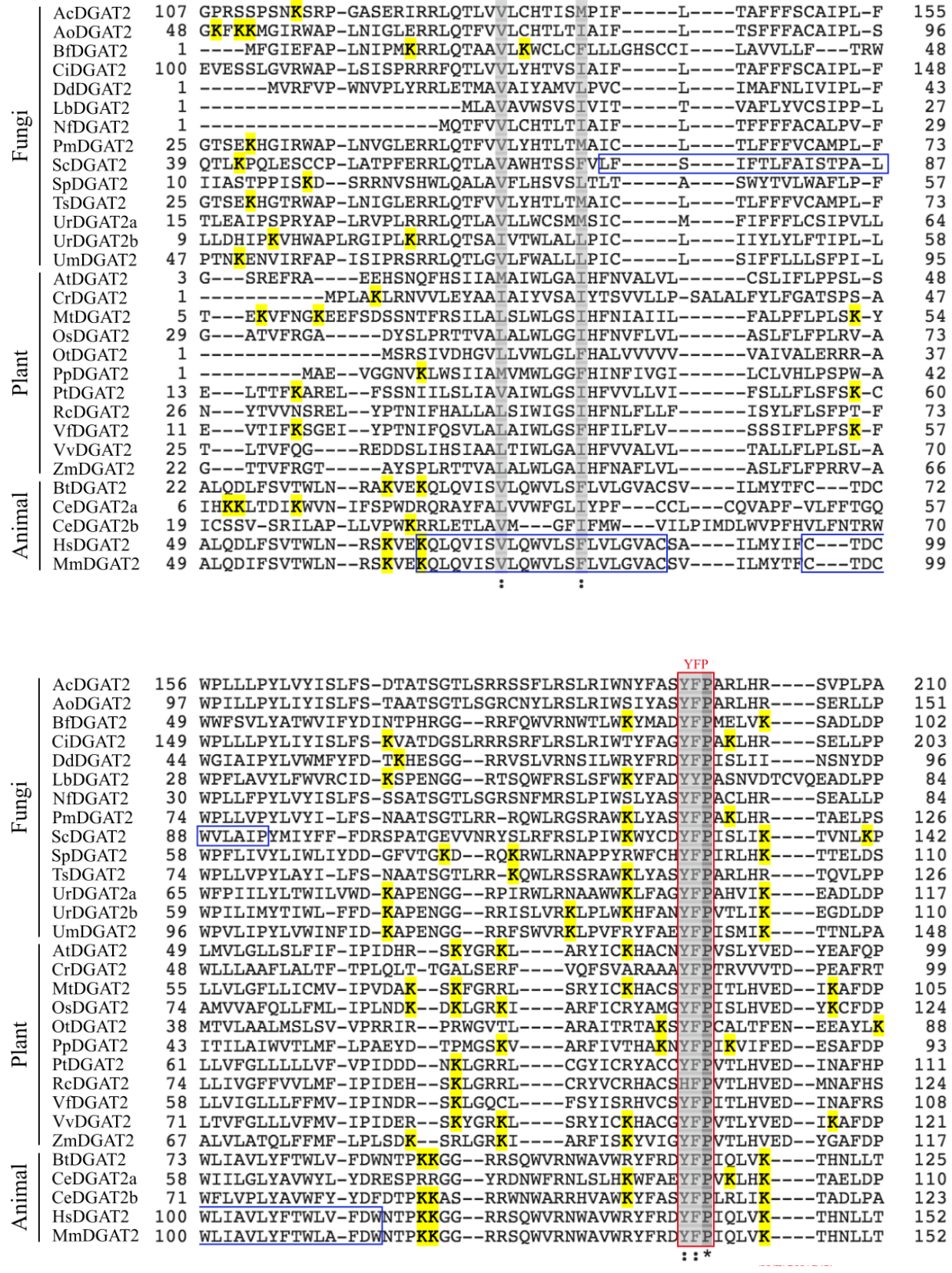
Fungi
Plant
Animal
AcDGAT2 107 GPRSSPSNKSRP-GASERIRRLQTLVVLCHTISMPIF-----L----TAFFFSCAIPL-F 155
AoDGAT2 48 GKFKKMGIRWAP-LNIGLERRLQTFVVLCHTLTIAIF-----L----TSFFFACAIPL-S 96
BfDGAT2 1 ----MFGIEFAP-LNIPMKRRLQTAAVLKWCLCFLLLGHSCCI----LAVVLLF---TRW 48
CiDGAT2 100 EVESSLGVRWAP-LSISPRRRFQTLVVLYHTVSIAIF-----L----TAFFFSCAIPL-F 148
DdDGAT2 1 ------MVRFVP-WNVPLYRRLETMAVAIYAMVLPVC-----L----IMAFNLIVIPL-F 43
LbDGAT2 1 ----------MLAVAVWSVSIVIT-----T----VAFLYVCSIPP-L 27
NfDGAT2 1 ----------MQTFVVLCHTLTIAIF-----L----TFFFFACALPV-F 29
PmDGAT2 25 GTSEKHGIRWAP-LNVGLERRLQTFVVLYHTLTMAIC-----L----TLFFFVCAMPL-F 73
ScDGAT2 39 QTLKPQLESCCP-LATPFERRLQTLAVAWHTSSFVLF-----S----IFTLFAISTPA-L 87
SpDGAT2 10 IIASTPPISKD--SRRNVSHWLQALAVFLHSVSLTLT-----A----SWYTVLWAFLP-F 57
TsDGAT2 25 GTSEKHGTRWAP-LNIGLERRLQTFVVLYHTLTMAIC-----L----TLFFFVCAMPL-F 73
UrDGAT2a 15 TLEAIPSPRYAP-LRVPLRRRLQTLAVLLWCSMMSIC-----M----FIFFFLCSIPVLL 64
UrDGAT2b 9 LLDHIPKVHWAPLRGIPLKRRLQTSAIVTWLALLPIC-----L----IIYLYLFTIPL-L 58
UmDGAT2 47 PTNKENVIRFAP-ISIPRSRRLQTLGVLFWALLLPIC-----L----SIFFLLLSFPI-L 95
AtDGAT2 3 G---SREFRA----EEHSNQFHSIIAMAIWLGAIHFNVALVL------CSLIFLPPSL-S 48
CrDGAT2 1 ----------MPLAKLRNVVLEYAAIAIYVSAIYTSVVLLP-SALALFYLFGATSPS-A 47
MtDGAT2 5 T---EKVFNGKEEFSDSSNTFRSILALSLWLGSIHFNIAIIL------FALPFLPLSK-Y 54
OsDGAT2 29 G---ATVFRGA-----DYSLPRTTVALALWLGGIHFNVFLVL------ASLFLFPLRV-A 73
OtDGAT2 1 ----------------MSRSIVDHGVLLVWLGLFHALVVVVV------VAIVALERRR-A 37
PpDGAT2 1 ---------MAE--VGGNVKLWSIIAMVMWLGGFHINFIVGI------LCLVHLPSPW-A 42
PtDGAT2 13 E---LTTFKAREL--FSSNIILSLIAVAIWLGSIHFVVLLVI------FSLLFLSFSK-C 60
RcDGAT2 26 N---YTVVNSREL--YPTNIFHALLALSIWIGSIHFNLFLLF------ISYLFLSFPT-F 73
VfDGAT2 11 E---VTIFKSGEI--YPTNIFQSVLALAIWLGSFHFILFLV-------SSSIFLPFSK-F 57
VvDGAT2 25 T---LTVFQG----REDDSLIHSIAALTIWLGAIHFVVALVL------TALLFLPLSL-A 70
ZmDGAT2 22 G---TTVFRGT-----AYSPLRTTVALALWLGAIHFNAFLVL------ASLFLFPRRV-A 66
BtDGAT2 22 ALQDLFSVTWLN--RAKVEKQLQVISVLQWVLSFLVLGVACSV----ILMYTFC---TDC 72
CeDGAT2a 6 IHKKLTDIKWVN-IFSPWDRQRAYFALVVWFGLIYPF---CCL---CQVAPF-VLFFTGQ 57
CeDGAT2b 19 ICSSV-SRILAP-LLVPWKRRLETLAVM---GFIFMW---VILPIMDLWVPFHVLFNTRW 70
HsDGAT2 49 ALQDLFSVTWLN--RSKVEKQLQVISVLQWVLSFLVLGVACSA----ILMYIFC---TDC 99
MmDGAT2 49 ALQDIFSVTWLN--RSKVEKQLQVISVLQWVLSFLVLGVACSV----ILMYTFC---TDC 99
YFP
AcDGAT2 156 WPLLLPYLVYISLFS-DTATSGTLSRRSSFLRSLRIWNYFASYFPARLHR----SVPLPA 210
AoDGAT2 97 WPILLPYLIYISLFS-TAATSGTLSGRCNYLRSLRIWSIYASYFPARLHR----SERLLP 151
BfDGAT2 49 WWFSVLYATWVIFYDINTPHRGG--RRFQWVRNWTLWKYMADYFPMELVK----SADLDP 102
CiDGAT2 149 WPLLLPYLIYISLFS-KVATDGSLRRRSRFLRSLRIWTYFAGYFPAKLHR----SELLPP 203
DdDGAT2 44 WGIAIPYLVWMFYFD-TKHESGG--RRVSLVRNSILWRYFRDYFPISLII----NSNYDP 96
LbDGAT2 28 WPFLAVYLFWVRCID-KSPENGG--RTSQWFRSLSFWKYFADYYPASNVDTCVQEADLPP 84
NfDGAT2 30 WPLLFPYLVYISLFS-SSATSGTLSGRSNFMRSLPIWSLYASYFPACLHR----SEALLP 84
PmDGAT2 74 WPLLVPYLVYI-LFS-NAATSGTLRR-RQWLRGSRAWKLYASYFPAKLHR----TAELPS 126
ScDGAT2 88 WVLAIPYMIYFF-FDRSPATGEVVNRYSLRFRSLPIWKWYCDYFPISLIK----TVNLKP 142
SpDGAT2 58 WPFLIVYLIWLIYDD-GFVTGKD--RQKRWLRNAPPYRWFCHYFPIRLHK----TTELDS 110
TsDGAT2 74 WPLLVPYLAYI-LFS-NAATSGTLRR-KQWLRSSRAWKLYASYFPARLHR----TQVLPP 126
UrDGAT2a 65 WFPIILYLTWILVWD-KAPENGG--RPIRWLRNAAWWKLFAGYFPAHVIK----EADLDP 117
UrDGAT2b 59 WPILIMYTIWL-FFD-KAPENGG--RRISLVRKLPLWKHFANYFPVTLIK----EGDLDP 110
UmDGAT2 96 WPVLIPYLVWINFID-KAPENGG--RRFSWVRKLPVFRYFAEYFPISMIK----TTNLPA 148
AtDGAT2 49 LMVLGLLSLFIF-IPIDHR--SKYGRKL----ARYICKHACNYFPVSLYVED--YEAFQP 99
CrDGAT2 48 WLLLAAFLALTF-TPLQLT-TGALSERF----VQFSVARAAAYFPTRVVVTD--PEAFRT 99
MtDGAT2 55 LLVLGFLLICMV-IPVDAK--SKFGRRL----SRYICKHACSYFPITLHVED--IKAFDP 105
OsDGAT2 74 AMVVAFQLLFML-IPLNDK--DKLGRKI----ARFICRYAMGYFPISLHVED--YKCFDP 124
OtDGAT2 38 MTVLAALMSLSV-VPRRIR--PRWGVTL----ARAITRTAKSYFPCALTFEN--EEAYLK 88
PpDGAT2 43 ITILAIWVTLMF-LPAEYD--TPMGSKV----ARFIVTHAKNYFPIKVIFED--ESAFDP 93
PtDGAT2 61 LLVFGLLLLLVF-VPIDDD--NKLGRRL----CGYICRYACCYFPVTLHVED--INAFHP 111
RcDGAT2 74 LLIVGFFVVLMF-IPIDEH--SKLGRRL----CRYVCRHACSHFPVTLHVED--MNAFHS 124
VfDGAT2 58 LLVIGLLLFFMV-IPINDR--SKLGQCL----FSYISRHVCSYFPITLHVED--INAFRS 108
VvDGAT2 71 LTVFGLLLVFMV-IPIDER--SKYGRKL----SRYICKHACGYFPVTLYVED--IKAFDP 121
ZmDGAT2 67 ALVLATQLFFMF-LPLSDK--SRLGRKI----ARFISKYVIGYFPVTLHVED--YGAFDP 117
BtDGAT2 73 WLIAVLYFTWLV-FDWNTPKKGG--RRSQWVRNWAVWRYFRDYFPIQLVK----THNLLT 125
CeDGAT2a 58 WIILGLYAVWYL-YDRESPRRGG--YRDNWFRNLSLHKWFAEYFPVKLHK----TAELDP 110
CeDGAT2b 71 WFLVPLYAVWFY-YDFDTPKKAS--RRWNWARRHVAWKYFASYFPLRLIK----TADLPA 123
HsDGAT2 100 WLIAVLYFTWLV-FDWNTPKKGG--RRSQWVRNWAVWRYFRDYFPIQLVK----THNLLT 152
MmDGAT2 100 WLIAVLYFTWLA-FDWNTPKKGG--RRSQWVRNWAVWRYFRDYFPIQLVK----THNLLT 152

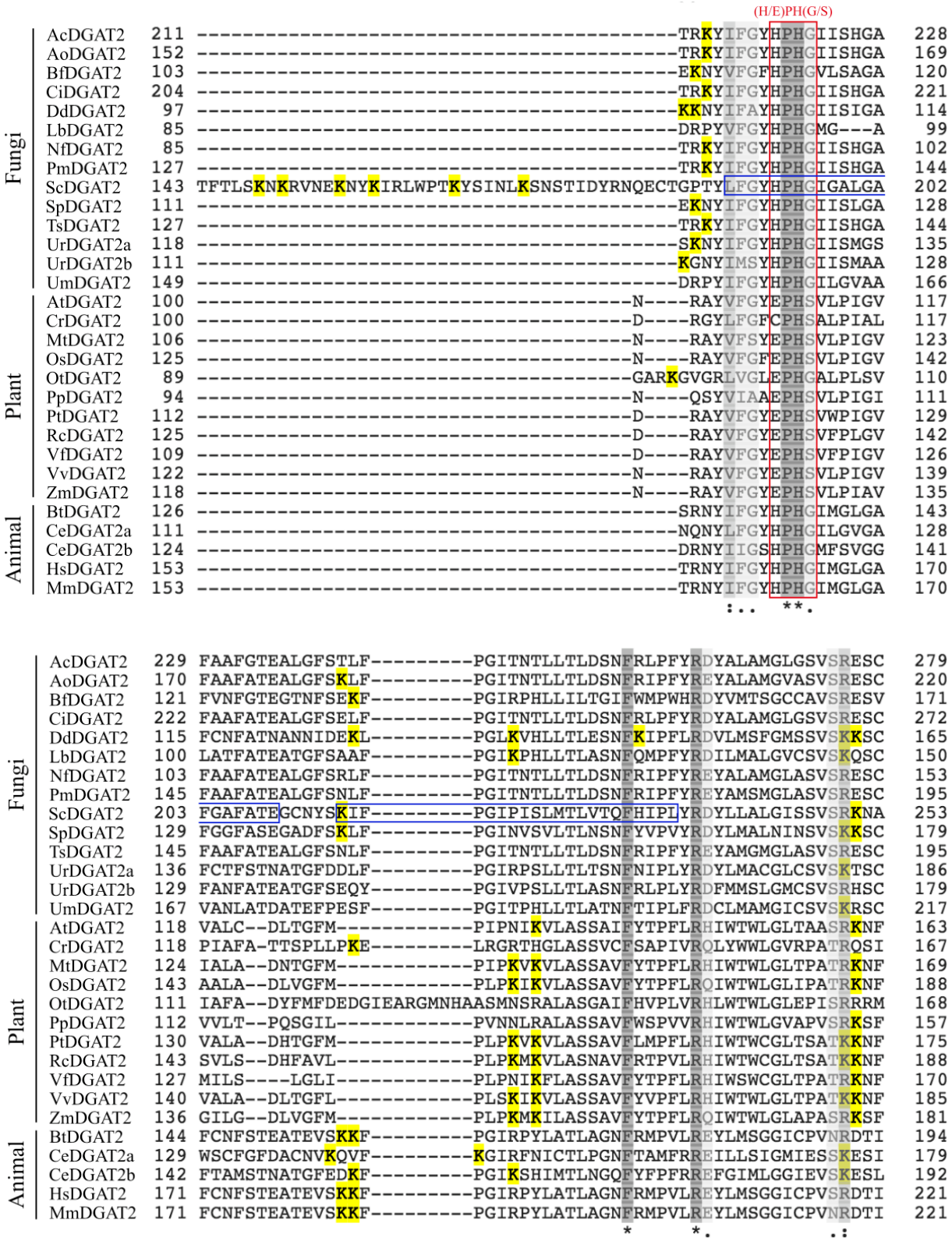
(H/E)PH(G/S)
Fungi
Plant
Animal
AcDGAT2 211 TRKYIFGYHPHGIISHGA 228
AoDGAT2 152 TRKYIFGYHPHGIISHGA 169
BfDGAT2 103 EKNYVFGFHPHGVLSAGA 120
CiDGAT2 204 TRKYIFGYHPHGIISHGA 221
DdDGAT2 97 KKNYIFAYHPHGIISIGA 114
LbDGAT2 85 DRPYVFGYHPHGMG---A 99
NfDGAT2 85 TRKYIFGYHPHGIISHGA 102
PmDGAT2 127 TRKYIFGYHPHGIISHGA 144
ScDGAT2 143 TFTLSKNKRVNEKNYKIRLWPTKYSINLKSNSTIDYRNQECTGPTYLFGYHPHGIGALGA 202
SpDGAT2 111 EKNYIFGYHPHGIISLGA 128
TsDGAT2 127 TRKYIFGYHPHGIISHGA 144
UrDGAT2a 118 SKNYIFGYHPHGIISMGS 135
UrDGAT2b 111 KGNYIMSYHPHGIISMAA 128
UmDGAT2 149 DRPYIFGYHPHGILGVAA 166
AtDGAT2 100 N----RAYVFGYEPHSVLPIGV 117
CrDGAT2 100 D----RGYLFGFCPHSALPIAL 117
MtDGAT2 106 N----RAYVFSYEPHSVLPIGV 123
OsDGAT2 125 N----RAYVFGFEPHSVLPIGV 142
OtDGAT2 89 GARKGVGRLVGLEPHGALPLSV 110
PpDGAT2 94 N----QSYVIAAEPHSVLPIGI 111
PtDGAT2 112 D----RAYVFGYEPHSVWPIGV 129
RcDGAT2 125 D----RAYVFGYEPHSVFPLGV 142
VfDGAT2 109 D----RAYVFGYEPHSVFPIGV 126
VvDGAT2 122 N----RAYVFGYEPHSVLPIGV 139
ZmDGAT2 118 N----RAYVFGYEPHSVLPIAV 135
BtDGAT2 126 SRNYIFGYHPHGIMGLGA 143
CeDGAT2a 111 NQNYLFGYHPHGILGVGA 128
CeDGAT2b 124 DRNYIIGSHPHGMFSVGG 141
HsDGAT2 153 TRNYIFGYHPHGIMGLGA 170
MmDGAT2 153 TRNYIFGYHPHGIMGLGA 170
AcDGAT2 229 FAAFGTEALGFSTLF---------PGITNTLLTLDSNFRLPFYRDYALAMGLGSVSRESC 279
AoDGAT2 170 FAAFATEALGFSKLF---------PGITNTLLTLDSNFRIPFYREYALAMGVASVSRESC 220
BfDGAT2 121 FVNFGTEGTNFSEKF---------PGIRPHLLILTGIFWMPWHRDYVMTSGCCAVSRESV 171
CiDGAT2 222 FAAFATEALGFSELF---------PGITNTLLTLDSNFRLPFYRDYALAMGLGSVSRESC 272
DdDGAT2 115 FCNFATNANNIDEKL---------PGLKVHLLTLESNFKIPFLRDVLMSFGMSSVSKKSC 165
LbDGAT2 100 LATFATEATGFSAAF---------PGIKPHLLTLASNFQMPFYRDILMALGVCSVSKQSC 150
NfDGAT2 103 FAAFATEALGFSRLF---------PGITNTLLTLDSNFRIPFYREYALAMGLASVSRESC 153
PmDGAT2 145 FAAFATEALGFSNLF---------PGITNTLLTLDSNFRIPFYREYAMSMGLASVSRESC 195
ScDGAT2 203 FGAFATEGCNYSKIF---------PGIPISLMTLVTQFHIPLYRDYLLALGISSVSRKNA 253
SpDGAT2 129 FGGFASEGADFSKLF---------PGINVSVLTLNSNFYVPVYRDYLMALNINSVSKKSC 179
TsDGAT2 145 FAAFATEALGFSNLF---------PGITNTLLTLDSNFRIPFYREYAMGMGLASVSRESC 195
UrDGAT2a 136 FCTFSTNATGFDDLF---------PGIRPSLLTLTSNFNIPLYRDYLMACGLCSVSKTSC 186
UrDGAT2b 129 FANFATEATGFSEQY---------PGIVPSLLTLASNFRLPLYRDFMMSLGMCSVSRHSC 179
UmDGAT2 167 VANLATDATEFPESF---------PGITPHLLTLATNFTIPLFRDCLMAMGICSVSKRSC 217
AtDGAT2 118 VALC--DLTGFM----------PIPNIKVLASSAIFYTPFLRHIWTWLGLTAASRKNF 163
CrDGAT2 118 PIAFA-TTSPLLPKE---------LRGRTHGLASSVCFSAPIVRQLYWWLGVRPATRQSI 167
MtDGAT2 124 IALA--DNTGFM----------PIPKVKVLASSAVFYTPFLRHIWTWLGLTPATRKNF 169
OsDGAT2 143 AALA--DLVGFM----------PLPKIKVLASSAVFYTPFLRQIWTWLGLIPATRKNF 188
OtDGAT2 111 IAFA--DYFMFDEDGIEARGMNHAASMNSRALASGAIFHVPLVRHLWTWLGLEPISRRRM 168
PpDGAT2 112 VVLT--PQSGIL----------PVNNLRALASSAVFWSPVVRHIWTWLGVAPVSRKSF 157
PtDGAT2 130 VALA--DHTGFM----------PLPKVKVLASSAVFLMPFLRHIWTWCGLTSATKKNF 175
RcDGAT2 143 SVLS--DHFAVL----------PLPKMKVLASNAVFRTPVLRHIWTWCGLTSATKKNF 188
VfDGAT2 127 MILS----LGLI----------PLPNIKFLASSAVFYTPFLRHIWSWCGLTPATRKNF 170
VvDGAT2 140 VALA--DLTGFL----------PLSKIKVLASSAVFYVPFLRHIWTWLGLTPATKKNF 185
ZmDGAT2 136 GILG--DLVGFM----------PLPKMKILASSAVFYTPFLRQIWTWLGLAPASRKSF 181
BtDGAT2 144 FCNFSTEATEVSKKF---------PGIRPYLATLAGNFRMPVLREYLMSGGICPVNRDTI 194
CeDGAT2a 129 WSCFGFDACNVKQVF---------KGIRFNICTLPGNFTAMFRREILLSIGMIESSKESI 179
CeDGAT2b 142 FTAMSTNATGFEDKF---------PGIKSHIMTLNGQFYFPFRREFGIMLGGIEVSKESL 192
HsDGAT2 171 FCNFSTEATEVSKKF---------PGIRPYLATLAGNFRMPVLREYLMSGGICPVSRDTI 221
MmDGAT2 171 FCNFSTEATEVSKKF---------PGIRPYLATLAGNFRMPVLREYLMSGGICPVNRDTI 221

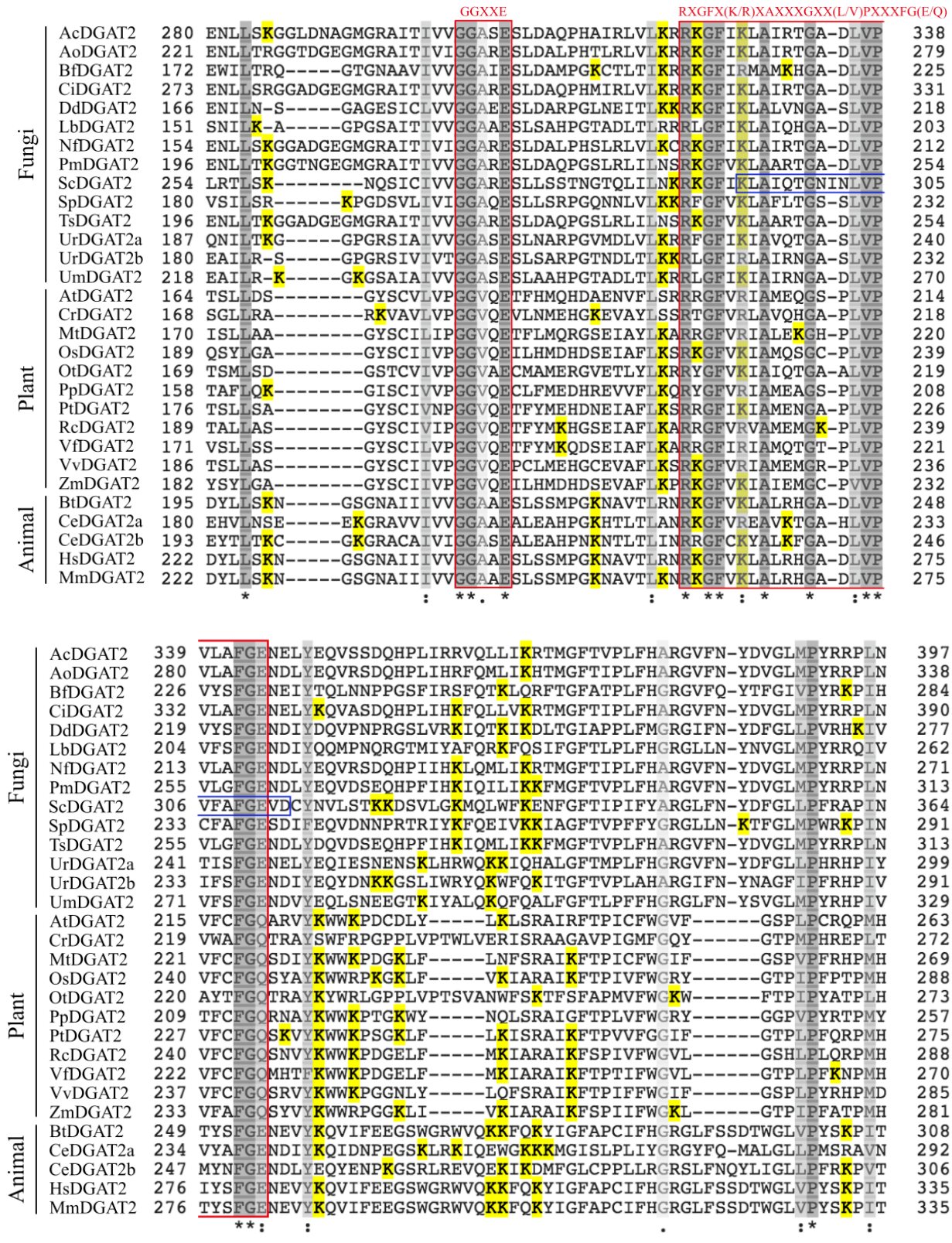
GGXXE
RXGFX(K/R)XAXXXGXX(L/V)PXXXFG(E/Q)
Fungi
Plant
Animal
AcDGAT2 280 ENLLSKGGLDNAGMGRAITIVVGGASESLDAQPHAIRLVLKRRKGFIKLAIRTGA-DLVP 338
AoDGAT2 221 ENLLTRGGTDGEGMGRAITIVIGGARESLDALPHTLRLVLKRRKGFIKLAIRTGA-DLVP 279
BfDGAT2 172 EWILTRQ-----GTGNAAVIVVGGAIESLDAMPGKCTLTIKRRKGFIRMAMKHGA-DLVP 225
CiDGAT2 273 ENLLSRGGADGEGMGRAITIVVGGARESLDAQPHMIRLVLKRRKGFIKLAIRTGA-DLVP 331
DdDGAT2 166 ENILN-S-----GAGESICLVVGGAEESLDARPGLNEITLKKRKGFIKLALVNGA-SLVP 218
LbDGAT2 151 SNILK-A-----GPGSAITIVVGGAAESLSAHPGTADLTLRRRLGFIKLAIQHGA-DLVP 203
NfDGAT2 154 ENLLSKGGADGEGMGRAITIVIGGARESLDALPHSLRLVLKCRKGFIKLAIRTGA-DLVP 212
PmDGAT2 196 ENLLTKGGTNGEGMGRAITIVVGGARESLDAQPGSLRLILNSRKGFVKLAARTGA-DLVP 254
ScDGAT2 254 LRTLSK--------NQSICIVVGGARESLLSSTNGTQLILNKRKGFIKLAIQTGNINLVP 305
SpDGAT2 180 VSILSR------KPGDSVLIVIGGAQESLLSRPGQNNLVLKKRFGFVKLAFLTGS-SLVP 232
TsDGAT2 196 ENLLTKGGADGEGMGRAITIVVGGARESLDAQPGSLRLILNSRKGFVKLAARTGA-DLVP 254
UrDGAT2a 187 QNILTKG-----GPGRSIAIVVGGASESLNARPGVMDLVLKRRFGFIKIAVQTGA-SLVP 240
UrDGAT2b 180 EAILR-S-----GPGRSIVIVTGGASESLSARPGTNDLTLKKRLGFIRLAIRNGA-SLVP 232
UmDGAT2 218 EAILR-K-----GKGSAIAIVVGGASESLAAHPGTADLTLKRRLGFIKIAIRNGA-DLVP 270
AtDGAT2 164 TSLLDS--------GYSCVLVPGGVQETFHMQHDAENVFLSRRRGFVRIAMEQGS-PLVP 214
CrDGAT2 168 SGLLRA--------RKVAVLVPGGVQEVLNMEHGKEVAYLSSRTGFVRLAVQHGA-PLVP 218
MtDGAT2 170 ISLLAA--------GYSCILIPGGVQETFLMQRGSEIAYLKARRGFVRIALEKGH-PLVP 220
OsDGAT2 189 QSYLGA--------GYSCIIVPGGVQEILHMDHDSEIAFLKSRKGFVKIAMQSGC-PLVP 239
OtDGAT2 169 TSMLSD--------GSTCVIVPGGVAECMAMERGVETLYLKRRYGFVKIAIQTGA-ALVP 219
PpDGAT2 158 TAFLQK--------GISCIVVPGGVQECLFMEDHREVVFLKQRYGFVRIAMEAGS-PLVP 208
PtDGAT2 176 TSLLSA--------GYSCIVNPGGVQETFYMEHDNEIAFLKSRRGFIKIAMENGA-PLVP 226
RcDGAT2 189 TALLAS--------GYSCIVIPGGVQETFYMKHGSEIAFLKARRGFVRVAMEMGK-PLVP 239
VfDGAT2 171 VSLLSS--------GYSCILVPGGVQETFYMKQDSEIAFLKARRGFIRIAMQTGT-PLVP 221
VvDGAT2 186 TSLLAS--------GYSCIIVPGGVQEPCLMEHGCEVAFLKSRKGFVRIAMEMGR-PLVP 236
ZmDGAT2 182 YSYLGA--------GYSCIIVPGGVQEILHMDHDSEVAFLKPRKGFVKIAIEMGC-PVVP 232
BtDGAT2 195 DYLLSKN-----GSGNAIIIVVGGAAESLSSMPGKNAVTLRNRKGFVKLALRHGA-DLVP 248
CeDGAT2a 180 EHVLNSE-----EKGRAVVIVVGGAAEALEAHPGKHTLTLANRKGFVREAVKTGA-HLVP 233
CeDGAT2b 193 EYTLTKC-----GKGRACAIVIGGASEALEAHPNKNTLTLINRRGFCKYALKFGA-DLVP 246
HsDGAT2 222 DYLLSKN-----GSGNAIIIVVGGAAESLSSMPGKNAVTLRNRKGFVKLALRHGA-DLVP 275
MmDGAT2 222 DYLLSKN-----GSGNAIIIVVGGAAESLSSMPGKNAVTLKNRKGFVKLALRHGA-DLVP 275
AcDGAT2 339 VLAFGENELYEQVSSDQHPLIRRVQLLIKRTMGFTVPLFHARGVFN-YDVGLMPYRRPLN 397
AoDGAT2 280 VLAFGENDLYEQVRSDQHPLIHRFQMLIKHTMGFTIPLFHARGVFN-YDVGLMPYRRPLN 338
BfDGAT2 226 VYSFGENEIYTQLNNPPGSFIRSFQTKLQRFTGFATPLFHGRGVFQ-YTFGIVPYRKPIH 284
CiDGAT2 332 VLAFGENELYKQVASDQHPLIHKFQLLVKRTMGFTIPLFHARGVFN-YDVGLMPYRRPLN 390
DdDGAT2 219 VYSFGENDIYDQVPNPRGSLVRKIQTKIKDLTGIAPPLFMGRGIFN-YDFGLLPVRHKIV 277
LbDGAT2 204 VFSFGENDIYQQMPNQRGTMIYAFQRKFQSIFGFTLPLFHGRGLLN-YNVGLMPYRRQIV 262
NfDGAT2 213 VLAFGENDLYEQVRSDQHPIIHKLQMLIKRTMGFTIPLFHARGVFN-YDVGLMPYRRPLN 271
PmDGAT2 255 VLGFGENDLYEQVDSEQHPFIHKIQILIKKFMGFTVPLFHARGVFN-YDVGLMPYRRPLN 313
ScDGAT2 306 VFAFGEVDCYNVLSTKKDSVLGKMQLWFKENFGFTIPIFYARGLFN-YDFGLLPFRAPIN 364
SpDGAT2 233 CFAFGESDIFEQVDNNPRTRIYKFQEIVKKIAGFTVPFFYGRGLLN-KTFGLMPWRKPIN 291
TsDGAT2 255 VLGFGENDLYDQVDSEQHPFIHKIQMLIKKFMGFTVPLFHARGVFN-YDVGLMPYRRPLN 313
UrDGAT2a 241 TISFGENELYEQIESNENSKLHRWQKKIQHALGFTMPLFHGRGVFN-YDFGLLPHRHPIY 299
UrDGAT2b 233 IFSFGENDIYEQYDNKKGSLIWRYQKWFQKITGFTVPLAHARGIFN-YNAGFIPFRHPIV 291
UmDGAT2 271 VFSFGENDVYEQLSNEEGTKIYALQKQFQALFGFTLPFFHGRGLFN-YSVGLMPYRHPIV 329
AtDGAT2 215 VFCFGQARVYKWWKPDCDLY-----LKLSRAIRFTPICFWGVF------GSPLPCRQPMH 263
CrDGAT2 219 VWAFGQTRAYSWFRPGPPLVPTWLVERISRAAGAVPIGMFGQY------GTPMPHREPLT 272
MtDGAT2 221 VFCFGQSDIYKWWKPDGKLF-----LNFSRAIKFTPICFWGIF------GSPVPFRHPMH 269
OsDGAT2 240 VFCFGQSYAYKWWRPKGKLF-----VKIARAIKFTPIVFWGRY------GTPIPFPTPMH 288
OtDGAT2 220 AYTFGQTRAYKYWRLGPPLVPTSVANWFSKTFSFAPMVFWGKW------FTPIPYATPLH 273
PpDGAT2 209 TFCFGQRNAYKWWKPTGKWY-----NQLSRAIGFTPLVFWGRY------GGPVPYRTPMY 257
PtDGAT2 227 VFCFGQSKVYKWWKPSGKLF-----LKISRAIKFTPVVFGGIF------GTPLPFQRPMH 275
RcDGAT2 240 VFCFGQSNVYKWWKPDGELF-----MKIARAIKFSPIVFWGVL------GSHLPLQRPMH 288
VfDGAT2 222 VFCFGQMHTFKWWKPDGELF-----MKIARAIKFTPTIFWGVL------GTPLPFKNPMH 270
VvDGAT2 237 VFCFGQSRVYKWWKPGGNLY-----LQFSRAIKFTPIFFWGIF------GSPLPYRHPMD 285
ZmDGAT2 233 VFAFGQSYVYKWWRPGGKLI-----VKIARAIKFSPIIFWGKL------GTPIPFATPMH 281
BtDGAT2 249 TYSFGENEVYKQVIFEEGSWGRWVQKKFQKYIGFAPCIFHGRGLFSSDTWGLVPYSKPIT 308
CeDGAT2a 234 VYAFGENDIYKQIDNPEGSKLRKIQEWGKKKMGISLPLIYGRGYFQ-MALGLLPMSRAVN 292
CeDGAT2b 247 MYNFGENDLYEQYENPKGSRLREVQEKIKDMFGLCPPLLRGRSLFNQYLIGLLPFRKPVT 306
HsDGAT2 276 IYSFGENEVYKQVIFEEGSWGRWVQKKFQKYIGFAPCIFHGRGLFSSDTWGLVPYSKPIT 335
MmDGAT2 276 TYSFGENEVYKQVIFEEGSWGRWVQKKFQKYIGFAPCIFHGRGLFSSDTWGLVPYSKPIT 335

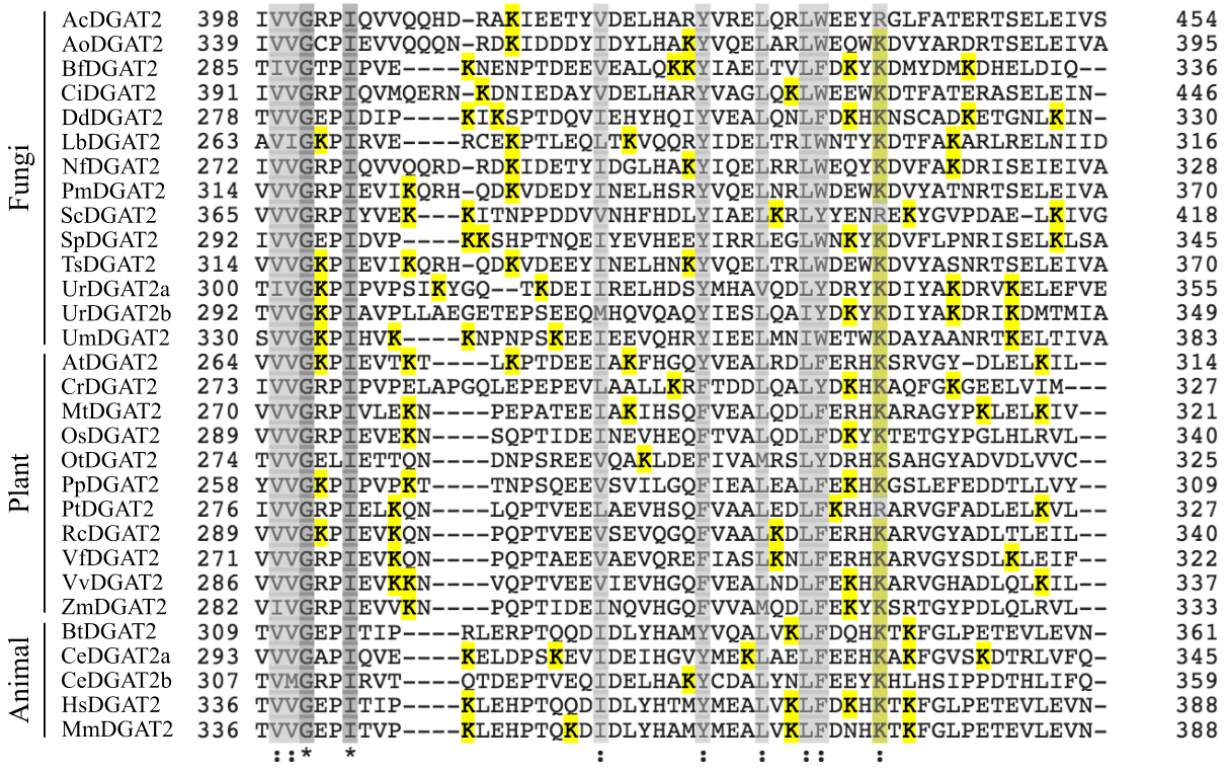

Figure 9.1. DGAT2 is highly conserved among species – Multiple sequence alignment of DGAT2 orthologs. Species are as follows: *Ajellomyces capsulatus*, AcDGAT2; *Aspergillus oryzae*, AoDGAT2; *Branchiostoma floridae*, BfDGAT2; *Coccidioides immitis*, CiDGAT2; *Dictyostelium discoideum*, DdDGAT2; *Laccaria bicolor*, LbDGAT2; *Neosartorya fischeri*, NfDGAT2; *Penicillium marneffei*, PmDGAT2; *Saccharomyces cerevisiae*, ScDGAT2; *Schizosaccharomyces pombe*, SpDGAT2; *Talaromyces stipitatus*, TsDGAT2; *Umbelopsis ramanniana*, UrDGAT2a, UrDGAT2b; *Ustilago maydis*, UmDGAT2; *Arabidopsis thaliana*, AtDGAT2; *Chlamydomonas reinhardtii*, CrDGAT2; *Medicago truncatula*, MtDGAT2; *Oryza sativa*, OsDGAT2; *Ostreococcus tauri*, OtDGAT2; *Physcomitrella patens*, PpDGAT2; *Populus trichocarpa*, PtDGAT2; *Ricinus communis*, RcDGAT2; *Vernicia fordii*, VfDGAT2; *Vitis vinifera*, VvDGAT2; *Zea mays*, ZmDGAT2; *Bos taurus*, BtDGAT2; *Caenorhabditis elegans*, CeDGAT2a, CeDGAT2b; *Homo sapiens*, HsDGAT2; *Mus musculus*, MmDGAT2. '*' denotes identical residues. ':' refers to conservation between groups of strongly similar properties. '.' refers to conservation between groups of weakly similar properties. Conserved domains are marked in red boxes. The position of transmembrane domains in ScDGAT2 and MmDGAT2 are marked in blue boxes (Liu *et al.*, 2011; Stone *et al.*, 2006; McFie *et al.*, 2014). The position of lysine residues are highlighted in yellow.

Table 9.1. DGAT2 interacting proteins detected by mass spectrometry

Protein	Accession Number	Unique Peptide Count	Percent Coverage	Frequency in Contaminant Repository
Eukaryotic initiation factor 4A-I	IF4A1_HUMAN	4	4.93%	0.381924
DNA replication licensing factor MCM6	MCM6_HUMAN	4	1.95%	0.166181
Glyceraldehyde-3-phosphate dehydrogenase	G3P_HUMAN	3	7.16%	0.577259
ATP synthase F(0) complex subunit B1, mitochondrial	AT5F1_HUMAN	3	7.42%	0.084548
Diacylglycerol O-acyltransferase 2	DGAT2_HUMAN	3	5.15%	N/A
T-complex protein 1 subunit alpha	TCPA_HUMAN	3	3.96%	0.396501
Importin subunit beta-1	IMB1_HUMAN	3	3.88%	0.314869
Importin-4	IPO4_HUMAN	3	1.76%	0.055394
Peptidyl-tRNA hydrolase 2, mitochondrial	PTH2_HUMAN	2	12.80%	0.020408
Small nuclear ribonucleoprotein Sm D1	SMD1_HUMAN	2	10.90%	0.422741
Sideroflexin-1 OS=Homo sapiens	SFXN1_HUMAN	2	8.39%	0.058309
Eukaryotic translation initiation factor 3 subunit G	EIF3G_HUMAN	2	7.81%	0.172012
Sterol-4-alpha-carboxylate 3-dehydrogenase, decarboxylating	NSDHL_HUMAN	2	3.49%	0.023324
26S proteasome non-ATPase regulatory subunit 11	PSD11_HUMAN	2	3.08%	0.195335
Calnexin	CALX_HUMAN	2	2.53%	0.239067
Erythroid differentiation-related factor 1	EDRF1_HUMAN	2	2.26%	N/A
Delta-1-pyrroline-5-carboxylate synthase	P5CS_HUMAN	2	2.26%	0.166181
Coatomer subunit beta'	COPB2_HUMAN	2	2.10%	0.131195
Coatomer subunit gamma-1	COPG1_HUMAN	2	1.95%	0.113703
Heat shock cognate 71 kDa protein	HSP7C_HUMAN	2	1.70%	0.962099
DNA mismatch repair protein Msh6	MSH6_HUMAN	2	1.32%	0.093294
Eukaryotic translation initiation factor 3 subunit C	EIF3C_HUMAN (+1)	2	1.20%	0.209913

60S ribosomal protein L11	RL11_HUMAN	1	7.87%	0.443149
ADP/ATP translocase 3	ADT3_HUMAN	1	7.05%	0.451895
Heat shock protein 75 kDa, mitochondrial	TRAP1_HUMAN	1	1.99%	0.198251
Cytochrome c oxidase subunit NDUFA4	NDUA4_HUMAN	1	14.80%	0.034985
60S ribosomal protein L23	RL23_HUMAN	1	14.30%	0.571429
40S ribosomal protein S20	RS20_HUMAN	1	10.10%	0.373178
40S ribosomal protein S13	RS13_HUMAN	1	9.93%	0.405248
ATP synthase subunit g, mitochondrial	ATP5L_HUMAN	1	8.74%	0.055394
Tafazzin	TAZ_HUMAN	1	8.56%	N/A
Prostaglandin E synthase 3	TEBP_HUMAN	1	8.12%	0.084548
Heat shock protein beta-1	HSPB1_HUMAN	1	7.80%	0.163265
Ubiquitin-60S ribosomal protein L40	RL40_HUMAN (+3)	1	7.03%	0.61516
Kallikrein-7	KLK7_HUMAN	1	6.72%	0.020408
Dolichyl-diphosphooligosaccharide--protein glycosyltransferase 48 kDa subunit	OST48_HUMAN	1	6.36%	0.081633
Guanine nucleotide-binding protein subunit beta-2-like 1	GBLP_HUMAN	1	6.31%	0.233236
Signal recognition particle receptor subunit beta	SRPRB_HUMAN	1	5.90%	0.037901
Methylosome subunit pICln	ICLN_HUMAN	1	5.49%	0.341108
Ras-related protein Rab-13	RAB13_HUMAN	1	5.42%	0.06414
CMT1A duplicated region transcript 15 protein	CDRTF_HUMAN	1	5.32%	N/A
Leucine-rich repeat-containing protein 59	LRC59_HUMAN	1	5.21%	0.148688
Ras-related protein Rab-15	RAB15_HUMAN	1	5.19%	N/A
Replication factor C subunit 3	RFC3_HUMAN	1	5.06%	0.069971
Uridine-cytidine kinase 2	UCK2_HUMAN	1	4.98%	0.008746
NADH dehydrogenase [ubiquinone] iron-sulfur protein 3, mitochondrial	NDUS3_HUMAN	1	4.92%	0.03207
Pyruvate dehydrogenase E1 component subunit beta, mitochondrial	ODPB_HUMAN	1	4.46%	0.084548
Putative uncharacterized protein FLJ37770	YK006_HUMAN	1	4.33%	N/A
Hydroxysteroid dehydrogenase-like protein 2	HSDL2_HUMAN	1	4.31%	0.011662

Dolichol-phosphate mannosyltransferase subunit 1	DPM1_HUMAN	1	4.23%	0.055394
Stomatin-like protein 2, mitochondrial	STML2_HUMAN	1	4.21%	0.090379
26S proteasome non-ATPase regulatory subunit 14	PSDE_HUMAN	1	4.19%	0.139942
Transmembrane emp24 domain-containing protein 10	TMEDA_HUMAN	1	4.11%	0.043732
Heterogeneous nuclear ribonucleoprotein F	HNRPF_HUMAN	1	4.10%	0.516035
Alpha-centractin	ACTZ_HUMAN	1	3.99%	0.169096
Cytochrome b-c1 complex subunit 2, mitochondrial	QCR2_HUMAN	1	3.97%	0.06414
Voltage-dependent anion-selective channel protein 1	VDAC1_HUMAN	1	3.89%	0.084548
T-complex protein 1 subunit epsilon	TCPE_HUMAN	1	3.70%	0.376093
B-cell receptor-associated protein 31	BAP31_HUMAN	1	3.66%	0.075802
Very-long-chain enoyl-CoA reductase	TECR_HUMAN	1	3.57%	0.110787
Pachytene checkpoint protein 2 homolog	PCH2_HUMAN	1	3.47%	N/A
26S protease regulatory subunit 7	PRS7_HUMAN	1	3.23%	0.212828
Pyruvate kinase PKM	KPYM_HUMAN	1	3.20%	0.556851
Sulfotransferase 4A1	ST4A1_HUMAN	1	3.17%	N/A
Serpin H1	SERPH_HUMAN	1	3.11%	0.107872
Mitochondrial import receptor subunit TOM40 homolog	TOM40_HUMAN	1	3.05%	0.03207
Tyrosine-protein kinase CSK	CSK_HUMAN	1	2.89%	0.017493
Acetyl-CoA acetyltransferase, mitochondrial	THIL_HUMAN	1	2.81%	0.116618
Trace amine-associated receptor 1	TAAR1_HUMAN	1	2.65%	N/A
Minor histocompatibility antigen H13	HM13_HUMAN	1	2.65%	0.037901
Phosphoglycerate kinase 1	PGK1_HUMAN	1	2.64%	0.177843
NADH dehydrogenase [ubiquinone] iron-sulfur protein 2, mitochondrial	NDUS2_HUMAN	1	2.59%	0.029155
ATP-dependent RNA helicase DDX3X	DDX3X_HUMAN (+1)	1	2.57%	0.443149
THO complex subunit 3	THOC3_HUMAN	1	2.56%	0.043732

E3 ubiquitin-protein ligase TRIM13	TRI13_HUMAN	1	2.46%	N/A
Basic leucine zipper and W2 domain-containing protein 1	BZW1_HUMAN	1	2.39%	0.03207
Bicaudal D-related protein 2	BICR2_HUMAN	1	2.36%	N/A
Kelch-like protein 10	KLH10_HUMAN	1	2.30%	N/A
T-complex protein 1 subunit beta	TCPB_HUMAN	1	2.24%	0.381924
Glutaminase kidney isoform, mitochondrial	GLSK_HUMAN	1	2.24%	0.029155
Katanin p60 ATPase-containing subunit A1	KTNA1_HUMAN	1	2.24%	0.023324
Sarcoplasmic/endoplasmic reticulum calcium ATPase 2	AT2A2_HUMAN	1	2.21%	0.157434
Cytochrome P450 3A43	CP343_HUMAN	1	2.19%	N/A
COP9 signalosome complex subunit 1	CSN1_HUMAN	1	2.04%	0.046647
Calcium-binding and coiled-coil domain-containing protein 2	CACO2_HUMAN	1	2.02%	0.011662
T-complex protein 1 subunit gamma	TCPG_HUMAN	1	2.02%	0.361516
Asparagine synthetase [glutamine-hydrolyzing]	ASNS_HUMAN	1	1.96%	0.052478
DNA replication licensing factor MCM5	MCM5_HUMAN	1	1.91%	0.201166
ATP-dependent Clp protease ATP-binding subunit clpX-like, mitochondrial	CLPX_HUMAN	1	1.90%	0.040816
Tyrosine--tRNA ligase, cytoplasmic	SYYC_HUMAN	1	1.89%	0.110787
Complement C1r subcomponent-like protein	C1RL_HUMAN (+1)	1	1.85%	N/A
cAMP-dependent protein kinase type I-beta regulatory subunit	KAP1_HUMAN	1	1.84%	N/A
Cytoskeleton-associated protein 4	CKAP4_HUMAN	1	1.83%	0.122449
Telomere repeats-binding bouquet formation protein 1	TERB1_HUMAN	1	1.79%	N/A
Eukaryotic translation initiation factor 3 subunit L	EIF3L_HUMAN	1	1.77%	0.247813
Transmembrane protein 200C	T200C_HUMAN	1	1.77%	N/A
Coiled-coil domain-containing protein 181	CC181_HUMAN	1	1.77%	N/A

Centromere/kinetochore protein zw10 homolog	ZW10_HUMAN	1	1.67%	0.026239
Early endosome antigen 1	EEA1_HUMAN	1	1.63%	0.014577
WD repeat-containing protein 44	WDR44_HUMAN	1	1.53%	0.011662
Zinc finger protein 408	ZN408_HUMAN	1	1.53%	N/A
Zinc finger protein 671	ZN671_HUMAN	1	1.50%	N/A
NACHT, LRR and PYD domains-containing protein 6	NALP6_HUMAN	1	1.46%	N/A
Extended synaptotagmin-1	ESYT1_HUMAN	1	1.45%	0.061224
Exportin-7	XPO7_HUMAN	1	1.38%	0.046647
Solute carrier family 12 member 2	S12A2_HUMAN	1	1.32%	0.011662
Putative ATP-dependent RNA helicase DDX11-like protein 8	D11L8_HUMAN (+2)	1	1.32%	N/A
tRNA (cytosine(34)-C(5))-methyltransferase	NSUN2_HUMAN	1	1.30%	0.142857
Vacuolar protein sorting-associated protein 35	VPS35_HUMAN	1	1.26%	0.078717
116 kDa U5 small nuclear ribonucleoprotein component	U5S1_HUMAN	1	1.23%	0.314869
X-ray repair cross-complementing protein 5	XRCC5_HUMAN	1	1.23%	0.390671
Dynactin subunit 1	DCTN1_HUMAN	1	1.10%	0.116618
Band 4.1-like protein 2	E41L2_HUMAN	1	1.09%	0.078717
Desmocollin-1	DSC1_HUMAN	1	1.01%	0.110787
Short transient receptor potential channel 1	TRPC1_HUMAN	1	1.01%	N/A
DNA mismatch repair protein Msh2	MSH2_HUMAN	1	0.96%	0.072886
X-linked retinitis pigmentosa GTPase regulator-interacting protein 1	RPGR1_HUMAN	1	0.93%	N/A
DNA-directed RNA polymerase II subunit RPB1	RPB1_HUMAN	1	0.91%	0.104956
Zinc finger protein basonuclin-2	BNC2_HUMAN	1	0.91%	0.005831
Nebulin-related-anchoring protein	NRAP_HUMAN	1	0.81%	N/A
Hermansky-Pudlak syndrome 3 protein	HPS3_HUMAN	1	0.80%	N/A
Zinc finger protein 197	ZN197_HUMAN	1	0.78%	N/A
ATP-binding cassette sub-family A member 7	ABCA7_HUMAN	1	0.75%	N/A

Slit homolog 3 protein	SLIT3_HUMAN	1	0.72%	N/A
Brefeldin A-inhibited guanine nucleotide-exchange protein 3	BIG3_HUMAN	1	0.64%	N/A
Tetratricopeptide repeat protein 37	TTC37_HUMAN	1	0.64%	0.037901
ATPase family AAA domain-containing protein 5	ATAD5_HUMAN	1	0.49%	N/A
Golgi-specific brefeldin A-resistance guanine nucleotide exchange factor 1	GBF1_HUMAN	1	0.48%	0.017493
Filaggrin-2	FILA2_HUMAN	1	0.46%	0.206997
Nuclear pore complex protein Nup98-Nup96	NUP98_HUMAN	1	0.44%	0.040816
Coiled-coil domain-containing protein 168	CC168_HUMAN	1	0.33%	N/A
Nucleosome-remodeling factor subunit BPTF	BPTF_HUMAN	1	0.30%	0.046647
Centromere protein F	CENPF_HUMAN	1	0.28%	0.040816
Nesprin-2	SYNE2_HUMAN	1	0.15%	0.058309

CHAPTER 10: References

Abo-Hashema, K.A.H., Cake, M.H., Power, G.W., and Clarke D. (1999). Evidence for triacylglycerol synthesis in the lumen of microsomes via a lipolysis-esterification pathway involving carnitine acyltransferases. J. Biol. Chem. *274*, 35577–35582.

Abumrad, N.A., and Davidson, N.O. (2012). Role of the gut in lipid homeostasis. Physiol. Rev. *92*, 1061–1085.

Agarwal, A.K., Arioglu, E., De Almeida, S., Akkoc, N., Taylor, S.I., Bowcock, A.M., Barnes, R.I., and Garg, A. (2002). AGPAT2 is mutated in congenital generalized lipodystrophy linked to chromosome 9q34. Nat. Genet. *31*, 21-23.

Aguilera, M., Oliveros, M., Martinez-Padron, M., Barbas, J.A. and Ferrus, A. (2000). Ariadne-1: a vital *Drosophila* gene is required in development and defines a new conserved family of ring-finger proteins. Genetics. *155*, 1231–1244.

Ahmadian, M., Abbott, M.J., Tang, T., Hudak, C.S., Kim, Y., Bruss, M., Hellerstein, M.K., Lee, H. Y., Samuel V.T., Shulman, G. I., Wang, Y., Duncan, R.E., Kang, C., and Sul, H.S. (2011). Desnutrin/ATGL is regulated by AMPK and is required for a brown adipose phenotype. Cell Metab. *13*, 739–748.

Aletrari, M.O., McKibben, C., Williams, H., Pawar, V., Lord, J.M., Flitsch S.L., Whitehead, R., Swanton, E., High, S., and Spooner, R.A. (2011). Eeyarestatin 1 interferes with both retrograde and anterograde intracellular trafficking pathways. PLoS One. *6*, e22713.

Anderson, H., Nilsson, I., and von Heijne, G. (1996). Calnexin can interact with *N*-linked glycans located close to the endoplasmic reticulum membrane. FEBS Lett. *397*, 321–324.

Anthonsen, M.W., Ronnstrand, L., Wernstedt, C., Degerman, E., and Holm, C. (1998). Identification of novel phosphorylation sites in hormone-sensitive lipase that are phosphorylated in response to isoproterenol and govern activation properties in vitro. J. Biol. Chem. *273*, 215–221.

Armand, M., Borel, P., Pasquier, B., Dubois, C., Senft, M., Andre, M., Peyrot, J., Salducci, J., and Lairon, D. (1996). Physicochemical characteristics of emulsions during fat digestion in human stomach and duodenum. Am. J. Physiol. *271*, G172–G183.

Ballar, P., Ors, A.U., Yang, H., and Fang, S. (2010). Differential regulation of CFTRΔF508 degradation by ubiquitin ligases gp78 and Hrd1. Int. J. Biochem. Cell Biol. *42*,167–173.

Ballar, P., Pabuccuoglu, A., and Kose, F.A. (2011). Different p97/VCP complexes function in retrotranslocation step of mammalian Er-associated degradation (ERAD). Int. J. Biochem. Cell Biol. *43*: 613–621.

Ballar, P., Shen, Y., Yang, H., and Fang S. (2006). The role of a novel p97/valosin-containing protein-interacting motif of gp78 in endoplasmic reticulum-associated degradation. J. Biol.

Chem. *281*, 35359–35368.

Bankaitis, V.A. (2009). The Cirque du Soleil of Golgi membrane dynamics. J. Cell Biol. *186*,169-171.

Bartz, R., Li, W.H, Venables, B., Zehmer, J.K., Roth, M.R., Welt, R., Anderson, R.G., Liu, P., and Chapman, K.D. (2007a). Lipidomics reveals that adiposomes store ether lipids and mediate phospholipid traffic. J. Lipid Res. *48*, 837–847.

Bartz, R., Zehmer, J.K., Zhu, M., Chen, Y., Serrero, G., Zhao, Y., and Liu, P. (2007b). Dynamic activity of lipid droplets: protein phosphorylation and GTP-mediated protein translocation. J. Proteome Res. *6*, 3256–3265

Bays, N.W., Wilhovsky, S.K., Goradia, A., Hodgkiss-Harlow, K. and Hampton R.Y. (2001). HRD4/NPL4 is required for the proteasomal processing of ubiquitinated ER proteins. Mol. Biol. Cell. *12*, 4114–4128.

Beigneux, A.P., Vergnes, L., Qiao, X., Quatela, S., Davis, R.G., Watkins, S.M., Coleman, R.A., Walzem, R.L., Philips, M., Reue, K., and Young, S.G. (2006). J. Lipid Res. *47*, 734-744.

Bell, R. M., and Coleman, R.A. (1980). Enzymes of glycerolipid synthesis in eukaryotes. Annu. Rev. Biochem. *49***,** 459–487.

Benyair, R., Ogen-Shtern, N., and Lederkremer, G.Z. (2015). Glycan regulation of ER-associated degradation through compartmentalization. Semin. Cell Dev. Biol. *41*, 99-109.

Bhamidipati, A., Denic, V., Quan, E.M., and Weissman, J.S. (2005). Exploration of the topological requirements of ERAD identifies Yos9p as a lectin sensor of misfolded glycoproteins in the ER lumen. Mol. Cell. *19*, 741–751.

Bou Khalil, M., Sundaram, M., Zhang, H.Y., Links, P.H., Raven, J.F., Manmontri, B., Sariahmetoglu, M., Tran, K., Reue, K., Brindley, D.N., and Yao, Z. (2009). J. Lipid Res. *50*, 47-58.

Bouchoux, J., Beilstein, F., Pauquai, T., Guerrera, I.C., Chateau, D., Ly, N., Alqub, M., Klein, C., Chambaz, J., Rousset, M., Lacorte, J.M., Morel, E., and Dignot, S. (2011). The proteome of cytosolic lipid droplets isolated from differentiated Caco-2/TC7 enterocytes reveals cell-specific characteristics. Biol Cell. *103*, 499–517.

Bozza, P.T., Yu, W., Penrose, J.F., Morgan, E.S., Dvorak, A.M., and Weller, P.F. (1997). Eosinophil lipid bodies: Specific, inducible intracellular sites for enhanced eicosanoid formation. J. Exp. Med. *186*, 909–920.

Braakman, I., and Hebert, D.N. (2013). Protein folding in the endoplasmic reticulum. Cold Spring Harb. Perspect. Biol. *5*, a013201.

Brandt, C., McFie, P.J., and Stone, S.J. (2016a). Biochemical characterization of human acyl coenzyme A: 2-monoacylglycerol acyltransferase-3 (MGAT3). Biochem. Biophys. Res. Commun. *475*, 264-270.

Brandt, C., McFie, P.J., and Stone, S.J. (2016b). Diacylglycerol acyltransferase-2 and monoacylglycerol acyltransferase-2 are ubiquitinated proteins that are degraded by the 26S proteasome. Biochem. J. *473*, 3621-3637.

Brasaemle, D.L. (2007). Thematic review series: adipocyte biology. The perilipin family of structural lipid droplet proteins: stabilization of lipid droplets and control of lipolysis. J. Lipid. Res. *48,* 2547-2559.

Brasaemle, D.L., Dolios, G., Shapiro, L. and Wang, R. (2004). Proteomic analysis of proteins associated with lipid droplets of basal and lipolytically stimulated 3T3–L1 adipocytes. J. Biol. Chem. *279*, 46835–46842

Bronnikov, G.E., Aboulaich, N., Vener, A.V., and Stralfors, P. (2008). Acute effects of insulin on the activity of mitochondrial GPAT1 in primary adipocytes. Biochem. Biophys. Res. Commun. *367*, 201-207

Buhman, K.K., Chen, H.C., and Farese, R.V.Jr. (2001). The enzymes of neutral lipid synthesis. J. Biol. Chem. *276*, 40369–40372.

Buhman, K.K., Smith, S.J., Stone, S.J., Repa, J.J., Wong, J.S., Knapp, F.F. Burri, B.J. Hamilton, R.L. Abumrad, N.A., and Farese, R.V.Jr. (2002). DGAT1 is not essential for intestinal triacylglycerol absorption or chylomicron synthesis. J. Biol. Chem. *277*, 25474–25479.

Caldas, H., and Herman, G.E. (2003). NSDHL, an enzyme involved in cholesterol biosynthesis, traffics through the Golgi and accumulates on ER membranes and on the surface of lipid droplets. Hum. Mol. Genet. *12*, 2981-2991.

Canadian Health Measures Survey. (2012). Retrieved from: http://publications.gc.ca/collections/collection_2012/statcan/82-626-x/82-626-x2012002-eng.pdf

Cao, J., Burn, P., and Shi, Y. (2003a). Properties of the mouse intestinal acyl-CoA:monoacylglycerol acyltransferase, MGAT2. J. Biol. Chem. *278*, 25657–25663.

Cao, J., Cheng, L., and Shi, Y. (2007). Catalytic properties of MGAT3, a putative triacylgycerol synthase. J. Lipid Res. *48*, 583–591.

Cao, J., Li, J.L., Li, D., Tobin, J.F., and Gimeno, R.E. (2006). Molecular identification of microsomal acyl-CoA:glycerol-2-phosphate, a key enzyme in de nova triacylglycerol synthesis Proc. Natl. Acad. Sci. U S A. *103*, 19695-19700.

Cao, J., Lockwood, J., Burn, P., and Shi, Y. (2003b). Cloning and functional characterization of a mouse intestinal acyl-CoA:monoacylglycerol acyltransferase, MGAT2. J. Biol. Chem. *278*, 13860-13866.

Carey, M.C., and Hernell, O. (1992). Digestion and absorption of fat. Semin. Gastrointest. Dis. *3*, 189-208.

Carman, G.M., and Han, G.S. (2006). Roles of phosphatidate photsphatase enzymes in lipid metabolism. Trends Biochem. Sci. *31*, 694-699.

Carmen, G.Y., and Victor, S.M. (2006). Signalling mechanisms regulating lipolysis. Cell Signal. *18*, 401–408.

Carvalho, P., Goder, V., and Rapoport, T.A. (2006). Distinct ubiquitin-ligase complexes define convergent pathways for the degradation of ER proteins. Cell. *126*, 361–373.

Carvalho, P., Stanley, A.M., and Rapoport, T.A. (2010). Retrotranslocation of a misfolded luminal ER protein by the ubiquitin-ligase Hrd1p. Cell. *143*, 579–591.

Cascales, C., Mangiapane, E.H., and Brindley, D.N. (1984). Oleic acid promotes the activation and translocation of phosphatidate phosphohydrolase from the cytosol to particulate fractions of isolated rat hepatocytes. Biochem. J. *219*, 911-916.

Cases, S., Smith, S.J., Zheng, Y.W., Myers, H.M., Lear, S.R., Sande, E., Novak, S., Collins, C., Welch, C.B., Lusis, A.J., Erickson S.K., and Farese R.V.Jr. (1998). Identification of a gene encoding an acyl CoA:diacylglycerol acyltransferase, a key enzyme in triacylglycerol synthesis. Proc. Natl. Acad. Sci. U S A. *95*, 13018-13023.

Cases, S., Stone, S.J., Zhou, P., Yen, E., Tow, B., Lardizabal, K.D., Voelker, T., and Farese, R.V.Jr. (2001). Cloning of DGAT2, a second mammalian diacylglycerol acyltransferase, and related family members. J. Biol. Chem. *276*, 38870–38876.

Chakraborty, T.R., Vancura, A., Balija, V.S., and Haldar, D. (1999). Phosphatidic acid synthesis in mitochondria. Topography of formation and transmembrane migration. J. Biol. Chem. *274*, 29786-29790.

Chan, W.M., Mak, M.C., Fung T.K., Lau, A., Siu, W.Y., and Poon R.Y. (2006). Ubiquitination of p53 at multiple sites in the DNA-binding domain. Mol. Cancer Res. *4*, 15-25.

Chandak, P.G., Radovic, B., Aflaki, E., Kolb, D., Buchebner, M., Frohlich, E., Magnes, C., Sinner, F., Haemmerle, G., Zechner, R., Tabas, I., Levak-Frank, S., and Kratky, D. (2010). Efficient phagocytosis requires triacylglycerol hydrolysis by adipose triglyceride lipase. J. Biol. Chem. *285*, 20192–20201.

Chang, T.Y., Li, B.L., Chang, C.C., and Urano, Y. (2009). Acyl-coenzyme a: Cholesterol acyltransferases. Am. J. Physiol. Endocrinol. Metab. *297*, E1-E9.

Chen, W., Chang, B., Wu, X., Li, L., Sleeman, M., and Chan, L. (2013). Inactivation of Plin4 downregulates Plin5 and reduces cardiac lipid accumulation in mice. Am. J. Physiol. Endocrinol. Metab. *304*, E770–E779.

Chen, H.C., Jensen, D.R., Myers, H.M., Eckel, R.H., and Farese, R.V., Jr. (2003a). Obesity resistance and enhanced glucose metabolismin mice transplanted with white adipose tissue lacking acyl CoA:diacylglycerol acyltransferase 1. J. Clin. Invest. *111*, 1715–1722.

Chen, H.C., Ladha, Z., Smith, S.J., and Farese, R.V., Jr. (2003b). Analysis of energy expenditure at different ambient temperatures in mice lacking DGAT1. Am. J. Physiol. Endocrinol. Metab. *284*, E213–E218.

Chen, H.C., Smith, S.J., Ladha, Z., Jensen, D.R., Ferreira, L.D., Pulawa, L.K., McGuire, J.G., Pitas, R.E., Eckel, R.H., and Farese, R.V.Jr. (2002). Increased insulin and leptin sensitivity in mice lacking acyl CoA:diacylglycerol acyltransferase 1. J. Clin. Invest. *109*, 1049–1055.

Chen, M., Yang, Y., Braunstein, E. Georgeson, K. E., and Harmon, C.M. (2001). Gut expression and regulation of FAT/CD36: possible role in fatty acid transport in rat enterocytes. Am. J. Physiol. Endocrinol. Metab. *281*, E916–E923.

Cheng, D., Meegalla, R.L., He, B., Cromley, D.A., Billheimer, J.T., and Young, P.R. (2001). Human acyl-CoA: diacylglycerol acyltransferase is a tetrameric protein. Biochem. J. *359*, 707-714.

Cheng, D., Nelson, T.C., Chen, J., Walker, S.G., Wardwell-Swanson, J., Meegalla, R., Taub, R., Billheimer, J.T., Ramaker, M., and Feder, J.N. (2003). Identification of acyl coenzyme A:monoacylglycerol acyltransferase 3, an intestinal specific enzyme implicated in dietary fat absorption. J. Biol. Chem. *278*, 13611–13614.

Cho, S.Y., Shin, E.S., Park, P.J., Shin, D.W., Chang, H.K., Kim, D., Lee, H.H., Lee, J.H., Kim, S.H., Song, M.J., Chanf, I.S., Lee, O.S., and Lee, T.R. (2007). Identification of mouse Prp19p as a lipid droplet-associated protein and its possible involvement in the biogenesis of lipid droplets. J. Biol. Chem. *282*, 2456–2465.

Choi, K., Kim, H., Kang, H., Lee, S.Y., Lee, S.J., Back, S.H., Lee, S.H., Kim, M.S., Lee, J.E., Park, J.Y., Kim, J., Kim, S., Song, J.H., Choi, Y., Lee, S., Lee, H.J., Kim, J.H., and Cho, S. (2014). Regulation of diacylglycerol acyltransferase 2 protein stability by gp78-associated endoplasmic-reticulum-associated degradation. FEBS J. *281*, 3048–3060.

Chon, S.H., Zhou, Y.X., Dixon, J.L., and Storch, J. (2007). Intestinal monoacylglycerol metabolism: developmental and nutritional regulation of monoacylglycerol lipase and monoacylglycerol acyltransferase. J. Biol. Chem. *282*, 33346–33357.

Christianson, J.C., Olzmann, J.A., Shaler, T.A., Sowa, M.E., Bennett, E.J., Richter, C.M., Tyler, R.E., Greenblatt, E.J., Harper, J.W., and Kopito, R.R. (2012). Defining human ERAD networks through an integrative mapping strategy. Nat Cell Biol. *14*, 93–105.

Christie, D.A., Lemke, C.D., Elias, I.M., Chau, L.A., Kirchhof, M.G., Li, B., Ball, E.H., Dunn, S.D., Hatch, G.M., and Madrenas, J. (2011). Stomatin-like protein 2 binds cardiolipin and regulates mitochondrial biogenesis and function**.** Mol. Cell. Biol. *31*, 3845-3856.

Ciechanover, A., and Ben, S.R, (2004). N-terminal ubiquitination: more protein substrates join in. Trends Cell. Biol. *14*, 103–106.

Cinti, S. (2001). The adipose organ: morphological perspectives of adipose tissues. Proc. Nutr. Soc. *60*, 319-328.

Cleland W.W. (1963a). The kinetics of enzyme-catalyzed reactions with two or more substrates or products. I. Nomenclature and rate equations. Biochim. Biophys. Acta. *67*, 104–137.

Cleland W.W. (1963b). The kinetics of enzyme-catalyzed reactions with two or more substrates or products. II. Inhibition: nomenclature and theory. Biochim. Biophys. Acta. *67*, 173–187.

Coe, N.R., Simpson, M.A., and Bernlohr, D.A. (1999). Targeted disruption of the adipocyte lipid-binding protein (aP2 protein) gene impairs fat cell lipolysis and increases cellular fatty acid levels. J. Lipid Res. *40*, 967–972.

Coleman, R.A., and Lee, D.P. (2004). Enzymes of triacylglycerol synthesis and their regulation. Prog. Lipid Res. *43*, 134-176.

Coleman, R.A., Lewin, T.M., and Muoio, D.M. (2000). Pysiological and nutritional regulation of enzymes of triacylglycerol. Annu. Rev. Nutr. *20*, 77-103.

Coleman, R. A., Lewin, T.M., Van Horn, C.G., and Gonzalez-Baro, M.R. (2002). Do long-chain acyl-CoA synthetases regulate fatty acid entry into synthetic versus degradative pathways? J. Nutr. *132*, 2123–2126.

Coleman, R.A. and Mashek, D.G. (2011). Mammalian triacylglycerol metabolism: synthesis, lipolysis and signaling. Chem Rev. *10*, 6359–6386.

Collison, L.W., and Jolly, C.A. (2006). Phosphorylation regulates mitochondrial glycerol-3-phosphate-1 acyltransferase activity in T-lymphocytes. Biochim. Biophys. Acta. *1761*, 129-139.

Cook, K. G., Yeaman, S. J., Stralfors, P., Fredrikson, G., and Belfrage, P. (1982). Direct evidence that cholesteryl ester hydrolase from adrenal cortex is the same enzyme as hormone-sensitive lipase from adipose tissue. Eur. J. Biochem. *125*, 245–249.

Cross, B.C., McKibbin, C., Callan, A.C., Roboti, P., Piacenti, M., Rabu, C., Wilson, C.M., Whitehead, R., Flitsch, S.L., Pool, M.R., High, S., and Swanton, E. (2009). Eeyarestatin I inhibits Sec61-mediated protein translocation at the endoplasmic reticulum. J. Cell Sci. ***122*****,** 4393-4400.

Csaki, L.S., and Reue, K. (2010). Lipins: multifunctional lipid metabolism proteins. Annu. Rev. Nutr. *30*, 257-272.

Cui, Z., Vance, J.E., Chen, M.H., Voelker, D.R., and Vance, D.E. (1993). Cloning and expression of a novel phosphatidylethanolamine N- methyltransferase. A specific biochemical and cytological marker for a unique membrane fraction in rat liver. J. Biol. Chem. *268*, 16655-16663.

Czabany, T., Wagner, A., Zweytick, D., Lohner, K., Leitner, E., Ingolic, E., and Daum, G. (2008). Structural and biochemical properties of lipid particles from the yeast Saccharomyces cerevisiae. J. Biol. Chem. *283*, 17065-17074.

Dalen, K.T., Schoonjans, K., Ulven, S.M., Weedon-Fekjaer, M.S., Bentzen, T.G., Koutnikova, H., Auwerx, J., and Nebb, H.I. (2004). Adipose tissue expression of the lipid droplet-associating proteins S3-12 and perilipin is controlled by peroxisome proliferator-activated receptor-gamma. Diabetes. *53*, 1243-1252.

Danilczyk, U.G., and Williams, D.B. (2001). Thelectinchaperonecalnexinutilizes polypeptide-based interactions to associate with many of its substrates in vivo. J. Biol. Chem. *276*, 25532–25540.

Demignot, S., Beilstein, F., and Morel, E. (2014). Triglyceride-rich lipoproteins and cytosolic lipid droplets in enterocytes: Key players in intestinal physiology and metabolic disorders. Biochimie. *96*, 48-55.

Denic, V., Quan, E.M., and Weissman, J.S. (2006). A luminal surveillance complex that selects misfolded glycoproteins for ER-associated degradation. Cell. *126*, 349–359.

Denison, H., Nilsson, C., Kujacic, M., Lofgren, L., Karlsson, C., Knutsson, M., and Eriksson, J.W. (2013). Proof of mechanism for the DGAT1 inhibitor AZD7687: results from a first-time-in-human single dose study. Diabetes, Obes. Metab. *15*, 136−143.

Denison, H., Nilsson, C., Lofgren, L., Himmelmann, A., Martensson, G., Knutsson, M., Al-Shurbaji, A., Tornqvist, H., and Eriksson, J.W. (2014). Diacylglycerol acyltransferase 1 inhibition with AZD7687 alters lipid handling and hormone secretion in the gut with intolerable side effects: a randomized clinical trial. Diabetes Obes. Metab. *16*, 334–343.

Deruyffelaere, C., Bouchez, I., Morin, H., Guillot, A., Miquel, M., Froissard, M., Chardot, T., and D'Andrea, S. (2015). Ubiquitin-mediated proteasomal degradation of oleosins is involved in oil body mobilization during post-germinative seedling growth in Arabidopsis. Plant Cell Physiol. *56*, 1374–1387

Dikic, I., Wakatsuki, S., and Walters, K.J. (2009). Ubiquitin-binding domains - from structures to functions. Nature Rev. Mol. Cell Biol. *10*, 659–671.

Donkor, J., Sariahmetoglu, M., Dewald, J., Brindley, D.N., and Reue, K.J. (2007). Three mammalian lipins act as phosphatidate phosphatases with distinct tissue expression patterns.

Biol. Chem. *282*, 3450-3457

Duda, D.M., Olszewski, J.L., Shuermann, J.P., Kurinov, I., Miller, D.J., Nourse, A., Alpi, A.F., and Schulman, B.A. (2013). Structure of HHARI, a RING-IBR-RING ubiquitin ligase: autoinhibition of an Ariadne-family E3 and insights into ligation mechanism. Structure. *21*, 1030–1041.

Duncan, R.E., Ahmadian, M., Jaworski, K., Sarkadi-Nagy, E., and Sul, H.S. (2007). Regulation of Lipolysis in Adipocytes. Annu. Rev. Nutr. *27*, 79-101.

Dvorak, A.M., Morgan, E., Schleimer, R.P., Ryeom, S.W., Lichtenstein, L.M., and Weller, P.F. (1992). Ultrastructural immunogold localization of prostaglandin endoperoxide synthase (cyclooxygenase) to non-membrane-bound cytoplasmic lipid bodies in human lung mast cells, alveolar macrophages, type ii pneumocytes, and neutrophils. J. Histochem. Cytochem. *40*, 759-769.

Eberhardt, C., Gray, P.W., and Tjoelker, L.W. (1997). Human lysophosphatidic acid acyltransferase. cDNA cloning, expression, and localization to chromosome 9q34.3. J. Biol. Chem. *272*, 20299-20305.

Ellis, J. M., Frahm, J.L., Li, L.O., and Coleman, R.A. (2010). Acyl-coenzyme A synthetases in metabolic control. Curr. Opin. Lipidol. *21*, 212–217.

Ericsson, J., Jackson, S.M., Kim, J.B., Spiegelman, B.M., and Edwards, P.A. (1997). Identification of glycerol-3-phosphate acyltransferase as an adipocyte determination and differentiation factor 1 and sterol regulatory element-binding protein-responsive gene. J. Biol. Chem. *272*, 7298-7305.

Ernst, R., Mueller, B. Ploegh, H.L., and Schlieker, C. (2009). The otubain YOD1 is a deubiquitinating enzyme that associates with p97 to facilitate protein dislocation from the ER. Mol. Cell. *36*, 28–38.

Fain, J.N., and Garcija-Sainz, J.A. (1983). Adrenergic regulation of adipocyte metabolism. J. Lipid Res. *24*, 945–966.

Fang, S., Ferrone, M., Yang, C., Jensen, J.P., Tiwari, S., and Weissman, A.M. (2001). The tumor autocrine motility factor receptor, gp78, is a ubiquitin protein ligase implicated in degradation from the endoplasmic reticulum. Proc. Natl. Acad. Sci. U S A. *98*, 14422–14427.

Farese, R.V.Jr., Cases, S., and Smith, S.J. (2000). Triglyceride synthesis: Insights from the cloning of diacylglycerol acyltransferase. Curr. Opin. Lipidol. *11*, 229–234.

Farese. R.V.Jr., and Walther, T.C. (2009). Lipid droplets finally get a little R-E-S-P-E-C-T. Cell. *139*, 855–860.

Finck, B.N., Gropler, M.C., Chen, Z., Leone, T.C., Croce, M.A., Harris, T.E., Lawrence, J.C. Jr, and Kelly, D.P. (2006). Lipin 1 is an inducible amplifier of the hepatic PGC-1alpha/PPARalpha regulatory pathway. Cell Metab. *4*, 199-210.

Finley, D. (2009). Recognition and processing of ubiquitin-protein conjugates by the proteasome. Annu. Rev. Biochem. *78*, 477–513.

First Nations Regional Health Survey (RHS). (2012). Retrieved from: http://fnigc.ca/sites/default/files/docs/first_nations_regional_health_survey_rhs_2008-10_-_national_report.pdf

Fisher, E.A., Lapierre, L.R., Junkins, R.D., and McLeod, R.S. (2008). The AAA-ATPase p97 facilitates degradation of apolipoprotein B by the ubiquitin-proteasome pathway. J. Lipid. Res. *49*, 2149–2160.

Fisher, E.A., Zhou, M., Mitchell, D.M., Wu, X., Omura, S., Wang, H., Goldberg, A.L., and Ginsberg, H.N. (1997). The degradation of apolipoprotein B100 is mediated by the ubiquitin-proteasome pathway and involves heat shock protein 70. J. Biol. Chem. *272*, 20427–20434.

Flegal, K.M., Kit, B.K., Orpana, H., and Graubard, B.L. (2013). Association of all-cause mortality with overweight and obesity using standard body mass index categories: a systematic review and meta-analysis. JAMA. *309*, 71-82.

Franke, W.W., and Kartenbeck, J. (1971). Outer mitochondrial membrane continuous with endoplasmic reticulum, Protoplasma. *73*, 35–41.

Frenkel, Z., Gregory, W., Kornfeld, S., and Lederkremer, G.Z. (2003). Endoplasmic reticulum-associated degradation of mammalian glycoproteins involves sugar chain trimming to Man6-5GlcNAc2. J. Biol. Chem. *278*, 34119 – 34124.

Friedel, S., Reichwald, K., Scherag, A., Brumm, H., Wermter, A., Fries, H., Koberwitz, K., Wabitsch, M., Meitinger, T., Platzer, M., Biebermann, H., Hinney, A., and Hebebrand, J. (2007). Mutation screen and association studies in the diacylglycerol O-acyltransferase homolog 2 gene (DGAT2), a positional candidate gene for early onset obesity on chromosome 11q13. BMC Genet. *8*, 17.

Fujimoto, T., and Parton, R.G. (2011). Not just fat: the structure and function of the lipid droplet. Cold Spring Harb. Perspect. Biol. *3*, 3.

Fung, T.K., Yam, C.H., and Poon, R.Y. (2005). The N-terminal regulatory domain of cyclin A contains redundant ubiquitination targeting sequences and acceptor sites. Cell Cycle. *4*, 1411-1420.

Futatsugi, K., Kung, D.W., Orr, S.T.M. (2015). Discovery and optimization of imidazopyridine-based inhibitors of diacylglycerol acyltransferase 2 (DGAT2). J. Med. Chem. *58*, 7173-7185.

Gale, S.E., Frolov, A., Han, X., Bickel, P.E., Cao, L., Bowcock, A.M., Schaffer, J.E., and Ory, D.S. (2006). A regulatory role for 1-acylglycerol-3-phosphate-O-acyltransferase 2 in adipocyte differentiation. J. Biol. Chem. *281*, 11082-11089.

Gandotra, S, Le Dour, C., Bottomley, W., Cervera, P., Giral, P., Reznik, Y., Charpentier, G., Auclair, M., Delépine, M., Barroso, I., Semple, R.K., Lathrop, M., Lascols, O., Capeau, J., O'Rahilly, S., Magré, J., Savage, D.B., and Vigouroux, C (2011). Perilipin deficiency and autosomal dominant partial lipodystrophy. N. Engl. J. Med. *364*, 740-748.

Gauss, R., Jarosch, E. Sommer, T. and Hirsch, C. (2006). A complex of Yos9p and the HRD ligase integrates endoplasmic reticulum quality control into the degradation machinery. Nat. Cell Biol. *8*, 849–854.

Gidda, S.K., Shockey, J.M., Falcone, M., Kim, P.K., Rothstein, S.J., Andrews, D.W., Dyer, J.M., and Mullen, R.T. (2011). Hydrophobic-domain-dependent protein-protein interactions mediate the localization of GPAT enzymes to ER subdomains. Traffic. *12*, 452–472.

Glenney, J., and Soppet, D. (1992). Sequence and expression of caveolin, a protein component of caveolae plasma membrane domains phosphorylated on tyrosine in Rous sarcoma virus-transformed fibroblasts. Proc. Natl. Acad. Sci. U S A. *89*, 10517–10521.

Glickman, M.H., and Raveh, D. (2005). Proteasome plasticity. FEBS Lett. *579*, 3214–3223.

Goetz, J.G., Genty, H., St. Pierre, P., Dang, T., Joshi, B., Sauvé, R., Vogl, W., and Nabi, I.R. (2007). Reversible interactions between smooth domains of the endoplasmic reticulum and mitochondria are regulated by physiological cytosolic calcium levels. J. Cell Sci. *120*, 3553–3564.

Goldstein, J.L. and Brown, M.S. (1990). Regulation of the mevalonate pathway. Nature. *343*, 425–430.

Gong, J., Sun, Z., Wu, L., Xu, W., Schieber, N., Xu, D., Shui, G., Yang, H., Parton, R.G., and Li, P. (2011). Fsp27 promotes lipid droplet growth by lipid exchange and transfer at lipid droplet contact sites. J. Cell Biol. *195*, 953-963.

Gonzalez-Baró, M.R., Granger, D.A., and Coleman, R.A. (2001). Mitochondrial glycerol phosphate acyltransferase contains two transmembrane domains with the active site in the N-terminal domain facing the cytosol. J. Biol. Chem. *276*, 43182-43188.

Grabbe, C. and Dikic, I. (2009). Functional roles of ubiquitin-like domain (ULD) and ubiquitin-binding domain (UBD) containing proteins. Chem. Rev. *109,* 1481–1494.

Grahn, T.H., Zhang, Y., Lee, M.J., Sommer, A.G., Mostoslavsky, G., Fried, S.K., Greenberg, A.S., and Puri, V. (2013). FSP27 and PLIN1 interaction promotes the formation of large lipid droplets in human adipocytes. Biochem. Biophys. Res. Commun. *432*, 296-301.

Grasselli. E., Voci, A., Pesce, C., Canesi, L., Fugassa, E., Gallo. G., and Vergani, L. (2010). PAT protein mRNA expression in primary rat hepatocytes: Effects of exposure to fatty acids. Int. J. Mol. Med. *25*, 505-512.

Greenberg, A.S., Egan, J.J., Wek, S.A., Garty, N.B., Blanchette-Mackie, E.J., and Londos, C.

(1991). Perilipin, a major hormonally regulated adipocyte-specific phosphoprotein associated with the periphery of lipid storage droplets. J. Biol. Chem. *266*, 11341–11346.

Grevengoed, T.J., Klett, E.L. and Coleman, R.A. (2014). Acyl-CoA metabolism and partitioning. Annu. Rev. Nutr. *34*, 1–30.

Grimsey, N., Han, G.S., O'Hara, L., Rochford, J.J., Carman, G.M., and Siniossoglou, S.J. (2008). Temporal and spatial regulation of the phosphatidate phosphatases lipin 1 and 2. Biol. Chem. *283*, 29166-29174.

Groot, P.H., Scholte, H.R., and Hulsmann, W.C. (1976). Fatty acid activation: specificity, localization, and function. Adv. Lipid Res. *14*, 75–126.

Gropler, M.C., Harris, T.E., Hall, A.M., Wolins, N.E., Gross, R.W., Han, X., Chen, Z., and Finck, B.N. (2009). Lipin 2 is a liver-enriched phosphatidate phosphohydrolase enzyme that is dynamically regulated by fasting and obesity in mice. J. Biol. Chem. *284*, 6763-6772.

Guerriero, C.J., and Brodsky, J.L. (2012). The delicate balance between secreted protein folding and endoplasmic reticulum-associated degradation in human physiology. Physiol. Rev. *92*, 537–576.

Guh, D.P, Zhang, W., Bansback, N., Amarsi, Z., Birmingham, C.L., and Anis, A.H. (2009). The incidence of co-morbidities related to obesity and overweight: a systematic review and meta-analysis. BMC Public Health. *9*, 88.

Guo, Y., Walther, T.C., Rao, M., Stuurman, N., Goshima, G., Terayama, K., Wong, J.S., Vale, R.D., Walter, P., and Farese, R.V.Jr. (2008). Functional genomic screen reveals genes involved in lipid-droplet formation and utilization. Nature. *453*, 657-661.

Gurnell, M., Wentworth, J., Agostini, M., Adams, M., Collingwood, T., Provenzano, C., Browne, P., Rajanayagam, O., Burris, T., Schwabe, J., Lazar, M., and Chatterjee, V. (2000). A dominant-negative peroxisome proliferator-activated receptor gamma (PPARgamma) mutant is a constitutive repressor and inhibits PPARgamma-mediated adipogenesis. J. Biol. Chem. *275*, 5754-5759.

Haas, A.L., Warms, J.V., Hershko, A., and Rose, I.A., (1982). Ubiquitin-activating enzyme–Mechanism and role in protein-ubiquitination conjugation. J. Biol Chem. *257*, 2543-2548.

Haas, J.T., Winter, H.S., Lim, E., Kirby, A., Blumenstiel, B., DeFelice, M., Gabriel, S., Jalas, C., Branski, D., Grueter, C.A., Toporovski, M.S., Walther, T.C., Daly, M.J., and Farese R.V.Jr. (2012). DGAT1 mutation is linked to a congenital diarrheal disorder. J. Clin. Invest. *122*, 4680-4684.

Hall, A.M., Kou, K., Chen, Z., Pietka, T.A., Kumar, M., Korenblat, K.M., Lee, K., Ahn, K., Fabbrini, E., Klein, S., Goodwin, B., and Finck, B.N. (2012). Evidence for regulated monoacylglycerol acyltransferase expression and activity in human liver. J. Lipid. Res. *53*, 990-999.

Haemmerle, G., Lass, A., Zimmermann, R., Gorkiewicz, G., Meyer, C., Rozman, J., Heldmaier, G., Maier, R., Theussl, C., Eder, S., Kratky, D., Wagner, E.F., Klingenspor, M., Hoefler, and G., Zechner, R. (2006). Defective lipolysis and altered energy metabolism in mice lacking adipose triglyceride lipase. Science. *312*, 734–737

Haemmerle, G., Moustafa, T., Woelkart, G., *et al.* (2011). ATGL-mediated fat catabolism regulates cardiac mitochondrial function via PPAR-alpha and PGC-1. Nat. Med. *17*, 1076–1085.

Hammond, L.E., Albright, C.D., He, L., Rusyn, I., Watkins, S.W., Doughman, S.D., Lemasters, J.J., and Coleman, R.A. (2007). Increased oxidative stress is associated with balanced increases in hepatocyte apoptosis and proliferation in glycerol-3-phosphate acyltransferase-1 deficient mice. Exper. Molec. Pathol. *82*, 210-219

Hammond, C., Braakman, I., and Helenius, A. (1994). Role of N-linked oligosaccharides, glucose trimming and calnexin during glycoprotein folding in the endoplasmic reticulum. Proc. Natl. Acad. Sci. U S A. *91*, 913 – 917.

Hammond, C., and Helenius, A.A. (1993). Chaperone with a sweet tooth. Curr. Biol. *3*, 884 – 885.

Hammond, L.E., Neschen, S., Romanelli, A.J., Cline, G.W., Ilkayeva, O.R., Shulman, G.I., Muoio, D.M., and Coleman, R.A. (2005). Mitochondrial glycerol-3-phosphate acyltransferase-1 is essential in liver for the metabolism of excess acyl-CoAs. J. Biol. Chem. *280*, 25629-25636.

Han, G.S., and Carman, G.M. (2010). Characterization of the human LPIN1-encoded phosphatidate phosphatase isoforms. J. Biol. Chem. *285*, 14628-14638.

Han, G.S., Wu, W.I., and Carman, G.M. (2006). The Saccharomyces cerevisiae Lipin homolog is a Mg2+-dependent phosphatidate phosphatase enzyme. J. Biol. Chem. *281*, 9210-9218.

Harris, C.A., Haas, J.T., Streeper, R.S., Stone, S.J., Kumari, M., Yang, K., Han, X., Brownell, N., Gross, R.W., Zechner, R., and Farese, R.V.Jr. (2011). DGAT enzymes are required for triacylglycerol synthesis and lipid droplets in adipocytes. J. Lipid Res. *52*, 657–667.

Harris, T.E., Huffman, T.A., Chi, A., Shabanowitz, .J, Hunt, D.F., Kumar, A., and Lawrence, J.C.Jr. (2007). Insulin controls subcellular localization and multisite phosphorylation of the phosphatidic acid phosphatase, lipin 1. J. Biol. Chem. *282*, 277-286.

Hartl, F.U., and Hayer-Hartl, M. (2009). Converging concepts of protein folding in vitro and in vivo. Nat. Struct. Mol. Biol. *16*, 574–581.

Hartman, I.Z., Liu, P., Zehmer, J.K., Luby-Phelps, K., Jo, Y., Anderson, R.G., and DeBose-Boyd, R.A. (2010). Sterol-induced dislocation of 3-hydroxy-3-methylglutaryl coenzyme A reductase from endoplasmic reticulum membranes into the cytosol through a subcellular compartment resembling lipid droplets. J. Biol. Chem. *285*, 19288–19298

Health Canada. (2003). Canadian guidelines for body weight classification in adults. Ottawa, ON: Health Canada Publications Centre.

Hebert, D.N., and Molinari, M. (2007). In and out of the ER: protein folding, quality control, degradation, and related human diseases. Physiol. Rev. *87*,1377–1408.

Heid, H.W., Moll, R., Schwetlick, I., Rackwitz, H.R., and Keenan, T.W. (1998). Adipophilin is a specific marker of lipid accumulation in diverse cell types and diseases. Cell Tissue Res. *294*, 309-321.

Heifetz, A., Keenan, R.W., and Elbein, A.D. (1979). Mechanism of action of tunicamycin on UDP-GlcNAc:dolichyl-phosphate Glc-NAc-1-phosphate transferase. Biochem. *18*, 2186-2192.

Helenius A. (1994). How N-linked oligosaccharides affect glycoprotein folding in the endoplasmic reticulum. Mol. Biol. Cell. *5*, 253 – 265.

Hershko, A., Ciechanover, A., Heller, H., Haas, A.L., and Rose, I.A. (1980). Proposed role of ATP in protein breakdown: conjugation of protein with multiple chains of the polypeptide of ATP-dependent proteolysis. Proc. Natl. Acad. Sci. U S A. *77*, 1783–1786.

Hickenbottom, S., Kimmel, A., Londos, C., and Hurley, J. (2004). Structure of a lipid droplet protein; the PAT family member TIP47. Structure. *12*, 1199–1207.

Hillman, N., and Hillman, R. (1975). Ultrastructural studies of tw32/tw32 mouse embryos. J. Embryol. Exp. Morphol. *33*, 685–695.

Hirsch, C., Gauss, R., Horn, S. C., Neuber, O., and Sommer, T. (2009). The ubiquitylation machinery of the endoplasmic reticulum. Nature. *458*, 453–460.

Hirschhorn, J.N., Lindgren, C.M., Daly, M.J., Kirby, A., Schaffner, S.F., Burtt, N.P., Altshuler, D., Parker, A., Rioux, J.D., Platko, J., Gaudet, D., Hudson, T.J., Groop, L.C., and Lander, E.S. (2001). Genomewide linkage analysis of stature in multiple populations reveals several regions with evidence of linkage to adult height. Am. J. Hum. Genet. *69*, 106–16.

Ho, S.Y., and Storch, J. (2001). Common mechanisms of monoacylglycerol and fatty acid uptake by human intestinal Caco-2 cells. Am. J. Physiol. Cell Physiol. *281*, C1106–C1117.

Hodges, B.D., and Wu, C.C. (2010). Proteomic insights into an expanded cellular role for cytoplasmic lipid droplets. J. Lipid Res. *51*, 262–273.

Hofmann, K. (2000). A superfamily of membrane-bound O-acyltransferases with implications for wnt signaling. Trends Biochem. Sci. *25*, 111–112.

Holm, C. (2003). Molecular mechanisms regulating hormone-sensitive lipase and lipolysis. Biochem Soc. Trans. *31*, 1120–1124.

Holm, C., Kirchgessner, T.G., Svenson, K.L., Fredrikson, G., Nilsson, S., Miller, C.G., Shively, J.E., Heinzmann, C., Sparkes, R.S., Mohandas, T., Lusis, A.J., Belfrage, P., and Schotz, M.C. (1988). Hormone-sensitive lipase: sequence, expression, and chromosomal localization to 19 cent-q13.3. Science. *241*, 1503–1506.

Hong, Y.B., Kang, J., Kim, J.H., Lee, J., Kwak, G., Hyun, Y.S., Nam, S.H., Hong, H.D., Choi, Y.R., Jung, S.C., Koo, H., Lee, J.E., Choi, B.O., and Chung, K.W. (2016). DGAT2 Mutation in a Family with Autosomal Dominant Early-Onset Axonal Charcot-Marie-Tooth Disease. Hum. Mutat. *37*, 473-480.

Hopewell, R., Martin-Sanz, P., Martin, A., Saxton, J., and Brindley, D.N. (1985). Regulation of the translocation of phosphatidate phosphohydrolase between the cytosol and the endoplasmic reticulum of rat liver. Effects of unsaturated fatty acids, spermine, nucleotides, albumin and chlorpromazine. Biochem. J. *232*, 485-491.

Horn, S.C., Hanna, J., Hirsch, C., Volkwein, C., Schütz, A., Heinemann, U., Sommer, T., and Jarosch, E. (2009). Usa1 functions as a scaffold of the HRD- ubiquitin ligase. Mol. Cell. *36*, 782–793.

Hornick, C.A., Thouron, C., DeLamatre, J.G., and Huang, J. (1992). Triacylglycerol Hydrolysis in Isolated Hepatic Endosome. J. Biol. Chem. *267*, 3396-3401.

Huffman, T.A., Mothe-Satney, I., and Lawrence, J.C. Jr. (2002). Insulin-stimulated phosphorylation of lipin mediated by the mammalian target of rapamycin. Proc. Natl. Acad. Sci. U S A. *99*, 1047-1052.

Husnjak, K., Elasser, S., Zhang, N., Chen, X., Randles, L., Shi, Y., Hoffmann, K., Walter, K.J., Finley, D., and Dikic, I. (2008). Proteasome subunit Rpn13 is a novel ubiquitin receptor. Nature. *453*, 481–488.

Hussain, M.M. (2014). Intestinal lipid absorption and lipoprotein formation. Curr. Opin. Lipidol. *25*, 200–206.

Hussain, M.M., Shi, J., and Dreizen, P. (2003). Microsomal triglyceride transfer protein and its role in apoB-lipoprotein assembly. J. Lipid. Res. *44*, 22–32.

Ikeda, F., and Dikic, I. (2008). Atypical ubiquitin chains: new molecular signals - Protein modifications: beyond the usual suspects' review series. EMBO Rep. *9*, 536–542.

Ikeda, Y., Yamamoto, J., Okamura, M., Fujino, T., Takahashi, S., Takeuchi, K., Osborne, T., Yamamoto, T., Ito, S., and Sakai, J. (2001). Transcriptional regulation of the murine acetyl CoA synthetase 1 gene through multiple clustered binding sites for SREBPs and a single neighboring site for Sp1. J. Biol. Chem. *276*, 34259–34269.

Imai, Y., Soda, M., Hatakeyama, S., Akagi, T., Hashikawa, T., Nakayama, K.I., and Takahashi, R. (2002). CHIP is associated with Parkin, a gene responsible for familial Parkinson's disease, and enhances its ubiquitin ligase activity. Mol. Cell. *10*, 55–67.

Ishimoto, K., Nakamura, H., Tachibana, K., Yamasaki, D., Ota, A., Hirano, K., Tanaka, T., Hamakubo, T., Sakai, J., Kodama, T., and Doi, T.J. (2009). Sterol-mediated regulation of human lipin 1 gene expression in hepatoblastoma cells. Biol. Chem. *284*, 22195-22205.

Iwai, K., and Tokunaga, F. (2009). Linear polyubiquitination: a new regulator of NF-κB activation. EMBO Rep. *10*, 706–713.

Jaekel S., and Goerlich D. (1998). Importin beta, transportin, RanBP5 and RanBP7 mediate nuclear import of ribosomal proteins in mammalian cells. EMBO J. *17*, 4491-4502.

Jaekel S., Mingot J.M., Schwarzmaier P., Hartmann E., and Goerlich D. (2002). Importins fulfill a dual function as nuclear import receptors and cytoplasmic chaperones for exposed basic domains. EMBO J. *21*, 377-386.

Jacobs, R.L., Lingrell, S., Zhao, Y., Francis, G.A., and Vance, D.E. (2008). Hepatic ctp: Phosphocholine cytidylyltransferase-a is a critical predictor of plasma high density lipoprotein and very low density lipoprotein. J. Biol. Chem. *283*, 2147– 2155.

Jacquier, N., Choudhary, V., Mari, M., Toulmay, A., Reggiori, F., and Schneiter, R. (2011). Lipid droplets are functionally connected to the endoplasmic reticulum in Saccharomyces cerevisiae. J. Cell Sci. *124*, 2424–2437.

Janssen, I. (2013). The public health burden of obesity in Canada. Can. J. Diabetes. *37*, 90-96.

Jarosch, E., Taxis, C., Volkwein, C., Bordallo, J., Finley, D., Wolf, D.H., and Sommer, T. (2002). Protein dislocation from the ER requires polyubiquitination and the AAA-ATPase Cdc48. Nat. Cell Biol. *4*, 134–139.

Jentsch, S., and Rumpf, S. (2007). Cdc48 (p97): a "molecular gearbox" in the ubiquitin pathway? Trends Biochem. Sci. *32*, 6–11.

Ji, Z.S., Dichel, H.S., Miranda, R.D., and Mahley, R.W. (1997). Heparan sulfate proteoglycans participate in hepatic lipase and apolipoprotein E-mediated binding and uptake of plasma lipoproteins, including high density lipoproteins. J. Biol. Chem. 272, 31285-31292.

Jiang, H.P., and Serrero, G. (1992). Isolation and characterization of a full-length cDNA coding for an adipose differentiation-related protein. Proc. Natl. Acad. Sci. U S A. *89,* 7856-7860.

Jin, Y., McFie, P.J., Banman, S.L., Brandt, C., and Stone, S.J. (2014). Diacylglycerol acyltransferase-2 (DGAT2) and monoacylglycerol acyltransferase-2 (MGAT2) interact to promote triacylglycerol synthesis. J. Biol. Chem. *289*, 28237-28248.

Jo, Y., Hartman, I.Z., and DeBose-Boyd, R.A. (2013) Ancient ubiquitous protein-1 mediates sterol- induced ubiquitination of 3-hydroxy-3-methylglutaryl CoA reductase in lipid droplet-associated endoplasmic reticulum membranes. Mol. Biol. Cell. *24*, 169–183.

Jo, Y., Lee, P.C., Sguigna, P.V., and DeBose-Boyd RA. (2011). Sterol-induced degradation of HMG CoA reductase depends on interplay of two Insigs and two ubiquitin ligases, gp78 and Trc8. Proc. Natl. Acad. Sci. U S A. *108*, 20503–20508.

Johnson, E.S., Ma, P.C., Ota, I.M., and Varshavsky, A. (1995). A proteolytic pathway that recognizes ubiquitin as a degradation signal. J. Biol. Chem. *270*, 17442–17456.

Johnston, J. M., and Rao, G.A. (1967). Intestinal absorption of fat. Protoplasma. *63***,** 40–44.

Kalderon, B., Mayorek, N., Berry, E., Zevit, N., and Bar-Tana, J. (2000). Fatty acid cycling in the fasting rat. Am. J. Physiol. Endocrinol. Metab. *279*, E221–E227.

Kalies, K.U., Allan, S., Sergeyenko, T., Kröger, H., and Römisch, K. (2005). The protein translocation channel binds proteasomes to the endoplasmic reticulum membrane. EMBO J. *24,* 2284–2293.

Kantartzis, K., Machicao, F., Machann, J., Schick, F., Fritsche, A., Haring, H.U., and Stefan, N. (2009). The *DGAT2* gene is a candidate for the dissociation between fatty liver and insulin resistance in humans. Clin. Sci. *116*, 531-537.

Karlsson, M., Contreras, J.A., Hellman, U., Tornqvist, H., and Holm, C. (1997). cDNA cloning, tissue distribution, and identification of the catalytic triad of monoglyceride lipase. Evolutionary relationship to esterases, lysophospholipases, and haloperoxidases. J. Biol. Chem. *272*, 27218–27223.

Kasper, H. (1970). Faecal fat excretion, diarrhea, and subjective complaints with highly dosed oral fat intake. Digestion*. 3*, 321-330.

Kato, H., Sakaki, K., and Mihara, K. (2006). Ubiquitin-proteasome-dependent degradation of mammalian ER stearoyl-CoA desaturase. J. Cell Sci. *119*, 2342–2353.

Katzmarzyk, P.T. (2002). The Canadian obesity epidemic: an historical perspective. Obes. Res. *10*, 666-674.

Kaushik, S., and Cuervo, A.M. (2015). Degradation of lipid droplet-associated proteins by chaperone-mediated autophagy facilitates lipolysis. Nat. Cell Biol. *17*, 759–770.

Kennedy, E.P. (1957). Metabolism of Lipids. Annu. Rev. Bioc. *26*, 119-148.

Keys, A., Fidanza, F., Karvonen, M.J., Kimura, N., and Taylor, H.L. (1972). Indices of relative weight and obesity. J. Chronic Dis. *25*, 329–343.

Khalil, M.B., Blais, A., Figeys, D., and Yao, Z. (2010). Lipin - The bridge between hepatic glycerolipid biosynthesis and lipoprotein metabolism. Biochim. Biophys. Acta. *1801*, 1249-1259.

Kikkert, M., Doolman, R., Dai, M., Avner, R., Hassink, G., van Voorden, S., Thanedar, S.,

Roitelman, J., Chau, V., and Wiertz, E. (2004). Human HRD1 is an E3 ubiquitin ligase involved in degradation of proteins from the endoplasmic reticulum. J. Biol. Chem. *279*, 3525–3534.

Kim, M.O., Lee, S., Choi, K., Lee, S., Kim, H., Kang, H., Choi, M., Kwon, E.B., Kang, M.J., Kim, S., Lee, H.J., Lee, H.S., Kwak, Y.S., and Cho, S. (2014). Discovery of a Novel Class of Diacylglycerol Acyltransferase 2 Inhibitors with a 1H-Pyrrolo[2,3-b]Pyridine Core. Biol. Pharm. Bull. *37*, 1655−1660.

Kim, M.O., Lee, S.U., Lee, H.J., Choi, K., Kim, H., Lee, S., Oh, S.J., Kim, S., Kang, J.S., Lee, H.S., Kwak, Y.S., and Cho, S. (2013). Identification and validation of a selective small molecule inhibitor targeting the diacylglycerol acyltransferase 2 activity. Biol. Pharm. Bull. *36,* 1167−1173.

Kim, W., Spear, E.D., and Ng, D.T. (2005). Yos9p detects and targets misfolded glycoproteins for ER-associated degradation. Mol. Cell. *19*, 753-764.

Kimmel, A.R., Brasaemle, D.L., McAndrews-Hill, M., Sztalryd, C., and Londos, C. (2010). Adoption of perilipin as a unifying nomenclature for the mammalian pat-family of intra-cellular lipid storage droplet proteins. J. Lipid Res. *51*, 468-471.

Kindel, T., Lee, D.M., and Tso, P. (2010). The mechanism of the formation and secretion of chylomicrons. Atheroscler. Suppl. *11*, 11-16.

Kirkin, V., McEwan, D.G., Novak, I., and Dikic, I (2009). A role for ubiquitin in selective autophagy. Mol. Cell. *34*, 259-269.

Kirkpatrick, D.S., Hathaway, N.A., Hanna, J., Elsasser, S., Rush, J., Finley, D., King, R.W., and Gygi, S.P. (2006). Quantitative analysis of in vitro ubiquitinated cyclin B1 reveals complex chain topology. Nat. Cell Biol. *8*, 700-710.

Klein, R.L., and Rudel, L.L. (1983). Effect of dietary cholesterol level on the composition of thoracic duct lymph lipoproteins isolated from nonhuman primates. J. Lipid Res. *24*, 357-367.

Klemm, E.J., Spooner, E., and Ploegh, and H.L. (2011). Dual role of ancient ubiquitous protein 1 (AUP1) in lipid droplet accumulation and endoplasmic reticulum (ER) protein quality control. J. Biol. Chem. *286*, 37602–37614.

Klinge, S., Voigts-Hoffmann, F., Leibundguy, M., Arpagaus, and S., Ban, N. (2011). Crystal structure of the eukaryotic 60S ribosomal subunit in complex with initiation factor 6. Science. *18*, 941-948.

Koegl, M., Hoppe, T., Schlenker, S., Ulrich, H.D., Mayer, T.U., and Jentsch, S. (1999). A novel ubiquitination factor, E4, is involved in multiubiquitin chain assembly. Cell. *96*, 635–644.

Kohler, A., Cascio, P., Leggett, D.S., Woo, K.M., Goldberg A.L., and Finley, D. (2001). The axial channel of the proteasome core particle is gated by the Rpt2 ATPase and controls both substrate entry and product release. Mol. Cell. *7*, 1143-1152.

Kraemer, F.B., Patel, S. Saedi, M.S., and Sztalryd, C. (1993). Detection of hormone-sensitive lipase in various tissues. I. Expression of an HSL/bacterial fusion protein and generation of anti-HSL antibodies. J. Lipid Res. *34*, 663-671.

Kreft, S.G., Wang, L., and Hochstrasser, M. (2006). Membrane topology of the yeast endoplasmic reticulum-localized ubiquitin ligase Doa10 and comparison with its human ortholog TEB4 (MARCH-VI). J. Biol. Chem. *281*, 4646-4653.

Krintel, C., Morgelin, M., Logan, D.T., and Holm, C. (2009). Phosphorylation of hormone-sensitive lipase by protein kinase A in vitro promotes an increase in its hydrophobic surface area. FEBS J. *276*, 4752-4762.

Krull, S., Thyberg, J., Bjorkroth, B., Rackwitz, H.R., and Cordes, V.C. (2004). Nucleoporins as components of the nuclear pore complex core structure and Tpr as the architectural element of the nuclear basket. Mol. Biol. Cell. *15*, 4261-4277.

Kuerschner, L., Moessinger, C., and Thiele, C. (2008). Imaging of Lipid Biosynthesis: How a Neutral Lipid Enters Lipid Droplets. Traffic. *9*, 338-352.

Lagakos, W.S., Guan, X., Ho, S.Y., Sawicki, L.R., Corsico, B., Kodukula, S., Murota, K., Stark, R.E., and Storch, J. (2013). Liver fatty acid-binding protein binds monoacylglycerol in vitro and in mouse liver cytosol. J. Biol. Chem. *288*, 19805–19815.

Langner, C.A., Birkenmeier, E.H., Ben-Zeev, O., Schotz, M.C., Sweet, H.O., Davisson, M.T., and Gordon, J.I. (1989). The fatty liver dystrophy (fld) mutation. A new mutant mouse with a developmental abnormality in triglyceride metabolism and associated tissue-specific defects in lipoprotein lipase and hepatic lipase activities. J. Biol. Chem. *264*, 7994-8003.

Langner, C.A., Birkenmeier, E.H., Roth, K.A., Bronson, R.T., and Gordon, J.I. (1991). Characterization of the peripheral neuropathy in neonatal and adult mice that are homozygous for the fatty liver dystrophy (fld) mutation. J. Biol. Chem. *266*, 11955-11964.

Lapierre, L.R., Currie, D.L. Yao, Z. Wang, J. and McLeod, R.S. (2004). Amino acid sequences within the b1 domain of human apolipoprotein B can mediate rapid intracellular degradation. J. Lipid Res. *45*, 366-377.

Lass, A., Zimmermann, R., Oberer, M., and Zechner, R. (2011). Lipolysis - a highly regulated multi-enzyme complex mediates the catabolism of cellular fat stores. Prog. Lipid Res. *50*, 14-27.

Lau, D.C., Douketis, J.D., Morrison, K.M., Hramiak, I.M., Sharma, A.M., and Ur, E. (2007). 2006 Canadian clinical practice guidelines on the management and prevention of obesity in adults and children [summary]. CMAJ. *176*, S1-13.

Layerenza, J.P., González, P., García de Bravo, M.M., Polo, M.P., Sisti, M.S., and Ves-Losada, A. (2013). Nuclear lipid droplets: A novel nuclear domain. Biochim. Biophys. Acta. *1831*, 327-340.

Lee, K., Kim, M., Lee, B., Goo, J., Kim, J., Naik, R., Seo, J.H., Kim, M.O., Byun, Y., Song, G.Y., Lee, H.S., and Choi, Y. (2013). Discovery of indolyl acrylamide derivatives as human diacylglycerol acyltransferase-2 selective inhibitors. Org. Biomol. Chem. *11*, 849-858.

Lee, Y.J., Ko, E.H., Kim, J.E., Kim, E., Lee, H., Choi, H., Yu, J.H., Kim, H.J., Seong, J.K., Kim, K.S., and Kim, J.W. (2012). Nuclear receptor PPARgamma-regulated monoacylglycerol O-acyltransferase 1 (MGAT1) expression is responsible for the lipid accumulation in diet-induced hepatic steatosis, Proc. Natl. Acad. Sci. U S A. *109*, 13656-13661.

Lee, P.C., Nguyen, A.D., and DeBose-Boyd, R.A. (2007). Mutations within the membrane domain of HMG-CoA reductase confer resistance to sterol-accelerated degradation 1. J. Lipid. Res. *48*, 318-327.

Lee, A., Scapa, E., Cohen, D., and Glimcher, L. (2008). Regulation of hepatic lipogenesis by the transcription factor XBP1. Science. *320*, 1492–1496.
Lee, J.N., Song, B., Debose-Boyd, R.A., and Ye, J. (2006). Sterol-regulated degradation of Insig-1 mediated by the membrane-bound ubiquitin ligase, gp78. J. Biol. Chem. *281*, 39308–39315.

Leber, R., Zinser, E., Zellnig, G., Paltauf, F., and Daum, G. (1994). Characterization of lipid particles of the yeast, Saccharomyces cerevisiae. Yeast. *10*, 1421–1428.

Lehner, R., and Kuksis, A. (1993). Triacylglycerol synthesis by an sn-1,2(2,3)-diacylglycerol transacylase from rat intestinal microsomes. J. Biol. Chem. *268*, 8781–8786.

Lehner, R., and Kuksis, A. (1996). Biosynthesis of triacylglycerols. Prog. Lipid Res. *35***,** 169-201.

Lehner, R., Lian, J., and Quiroga, A.D. (2012). Lumenal lipid metabolism: implications for lipoprotein assembly. Arterioscler. Thromb. Vasc. Biol. *32*, 1087-1093.

Lerner, M., Corcoran, M., Cepeda, D., Nielsen, M.L., Zubarev, R., Ponten, F., Uhlen, M., Hober, S., Grander, D., and Sangfelt. O. (2007). The RBCC Gene *RFP2* (*Leu5*) Encodes a Novel Transmembrane E3 Ubiquitin Ligase Involved in ERAD. Mol. Biol. Cell. *18*, 1670-1682.

Leung, D.W. (2001). The structure and functions of human lysoophosphatidic acid acyltransferase. Front. Biosci. *6*, D944-D953.

Lewin, T.M., de Jong, H., Schwerbrock, N.J., Hammond, L.E., Watkins, S.M., Combs, T.P., and Coleman, R.A. (2008). Mice deficient in mitochondrial glycerol-3-phosphate acyltransferase-1 have diminished myocardial triacylglycerol accumulation during lipogenic diet and altered phospholipid fatty acid composition. Biochim. Biophys. Acta. *1781*, 352-358.

Lewin, T.M., Granger, D.A., Kim, J.H., and Coleman, R.A. (2001). Regulation of mitochondrial sn-glycerol-3-phosphate acyltransferase activity: response to feeding status is unique in various rat tissues and is discordant with protein expression. Arch. Biochem. Biophys. *396*, 119-127.

Lewin, T.M., Schwerbrock, N.M.J., Lee, D.P., and Coleman, R.A. (2004). Identification of a new glycerol-3-phosphate acyltransferase isoenzyme, mtGPAT2, in mitochondria. J. Biol. Chem. *279*, 13488-13495.

Li, X. (2013). SIRT1 and Energy Metabolism. Acta. Biochimica. Biophysica. Sinica. *45*, 51-60.

Li, M., Brooks, C.L., Wu-Baer, F., Chen, D., Baer, R., and Gu, W. (2003). Mono versus polyubiquitination: differential control of p53 fate by Mdm2. Science. *302*, 1972–1975.

Li, C., Li, L., Lian, J., Watts, R., Nelson, R., Goodwin, B., and Lehner, R. (2015). Roles of Acyl-CoA:Diacylglycerol Acyltransferases 1 and 2 in Triacylglycerol Synthesis and Secretion in Primary Hepatocytes. Arterioscler. Thromb. Vasc. Biol. *35*, 1080-1091.

Liang, J., Oelkers, P., Guo, C., Chu, P., Dixon, J., Ginsberg, H., and Sturley, S. (2004). Overexpression of human diacylglycerol acyl-transferase 1, acyl-coa:cholesterol acyltransferase 1, or acyl-CoA: cholesterol acyltransferase 2 stimulates secretion of apolipoprotein B-containing lipoproteins in McA-RH7777 cells. J. Biol. Chem. *279*, 44938-44944.

Lilley, B.N., and H.L. Ploegh. (2004). A membrane protein required for dislocation of misfolded proteins from the ER. Nature. *429*, 834–840.

Listenberger, L.L., Han, X., Lewis, S.E., Cases, S., Farese, R.V.Jr., Ory, D.S., and Schaffer, J.E. (2003). Triglyceride accumulation protects against fatty acid-induced lipotoxicity. Proc. Natl. Acad. Sci. U S A. *100*, 3077–3082.

Listenberger, L.L., Ostermeyer-Fay, A.G., Goldberg, E.B., Brown, W.J., and Brown, D.A. (2007). Adipocyte differentiation related protein reduces the lipid droplet association of adipose triglyceride lipase and slows triacylglycerol turnover. J. Lipid Res. *48*, 2751–276.1

Liu, G.H., and Gerace, L. (2009). Sumoylation regulates nuclear localization of lipin-1alpha in neuronal cells. PLoS One. *4*, e7031.

Liu, Y., Millar, J., Cromley, D., Graham, M., Crooke, R., Billheimer, J., and Rader D. (2008). Knockdown of acyl-CoA:diacyl- glycerol acyltransferase 2 with antisense oligonucleotide reduces VLDL TG and ApoB secretion in mice. Biochim. Biophys. Acta. *1781*, 97–104.

Liu, Q., Siloto, R.M.P., Lehner, R., Stone, S.J., and Weselake, R.J. (2012). Acyl-CoA:diacylglcerol acyltransferase: Molecular biology, biochemistry and biotechnology. Prog. Lipid Res. *51*, 350-377.

Liu, Q., Siloto, R.M.P., Snyder, C.L., and Weselake, R.J. (2011). Functional and topological

analysis of yeast acyl-Coa:diacylglycerol acyltransferase 2, an endoplasmic reticulum enzyme essential for triacylglycerol biosynthesis. J. Bio. Chem. *286*, 13115-13126.

Londos, C., Sztalryd, C., Tansey, J., and Kimmel, A. (2005). Role of PAT proteins in lipid metabolism. Biochimie. *87*, 45–49.

Lu, B., Jiang, Y.J., Zhou, Y., Xu, F.Y., Hatch, G.M., and Choy, P.C. (2005). Cloning and characterization of murine 1-acyl-sn-glycerol 3-phosphate acyltransferases and their regulation by PPARalpha in murine heart. Biochem. J. *385*, 469-477.

Lu, B., Morrow, J.A., and Weisgraber, K.H. (2000). Conformational reorganization of the four-helix bundle of human apolipoprotein E in binding to phospholipids. J. Biol. Chem. *275*, 20775–20781.

Ludwig, E.H., Mahley, R.W., Palaoglu, E., Balestra, M.E., Borecki, I.B., Innerarity, T.L., and Farese, R.V. Jr. (2002). DGAT1 promoter polymorphism associated with alterations in body mass index, high density lipoprotein levels and blood pressure in Turkish women. Clin. Genet. *62*, 68–73.

Lynes E.M., Raturi, A., Shenkman, M., Ortiz Sandoval C., Yap, M.C., Wu, J., Janowicz, A., Myhill N., Benson, M.D., Campbell, R.E., Berthiaume, L.G., Lederkremer, G.Z., and Simmen, T. (2013). Palmitoylation is the switch that assigns calnexin to quality control or ER calcium signaling. J. Cell Sci. *126*, 3893–3903.

Maciejewski, B.S., LaPerle, J.L., Chen, D., Ghosh, A., Zavadoski, W.J., McDonald, T.S., Manion, T.B., Mather, D., Patterson, T.A., Hanna, M., Watkins, S., Gibbs, E.M., Calle, R.A., and Steppan, C.M. (2013). Pharmacological inhibition to examine the role of DGAT1 in dietary lipid absorption in rodents and humans. Am. J. Physiol. Gastrointest. Liver Physiol. *304*, G958−G969.

Madsen, L., Kriegenburg, F., Vala, A., Best, D., Prag, S., Hofmann, K., Seeger, M., Adams, I.R., and Hartmann-Petersen, R. (2011). The tissue-specific Rep8/UBXD6 tethers p97 to the endoplasmic reticulum membrane for degradation of misfolded proteins. PLoS One. *6*, e25061.

Maffeis, C., Schutz, Y., Grezzani, A., Provera, S., Piacentini, G., and Tato, L. (2001). Meal-induced thermogenesis and obesity: is a fat meal a risk factor for fat gain in children? J. Clin. Endocrinol. Metab. *86*, 214–219.

Man, W.C., Miyazaki, M., Chu, K., and Ntambi, J. (2006). Colocalization of SCD1 and DGAT2: implying preference for endogenous monounsaturated fatty acids in triglyceride synthesis. J. Lipid Res. *47*, 1928-1939.

Manmontri, B., Sariahmetoglu, M., Donkor, J., Bou Khalil, M., Sundaram, M., Yao, Z., Reue, K., Lehner, R., and Brindley, D.N. (2008). Glucocorticoids and cyclic AMP selectively increase hepatic lipin-1 expression, and insulin acts antagonistically. J. Lipid Res. *49*, 1056-1067.

Martin, S., and Parton, R.G. (2006). Lipid droplets: a unified view of a dynamic organelle. Nat. Rev. Mol. Cell Biol. *7*, 373–378.

Martinez-Botas, J., Anderson, J.B., Tessier, D., Lapillonne, A., Chang, B.H., Quast, M.J., Gorenstein, D., Chen, K.H., and Chan L. (2000). Absence of perilipin results in leanness and reverses obesity in Lepr(db/db) mice. Nat Genet. *26*, 474-479.

Mansbach, C.M., and Dowell, R. (2000). Effect of increasing lipid loads on the ability of the endoplasmic reticulum to transport lipid to the Golgi. J. Lipid Res. *41,* 605–612.

Mansbach, C.M., and Siddiqi, S.A. (2010). The biogenesis of chylomicrons. Annu. Rev. Physiol. *72,* 315–333.

Mashek, D.G., and Coleman, R.A. (2006). Cellular fatty acid up-take: the contribution of metabolism. Curr. Opin. Lipidol. *17*, 274–278.

Mbonye, U.R., Wada, M., Rieke, C.J., Tang, H.Y., Dewitt, D.L. and Smith, W.L. (2006). The 19-amino acid cassette of cyclooxygenase-2 mediates entry of the protein into the endoplasmic reticulum-associated degradation system. J. Biol. Chem. *281*, 35770-35778.

McFie, P.J., Banman, S.L., Kary, S., and Stone, S.J. (2011). Murine diacylglycerol acyltransferase-2 (DGAT2) can catalyze triacylglycerol synthesis and promote lipid droplet formation independent of its localization to the endoplasmic reticulum. J. Biol. Chem. *286*, 28235-28246.

McFie, P.J., Izzard, S., Vu, H., Jin, Y., Beauchamp, E., Bertiaume, L.G., and Stone, S.J. (2016). Membrane topology of human monoacylglycerol acyltransferase-2 and identification of regions important for its localization to the endoplasmic reticulum. Biochim. Biophys. Acta. *1861*, 1192-1204.

McFie, P.J., Jin, Y., Banman S.L., Beauchamp, E., Berthiaume, L.G., and Stone, S.J. (2014). Characterization of the interaction of diacylglycerol acyltransferase-2 with the endoplasmic reticulum and lipid droplets. Biochim. Biophys. Acta. *1841*, 1318–1328.

McFie, P. J., and Stone, S.J. (2011) A fluorescent assay to quantitatively measure in vitro Acyl CoA:Diacylglycerol acyltransferase activity. J. Lipid Res. *52*, 1760-1764.

McFie, P.J., Stone, S.L., Banman, S.L., and Stone, S.J. (2010). Topological Orientation of Acyl-CoA:Diacylglycerol Acyltransferase-1 (DGAT1) and Identification of a Putative Active Site Histidine and the Role of the N Terminus in Dimer/Tetramer Formation. J. Biol. Chem. *285*, 37377-37387.

Meacham, G.C., Patterson, C., Zhang, W., Younger, J.M., and Cyr, D.M. (2001). The Hsc70 co-chaperone CHIP targets immature CFTR for proteasomal degradation. Nat. Cell Biol. *3*, 100-105.

Meegalla, R.L., Billheimer, J.T., and Cheng, D. (2002). Concerted elevation of acyl-coenzyme

A:diacylglycerol acyltransferase (DGAT) activity through independent stimulation of mRNA expression of DGAT1 and DGAT2 by carbohydrate and insulin. Biochem. Biophys. Res. Commun. *298*, 317–323.

Mehnert, M., Sommer, T., and Jarosch, E. (2014). Der1 promotes movement of misfolded proteins through the endoplasmic reticulum membrane. Nat. Cell Biol. *16*, 77-86.

Mellacheruvu, D., Wright, Z., Couzens, A.L., et al. (2013). The CRAPome: a contaminant repository for affinity purification mass spectrometry data. Nature Methods. *10*, 730-736.

Meller, N., Morgan, M.E., Wong, W.P., Altemus, J.B., and Sehayek, E. (2013). Targeting of acyl-CoA synthetase 5 decreases jejunal fatty acid activation with no effect on dietary long-chain fatty acid absorption. Lipids Health Dis. *12*, 88.

Millar, J., Stone, S.J., Tietge, U. Tow, B., Billheimer, J. Wong, J., Hamilton, R. Farese, R.V.Jr., and Rader, D. (2006). Short-term over-expression of DGAT1 or DGAT2 increases hepatic triglyceride but not VLDL triglyceride or apoB production. J. Lipid Res. *47*, 2297–2305.

Mingot, J.M., Bohnsack, M.T., Jaekle, U., and Goerlich, D. (2004). Exportin 7 defines a novel general nuclear export pathway. EMBO J. *23*, 3227-3236.

Mitchell, D.M., Zhou, M., Pariyarath, R., Wang, H., Aitchison, J.D., Ginsberg, H.N., and Fisher, E.A. (1998). Apoprotein B100 has a pro-longed interaction with the translocon during which its lipidation and translocation change from dependence on the microsomal triglyceride transfer protein to independence. Proc. Natl. Acad. Sci. U S A. *95*, 14733–14738.

Monetti, M., Levin, M.C., Watt, M.J., Sajan, M.P., Marmor, S., Hubbard, B.K., Stevens, R.D., Bain, J.R., Newgard, C.B., Farese, R.V. Sr., Hevener A.L., Farese, R.V.Jr. (2007). Dissociation of Hepatic Steatosis and Insulin Resistance in Mice Overexpressing DGAT in the Liver. Cell Metab. *6*, 69-78.

Moon, Y., and Horton, J.D. (2003). Identification of two mammalian reductases involved in the two-carbon fatty acyl elongation cascade. J. Biol. Chem. *278*, 7335-7343.

Morak, M., Schmidinger, H., Riesenhuber, G., Rechberger, G.N., Kollroser, M., Haemmerle, G., Zechner, R., Kronenberg, F., and Hermetter, A. (2012). Adipose triglyceride lipase (ATGL) and hormone-sensitive lipase (HSL) deficiencies affect expression of lipolytic activities in mouse adipose tissues. Mol. Cell. Proteomics. *11*, 1777–1789.

Morito, D., Hirao, K., Oda, Y., Hosokawa, N., Tokunaga, F., Cyr, D.M., Tanaka, K., Iwai, K., and Nagata, K. (2008). Gp78 cooperates with RMA1 in endoplasmic reticulum-associated degradation of CFTRΔF508. Mol. Biol. Cell. *19*, 1328–1336.

Morré, D.J., Merritt, W.D., and Lembi, C.A. (1971). Connections between mitochondria and endoplasmic reticulum in rat liver and onion stem. Proc. Natl. Acad. Sci. U S A. *73*, 43–49.

Mueller, B., Klemm, E.J., Spooner, E., Claessen, J.H. and Ploegh H.L. (2008). SEL1L

nucleates a protein complex required for dislocation of misfolded glycoproteins. Proc. Natl. Acad. Sci. U S A. *105*, 12325–12330.

Murphy, D.J., and Vance, J. (1999). Mechanisms of lipid body formation. Trends Biochem. Sci. *24*, 109–115.

Nadav, E., Shmueli, A., Barr, H., Gonen, H., Ciechanover, A., and Reiss, Y. (2003). A novel mammalian endoplasmic reticulum ubiquitin ligase homologous to the yeast Hrd1. Biochem. Biophys. Res. Commun. *303*, 91–97.

Nadra, K., de Preux, Charles, A.S., Medard, J.J., Hendriks, W.T., Han, G.S., Gres, S., Carman, G.M., Saulnier-Blache, J.S., Verheijen, M.H., and Chrast, R. (2008). Phosphatidic acid mediates demyelination in Lpin1 mutant mice. Genes Dev. *22,* 1647-1661.

Nagai, S., Shimizu, C., Umetsu, M., Taniguchi, S., Endo, M., Miyoshi, H., Yoshioka, N., Kubo, M., and Koike, T. (2004). Identification of a functional peroxisome proliferator-activated receptor responsive element within the murine perilipin gene. Endocrinology. *145*, 2346-2356.

Nagle, C.A., Verges, L., Wang, S., deJong, H., Wang, S., Lewin, T.M., Reue, K., and Coleman, R.A. (2008). Identification of a novel sn-glycerol-3-phosphate acyltransferase isoform, GPAT4, as the enzyme deficient in Agpat6-/- mice. J. Lipid Res. *49*, 823-831.

Naik, R., Obiang-Obounou, B.W., Kim, M., Choi, Y., Lee, H.S., and Lee, K. (2014). Therapeutic Strategies for Metabolic Diseases: Small-Molecule Diacylglycerol Acyltransferase (DGAT) Inhibitors. ChemMedChem. *9*, 2410−2424.

Nakatsukasa, K., and Brodsky, J.L. (2008). The recognition and retrotranslocation of misfolded proteins from the endoplasmic reticulum. Traffic. *9*, 861–870.

Nelson, D.L., and Cox, M.M., (2008). Fatty Acid Catabolism. Lehninger principles of biochemistry fifth edition. W.H. Freeman and Company, New York, USA, pp. 647-667.

Neuber, O., Jarosch, E. Volkwein, C. Walter, J. and Sommer, T. (2005). Ubx2 links the Cdc48 complex to ER-associated protein degradation. Nat. Cell Biol. *7*, 993-998.

Neutzner, A., Neutzner, M., Benischke, A.S., Ryu, S.W., Frank, S., Youle, R.J., Karbowski, M. (2011). A systematic search for endoplasmic reticulum (ER) membrane-associated RING finger proteins identifies Nixin/ZNRF4 as a regulator of calnexin stability and ER homeostasis. J. Biol. Chem. *286*, 8633–8643.

Nevin, P., Koelsch, D. and, Mansbach C.M.2nd. (1995). Intestinal triacylglycerol storage pool size changes under differing physiological conditions. J. Lipid Res. *36*, 2405–2412.

Newsholme, E.A., and Crabtree, B. (1976). Substrate cycles in metabolic regulation and in heat generation. Biochem. Soc. Symp. *41*, 61–109.

Niot, I., Poirier, H., Tran, T.T., and Besnard, P. (2009). Intestinal absorption of long-chain fatty

acids: evidence and uncertainties. Prog. Lipid Res. *48*, 101–115.

Norman, R.A., Thompson, D.B., Foroud, T., Garvey, W.T., Bennett, P.H., Bogardus, C., and Ravussin, E. (1997). Genomewide search for genes influencing percent body fat in Pima Indians: suggestive linkage at chromosome 11q21-q22. Pima Diabetes Gene Group. Am. J. Hum. Genet. *60*, 166-173.

Novartis. Clinical Trial Results Database. Retrieved from: http://www.novctrd. com/ctrdWebApp/clinicaltrialrepository/displayFile.do?trialResult= 4314. Accessed on: May 5, 2016.

Obrowsky, S., Chandak, P.G., Patankar, J.V., Povoden, S., Schlager, S., Kershaw, E.E., Bogner-Strauss, J.G., Hoefler, G., Levak- Frank, S., and Kratky, D. (2013). Adipose triglyceride lipase is a TG hydrolase of the small intestine and regulates intestinal PPARalpha signaling. J. Lipid Res. *54*, 425–435.

Ogden, C.L., Carroll, M.D., Kit, B.K., and Flegal, K.M. (2014). Prevalence of Childhood and Adult Obesity in the United States, 2011-2012. JAMA. *311*, 806-814.

Ohsaki, Y., Cheng, J., Fujita, A., Tokumoto, T., and Fujimoto, T. (2006). Cytoplasmic lipid droplets are sites of convergence of proteasomal and autophagic degradation of apolipoprotein B. Mol. Biol. Cell. *17*, 2674–2683.

Ohsaki, Y., Cheng, J., Suzuki, M., Shinohara, Y., Fujita, A., and Fujimoto, T. (2009). Biogenesis of cytoplasmic lipid droplets: From the lipid ester globule in the membrane to the visible structure. Biochim. Biophys. Acta. *1791*, 399–407.

Ohsaki, Y., Kawai, T., Yoshikawa, Y., Cheng, J., Jokitalo, E., and Fujimoto, Y. (2016). PML isoform II plays a critical role in nuclear lipid droplet formation. J. Cell Bio. *212*, 29-38.

Oleckno, W.A. (2002). Essential epidemiology: principles and applications. Long Grove, IL: Waveland Press.

Olzmann, J.A., and Kopito, R.R. (2011). Lipid droplet formation is dispensable for endoplasmic reticulum-associated degradation. J. Biol. Chem. *286*, 27872–27874.

Olzmann, J.A., Kopito, R.R., and Christianson, J.C., (2013a). The mammalian endoplasmic reticulum-associated degradation system. Cold Spring Harb. Perspect. Biol. *5*, a01385.

Olzmann, J.A., Richter, C.M., and Kopito, R.R. (2013b). Spatial regulation of UBXD8 and p97/ VCP controls ATGL-mediated lipid droplet turnover. Proc. Natl. Acad. Sci. U S A. *110*, 1345–1350.

Ong, K.T., Mashek, M.T., Bu, S.Y., Greenberg, A.S., and Mashek, D.G. (2011). Adipose triglyceride lipase is a major hepatic lipase that regulates triacylglycerol turnover and fatty acid signaling and partitioning. Hepatology. *53*, 116–126.

Onorato, T.M., Chakraborty, S., and Haldar, D. (2005). Phosphorylation of rat liver mitochondrial glycerol-3-phosphate acyltransferase by casein kinase 2. J. Biol. Chem. *280*, 19527-19534.

Orlicky, S., Tang, X., Willems, A., Tyers, M., and Sicheri, F. (2003). Structural Basis for Phosphodependent Substrate Selection and Orientation by the SCF(Cdc4) Ubiquitin Ligase. Cell. *112*, 243–256.

Ostermeyer, A., Ramcharan, L., Zeng, Y., Lublin, D, and Brown, D. (2004). Role of the hydrophobic domain in targeting caveolin-1 to lipid droplets. J. Cell Biol. *164*, 69–78.

Owen, M.R., Corstorphine, C.C., and Zammit, V.A. (1997). Overt and latent activities of diacylglycerol acytransferase in rat liver microsomes: possible roles in very-low-density lipoprotein triacylglycerol secretion. Biochem. J. *323*, 17–21.

Ozato, K., Shin, D.M., Chang, T.H., and Morse, H.C. (2008). TRIM family proteins and their emerging roles in innate immunity 3rdNat. Rev. Immunol. *8*, 849–860.

Palmer, A., Rivett, A.J., Thomson, S., Hendil, K.B., Butcher, G.W., Fuertes, and G., Knecht, E. (1996) Subpopulations of proteasomes in rat liver nuclei, microsomes and cytosol. Biochem. J. *316*, 401–407.

Patton, J.S., and Carey, M.C. (1979). Watching fat digestion. Science. *204*, 145–148.

Payne, V.A., Au, W.S., Gray, S.L., Nora E.D., Rahman, S.M., Sanders, R., Hadaschik, D., Friedman, J.E., O'Rahilly, S., and Rochford, J.J. (2007). Sequential regulation of diacylglycerol acyltransferase 2 expression by CAAT/enhancer-binding protein beta (C/EBPbeta) and C/EBPalpha during adipogenesis. J. Biol. Chem. *282*, 21005-21014.

Pellon-Maison, M., Montanaro, M.A., Coleman, R.A., and Gonzalez-Baro, M.R. (2007). Mitochondrial glycerol-3-P acyltransferase 1 is most active in outer mitochondrial membrane but not in mitochondrial associated vesicles (MAV). Biochim. Biophys. Acta. *1771*, 830-838.

Peng, J., Schwartz, D., Elias, J.E., Thoreen, C.C., Cheng, D., Marsischky, G., Roelofs, J., Finley, D., and Gygi, S.P. (2003). A proteomics approach to understanding protein ubiquitination. Nat. Biotechnol. *21*, 921-926.

Pestova, T.V., and Hellen, C.U. (2003). Translation elongation after assembly of ribosomes on the Cricket paralysis virus internal ribosomal entry site without initiation factors or initiator tRNA. Genes Dev. *17*, 181-186.

Peterfy, M., Harris, T.E., Fujita, N., and Reue, K.J. (2010). Insulin-stimulated interaction with 14-3-3 promotes cytoplasmic localization of lipin-1 in adipocytes. Biol. Chem. *285*, 3857-3864.

Peterfy, M., Phan, J., Xu, P., and Reue, K. (2001). Lipodystrophy in the fld mouse results from mutation of a new gene encoding a nuclear protein, lipin. Nat. Genet. *27*, 121-124.

Petroski, M.D. and Deshaies, R.J. (2003). Redundant Degrons Ensure the Rapid Destruction of Sic1 at the G1/S Transition of the Budding Yeast Cell Cycle. Cell Cycle. *2*, 409-410.

Phan, J., Peterfy, M., and Reue, K.J. (2004). Lipin expression preceding peroxisome proliferator-activated receptor-gamma is critical for adipogenesis in vivo and in vitro. Biol. Chem. *279*, 29558-29564.

Plemper, R.K., Bordallo, J., Deak, P.M., Taxis, C., Hitt, R., and Wolf, D.H. (1999). Genetic interactions of Hrd3p and Der3p/Hrd1p with Sec61p suggest a retro-translocation complex mediating protein transport for ER degradation. J. Cell Sci. *112*, 4123–4134.

Ploegh, H.L. (2007). A lipid-based model for the creation of an escape hatch from the endoplasmic reticulum. Nature. *448*, 435–438.

Pratley, R.E., Thompson, D.B., Prochazka, M., Baier, L., Mott, D., Ravussin, E., Sakul, H., Ehm, M.G., Burns, D.K, Foroud, T., Garvey, W.T., Hanson, R.L., Knowler, W.C., Bennett, P.H., and Bogardus, C. (1998). An autosomal genomic scan for loci linked to prediabetic phenotypes in Pima Indians. J. Clin. Invest. *101*, 1757–1764.

Prattes, S., Horl, G., Hammer, A., Blaschitz, A., Graier, W.F., Sattler, W., Zechner, R., and Steyrer, E. (2000). Intracellular distribution and mobilization of unesterified cholesterol in adipocytes: Triglyceride droplets are surrounded by cholesterol-rich ER-like surface layer structures. J. Cell Sci. *113*, 2977-2989.

Qi, J., Lang, W., Geisler, J. G., Wang, P., Petrounia, I., Mai, S., Smith, C., Askari, H., Struble, G.T., Williams, R., Bhanot, S., Monia, B.P., Bayoumy, S., Grant, E., Caldwell, G.W., Todd, M.J., Liang, Y., Gaul, M.D., Demarest, K.T., and Connelly, M.A. (2012). The use of stable isotope-labeled glycerol and oleic acid to differentiate the hepatic functions of DGAT1 and −2. J. Lipid Res. *53*, 1106−1116.

Rabinovich, E., Kerem, A., Fröhlich, K.U., Diamant, N., and Bar-Nun, S. (2002). AAA-ATPase p97/Cdc48p, a cytosolic chaperone required for endoplasmic reticulum-associated protein degradation. Mol. Cell. Biol. *22*, 626– 634.

Raiborg, C., and Stenmark, H. (2009). The ESCRT machinery in endosomal sorting of ubiquitylated membrane proteins. Nature. *458*, 445–452.

Ranganathan, G., Unal, R., Pokrovskaya, I., Yao-Borengasser, A., Phanavanh, B., Lecka-Czernik, B., Rasouli, N., and Kern, P. (2006). The lipogenic enzymes DGAT1, FAS, and LPL in adipose tissue: effects of obesity, insulin resistance, and TZD treatment. J. Lipid Res. *47*, 2444–2450.

Rao, H., Uhlmann, F., Nasmyth, K., and Varshavsky, A. (2001). Degradation of a cohesin subunit by the N-end rule pathway is essential for chromosome stability. Nature. *410*, 955–959.

Rapoport, T.A. (2007). Protein translocation across the eukaryotic endoplasmic reticulum and bacterial plasma membranes. Nature. *450*, 663–669.

Ravid, T., and Hochstrasser, M. (2008). Diversity of degradation signals in the ubiquitin-proteasome system. Nat. Rev. Mol. Cell. Biol. *9,* 679-690.

Redgrave, T.G. (1970). Formation of cholesteryl ester-rich particulate lipid during metabolism of chylomicrons. J. Clin. Invest. *49*, 465-471.

Riemer, .J, Hansen, H.G., Appenzeller-Herzog, C., Johansson, L., and Ellgaard, L. (2011). Identification of the PDI- family member ERp90 as an interaction partner of ERFAD. PLoS ONE. *6*, e17037.

Renaville, B., Bacciu, N., Lanzoni, M., Corazzin, M., and Piasentier, E. (2015). Polymorphism of fat metabolism genes as candidate markers for meat quality and production traits in heavy pigs. Meat Sci. *110*, 220-223.

Reverte, C.G., Ahearn, M.D., and Hake, L.E. (2001). CPEB degradation during Xenopus oocyte maturation requires a PEST domain and the 26S proteasome. Dev. Biol. *231*, 447-58.

Robenek, H., Robenek, M.J., and Troyer, D. (2005). Pat family proteins pervade lipid droplet cores. J. Lipid Res. *46,* 1331–1338.

Robenek, M.J., Severs, N.J., Schlattmann, K., Plenz, G., Zimmer, K.P., Troyer, D., and Robenek, H. (2004). Lipids partition caveolin-1 from er membranes into lipid droplets: Updating the model of lipid droplet biogenesis. FASEB J. *18*, 866–868.

Rodriguez, J.A., Ben Ali, Y., Abdelkafi, S., Mendoza, L.D., Leclaire, J., Fotiadu, F., Buono, G., Carrière, F., and Abousalham, A. (2010). In vitro stereoselective hydrolysis of diacylglycerols by hormone-sensitive lipase. Biochim. Biophys. Acta. *1801*, 77–83.

Roussel, A., Yang, Y., Ferrato, F. Verger, R. Cambillau, C. and Lowe, M. E. (1998). Structure and activity of rat pancreatic lipase related protein 2. J. Biol. Chem. *273*, 32121–32128.

Ruan, H., and Pownall, H.J. (2001). Overexpression of 1-acyl-glycerol-3-phosphate acyltransferase-alpha enhances lipid storage in cellular models of adipose tissue and skeletal muscle. Diabetes. *50*, 233-240.

Rumpf, S., and Jentsch, S. (2006). Functional division of substrate processing cofactors of the ubiquitin-selective Cdc48 chaperone. Mol. Cell. *21*, 261-269.

Rusinol, A.E., Cui, Z., Chen, M.H., and Vance, J.E. (1994). A unique mitochondria-associated membrane fraction from rat liver has a high capacity for lipid synthesis and contains pre-Golgi secretory proteins including nascent lipoproteins. J.Biol. Chem. *269*, 27494-27502.

Saar, K., Geller, F., Ruschendorf, F., Reis, A., Friedel, S., Schauble, N., Nurnberg, P., Siegfried, W., Goldschmidt, H.P., Schafer, H., Ziegler, A., Remschmidt, H., Hinney, A., and Hebebrand, J. (2003). Genome scan for childhood and adolescent obesity in German families. Pediatrics. *111*, 321-327.

Saito, Y., Ihara,Y., Leach,M.R., Cohen-Doyle, M.F., and Williams, D.B. (1999). Calreticulin functions in vitro as a molecular chaperone for both glycosylated and non-glycosylated proteins. EMBO J. *18*, 6718-6729.

Salter, A., Wiggins, D., Sessions, V., and Gibbons, G. (1998). The intracellular triacylglycerol/fatty acid cycle: a comparison of its activity in hepatocytes which secrete exclusively apolipoprotein (apo) B100 very-low-density lipoprotein (VLDL) and in those which secrete predominantly apoB48 VLDL. Biochem. J. *332*, 667–672.

Schmidt, J.A., and Brown, W.J. (2009). Lysophosphatidic acid acyltransferase 3 regulates Golgi complex structure and function. J. Cell Biol. *186*, 211-218.

Schmidt, J.A., Yvone, G.M., and Brown, W.J. (2010). Membrane topology of human AGPAT3 (LPAAT3). Biochem. Biophys. Res. Commun. *397*, 661-667.

Schneider-Poetsch, T., Ju, J., Eyler, D.E., Dang, Y., Bhat, S., Merrick, W.C., Green, R., Shen, B., and Liu, J.O. (2010). Inhibition of eukaryotic translation elongation by cycloheximide and lactimidomycin. Nat. Chem. Biol. *6*, 209-217.

Schrag, J.D., Bergeron, J.J., Li, Y., Borisova, S., Hahn, M., Thomas, D.Y., and Cygler, M. (2001). The structure of calnexin, an ER chaperone involved in quality control of protein folding. Mol. Cell. *8*, 633-644.

Schreiner, P., Chen, X., Husnjak, K., Randles, L., Zhang, N., Elasser, S., Finley, D., Dikic, I., Walters, K.J., and Groll, M. (2008). Ubiquitin docking at the proteasome through a novel pleckstrin-homology domain interaction. Nature. *453*, 548-552.

Schuberth, C., and A. Buchberger. (2005). Membrane-bound Ubx2 recruits Cdc48 to ubiquitin ligases and their substrates to ensure efficient ER-associated protein degradation. Nat. Cell Biol. *7*, 999–1006.

Schulthess, G., Lipka, G., Compassi, S., Boffelli, D., Weber, F.E., Paltauf, F. and Hauser, H. (1994). Absorption of monoacylglycerols by small intestinal brush border membrane. Biochemistry. *33*, 4500-4508.

Scott, D.C., and Schekman. R. (2008). Role of Sec61p in the ER-associated degradation of short-lived transmembrane proteins. J. Cell Biol. *181*, 1095-1105.

Serrano-Wu, Coppola, G., Gong, Y., *et al.* (2012). Intestinally Targeted Diacylglycerol Acyltransferase 1 (DGAT1) Inhibitors Robustly Suppress Postprandial Triglycerides. ACS Med. Chem. Lett. *3*, 411-415

Sever, N., Song, B.L., Yabe, D., Goldstein, J.L., Brown, M.S., and DeBose-Boyd R.A. (2003). Insig-dependent ubiquitination and degradation of mammalian 3-hydroxy-3-methylglutaryl-CoA reductase stimulated by sterols and geranylgeraniol. J. Biol. Chem. *278*, 52479–52490.

Shan, D., Li, J.L., Wu, L., Li, D., Hurov, J., Tobin, J.F., Gimeno, R.E., and Cao, J.J. (2010). GPAT3 and GPAT4 are regulated by insulin-stimulated phosphorylation and play distinct roles in adipogenesis. Lipid Res. *51*, 1971-1981.

Shiao, Y.J., Balcerzak, B., and Vance, J.E. (1998). A mitochondrial membrane protein is required for translocation of phosphatidylserine from mitochondria-associated membranes to mitochondria. Biochem. J. *331*, 217-223.

Shiao, Y.J., Lupo, G., and Vance, J.E. (1995). Evidence that phosphatidylserine is imported into mitochondria via a mitochondria-associated membrane and that the majority of mitochondrial phosphatidylethanolamine is derived from decarboxylation of phosphatidylserine. J. Biol. Chem. *270*, 11190-11198.

Shimakata, T., Mihara, K. and Sato, R. (1972). Reconstitution of hepatic microsomal stearoyl-Coenzyme A desaturase from solubilized components. J. Biochem. *72*, 1163-1174.

Shimizu, Y., Okuda-Shimizu, Y., and Hendershot, L.M. (2010). Ubiquitylation of an ERAD substrate occurs on multiple types of amino acids. Mol. Cell. *40*, 917 – 926.

Shimizu, M., Yamashita, D., Yamaguchi, T., Hirose, F., and Osumi, T. (2006). Aspects of the regulatory mechanisms of PPAR functions: analysis of a bidirectional response element and regulation by sumoylation. Mol. Cell Biochem. *286*, 33-42.

Shmueli, A., Tsai, Y.C., Yang, M., Braun, M.A., and Weissman, A.M. (2009). Targeting of gp78 for ubiquitin-mediated proteasomal degradation by Hrd1: Cross-talk between E3s in the endoplasmic reticulum. Biochem. Biophys. Res. Commun. *390*, 758–762.

Shockey, J.M., Gidda, S.K., Chapital, D.C., Kuan, J.C., Dhanoa, P.K., Bland, J.M., Rothstein, S.J., Mullen, R.T., and Dyer, J.M. (2006). Tung tree DGAT1 and DGAT2 have nonredundant functions in triacylglycerol biosynthesis and are localized to different subdomains of the endoplasmic reticulum. Plant Cell. *18*, 2294-2313.

Shumway, S.D., Maki, M., and Miyamoto, S. (1999). The PEST domain of IkappaBalpha is necessary and sufficient for in vitro degradation by mu-calpain. J. Biol. Chem. *274*, 30874-30881.

Smith, S.J., Cases, S., Jensen, D.R., Chen, H.C., Sande, E., Tow, B., Sanan, D.A., Raber, J., Eckel, R.H., and Farese, R.V.Jr. (2000). Obesity resistance and multiple mechanisms of triglyceride synthesis in mice lacking DGAT. Nat. Genet. *25*, 87-90.

Song, B.L., Javitt, N.B., and DeBose-Boyd, R.A. (2005). Insig-mediated degradation of HMG CoA reductase stimulated by lanosterol, an intermediate in the synthesis of cholesterol. Cell Metab. *1*, 179-189.

Spandl, J., Lohmann, D., Kuerschner, L., Moessinger, C., and Thiele, C. (2011). Ancient ubiquitous protein 1 (AUP1) localizes to lipid droplets and binds the E2 ubiquitin conjugase G2 (Ube2g2) via its G2 binding region. J. Biol. Chem. *286*, 5599-5606.

Spencer, M.L., Theodosiou, M., and Noonan, D.J. (2004). NPDC-1, a novel regulator of neuronal proliferation, is degraded by the ubiquitin/proteasome system through a PEST degradation motif. J. Biol. Chem. *279*, 37069-37078.

Stahl, A., Hirsch, D.J., Gimeno, R.E., Punreddy, S., Ge, P., Watson, N., Patel, S., Kotler, M., Raimondi, A., Tartaglia, L.A., and Lodish, H.F. (1999). Identification of the major intestinal fatty acid transport protein. Mol. Cell. *4*, 299–308.

Statistics Canada (2012). Obesity. Retrieved from: http://www.statcan.gc.ca/eng/help/bb/info/obesity. Accessed Aug 1, 2016.

Stemberger, B.H., Walsh, R.M., and Patton, S. (1984). Morphometric evaluation of lipid droplet associations with secretory vesicles, mitochondria and other components in the lactating cell. Cell Tissue Res. *236*, 471-475.

Stone, S.J., Levin, M.C., and Farese, R.V.Jr. (2006). Membrane topology and identification of key functional amino acid residues of murine acyl-CoA:diacylglycerol acyltransferase-2. J. Biol. Chem. *281*, 40273-40282.

Stone, S.J., Levin, M.C., Zhou, P., Han, J., Walther, T.C., and Farese, R.V.Jr. (2009). The Endoplasmic Reticulum Enzyme DGAT2 Is Found in Mitochondria-associated Membranes and Has a Mitochondrial Targeting Signal That Promotes Its Association with Mitochondria. J. Biol. Chem. *284*, 5352-5361.

Stone, S.J., Myers, H.M., Watkins, S.M., Brown, B.E., Feingold, K.R., Elias, P.M., and Farese, R.V.Jr. (2004). Lipopenia and skin barrier abnormalities in DGAT2-deficient mice. J. Biol. Chem. *279*, 11767-11776.

Stone, S.J., and Vance, J.E. (2000). Phosphatidylserine synthase-1 and -2 are localized to mitochondria-associated membranes. J. Biol. Chem. *275*, 34534-34540.

Storch, J., and Corsico, B. (2008). The emerging functions and mechanisms of mammalian fatty acid-binding proteins. Annu. Rev. Nutr. *28*, 73-95.

Storch, J., and McDermott, L. (2009). Structural and functional analy- sis of fatty acid-binding proteins. J. Lipid Res. *50*, S126-S131.

Storch, J., and Thumser, A.E. (2000). The fatty acid transport func- tion of fatty acid-binding proteins. Biochim. Biophys. Acta. *1486*, 28-44.

Storch, J., Zhou, Y.X., and Lagakos, W.S. (2008). Metabolism of apical versus basolateral sn-2-monoacylglycerol and fatty acids in rodent small intestine. J. Lipid Res. *49*, 1762-1769.

Stremmel, W., Lotz, G., Strohmeyer, G., and Berk, P.D. (1985). Identification, isolation, and partial characterization of a fatty acid binding protein from rat jejunal microvillous membranes. J. Clin. Invest. *75*, 1068-1076.

Strittmatter, P., Spatz, L., Corcoran, D., Rogers, M. J., Setlow, B. and Redline, R. (1974). Purification and properties of rat liver microsomal stearyl coenzyme A desaturase. Proc. Natl. Acad. Sci. U S A. *71*, 4565-4569.

Sturley, S.L., and Hussain, M.M. (2012). Lipid droplet formation on opposing sides of the endoplasmic reticulum. J. Lipid Res. *53*, 1800-1810.

Su, C.L., Sztalryd, C., Contreras, J.A., Holm, C., Kimmel, A.R., and Londos, C. (2003). Mutational analysis of the hormone-sensitive lipase translocation reaction in adipocytes. J. Biol. Chem. *278*, 43615-43619.

Subauste, A.R., Elliott, B., Das, A.K., and Burant, C.F. Differentiation. (2010). A role for 1-acylglycerol-3-phosphate-O-acyltransferase-1 in myoblast differentiation. Differentiation. *80*, 140-146.

Sun, Z., Gong, J., Wu, H., Xu, W., Wu, L., Xu, D., Gao, J., Wu, J.W., Yang, H., Yang, M., and Li, P. (2013). Perilipin1 promotes unilocular lipid droplet formation through the activation of Fsp27 in adipocytes. Nat. Commun. *4*, 1594.

Suzuki, R., Tobe, K., Aoyama, M., Sakamoto, K., Ohsugi, M., Kamei, N., Nemoto, S., Inoue, A., Ito, Y. Uchida, S., Hara, K., Yamauchi, T., Kubota, N., Terauchi, Y., and Kadowski, T. (2005). Expression of DGAT2 in white adipose tissue is regulated by central leptin action. J. Biol. Chem. *280*, 3331–3337.

Swaminathan, R., King, R.F., Holmfield, J., Siwek, R.A., Baker, M., and Wales, J.K. (1985). Thermic effect of feeding carbohydrate, fat, protein and mixed meal in lean and obese subjects. Am. J. Clin. Nutr. *42*, 177-181.

Swanton, E., High, S., and Woodman, P. (2003). Role of calnexin in the glycan-independent quality control of proteolipid protein. EMBO J. *22*, 2948-2958.

Szathmary, R., Bielmann, R., Nita-Lazar, M., Burda, P., and Jakob, C.A. (2005). Yos9 protein is essential for degradation of misfolded glycoproteins and may function as lectin in ERAD. Mol. Cell. *19*, 765-775.

Sztalryd, C., Bell, M., Lu, X., Mertz, P., Hickenbottom, S., Chang, B.H., Chan, L., Kimmel, A.R., and Londos, C. (2006). Functional compensation for adipose differentiation-related protein (ADFP) by Tip47 in an ADFP null embryonic cell line. J. Biol. Chem. *281*, 34341-34348.

Sztalryd, C., Xu, G., Dorward, H., Tansey, J.T., Contreras, J.A., Kimmel, A.R., and Londos, C. (2003). Perilipin A is essential for the translocation of hormone-sensitive lipase during lipolytic activation. J. Cell Biol. *161*, 1093–1103.

Taghibiglou, C., Rudy, D., Van Iderstine, S. C., Aiton, A., Cavallo, D., Cheung, R., and Adeli, K. (2000). Intracellular mechanisms regulating apoB-containing lipoprotein assembly and secretion in primary hamster hepatocytes. J. Lipid Res. *41*, 499-513.

Tait, S.W., de Vries, E., Maas, C., Keller, A.M., D'Santos, C.S., Borst, J. (2007). Apoptosis induction by Bid requires unconventional ubiquitination and degradation of its N-terminal fragment. J. Cell Biol. *179*, 1453–1466.

Tanaka, T., Yoshida, N., Kishimoto, T., and Akira, S. (1997). Defective adipocyte differentiation in mice lacking the C/EBPbeta and/or C/EBPdelta gene. EMBO J. *16*, 7432-7443.

Tannous, A., Patel, N., Tamura, T., and Hebert, D.N. (2015). Reglucosylation by UDP-glucose: glycoprotein glucosyltransferase 1 delays glycoprotein secretion but not degradation. Mol. Biol. Cell. *26*, 390-405.

Tansey, J.T., Huml, A.M., Vogt, R., Davis, K.E., Jones, J.M., Fraser, K.A., Brasaemle, D.L., Kimmerl, A.R., and Londos, C. (2003). Functional studies on native and mutated forms of perilipins: A role in protein kinase A-mediated lipolysis of triacylglycerols. J. Biol. Chem. *278*, 8401-8406.

Tansey, J.T., Sztalryd, C., Gruia-Gray, J., Roush, D.L., Zee, J.V., Gavrilova, O., Reitman, M.L., Deng, C.X., Li, C., Kimmel, A.R., and Londos C. (2001). Perilipin ablation results in a lean mouse with aberrant adipocyte lipolysis, enhanced leptin production, and resistance to diet-induced obesity. Proc. Natl. Acad. Sci. U S A. *98*, 6494-9.

Taschler, U., Radner, F.P., Heier, C., Schreiber, R., Schweiger, M., Schoiswohl, G., Preiss-Landl, K., Jaeger, D., Reiter, B., Koefeler, H.C. Wojciechowski, J., Theussl, C., Penninger, J.M., Lass, A., Haemmerle, G., Zechner, R., and Zimmermann, R. (2011). Monoglyceride lipase deficiency in mice impairs lipolysis and attenuates diet-induced insulin resistance. J. Biol. Chem. *286*, 17467–17477.

Tauchi-Sato, K., Ozeki, S., Houjou, T., Taguchi, R., and Fujimoto, T. (2002). The surface of lipid droplets is a phospholipid monolayer with a unique fatty acid composition. J. Biol. Chem. *277*, 44507–44512.

Teasdale, R.D., and Jackson, M.R. (1996). Signal-mediated sorting of membrane proteins between the endoplasmic reticulum and the golgi apparatus. Annu. Rev. Cell Dev. Biol. *12*, 27-54.

Thiam, A.R., Farese, R.V.Jr., and Walther, T.C. (2013). The biophysics and cell biology of lipid droplets. Nat. Rev. Mol. Cell Biol. *14*, 775–786.

Thrower, J.S., Hoffman, L. Rechsteiner, M., and Pickart, C.M. (2000). Recognition of the polyubiquitin proteolytic signal. EMBO J. *19,* 94-102.

Tjepkema, M. (2006). Adult obesity. Health Rep. *17*, 9-25.

Tomar, D., Singh, R., Singh, A.K., and Pandya, C.D. (2012). TRIM13 regulates ER stress induced autophagy and clonogenic ability of the cells. Biochim. Biophys. Acta. *1823*; 316–326.

Tremblay, M.S., Katzmarzyk, P.T., and Willams, J.D. (2002). Temporal trends in overweight and obesity in Canada, 1981-1996. Int. J. Obes. Relat. Metab. Disord. *26*, 538e43.

Ulrich, H.D., and Walden, H. (2010). Ubiquitin signaling in DNA replication and repair. Nature Rev. Mol. Cell Biol. *11*, 479–489.

Tso, P., Liu, M., Kalogeris, T.J., and Thomson, A.B. (2001). The role of apolipoprotein A-IV in the regulation of food intake. Annu. Rev. Nutr. *21*, 231–254.

Turkish, A., and Sturley, S.L. (2007). Regulation of Triglyceride Metabolism. I. Eukaryotic neutral lipid synthesis: "Many ways to skin ACAT or a DGAT". Am. J. Physiol. Gastrointest. Liver Physiol. *292*, G953-957.

Turnbull, A.P., Rafferty, J.B., Sedelnikova, S.E., Slabas, A.R., Schierer, T.P., Kroon, J.T., Nishida, I., Murata, N., Simon, J.W., and Rice, D.W. (2001). Crystallization and preliminary X-ray analysis of the glycerol-3-phosphate 1-acyltransferase from squash (Cucurbita moschata). Acta. Crystallogr. D. Biol. Crystallogr. *57*, 451-453.

Turró, S., Ingelmo-Torres, M., Estanyol, J. M., Tebar, F., Fernández, M. A., Albor, C. V., Gaus, K., Grewal, T., Enrich, C., Pol, A. (2006). Identification and characterization of associated with lipid droplet protein 1: a novel membrane-associated protein that resides on hepatic lipid droplets. Traffic. *7*, 1254-1269.

Uzbekov, R., and P. Roingeard. (2013). Nuclear lipid droplets identified by electron microscopy of serial sections. BMC Res. Notes. *6*, 386.

Vance, J.E. (2014). MAM (mitochondria-associated membranes) in mammalian cells: lipids and beyond. Biochim. Biophys. Acta. *1841*, 595–609.

Vance, J.E., and Shiao, Y.J. (1996). Intracellular trafficking of phospholipids: import of phosphatidylserine into mitochondria. Anticancer Res. *16*, 1333-1339.

Vaz, F.M., Houtkooper, R.H., Valianpour, F., Barth, P.G., and Wanders, R.J. (2003). Only one splice variant of the human TAZ gene encodes a functional protein with a role in cardiolipin metabolism. J. Biol. Chem. *278, 43089-43094.*

Verger, R. (1997). Interfacial activation of lipases facts and artifacts. Trends. Biochem. Tech. *15*, 32–38.

Vergnes, L., Beigneux, A.P., Davis, R.G., Watkins, S.M., Young, S.G., Reue, K.J. (2006). Agpat6 deficiency causes subdermal lipodystrophy and resistance to obesity. Lipid Res. *47*, 745-754.

Wagner, S.A., Beli, P., Weinert, B.T., Scholz, C., Kelstrup, C.D., Young, C., Nielsen, M.L., Olsen, J.V., Brakebusch, C., and Choudhary, C. (2012). Proteomic analyses reveal divergent ubiquitylation site patterns in murine tissues. Mol. Cell Proteomics. *11*, 1578-1585.

Walter, P., and Ron, D. (2011). The unfolded protein response: from stress pathway to homeostatic regulation. Science. *334*, 1081–1086.

Walther, T.C., and Farese, R.V.Jr. (2009). The life of lipid droplets. Biochim. Biophys. Acta. *1791*, 459–466.

Wan, H.C., Melo, R.C.N., Jin, Z., Dvorak, A.M., and Weller, P.F. (2007). Roles and origins of leukocyte lipid bodies: proteomic and ultrastructural studies. FASEB J. *21*, 167–178.

Wang, Y., Guan, S., Acharya, P., Liu, Y., Thirumaran, R.K., Brandman, R., Schuetz, E.G., Burlingames, A.L., and Correia, A.C. (2012a). Multisite phosphorylation of human liver cytochrome P450 3A4 enhances its gp78-and CHIP-mediated ubiquitination. Mol. Cell. Proteomics. *11*, M111.010132.

Wang, H.J., Guay, G., Pogan, L., Sauve, R., and Nabi, I.R. (2000). Calcium regulates the association between mitochondria and a smooth subdomain of the endoplasmic reticulum. J. Cell Biol. *150*,1489–1498.

Wang, B., Heath-Engel, H., Zhang, D., Nguyen, N., Thomas, D.Y., Hanrahan, J.W., and Shore, G.C. (2008). BAP31 Interacts with Sec61 Translocons and Promotes Retrotranslocation of CFTRΔF508 via the Derlin-1 Complex. Cell. *133*, 1080–1092.

Wang, X., Herr R.A., and Hansen T.H. (2012b). Ubiquitination of substrates by esterification. Traffic. *13*, 19-24.

Wang, H., Hu, L., Dalen, K., Dorward, H., Marcinkiewicz, A., Russell, D., Gong, D., Londos, C., Yamaguchi, T., Holm, C., Rizzo, M.A., Brasaemle, D., and Sztalryd, C. (2009a)**.** Activation of hormone-sensitive lipase requires two steps, protein phosphorylation and binding to the PAT-1 domain of lipid droplet coat proteins. J. Biol. Chem. *284*, 32116–32125.

Wang, S., Lee, D.P., Gong, N., Schwerbrock, N.M.J., Mashek, D.G., Gonzalez-Baró, M.R., Stapleton, C.M., Li, L.O., Lewin, T.M., and Coleman, R.A. Arch. (2007). Cloning and functional characterization of a novel mitochondrial N-ethylmaleimide-sensitive glycerol-3-phosphate acyltransferase (GPAT2). Biochem. Biophys. *465*, 347-358.

Wang, Q., Li, L., and Ye, Y. (2006). Regulation of retrotranslocation by p97- associated deubiquitinating enzyme ataxin-3. J. Cell Biol. *174*, 963-971.

Wang, Q., Li, L., and Ye, Y. (2008). Inhibition of p97-dependent Protein Degradation by Eeyarestatin I. J. Biol. Chem. *283*, 7445-7454.

Wang, Y., Liao, M., Hoe, N., Acharya, P., Deng, C., Krutchinsky, A.N., and Correia, M.A. (2009b). A role for protein phosphorylation in cytochrome P450 3A4 ubiquitin-dependent proteasomal degradation. J. Biol. Chem. *284*, 5671-5684.

Wang, T.Y., Liu, M., Portincasa, P., and Wang, D.Q. (2013). New insights into the molecular mechanism of intestinal fatty acid absorption. Eur. J. Clin. Invest. *43*, 1203-1223.

Wang, X., Medzihradszky, K.F., Maltby, D., and Correia, M.A. (2001). Phosphorylation of native and heme-modified CYP3A4 by protein kinase C: A mass spectrometric characterization of the phosphorylated peptides. Biochemistry. *40*, 11318–11326.

Wang, Q., Shinkre, B.A., Lee, J., Weniger, M.A., Liu, Y., Chen, W., Wiestner, A., Trenkle, W.C., Ye, Yihong (2010). The ERAD Inhibitor Eeyarestatin I Is a Bifunctional Compound with a Membrane-Binding Domain and a p97/VCP Inhibitory Group. PLoS One. *5*, e15479.

Wang, H., Wei, E., Quiroga, A.D., Sun, X., Touret, N., and Lehner, R. (2010). Altered lipid droplet dynamics in hepatocytes lacking triacylglycerol hydrolase expression. Mol. Biol. Cell. *21*, 1991-2000.

Watanabe, R.M., Ghosh, S., Langefeld, C.D., *et al.* (2000). The Finland-United States investigation of non-insulin-dependent diabetes mellitus genetics (FUSION) study. II. An autosomal genome scan for diabetes-related quantitative-trait loci. Am. J. Hum. Genet. *67*, 1186-200.

Waterman, I.J., Price, N.T., and Zammit, V.A. (2002). Distinct ontogenic patterns of overt and latent DGAT activities of rat liver microsomes. J. Lipid Res. *43*, 1555-1562.

Wei, S., Lai, K., Patel, S., Piantedosi, R., Shen, H., Colantuoni, V., Kraemer, F.B., and Blaner, W.S. (1997). Retinyl ester hydrolysis and retinol efflux from BFC-1β adipocytes. J. Biol. Chem. *272*, 14159-14165.

Weiss, S.B., and Kennedy, E.P. (1956). The Enzymatic Synthesis of Triglycerides. J. Am. Chem. Soc. *78*, 3550-3550.

Wendel, A.A., Lewin, T.M., and Coleman, R.A. (2009). Glycerol-3-phosphate acyltransferases: rate limiting enzymes of triacylglycerol biosynthesis. Biochim. Biophys. Acta. *1791*, 501-506.

Wenner, C., Lorkowski, S., Engel, T., and Cullen, P. (2001). Apolipoprotein E in Macrophages and Hepatocytes Is Degraded via the Proteasomal Pathway. Biochem. Biophys. Res. Commun. *282*, 608-614.

Wenzel, D.M., Lissounov, A., Brzovic, P.S. and Klevit, R.E. (2011). UBCH7 reactivity profile reveals parkin and HHARI to be RING/HECT hybrids. Nature. *474*, 105–108.

Wertz, I.E., and Dixit, V.M. (2010). Regulation of death receptor signaling by the ubiquitin system. Cell Death Differ. *17*, 14-24.

West, J., Tompkins, C.K., Balantac, N., Nudelman, E., Meengs, B., White, T., Bursten, S., Coleman, J., Kumar, A., Singer, J.W., and Leung, D.W. (1997). Cloning and expression of two human lysophosphatidic acid acyltransferase cDNAs that enhance cytokine-induced signaling responses in cells. DNA Cell Biol. *16*, 691-701.

White, A.L., Guerra, B., Wang, J., and Lanford, R.E. (1999). Presecretory degradation of apolipoprotein[a] is mediated by the proteasome pathway. J. Lipid Res. *40*, 275-286.

Wiertz, E.J., Tortorella, D., Bogyo, M., Yu, J., Mothes, W., Jones, T.R., Rapoport, T.A., and Ploegh H.L. (1996). Sec61-mediated transfer of a membrane protein from the endoplasmic reticulum to the proteasome for destruction. Nature. *384*, 432–438.

Wijeyesakere, S.J., Rizvi, S.M., Raghavan, M. (2013). Glycan-dependent and -independent interactions contribute to cellular substrate recruitment by calreticulin. J. Biol. Chem. *288*, 35104-35116.

Wilfling, F., Haas, J.T., Walther, T.C., and Farese, R.V.Jr. (2014a). Lipid droplet biogenesis. Curr. Opin. Cell Biol. *29C*, 39-45.

Wilfling, F., Thiam, A.R., Olarte, M.J., Wang, J., Beck, R., Gould, T.J., Allgeyer, E.S., Pincet, F., Bewersdorf, J., Farese, R.V.Jr., and Walther, T.C. (2014b). Arf1/COPI machinery acts directly on lipid droplets and enables their connection to the ER for protein targeting. eLife *3*, e01607.

Wilfling, F., Wang, H., Krahmer, N., Gould, T.J., Uchida, A., Cheng, J.X., Graham, M., Christiano, R., Frohlich, F., Liu, X., Buhman, K.K., Coleman, R.A., Bewersdorf, J., Farese, R.V. Jr., Walther, T.C. (2013). Triacylglycerol synthesis enzymes mediate lipid droplet growth by relocalizing from the ER to lipid droplets. Dev Cell. *24*, 384-399.

Wilson, C., Wardell, M.R., Weisgraber, K.H., Mahley, R.W., and Agard, D.A. (1991). Three-dimensional structure of the LDL receptor-binding domain of human apolipoprotein. E. Science. *252*, 1817-1822.

Wolfe, R.R., Klein, S., Carraro, F., and Weber, J.M. (1990). Role of triglyceride-fatty acid cycle in controlling fat metabolism in humans during and after exercise. Am. J. Physiol. Endocrinol. Metab. *258*, E382-E389.

Wolins, N., Quaynor, B., Skinner, J., Schoenfish, M., Tzekov, A., and Bickel, P. (2005). S3-12, adipophilin, and TIP47 package lipid in adipocytes. J. Biol. Chem. *280*, 19146-19155.

Wolins, N.E., Quaynor, B.K., Skinner, J.R., Tzekov, A., Croce, M.A., Gropler, M.C., Varma, V., Yao-Borengasser, A., Rasouli, N., Kern, P.A., Finck, B.N., and Bickel, P.E. (2006). OXPAT/PAT-1 is a PPAR-induced lipid droplet protein that promotes fatty acid utilization. Diabetes. *55*, 3418-3428.

World Health Organization. (2000). Obesity: preventing and managing the global epidemic. Geneva: Report of a WHO Consultation on Obesity. pp. 1-252.

Wu, J.W., Wang, S.P., Casavant, S., Moreau, A., Yang, G.S., and Mitchell, G. A. (2012). Fasting energy homeostasis in mice with adipose deficiency of desnutrin/adipose triglyceride lipase. Endocrinology. *153*, 2198–2207.

Wurie, H.R., Buckett, L., and Zammit, V.A. (2012). Diacylglycerol acyltransferase 2 acts upstream of diacylglycerol acyltransferase 1 and utilizes nascent diglycerides and de novo synthesized fatty acids in HepG2 cells. FEBS J. *279*, 3033−3047.

Xie, P., Guo, F., Ma, Y., Zhu, H., Wang, F., Xue, B., Shi, H., Yang, J., and Yu, L. (2014). Intestinal Cgi-58 deficiency reduces postprandial lipid absorption. PLoS ONE. *9,* e91652.

Xu, G., Sztalryd, C., and Londos, C. (2006). Degradation of perilipin is mediated through ubiquitination-proteasome pathway. Biochim. Biophys. Acta. *1761*, 83-90.

Xu, G., Sztalryd, C., Lu, X., Tansey, J.T., Gan, J., Dorward, H., Kimmel, A. R., and Londos, C. (2005). Post-translational regulation of adipose differentiation-related protein by the ubiquitin/proteasome pathway. J. Biol. Chem. *280*, 42841-42847.

Xu, N., Zhang, S.O., Cole, R.A., McKinney, S.A., Guo, F., Haas, J.T., Bobba, S., Farese, R.V.Jr, and Mak, H.Y. (2012). The FATP1-DGAT2 complex facilitates lipid droplet expansion at the ER-lipid droplet interface. J. Cell Biol. *198*, 895–911.

Yamaguchi T., Omatsu N., Omukae A., and Osumi T. (2006). Analysis of interaction partners for perilipin and ADRP on lipid droplets. Mol. Cell. Biochem. *284*, 167–73.

Yamazaki, T., Sasaki, E., Kakinuma, C., Yano, T., Miura, S., and Ezaki, O. (2005). Increased very low density lipoprotein secretion and gonadal fat mass in mice overexpressing liver DGAT1. J. Biol. Chem. *280*, 21506–21514.

Yang, L.Y., Kuksis, A., Myher, J.J., and Steiner, G. (1995). Origin of triacylglycerol moiety of plasma very low density lipoproteins in the rat: structural studies. J. Lipid Res. *36*, 125–136.

Ye, Y., Meyer, H.H., and Rapoport, T.A. (2001). The AAA ATPase Cdc48/p97 and its partners transport proteins from the ER into the cytosol. Nature. *414*, 652–656.

Ye, Y., Meyer, H.H., and Rapoport, T.A. (2003). Function of the p97-Ufd1-Npl4 complex in retrotranslocation from the ER to the cytosol: dual recognition of nonubiquitinated polypeptide segments and polyubiquitin chains. J. Cell Biol. *162*, 71–84.

Ye, Y., and Rape, M. (2009). Building ubiquitin chains: E2 enzymes at work. Nat. Rev. Mol. Cell Bio. *10*, 755–764.

Ye, Y., Shibata, Y., Kikkert, M., van Voorden, S., Wiertz, E., Rapoport T.A. (2005) Recruitment of the p97 ATPase and ubiquitin ligases to the site of retrotranslocation at the endoplasmic reticulum membrane. Proc. Natl. Acad. Sci. U S A. *102*,14132–14138.

Yen, C.L., Cheong, M.L., Grueter, C., Zhou, P., Moriwaki, J., Wong, J.S., Hubbard, B., Marmor, S., and Farese, R.V.Jr. (2009). Deficiency of the intestinal enzyme acyl CoA:monoacylglycerol acyltransferase-2 protects mice from metabolic disorders induced by high-fat feeding. Nat. Med. *15*, 442–446.

Yen, C.L., and Farese, R.V.Jr. (2003). MGAT2, a monoacylglycerol acyltransferase expressed in the small intestine. J. Biol. Chem. *278*, 18532–18537.

Yen, C.L., Monetti, M., Burri, B.J., and Farese R.V.Jr. (2005). The triacylglycerol synthesis enzyme DGAT1 also catalyzes the synthesis of diacylglycerols, waxes, and retinyl esters. J. Lipid Res. *46*, 1502-1511.

Yen, C.L., Nelson, D.W., Yen M.I. (2015). Intestinal triacylglycerol synthesis in fat absorption and systemic energy metabolism. J. Lipid Res. *56*, 489-501.

Yen, C.L., Stone, S.J., Cases, S., Zhou, P., and Farese, R.V.Jr. (2002). Identification of a gene encoding MGAT1, a monoacylglylcerol acyltransferase. Proc. Natl. Acad. Sci. U S A. *99*, 8512–8517.

Yen, C.L., Stone, S.J., Koliwad, S., Harris, C., and Farese, R.V.Jr. (2008). Thematic Review Series: glycerolipids. DGAT enzymes and triacylglycerol biosynthesis. J. Lipid Res. *49*, 2283-2301.

Yin, Q., Yang, H., Han, X., Fan, B., and Liu, B. (2012). Isolation, mapping, SNP detection and association with backfat traits of the porcine CTNNBL1 and DGAT2 genes**.** Mol. Biol. Rep. *39*, 4485–4490.

Young, S.G., and Zechner, R. (2013). Biochemistry and pathophysiology of intravascular and intracellular lipolysis. Genes Dev. *27*, 459–484.

Younger, J.M., Chen, L., Ren, H.Y., Rosser, M.F., Turnbull, E.L., Fan, C.Y., Patterson, C., and Cyr, D.M. (2006). Sequential quality-control checkpoints triage misfolded cystic fibrosis transmembrane conductance regulator. Cell. *126*, 571–582.

Yu, X.X., Murray, S.F., Pandey, S.K., Booten, S.L., Bao, D., Song, X.Z., Kelly, S., Chen, S., McKay, R., Monia, B.P., and Bhanot, S. (2005). Antisense oligonucleotide reduction of DGAT2 expression improves hepatic steatosis and hyperlipidemia in obese mice. Hepatology. *42*, 362–371.

Yu, Y., Zhang, Y., Oelkers, P., Sturley, S.L., Rader, D.J., Ginsberg, H.N. (2002). Posttranscriptional control of the expression and function of diacylglycerol acyltransferase-1 in mouse adipocytes. J. Biol. Chem. *277*, 50876-50884.

Yue, Y.G., Chen, Y. Q., Zhang, Y., Wang, H., Qian, Y.W., Arnold, J.S., Calley, J.N., Li, S.D., Perry, W.L.3rd., Zhang, H.Y., Konrad, R.J., and Cao, G. (2011). The acyl coenzymeA:monoacylglycerol acyltransferase 3 (MGAT3) gene is a pseudogene in mice but encodes a functional enzyme in rats. Lipids. *46*, 513–520.

Zhang, Z.R., Bonifacino, J.S., and Hegde, R.S. (2013). Deubiquitinases sharpen substrate discrimination during membrane protein degradation from the ER. Cell. *154*, 609–622.

Zhang, P., O'Loughlin, L., Brindley, D.N., and Reue, K. (2008). Regulation of lipin-1 gene expression by glucocorticoids during adipogenesis. J. Lipid Res. *49*, 1519-1528.

Zhang, Z., Tan, M., Xie, Z., Dai, L., Chen, Y., and Zhao, Y. (2011). Identification of lysine succinylation as a new post-translational modification. Nat. Chem. Biol. *7*, 58–63.

Zhang, L.J., Wang, C., Yuan, Y., Wang, H., Wu, J., Liu, F., Li, F., Gao, X., Zhao, Y.L., Hu, P.Z., Li, P., and Ye, J. (2014). Cideb facilitates the lipidation of chylomicrons in the small intestine. J. Lipid Res. *55*, 1279–1287.

Zhou H., and Hylemon, P.B. (2014). Bile acids are nutrient signaling hormones. Steroids. *86*, 62-68.

Zimmermann, R., Lass, A., Haemmerle, G., and Zechner, R. (2009). Fate of fat: the role of adipose triglyceride lipase in lipolysis. Biochim. Biophys. Acta. *1791*, 494–500.

Zimmermann, R., Strauss, J.G., Haemmerle, G., Schoiswohl, G., Birner-Gruenberger, R., Riederer, M., Lass, A., Neuberger, G., Eisenhaber, F., Hermetter, A., and Zechner, R. (2004). Fat mobilization in adipose tissue is promoted by adipose triglyceride lipase. Science. *306*, 1383–1386.